doi.org/10.26434/chemrxiv.12404252.v1

Minimizing HCN in DIC/Oxyma Mediated Amide Bond Forming Reactions

Marion Erny, Marika Lundqvist, Jon H. Rasmussen, Olivier Ludemann-Hombouger, Frédéric Bihel, Jan Pawlas

Submitted date: 01/06/2020 • Posted date: 02/06/2020

Citation information: Erny, Marion; Lundqvist, Marika; Rasmussen, Jon H.; Ludemann-Hombouger, Olivier; Bihel, Frédéric; Pawlas, Jan (2020): Minimizing HCN in DIC/Oxyma Mediated Amide Bond Forming Reactions. ChemRxiv. Preprint. https://doi.org/10.26434/chemrxiv.12404252.v1

Aiming at advancing protocols for safer, environmentally sensible peptide synthesis we report our findings with regards to the occurrence of hydrogen cyanide (HCN, prussic acid) in amide bond forming reactions mediated by diisopropylcarbodiimide (DIC) and ethyl (hydroxyimino)cyanoacetate (Oxyma). We have determined that HCN is always formed in amide bond forming reactions on solid support in N,N-dimethylformamide (DMF) when employing DIC/Oxyma. In an attempt to minimize the formation of prussic acid by means of preventing the linear DIC/Oxyma adduct 2 from cyclizing to oxadiazole 3 and in turn releasing HCN, we evaluated a series of greener solvents such as N-butylpyrrolidinone (NBP), NBP/ethyl acetate (EtOAc, 1:1), methyl 5-(dimethylamino)-2-methyl-5-oxopentanoate (PolarClean, PC), and PC/EtOAc (1:1). We found that the ratio between 2 and 3 greatly depends on the solvent used and consequently, we further examined DMF, NBP, NBP/EtOAc (1:1) and NBP/EtOAc (1:4) as solvents for DIC/Oxyma mediated amidations on solid support and in solution. We found that using carboxylic acid/Oxyma/DIC in a 1:1:1 ratio the rate of HCN formation decreases in the following order DMF>NBP>NBP/EtOAc (1:1)>NBP/EtOAc (1:4) while the reaction rate increases in order of DMF~NBPin situ scavenging of the HCN formed. We carried out DIC/Oxyma mediated amidation of Fmoc-Gly-OH + (S)-(-)-1-phenylethylamine in DMF-d_7 with 0, 5 and 10 equiv of dimethyl trisulfide (DMTS) as HCN scavenger. The formation of HCN and rate of amidation was monitored by ^{1}H NMR, revealing that DMTS scavenges HCN without inhibiting the rate of amidation. DIC/Oxyma mediated amidations of Fmoc-Ser(t-Bu)-OH with (S)-(-)-1-phenylethylamine in DMF and NBP/EtOAc (1:4) with and without 10 equiv of DMTS were carried out and found to be comparable.

Minimizing HCN in DIC/Oxyma mediated amide bond forming reactions

Marion Erny,[a,c] Marika Lundqvist,[b] Jon H. Rasmussen,[b] Olivier Ludemann-Hombourger,[a] Frédéric Bihel[c] and Jan Pawlas[b,*]

[a]PolyPeptide Group, 7 rue de Boulogne, 67100 Strasbourg, France

[b]PolyPeptide Group, Limhamnsvägen 108, PO BOX 30089, 20061 Limhamn, Sweden

[c]Laboratoire d'Innovation Thérapeutique, UMR7200, CNRS, Université de Strasbourg, Faculty of Pharmacy, 74 Route du Rhin, 67401 Illkirch-Graffenstaden, France

[*]Corresponding author. E-mail: jan.pawlas@polypeptide.com

Abstract

Aiming at advancing protocols for safer, environmentally sensible peptide synthesis we report our findings with regards to the occurrence of hydrogen cyanide (HCN, prussic acid) in amide bond forming reactions mediated by diisopropylcarbodiimide (DIC) and ethyl (hydroxyimino)cyanoacetate (Oxyma). We have determined that HCN is always formed in amide bond forming reactions on solid support in N,N-dimethylformamide (DMF) when employing DIC/Oxyma. In an attempt to minimize the formation of prussic acid by means of preventing the linear DIC/Oxyma adduct **2** from cyclizing to oxadiazole **3** and in turn releasing HCN, we evaluated a series of greener solvents such as N-butylpyrrolidinone (NBP), NBP/ethyl acetate (EtOAc, 1:1), methyl 5-(dimethylamino)-2-methyl-5-oxopentanoate (PolarClean, PC), and PC/EtOAc (1:1). We found that the ratio between **2** and **3** greatly depends on the solvent used and consequently, we further examined DMF, NBP, NBP/EtOAc (1:1) and NBP/EtOAc (1:4) as solvents for DIC/Oxyma mediated amidations on solid support and in solution. We found that using carboxylic acid/Oxyma/DIC in a 1:1:1 ratio the rate of HCN formation decreases in the following order DMF>NBP>NBP/EtOAc (1:1)>NBP/EtOAc (1:4) while the reaction rate increases in order of DMF~NBP<NBP/EtOAc (1:1)<NBP/EtOAc (1:4). Of the solvents examined, the NBP/EtOAc (1:4) mixture gave the lowest rate of HCN formation and the highest rate of amide bond formation both in solution and on solid support. As altering the solvent for DIC/Oxyma mediated amidations resulted in suppressing HCN rather than its full elimination we evaluated the concept of *in situ* scavenging of the HCN formed. We carried out DIC/Oxyma mediated amidation of Fmoc-Gly-OH + (S)-(-)-1-phenylethylamine in DMF-d_7 with 0, 5 and 10 equiv of dimethyl trisulfide (DMTS) as HCN scavenger. The formation of HCN and rate of amidation was monitored by ^{1}H NMR, revealing that DMTS scavenges HCN without inhibiting the rate of amidation. DIC/Oxyma mediated amidations of Fmoc-Ser(*t*-Bu)-OH with (S)-(-)-1-phenylethylamine in DMF and NBP/EtOAc (1:4) with and without 10 equiv of DMTS were carried out and found to be comparable.

TOC Graphic

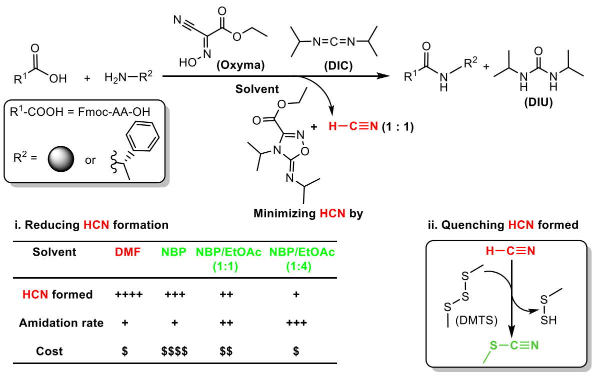

Solvent	DMF	NBP	NBP/EtOAc (1:1)	NBP/EtOAc (1:4)
HCN formed	++++	+++	++	+
Amidation rate	+	+	++	+++
Cost	$	$$$$	$$	$

The focus on sustainable chemistry as a means to contribute to the advancement of United Nations' Sustainable Development Goals has been increasing in recent years.[1] Adhering to the principles of Green Chemistry[2] is a key prerequisite for the development of sustainable chemical processes and due to the essential role of amide bonds in chemistry and biology,[3] greening of methods for the construction of amide bonds has received tremendous interest as of late,[4] for example within the areas of catalytic[5] and non-classical[6] amide bond forming reactions. Nevertheless, a vast majority of amide bonds are still being made using a wide range of conventional coupling reagents.[7] In fact, evaluating various environment, health and safety (EHS) aspects of using these coupling agents has seen growing attention as well.[8] Among the plethora of reagents available for amide bond formation, the combination of DIC[9] and Oxyma[10] has become established as one of the most widely used for efficient amide and peptide synthesis.[11] With regards to EHS considerations, DIC, which in itself promotes an efficient formation of amide bonds,[12] but is mostly used in the presence of various coupling additives,[7,13] has been deemed as one of the most preferred coupling reagents from the process safety standpoint.[8a] Oxyma has been reported to constitute a highly efficient, greener[4b] and safer alternative[14] to the hydroxybenzotriazole based coupling additives[7] which are also highly efficient racemization suppressants albeit their use in peptide synthesis has decreased considerably since explosive properties and classification of benzotriazole based coupling agents has been demonstrated.[15] Recently, McFarland et al. (Eli Lilly) reported that reacting DIC with Oxyma, either alone or in the presence of an amino acid (AA) component, leads to the formation of an oxadiazole byproduct **3** accompanied by an equimolar amount of HCN (Fig. 1a).[16] Although HCN has conceivably played a key role in the emergence of all life in the early days of our planet,[17] nowadays HCN is mostly associated with its very high toxicity.[18] In fact, the National Institute for Occupational Safety and Health (NIOSH) defines a level of 50 ppm of HCN gas as immediately dangerous to life or health.[19] The recent report by the scientists at Eli Lilly on occurrence of HCN upon reacting DIC with Oxyma[16] has therefore warranted a careful evaluation of possible EHS consequences of using DIC/Oxyma in amide and peptide synthesis. On this topic, it was recently noted by Albericio and coworkers[20] that the occurrence of this side reaction in the presence of an amino component, which corresponds to the real case in peptide synthesis, has not been reported. In fact, these authors indicated that the issue of HCN formation could be less pronounced than what was reported in the instances in which DIC/Oxyma was reacted in the absence of an amine.[16]

In connection with our ongoing interest and efforts in greening peptide chemistry[21] together with the fact that large quantities of DIC/Oxyma are used in the manufacturing of peptide therapeutics, these reports prompted us to investigate the extent of HCN formation under the conditions of DIC/Oxyma mediated amide bond forming reactions, and to identify possible courses of actions for mitigation. (Fig. 1b).

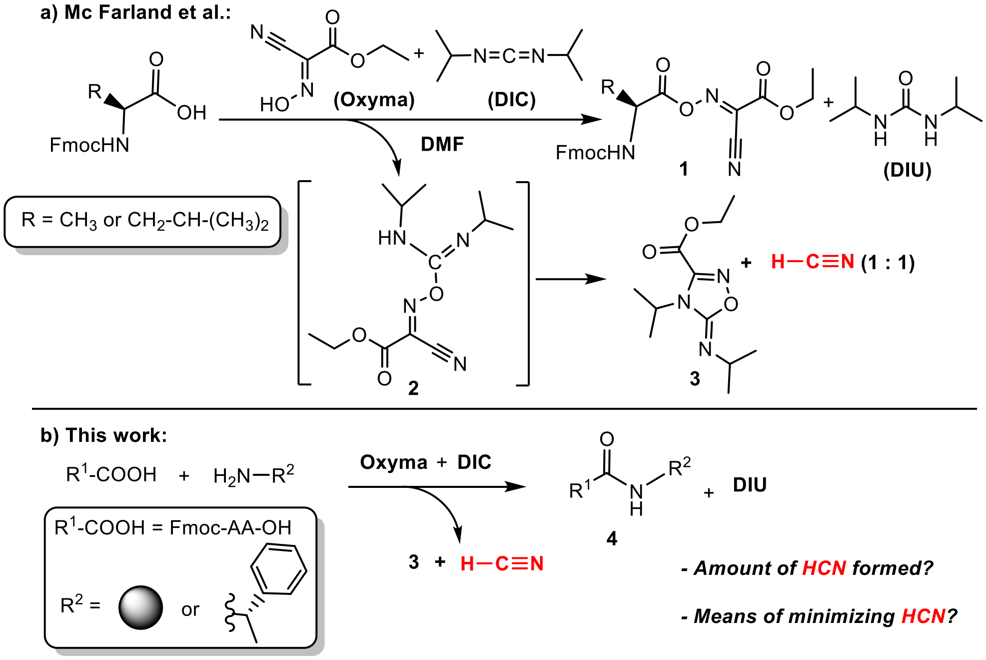

Figure 1. Schematic representation of HCN formation during DIC/Oxyma mediated reactions: (a) in reaction with Fmoc-Ala-OH or Fmoc-Leu-OH[16] (b) in amide bond forming reactions and assessment of HCN minimization.

First, we set out to assess the extent of HCN formation in a model DIC/Oxyma mediated amide bond forming reaction. As oxadiazole **3** is formed in an equimolar amount as HCN in reactions involving DIC and Oxyma (Fig. 1a),[16] we used the easily UV-detectable **3** as the marker of the HCN formation. As Merrifield's solid-phase peptide synthesis (SPPS)[22] constitutes the most widely used method for synthesis of peptides,[23] we assessed an amide bond forming reaction on a polymer support. The model system employed the Ramage linker[24] bound to an aminomethylstyrene (AMS) functionalized polystyrene/divinylbenzene (PS/DVB) resin[25] as nucleophile while using a Fluorenylmethyloxycarbonyl (Fmoc) protected AA activated by DIC/Oxyma as an acyl donor (Table 1). Thus, using the standard SPPS solvent DMF as the reaction medium, we carried out two amidations using AA/Oxyma/DIC starting materials in 1:1:1 and 1:1:3 stoichiometries. In both cases these starting materials were reacted for 1 h at room temperature (rt) after which the activated AA solutions were added to the resin and the resulting amide bond forming reactions were allowed to proceed for 20 h (Table 1). The formation of the HCN marker **3** was monitored throughout, and 0.3% Oxyma to **3** conversion was observed (and hence equimolar amounts of HCN) after 1 h of activation of Fmoc-Ser(*t*-Bu)-OH/Oxyma/DIC (1:1:1) in DMF. This corroborates the results obtained by McFarland et al. who reported a similar rate of HCN formation after reacting Fmoc-Leu-OH/Oxyma/DIC (1:1:1) in DMF for 1 h.[16] Further to this, during the monitoring of the subsequent amide bond forming process, we found that the formation of **3** steadily increased throughout the coupling process. Although in terms of chemical conversion of Oxyma to HCN the extent of HCN formation was not significant, appreciable amounts of HCN would have been formed if the reaction was carried out on mol scales customary in manufacturing on industrial scale. Upon completion of these couplings as determined by a colorimetric test (ninhydrin),[26] an appreciable amount of HCN was formed not only when 3 equiv DIC vs AA and Oxyma was used (~326 mg HCN mol^{-1} AA coupling) but also when 1 equiv of DIC vs AA and Oxyma was employed (~166 mg HCN mol^{-1} AA coupling). It is worth noting that upon allowing the reactions to proceed further for a total of 20 h, the content of HCN increased to ~328 mg HCN mol^{-1} AA coupling for AA/Oxyma/DIC used in 1:1:1 ratio and to ~2148 mg HCN mol^{-1} AA coupling for 1:1:3 ratio. This result shows that if the reactions are stopped as soon as the desired coupling conversion is attained, the total amount of formed HCN is reduced.

Table 1: Assessment of HCN formation during DIC/Oxyma mediated amide bond formation on solid support[1]

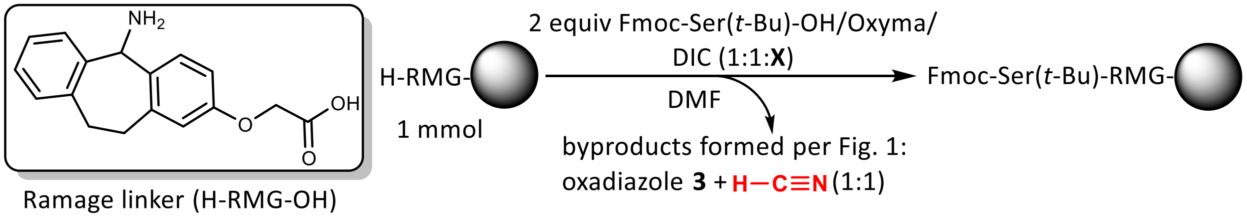

	AA activation (h)			Amide bond formation (h)		
X	0.0	0.5	1.0	0.5	2.5	20
	Oxyma to **3** conversion (mol %) (equimolar amounts of **HCN**) [2]					
1	0.00	0.21	0.28	0.32	0.48[3]	0.94
3	0.00	0.28	0.30	0.97[3]	1.66	6.37

[1] Reagents and conditions: Fmoc-Ser(*t*-Bu)-OH/Oxyma/DIC in DMF was reacted for 1 h at rt and the resulting mixture was added to H-RMG resin (swollen in DMF and drained). The slurry thus obtained was shaken at rt (300 rpm) for 20 h. [2] Aliquots of reaction mixtures were taken out throughout and analyzed by HPLC for the content of the HCN marker **3**. Using these contents of **3** Oxyma to HCN conversions were determined, see section 2 in the ESI for details. [3] Full conversion of the amide bond formation attained according to a qualitative (ninhydrin) color test.

As we determined that HCN formation occurs under commonly used conditions for use of DIC/Oxyma in peptide synthesis we set out to examine whether the extent of this side reaction could be minimized by suitably altering the parameters of the reaction between DIC and Oxyma. Recently, we reported that choice of solvent and/or addition of scavengers have a profound effect on the extent of side reactions initiated by conversion of Oxyma to the corresponding N-oxyl radical.[27] We reasoned that the reaction medium could alter the rate of the HCN forming side reaction as well and, thus, wanted to evaluate the solvent effects on the conversion of Oxyma to HCN. As oxadiazole **3** is directly associated with formation of HCN and the linear precursor **2** (Fig. 1a) is not, we decided to evaluate the rate of formation of both **3** and **2** in reactions between DIC/Oxyma solely and in solvents considered to be greener than the standard hazardous DMF,[28] but still relevant in the context of SPPS. Two greener dipolar aprotic solvents, NBP[29] and PC[30] were chosen. In addition, as we recently showed that using EtOAc, a suitable solvent for greener solution-phase amidations,[31] works well as a co-solvent in SPPS and even enables suppression of side reactions in peptide couplings on polymer supports,[32] we also examined 1:1 mixtures of NBP/EtOAc and PC/EtOAc. With regards to scavengers, addition of a suitable sulfur containing radical scavenger such as dithiothreitol (DTT) or diisopropylthiourea (DITU) was reported to inhibit the formation of N-Oxyl radical from Oxyma.[27] Therefore, all five solvents were evaluated in the presence of DITU (10 mol%) to discern any possible role of an N-Oxyl radical formed from Oxyma in the side reaction leading to the HCN formation. The progress of formation of **3** was assessed by HPLC over the course of 17 days, and the content of **2** and **3** was determined after 4 days by EIC (extracted ion chromatography) LC-MS (Fig. 2). We found that the rate of formation of **3** depends profoundly on the reaction medium (see ESI, section 3), and the **2**:**3** ratio could be altered by replacing DMF with any of the four greener solvents examined. Although in none of the experiments the occurrence of **3** could be minimized to an appreciable extent, we observed that the amount of **2** present increased in order of DMF~NBP<NBP/EtOAc~PC<PC/EtOAc. It is worth noting that the open chain DIC-Oxyma adduct **2** was detected at rt, whereas in the study by McFarland et al. it was only observed by NMR at -30 °C.[16] Regarding the addition of 10 mol % of DITU, we determined that it did not alter the **2**:**3** ratio appreciably irrespective of solvent (see ESI section 3) and this result disfavors a role of Oxyma based N-oxyl radical species in the formation of **3** and HCN.

Having evaluated the effect of solvents on formation of adduct **2** vs oxadiazole **3** and HCN in DIC/Oxyma mixtures, a screening of actual amide bond formations on a solid support in the different solvents was initiated. Thus, we examined DMF vs the greener NBP and NBP/EtOAc (1:1), which both constitute suitable SPPS solvents.[33,34] Moreover, to examine the role of NBP/EtOAc ratio on the formation of HCN, NBP/EtOAc (1:4) mixture was examined as well. With regards to PC and PC/EtOAc (1:1), these solvents were not further assessed since inferior amide bond formation kinetics were determined outside this work (unpublished data).

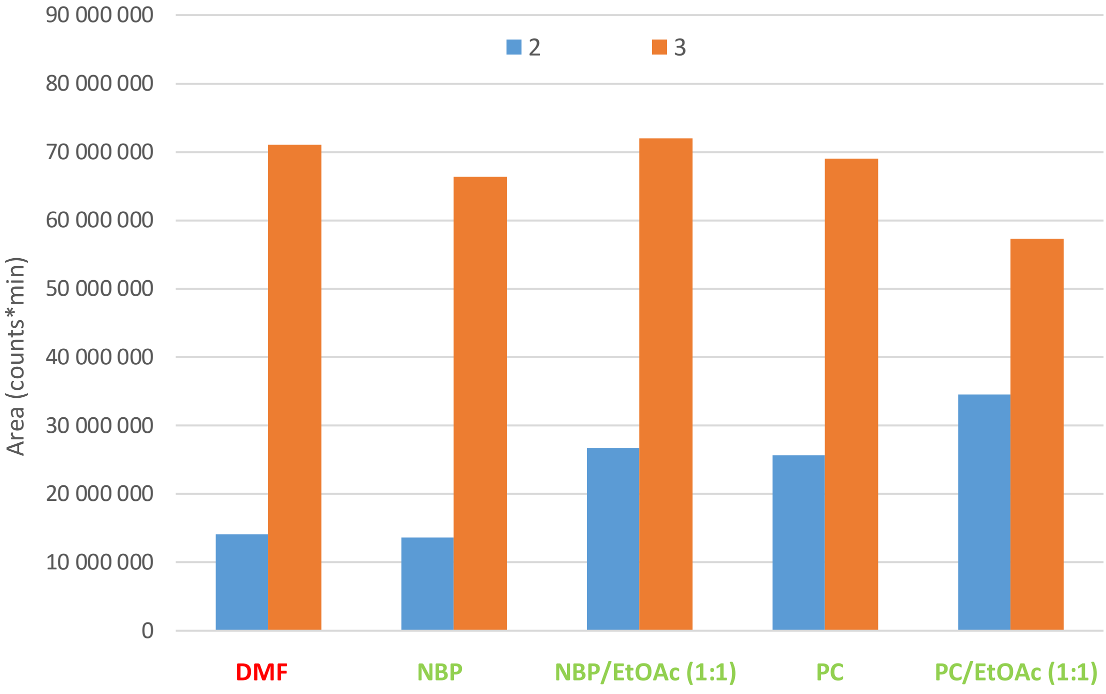

Figure 2. Schematic representation of EIC-MS contents of linear DIC/Oxyma adduct **2** and oxadiazole **3** in Oxyma/DIC (1.0:1.2) mixtures in five different solvents after 4 days at rt. For full details of HPLC analyses at different timepoints with and without 10 mol% DITU and LC-HRMS analyses confirming the presence of **2** and **3** in these reactions see ESI, section 3.

For the coupling screening, 2 equiv. of AA/Oxyma/DIC in 1:1:1 and 1:1:3 ratios were examined. To avoid the formation of HCN during AA/DIC/Oxyma activation, the amide bond forming reactions were carried out as ‘‘one-pot’’, i.e. to a slurry of dissolved AA, Oxyma and resin, DIC was added (Table 2). The coupling conversion was assessed by a colorimetric (ninhydrin) test[26] and the formation of **3** at the completion of the experiment was determined by LC-HRMS. According to the color test carried out after 0.5 h, all couplings using 1:1:3 AA/Oxyma/DIC were complete, while using the 1:1:1 AA/Oxyma/DIC ratio all reactions except for the NBP/EtOAc (1:4) run were incomplete. Interestingly, while the runs using 1:1:3 AA/Oxyma/DIC ratio all exhibited significant rate of **3** (and HCN) formation which increased in order of NBP<DMF<NBP/EtOAc (1:1)<NBP/EtOAc (1:4) the experiments run with 1:1:1 AA/Oxyma/DIC ratio showed a much slower rate of HCN formation, decreasing in order of DMF>NBP>NBP/EtOAc (1:1)>NBP/EtOAc (1:4). The exact nature of all the phenomena governing the rate of HCN formation depending on solvent and reagent stoichiometry is currently not known and will be the subject of future studies.

Nevertheless, we were intrigued by the low rate of HCN formation and the high rate of amide bond formation observed with the AA/Oxyma/DIC (1:1:1) in NBP/EtOAc (1:4) and we decided to further evaluate reaction kinetics using this protocol. As the AA/Oxyma/DIC (1:1:1) coupling in NBP/EtOAc (1:4) using 2 equiv was quite fast, we decreased the amount of AA to 1.3 equiv to slow down the coupling rate and facilitate the assessment of the kinetics. Furthermore, to also evaluate the solvent effect on the rate of HCN formation in a solution phase amidation, we carried out a DIC/Oxyma mediated coupling of Fmoc-Ser(*t*-Bu)-OH using (S)-(-)-1-phenylethylamine (1.0 equiv) as a nucleophile. The results of these experiments are summarized in Fig. 3, revealing that both in solution and on solid support the amidation kinetics increased in order of DMF~NBP<NBP/EtOAc (1:1)<NBP/EtOAc (1:4) while the rate of HCN formation decreased in a DMF>NBP>NBP/EtOAc (1:1)>NBP/EtOAc (1:4) order. In summary, using the inexpensive NBP/EtOAc (1:4)[35] as solvent gave the highest reaction rate and the lowest rate of HCN formation both in solution and on a solid support.

Table 2: Solvent effects on HCN formation during DIC/Oxyma mediated amide bond formation on solid support[1]

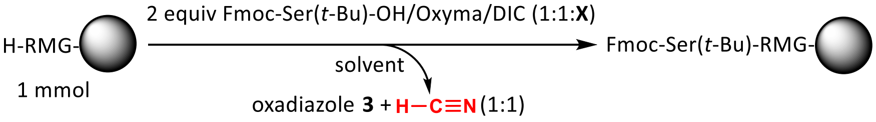

Solvent	**DMF**		**NBP**		**NBP/EtOAc (1:1)**		**NBP/EtOAc (1:4)**	
X	1	3	1	3	1	3	1	3
Kaiser test after 0.5 h[2]	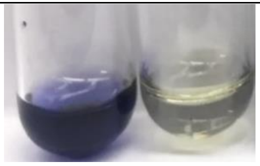		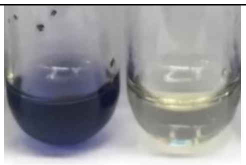		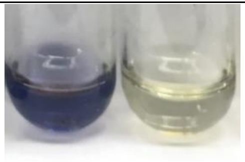			
Oxyma to HCN conv. after 20 h (%)[3]	**0.74**	**8.84**	**0.45**	**6.38**	**0.20**	**11.47**	**0.09**	**22.54**

[1] Reagents and conditions: Fmoc-Ser(*t*-Bu)-OH/Oxyma in solvent was added to H-RMG resin (swollen in solvent and drained). DIC was added and the slurry thus obtained was shaken at rt (300 rpm) for 20 h. [2] After 2.5 h the color test was negative for all runs. [3] Oxyma to HCN conversions were determined as in Table 1, see section 4 in the ESI for details.

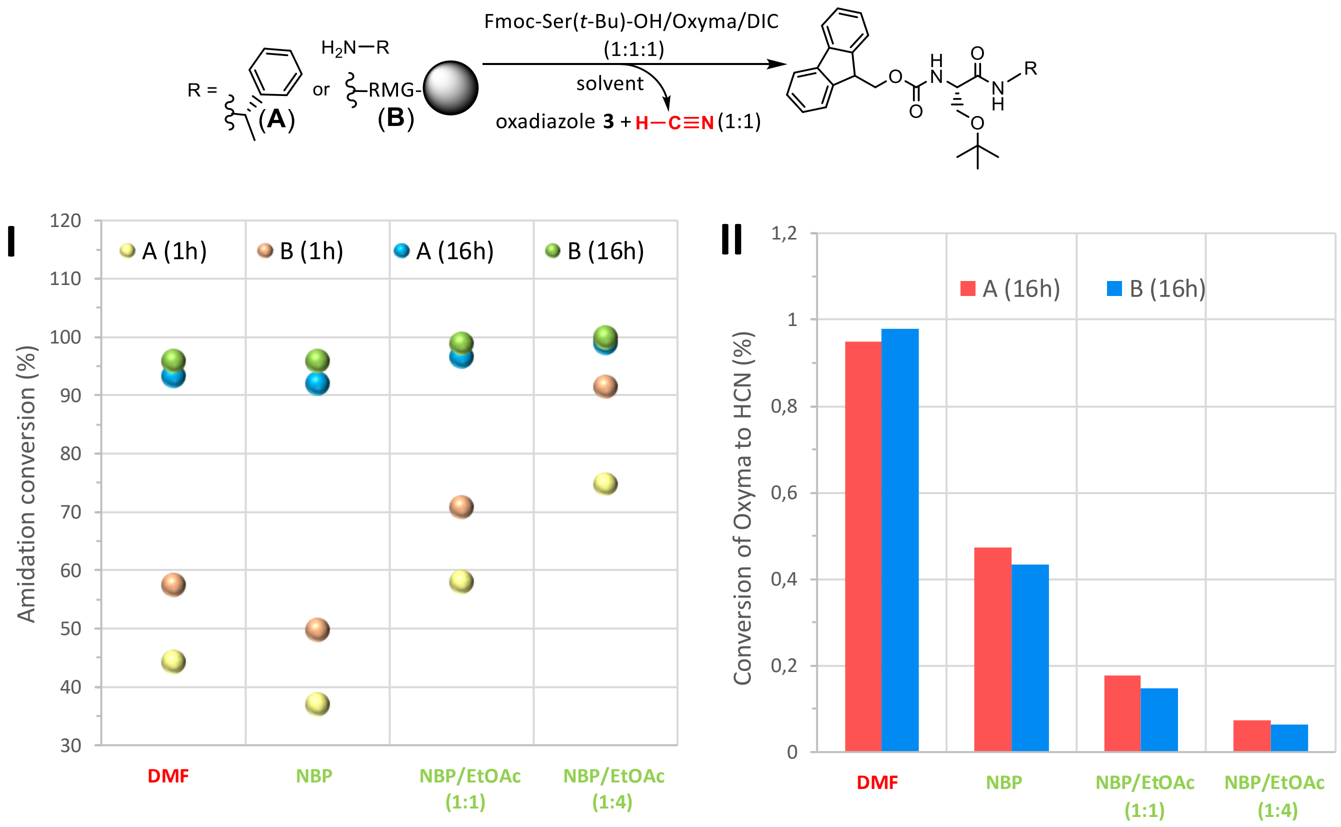

Figure 3. Solvent effects on **I)** amidation conversion **II)** HCN formation during DIC/Oxyma mediated amide bond formation in solution (R=**A**) and on solid support (R=**B**).

The encouraging results of minimizing HCN as well as improving reaction rates in NBP/EtOAc (1:4) represent an interesting perspective over the conventional DMF protocols. However, the occurrence of HCN was not fully eradicated. In a further pursuit of methods that would enable additional reduction of HCN, we evaluated the concept of in situ scavenging of the HCN formed. Mc Farland *et al.* showed that in DMF-d_7 mixtures of DIC/Oxyma, the amount of HCN in solution was appreciably lower than the amount of oxadiazole **3**, conceivably due to the loss of HCN to the vapor phase above the reaction solution.[16] This observation prompted us first to examine the effect of the concentration on the ratio of HCN vs **3** in solution prior to any test for HCN scavenging effects. We examined DMF-d_7 solutions of DIC/Oxyma at 0.3M, 0.4M and 0.5M by NMR spectroscopy (Fig. 4) and determined the amount of HCN versus **3**. Interestingly, a marked concentration dependence was observed. At 0.4M and 0.5M the relative amount of HCN (HCN vs **3**) in solution over time decreased quite significantly whereas at 0.3M the relative amount of HCN in solution remained much higher (Fig. 4A). The HCN lacking in solution due to loss of HCN to the gas phase would be more pronounced at higher concentrations in line with the generated results. To further test this hypothesis, future studies will be aimed at determining the content of HCN both in solution and in gas phase.[36]

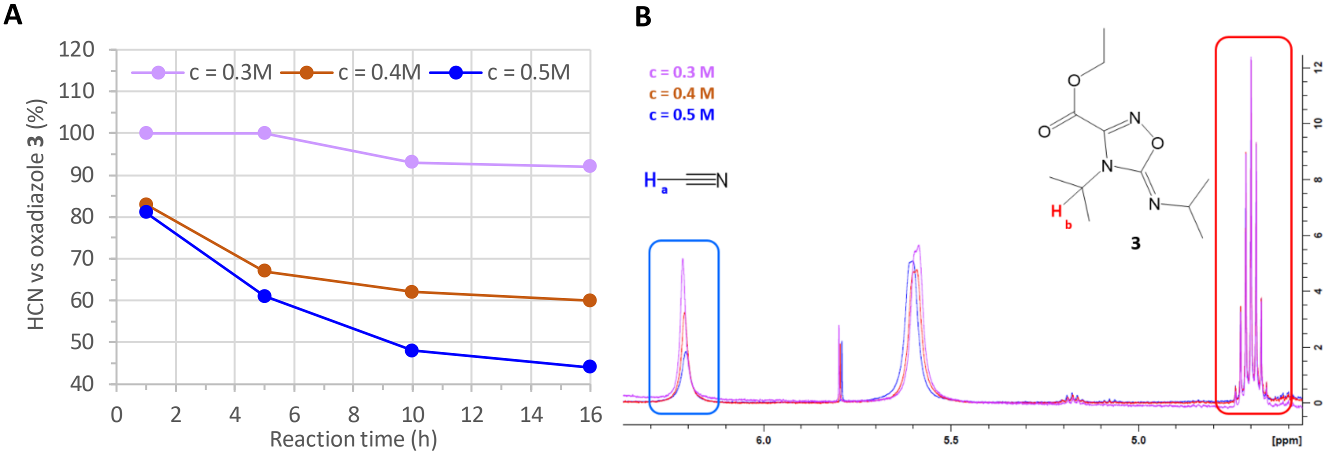

Figure 4. ^{1}H NMR assessment of the presence of HCN in 0.3M, 0.4M and 0.5M DMF-d_7 solutions of DIC/Oxyma (1:1) at rt. A) HCN vs oxadiazole **3** ratio at different DIC/Oxyma concentrations over time. B) An expansion of an overlay of ^{1}H NMR spectra of 0.3M, 0.4M and 0.5M DIC/Oxyma mixtures after 10 h. An integration of HCN H_a and oxadiazole **3** H_b peaks was used to determine HCN vs **3** ratios, for experimental details see ESI section 7.

With the result of the DIC/Oxyma concentration study (Fig. 4) in hand we moved on to the HCN scavenger proof of concept. The concentration of the amidation reactions was chosen to be at 0.1M to keep the HCN to be scavenged in solution, and the reaction was to be monitored by NMR. As an HCN scavenger DMTS[37] was employed using a reaction where DMTS transforms the HCN into the less hazardous methyl thiocyanate. Prior to engaging DMTS, it was first established that i) none of the starting materials used in DIC/Oxyma mediated amide bond formations react with the DMTS, and ii) activation of an AA by DIC/Oxyma is not impaired by the presence of DMTS (see ESI, section 8). Upon confirmation of these prerequisites, DIC/Oxyma mediated coupling of Fmoc-Gly-OH with (S)-(-)-1-phenylethylamine in DMF-d_7 at 0.1M concentration was carried out using 0, 5 and 10 equiv. of DMTS, respectively. NMR analyses showed that increasing the amount of DMTS resulted in lowering of the HCN concentration (Fig. 5), confirming that DMTS scavenges the HCN formed during the coupling reaction. Importantly, using NMR it was determined that HCN scavenging occurred without impairing the rate of the coupling reaction (Fig. 5). Additionally, we evaluated the impact of DMTS on the rate of amide bond formations in the different solvents. Thus, DIC/Oxyma mediated couplings of Fmoc-Ser(*t*-Bu)-OH and (S)-(-)-1-phenylethylamine in DMF and NBP/EtOAc (1:4) were carried out, with and without 10 equiv of DMTS. In keeping with the assessment of solvents effects on coupling kinetics shown in Fig. 3 the amidations in NBP/EtOAc (1:4) occurred at faster rates than the corresponding reactions in DMF and according to HPLC analyses, the couplings with and without DMTS proceeded comparably (see ESI, section 10).

In future studies we will continue to determine the amount of HCN as well as rate of amide bond formation in a broader range of solvents and in the presence of various potential HCN scavengers with the aim of establishing greener, safer coupling conditions.

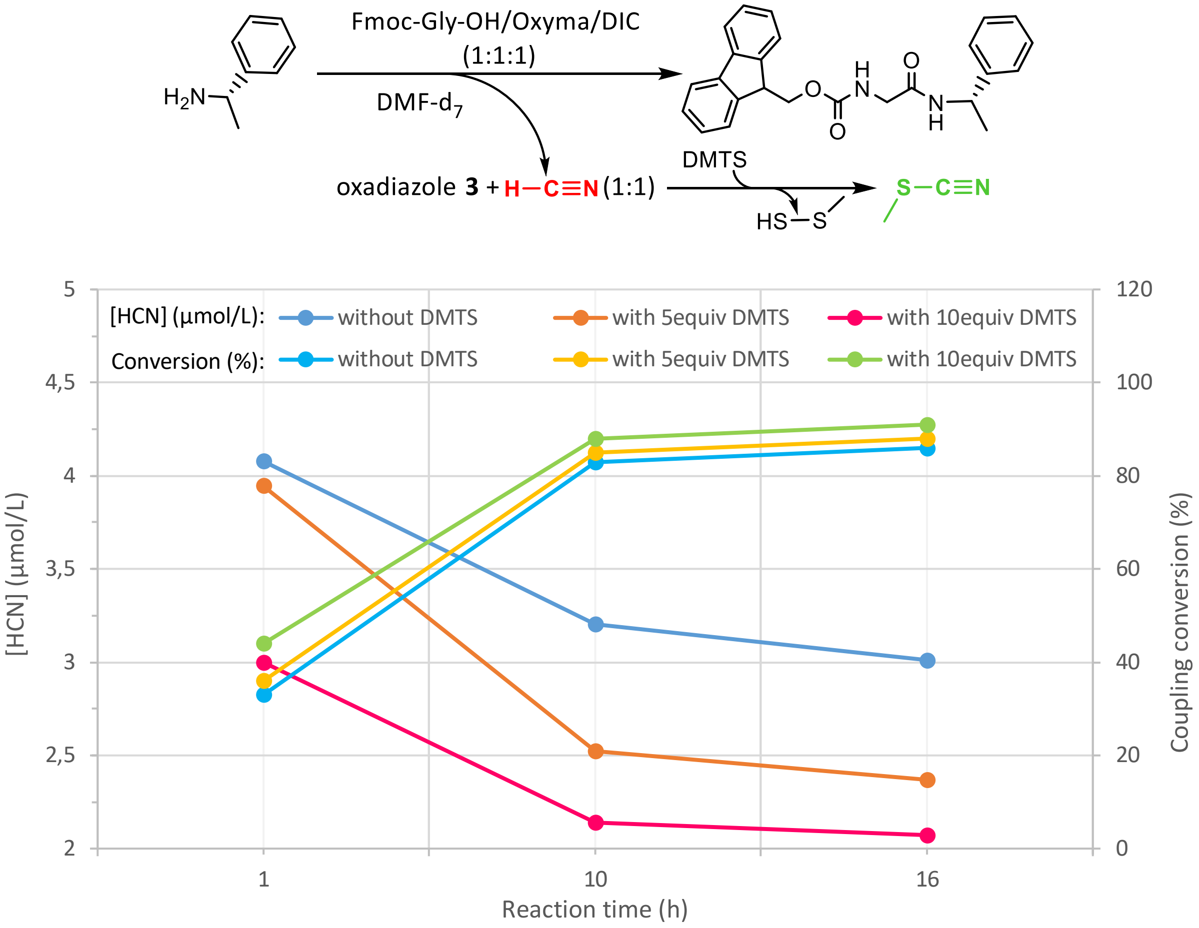

Figure 5. Effect of DMTS on conversion and presence of HCN during DIC/Oxyma mediated coupling of Fmoc-Gly-OH (1.0 equiv) and (S)-(-)-1-phenylethylamine in DMF-d$_7$ at rt.

Conclusions

In this initial work on understanding the HCN formation and identifying paths forward for control and prevention, we have demonstrated that DIC/Oxyma mediated amide bond forming reactions are accompanied by formation of HCN and that the HCN continues to build up in the reaction mixture. The rate of formation of HCN was found to be dependent on the solvent composition and the reagents ratios, and among the investigated greener alternatives, NPB/EtOAc (1:4) was found to minimize the formation while accelerating the actual coupling kinetics when employed with a 1:1:1 ratio of AA/Oxyma/DIC . The observed gap between the amounts of HCN and the amounts of **3**, attributed to release of HCN into the vapor phase, was investigated and a concentration of 0.3M (DIC and Oxyma) was found to contain the HCN in the solution significantly more effective than higher concentrations. Moreover, the concept of HCN scavenging during the DIC/Oxyma mediated coupling reactions was successfully tested with DMTS. We propose that combining the two HCN minimization concepts involving solvent engineering and *in situ* HCN scavenging may furnish protocols for efficient DIC/Oxyma mediated, HCN free synthesis of amides and peptides in green solvents. Further work on the development of such protocols as well as their implementation in industrial manufacturing of peptides is underway and will be reported in due course.

Experimental Section

All reagents, reactants and solvents were from standard suppliers of raw materials for peptide synthesis and were used as such.

Assessment of HCN formation and amide bond formation kinetics during DIC/Oxyma mediated coupling of 1.3 equiv Fmoc-Ser(t-Bu)-OH with H-RMG resin in different solvents.

4 x 1 mmol of dry H-RMG AMS resin was prepared as described in section 2 of the ESI. The dried H-RMG AMS resins were swollen in solvents specified for each reaction and drained. The amounts of residual solvent in the swollen and drained resins were determined to be ~5 mL. Next, in four reactions vessels, 4 x 498.5 mg (1.3 mmol, 1.0 equiv) of Fmoc-Ser(t-Bu)-OH and 184.7 mg (1.3 mmol, 1.0 equiv) of Oxyma were dissolved in 20 mL of solvents as specified for each reaction. The resulting Fmoc-Ser(t-Bu)-OH/Oxyma mixtures were added to the washed and drained batches of H-RMG AMS resins prepared above. To the resulting slurries of Fmoc Ser(t-Bu)-OH/Oxyma with H-RMG AMS resins 203.9 μL DIC (1.3 mmol, 1.0 equiv) was added in the following manner: experiment R1, DMF; experiment R2, NBP; experiment R3, NBP/EtOAc (1:1); experiment R4, NBP/EtOAc (1:4) and the resulting reaction mixtures were shaken at rt (300 rpm) for 16 h. Conversions of the amidation reactions were followed by determining the Fmoc content of the Fmoc Ser(t Bu)-RMG AMS resins and EIC MS analyses were used for the determination of **3** based on which Oxyma to HCN conversions were determined (see section 5 of the ESI for details).

Assessment of HCN formation and amide bond formation kinetics during DIC/Oxyma mediated coupling of 1.0 equiv Fmoc-Ser(t-Bu)-OH with (S)-(-)-1-phenylethylamine in different solvents.

Fmoc-Ser(t-Bu)-OH (191.8 mg, 0.5 mmol, 1.0 equiv) and Oxyma (71.0 mg, 0.5 mmol, 1.0 equiv) were weighed into four glass reaction vessels equipped with a magnetic stirrer. 10.0 mL of a solvent (DMF, NBP, NBP/EtOAc (1:1) and NBP/EtOAc (1:4)) was added to these vessels and all four reactions thus obtained were stirred at rt until all solid material was dissolved. To the resulting reaction mixtures (S)-(-)-1-phenylethylamine (62.9 μL, 0.5 mmol, 1.0 equiv) and DIC (78.3 μL, 0.5 mmol, 1.0 equiv) were added in the following manner: experiment R1, DMF ; experiment R2, NBP; experiment R3, NBP/EtOAc (1:1); experiment R4, NBP/EtOAc (1:4) and the resulting amidation reactions were allowed to stir at rt for 16 h. Conversions of the amidation reactions were followed by HPLC and EIC MS analyses were used for the determination of **3** based on which Oxyma to HCN conversions were determined (see section 6 of the ESI for details).

NMR analysis of HCN formation at different DIC/Oxyma concentrations

A solution was prepared by dissolving Oxyma (7.2 mg, 0.051 mmol, 1.0 equiv) and caffeine as internal standard (2.1 mg, 0.011 mmol, 0.22 equiv) in varying amount of DMF-d7 (see ESI section 7) to obtain 0.3, 0.4 and 0.5M concentration of Oxyma. The solution was mixed by using an ultrasound bath and DIC (8.0 μL, 0.051 mmol, 1.0 equiv) was added and the resulting mixture was transferred into a 3 mm NMR tube and transferred to the spectrometer for monitoring at 20°C. 1D ^{1}H NMR acquisition was done after 1 h, 5 h, 10 h and 16 h at which times HCN content in the solutions were determined (see ESI section 7).

NMR analysis of HCN formation during amide bond formations mediated by DIC/Oxyma with and without DMTS

Oxyma (10.1 mg, 0.071 mmol, 1.04 equiv), Fmoc-Gly-OH (20.3 mg, 0.068 mmol, 1.0 equiv) and caffeine (8.0 mg, 0.042 mmol, 0.62 equiv) were dissolved in 680 μL of DMF-d7 and (S)-(-)-1-phenylethylamine (8.77 μL, 0.068 mmol, 1.0 equiv) and DIC (10.65 μL, 0.068 mmol, 1.0 equiv) were added. 170 μL aliquots (25% v/v of the solution i.e. ~ 0.017 mmol based on Fmoc-Gly OH) of this solution were taken out and 0, 5, 10 equiv of DMTS were added to these solutions. The resulting reaction mixtures were transferred into 3 mm NMR tubes and 1D ^{1}H NMR acquisitions were done after 1 h, 5 h, 10 h and 16 h using which amidation conversions and contents of HCN were determined (see ESI section 9).

Conflicts of interest

There are no conflicts to declare.

References

---

[1] Anastas, P. T.; Zimmerman, J. B., The United Nations sustainability goals: How can sustainable chemistry contribute? *Curr. Opin. Green Sustainable Chem*. **2018**, *13*, 150.

[2] Erythropel, H. C.; Zimerman, J. B.; de Winter, T. M.; Petitjean, L.; Melnikov, F.; Lam, C. H.; Lounsbury, A. W.; Mellor, K. E.; Janković, N. Z.; Tu, Q.; Pincus, L. N.; Falinski, M. M.; Shi, W.; Coish, P.; Plata, D. L.; Anastas, P. T., The Green ChemisTREE: 20 years after taking root with the 12 principles. *Green Chem*. **2018**, *20*, 1929.

[3] See e.g. a) Canavelli,P.; Islam, S.; Powner, M. W., Peptide ligation by chemoselective aminonitrile coupling in water. *Nature,* **2019**, *571*, 546; b) Henninot, A.; Collins, J. C.; Nuss, J. M. The Current State of Peptide Drug Discovery: Back to the Future? *J. Med. Chem*. **2018**, *61*, 1382.

[4] a) Bryan, M. C.; Dunn, P. J.; Entwistle, D.; Gallou, F; Koenig, S. G.; Hayler, J. D.; Hickey, M. R.; Hughes, S,; Kopach, M. E.; Moine, G.; Richardson, P.; Roschangar, F.; Steven, A.; Weiberth, F. J., Key Green Chemistry research areas from a pharmaceutical manufacturers' perspective revisited. *Green Chem*. **2018**, *20*, 5082; b) Llobet, A. I.; Kenworthy, M. N.; Mukherjee, S.; Kopach, M. E.; Wegner, K.; Gallou, F.; Smith, A. G.; Roschangar, F., Sustainability Challenges in Peptide Synthesis and Purification: From R&D to Production. *J. Org. Chem.* **2019**, *84*, 4615; c) Amide Bond Formation Strategies: Latest Advances on a Dateless Transformation. *Eur. J. Org. Chem.* **2020**, 21, DOI: /10.1002/ejoc.202000080.

[5] a) Sabatini, M. T.; Boulton, L. T.; Sneddon, H. F.; Sheppard, T. D., A green chemistry perspective on catalytic amide bond formation. *Nature Cat.* **2019**, *2*, 10; b) Wang, X., Challenges and outlook for catalytic direct amidation reactions *Nature Cat.* **2019**, *2*, 98.

[6] de Figueiredo, R. M. ; Suppo, J.-S.; Campagne, Nonclassical Routes for Amide Bond Formation. J.-M. *Chem. Rev.* **2016**, *116*, 12029.

[7] El-Faham, A.; Albericio, F., Peptide Coupling Reagents, More than a Letter Soup. F., *Chem. Rev.* **2011**, *111*, 6557.

[8] See e.g. a) Sperry, J. B.; Minteer, J. B.; Tao, J.; Johnson, R.; Duzguner, R.; Hawksworth, M.; Oke, S.; Richardson, P. F.; Barnhart, R.; Bill, D. R.; Giusto, R. A.; Weaver III, J. D., Thermal Stability Assessment of Peptide Coupling Reagents Commonly Used in Pharmaceutical Manufacturing. *Org. Process Res. Dev*. **2018**, *22*, 1262; b) Treitler, D. S.; Marriott, A. S.; Chadwick, J.; Quirk, E., Mutagenic Impurities in 1-Hydroxybenzotriazole (HOBt). *Org. Process Res. Dev*. **2019**, *23*, *2562*; c) McKnelly, K. J.; Sokol, W.; Nowick, J. S., Anaphylaxis Induced by Peptide Coupling Agents: Lessons Learned from Repeated Exposure to HATU, HBTU, and HCTU. *J. Org. Chem.* **2020**, *85*, 1764.

[9] Benoiton, N. L.; Chen, F. M., Not the alkoxycarbonylamino-acid O-acylisourea. *J. Chem. Soc., Chem. Commun*., **1981**, 543.

[10] El-Faham, A.; Albericio, F., Synthesis and Application of N-Hydroxylamine Derivatives as Potential Replacements for HOBt. *Eur. J. Org. Chem*. **2009**, *10*, 1499.

[11] Albericio, F.; El-Faham, A., Choosing the Right Coupling Reagent for Peptides: A Twenty-Five-Year Journey. *Org. Process Res. Dev*. **2018**, *22*, 760.

[12] Fattahi, N.; Ayubi, M.; Ramazani, A., Amidation and esterification of carboxylic acids with amines and phenols by N,N'-diisopropylcarbodiimide: A new approach for amide and ester bond formation in water. *Tetrahedron Lett.* **2018**, *74*, 4351.

[13] Jad, J. E.; Khattab, S. N.; de la Torre, B. G.; Govender, T.; Kruger, H. G.; El-Faham, A.; Albericio, F., Oxyma-B, an excellent racemization suppressor for peptide synthesis. *Org. Biomol. Chem.* **2014**, *12*, 8379.

[14] Subirós-Funosas, R.; Prohens, R.; Barbas, R.; El-Faham, A.; Albericio, F., Oxyma: An Efficient Additive for Peptide Synthesis to Replace the Benzotriazole-Based HOBt and HOAt with a Lower Risk of Explosion. *Chem. Eur. J.* **2009**, *15*, 9394.

[15] Wehrstedt, K. D.; Wandrey, P. A.; Heitkamp, D., Explosive properties of 1-hydroxybenzotriazoles. *J. Hazard. Mater.* **2005**, *126*, 1.

[16] McFarland, A. D.; Buser, J. Y.; Embry, M. C.; Held, C. B.; Kolis, S. P., Generation of Hydrogen Cyanide from the Reaction of Oxyma (Ethyl cyano(hydroxyimino) acetate) and DIC (Diisopropylcarbodiimide). *Org. Process Res. Dev.* **2019**, *23*, 2099.

[17] Patel, B. H.; Percivalle, C.; Ritson, D. J.; Duffy, C. D.; Sutherland, J. D., Common origins of RNA, protein and lipid precursors in a cyanosulfidic protometabolism. *Nature Chem.* **2015**, *7*, 301.

[18] Udhayakumari, D., Chromogenic and fluorogenic chemosensors for lethal cyanide ion. A comprehensive review of the year 2016. *Sens. Actuators, B*, **2018**, *259*, 1022.

---

[19] CDC, hydrogen cyanide, in: NIOSH Pocket Guide to Chemical Hazards, retrieved from https://www.cdc.gov/niosh/npg/npgd0333.html, on May 14th 2020.

[20] Albericio, F.; Al Musaimi, O.; de la Torre, B. G., Greening Fmoc/tBu solid-phase peptide synthesis. *Green Chem*. **2020**, *22*, 996.

[21] Rasmussen, J. H.; Pawlas, J.; Ludemann-Hombourger, O.; Rekai, E. D., Aspects of greening peptide chemistry within the pharmaceutical manufacturing industry. *Chem. Today,* **2019**, *37*, 42.

[22] Merrifield, R. B., Solid Phase Peptide Synthesis. I. The Synthesis of a Tetrapeptide. *J. Am. Chem. Soc.,* **1963**, *85*, 2149.

[23] Petrou, C.; Sarigiannis, Y., Peptide synthesis: Methods, trends, and challenges. *Peptide Applications in Biomedicine, Biotechnology and Bioengineering.* S. Koutsopoulos, ed. Woodhead Publishing, Duxford, United Kingdom, 2018, 1.

[24] Ramage, R.; Irving, S. L.; McInnes, C. Design of a versatile linker for solid phase peptide synthesis: Synthesis of C-terminal primary/seconary amides and hydrazides. *Tetrahedron Lett.* **1993**, 34, 6599.

[25] Yan, B., The properties of resin supports and their effects on solid-phase organic synthesis. *Comb. Chem. High Throughput Screen*. **1998**, *1*, 215.

[26] Kaiser, E.; Colescott, R. L.; Bossinger, C. D.; Cook, P. I., Color test for detection of free terminal amino groups in the solid-phase synthesis of peptides. *Anal. Biochem.* **1970**, *34*, 595.

[27] Pawlas, J.; Rasmussen, J. H., *Re*Green SPPS: enabling circular chemistry in environmentally sensible solid-phase peptide synthesis *Green Chem.* **2019**, *21*, 5990.

[28] Byrne, F. P.; Jin, S.; Paggiola, G.; Petchey, T. H. M.; Clark, J. H.; Farmer, T. J.; Hunt, A. J.; McElroy, C. R.; Sherwood, J.; Tools and techniques for solvent selection: green solvent selection guides. *Sustain. Chem. Process*. **2016**, *4*, 1.

[29] Sherwood, J.; Parker, H. L.; Moonen, K.; Farmer, T. J.; Hunt, A. J., N-Butylpyrrolidinone as a dipolar aprotic solvent for organic synthesis. *Green Chem.* **2016**, *18*, 3990.

[30] a) Luciani, L.; Goff, E.; Lanari, D.; Santoro. S.; Vaccaro, L. Waste-minimised copper-catalysed azide–alkyne cycloaddition in Polarclean as a reusable and safe reaction medium. *Green Chem*. **2018**, *20*, 183; b) Cseri, L.; Szekely, G., Towards cleaner PolarClean: efficient synthesis and extended applications of the polar aprotic solvent methyl 5-(dimethylamino)-2-methyl-5-oxopentanoate. *Green Chem*. **2019**, *21*, 4178.

[31] MacMillan, D. S.; Murray, J.; Sneddon, H. F.; Jamieson, C., Watson, A. J. B., Evaluation of alternative solvents in common amide coupling reactions: replacement of dichloromethane and N,N-dimethylformamide. *Green. Chem.* **2013**, *15*, 596.

[32] Pawlas, J., Investigating racemization in HIS couplings in SPPS. *Proceedings of the 34th European Peptide Symposium and the 8th International Peptide Symposium*, A. Beck-Sickinger, K. Mörl, K. Bellmann-Sickert, S. Els-Heindl eds., Leipzig, Germany, 2016, p. 60.

[33] For use of NBP as SPPS solvent see: a) Lopez, J.; Pletscher, S.; Aemissegger, A.; Bucher, C.; Gallou, F., *Org. Process Res. Dev*. N-Butylpyrrolidinone as Alternative Solvent for Solid-Phase Peptide Synthesis. **2018**, *22*, 494; b) de la Torre, B. G.; Kumar, A.; Alhassan, M.; Bucher, C.; Albericio, F.; Lopez, J., Successful development of a method for the incorporation of Fmoc-Arg(Pbf)-OH in solid-phase peptide synthesis using N-butylpyrrolidinone (NBP) as solvent. *Green. Chem.* **2020**, *61*, DOI: 10.1039/C9GC03784E.

[34] For use of NBP/EtOAc as SPPS solvent see: a) Pawlas, J.; Nilsson, M.; Antonic, B.; Svensson, T.; Finnman, J.; Rasmussen, J. H., TamiSolve™ NxG as a suitable solvent for cost-efficient green SPPS. Poster PM1 at TIDES, Boston, MA, U.S.A, May 2018; https://www.polypeptide.com/wp-content/uploads/2019/10/Suitable-Solvent-for-cost-efficient-green-SPPS_TIDES2018-PM1.pdf; b) Pawlas, J.; Antonic, B.; Lundqvist, M.; Svensson, T.; Finnman, J.; Rasmussen, J. H., 2D green SPPS: green solvents for on-resin removal of acid sensitive protecting groups and lactamization. *Green Chem.* **2019**, *21*, 2594.

[35] For a comparison of the cost of DMF, NBP and NBP/EtOAc as SPPS solvents see ref. 34b.

[36] For examples of methods suitable for determining content of HCN in gas phase and in solution see e.g ref. 18 and a) Gotor, R.; Costero, A. M.; Gil, S.; Parra, M.; Martínez-Máñez, R.; Sancenón, F.; Gaviña, P., Selective and sensitive chromogenic detection of cyanide and HCN in solution and in gas phase. *Chem. Commun.* **2013**, *49*, 5669; b) Greenawald, L. A.; Snyder, J. L.; Fryc, N. L.; Sailor, M. J.; Boss, G. R.; Finklea, H. O.; Bell, S., Development of a cobinamide-based end-of-service-life indicatorfor detection of hydrogen cyanide gas. *Sens. Actuators, B*, **2015**, *221*, 379.

[37] a) Rockwood, G. A.; Thompson, D. E.; Petrikovics, I., Dimethyl trisulfide: A novel cyanide countermeasure. *Toxicol. Ind. Health*, **2016**, *32*, 2009; b) Bhadra, S.; Zhang, Z.; Zhou, W., Ochieng, F.; Rockwood, G. A.; Lippner, D.; Logue, B.

A., Analysis of potential cyanide antidote, dimethyl trisulfide, in whole blood by dynamic headspace gas chromatography-mass spectroscopy. *J. Chromatogr. A*, **2019**, *1591*, 71.

Electronic Supplementary Information (ESI)

Minimizing HCN in DIC/Oxyma mediated amide bond forming reactions

Marion Erny,[a,c] Marika Lundqvist,[b] Jon H. Rasmussen,[b] Olivier Ludemann-Hombourger,[a] Frédéric Bihel[c] and Jan Pawlas[b,*]

[a]PolyPeptide Group, 7 rue de Boulogne, 67100 Strasbourg, France

[b]PolyPeptide Group, Limhamnsvägen 108, PO BOX 30089, 20061 Limhamn, Sweden

[c]Laboratoire d'Innovation Thérapeutique, UMR7200, CNRS, Université de Strasbourg, Faculty of Pharmacy, 74 Route du Rhin, 67401 Illkirch-Graffenstaden, France

[*]Corresponding author. E-mail: jan.pawlas@polypeptide.com

Table of Contents

1. General information

All HPLC analyses were carried out on an Agilent 1100 or a Waters Alliance instruments. LC-MS analyses in section 3 of this ESI were performed on a tandem liquid chromatography mass spectrometry system consisting of an Agilent 1290, 1200 bar system with DAD, connected to an Agilent quadrupole time-of-flight (Q-TOF) mass spectrometer (Agilent, Santa Clara, CA, USA). The mass spectrometry system was operated in a positive mode using electron spray ionization (ESI), mass range 20-3200, mass accuracy at 0.02 u, resolution up to 20000 ppm. The following source settings were used: gas temp 300 ˚C, gas flow 8 l/min, nebulizer 30psig, sheath gas temperature 350 ˚C and sheat gas flow 7.5 l/min. Analytical separations were achieved using a Waters Acquity UPLC instrument. LC-MS analyses in sections 4 - 6 of this ESI were performed on a Horizon high performance liquid chromatography system (Thermo, Waltham, Massachusetts, U.S) with variable wavelength detector connected to a Qexactive orbitrap mass spectrometry system (Thermo, Waltham, Massachusetts, U.S). The mass spectrometry system was operated in a positive mode using sheath gas electrospray ionization (ESI), mass range 50-750, mass accuracy 5ppm, resolution up to 140 000 ppm. The following source settings were used: sheath gas flow rate 35, aux gas flow rate 10, sweep gas flow rate 1, spray voltage (kV) 3.50, capillary temp. 250 °C, S-lens RF level 50,0 and Aux gas heater temp. 200 °C. NMR spectra were recorded on a 400 MHz (for section 8.2) and 500 MHz Bruker system. Spectral data were processed using TopSpin software. All the samples were placed in 3 mm tubes from Norell.

2. Details of the assessment of HCN formation during DIC/Oxyma mediated coupling of 2.0 equiv Fmoc-Ser(t-Bu)-OH with H-RMG resin in DMF

Fmoc-RMG AMS resin (0.43 mmol/g) was prepared as previously described.[1] For each Fmoc-Ser(*t*-Bu)-OH coupling experiment the requisite H-RMG AMS resin was prepared as follows: 2.33 g (1.0 mmol) of the Fmoc-RMG AMS resin was swollen in DMF, drained and shaken at rt for 1 h with 20 mL piperidine (pip)/DMF (20% v/v). The resulting H-RMG AMS resin was washed with DMF (6 x 20 mL), isopropanol (*i*-PrOH, 3 x 20 mL) and diethyl ether (2 x 20 mL) and dried to constant weight *in vacuo.* The dried H-RMG AMS resin was swollen in DMF and drained. The amount of residual DMF in the swollen and drained resin was determined to be ~5 mL. Next, in two reactions vessels, 766.9 mg (2.0 mmol, 1.0 equiv) of Fmoc-Ser(*t*-Bu)-OH) and 284.2 mg (2.0 mmol, 1.0 equiv) of Oxyma were dissolved in 20 mL DMF. To the first vessel, 313.2 μL DIC (2.0 mmol, 1.0 equiv) was added and to the second vessel, 939 μL DIC (6.0 mmol, 3.0 equiv) was added. The resulting reaction mixtures were allowed to stir at rt for 1 h and added to the washed and drained batches of H-RMG AMS resin prepared above. The resulting slurries of DIC/Oxyma mediated couplings of Fmoc-Ser(*t*-Bu)-OH with H-RMG AMS resins were shaken at rt (300 rpm) for 20 h. Conversions of these amidation reactions were followed by a qualitative (ninhydrin) color test.[2] During the course of Fmoc-Ser(*t*-Bu)-OH/DIC/Oxyma activations as well as the subsequent amidation reactions of the activated mixtures with H-RMG AMS resin 50 μL reaction aliquots were taken out and quenched with MeCN (1.0 mL). The samples thus obtained were analysed for the content of oxadiazole **3** (section 2.1 of this ESI) based on which the conversions of Oxyma to HCN during these DIC/Oxyma mediated reactions were determined, see section 2.2 of this ESI.

2.1 HPLC analysis of samples of Fmoc-Ser(*t*-Bu)-OH/DIC/Oxyma reaction mixtures containing oxadiazole 3 and determination of Oxyma to HCN conversions in these reactions

Experimental conditions: column: Waters XSelect CSH130 C18 2.5 μm 4.6x150mm; detection wavelength: 220 nm; column temperature: 30°C; injection volume: 2 μL; sampler temperature: 10°C; flow: 0.5 ml/min; mobile phase A: 0.1 % TFA in water, mobile phase B: 0.08 % TFA in 90% MeCN/10 %water. Gradient (Time(min), %B): 0, 0; 40, 100; 54, 100; 55, 0; 62, 0.

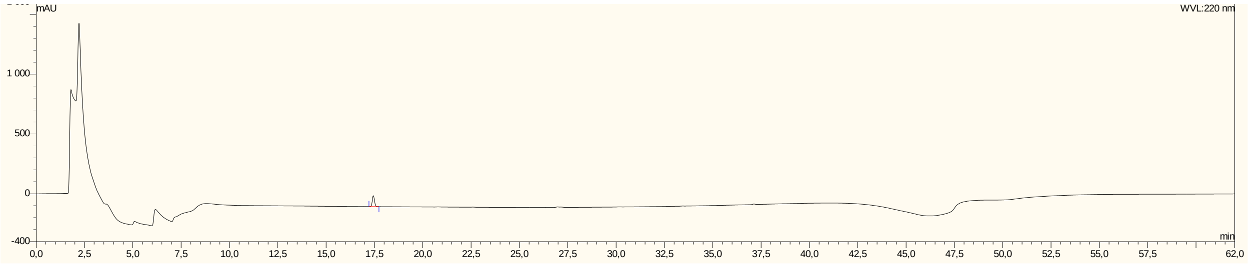

Figure S1. UV chromatogram overview of a 5 mg/mL reference sample of oxadiazole **3** in MeCN, 50 μL of which was diluted with MeCN (1.0 mL).

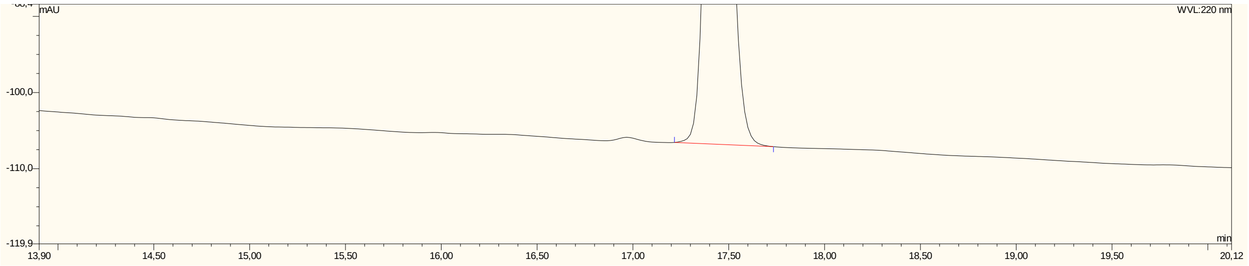

Figure S2. UV chromatogram zoom-in of a 5 mg/mL reference sample of oxadiazole **3** in MeCN, 50 μL of which was diluted with MeCN (1.0 mL).

Table S1. Area (mAu^{x}min) for the integrated peak of a 5 mg/mL reference sample of oxadiazole **3**, 50 μL of which was diluted with 0.5 % TFA/MeCN (1.0 mL).

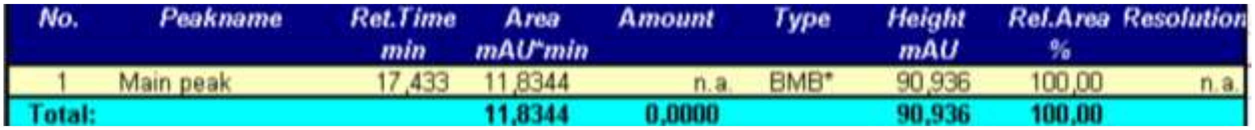

No.	Peakname	Ret.Time min	Area mAU*min	Amount	Type	Height mAU	Rel.Area %	Resolution
1	Main peak	17,433	11,8344	n.a.	BMB*	90,936	100,00	n.a.
Total:			11,8344	0,0000		90,936	100,00	

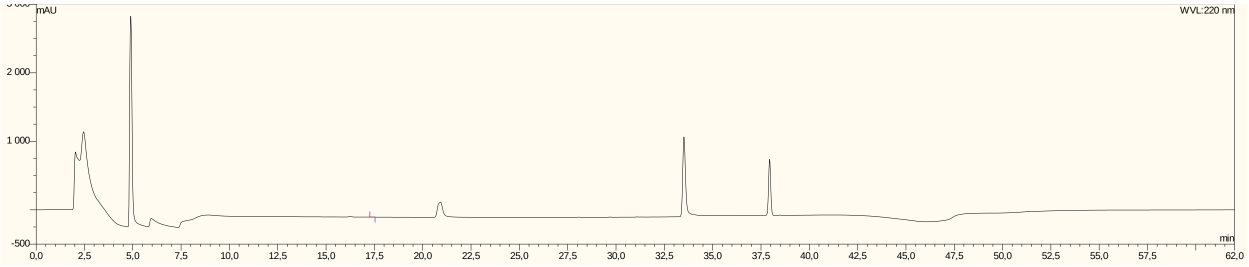

Figure S3. UV chromatogram overview of a reaction mixture of Fmoc-Ser(*t*-Bu)-OH/Oxyma/DIC (1:1:1) after 0.5 h at rt, 50 μL of this mixture was diluted with MeCN (1.0 mL).

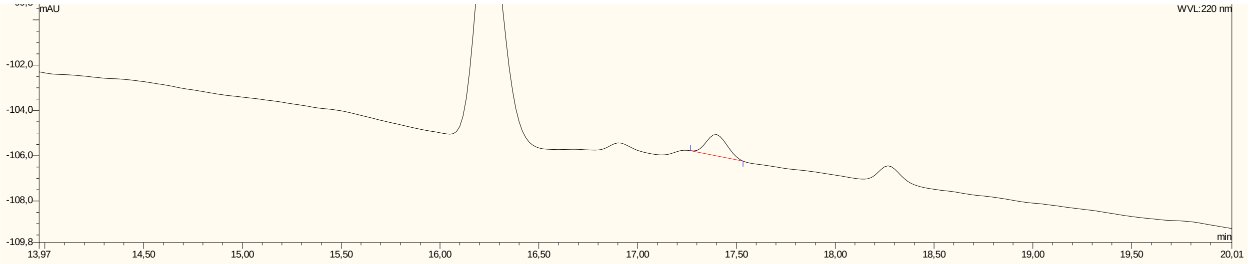

Figure S4. UV chromatogram zoom-in of a reaction mixture of Fmoc-Ser(*t*-Bu)-OH/Oxyma/DIC (1:1:1) after 0.5 h at rt, 50 μL of this mixture was diluted with MeCN (1.0 mL).

Table S2. Area (mAu^{x}min) for the integrated peak of oxadiazole **3** from the reaction mixture of Fmoc-Ser(*t*-Bu)-OH/Oxyma/DIC (1:1:1) after 0.5 h at rt, 50 μL of this mixture was diluted with MeCN (1.0 mL).

No.	Peakname	Ret.Time min	Area mAU*min	Amount	Type	Height mAU	Rel.Area %	Resolution
1	Main peak	17,400	0,1139	n.a.	BMB*	0,941	100,00	n.a.
Total:			0,1139	0,0000		0,941	100,00	

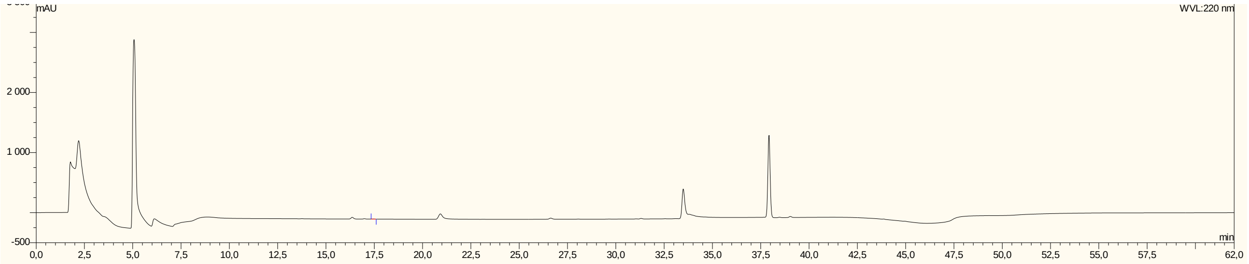

Figure S5. UV chromatogram overview of a reaction mixture of Fmoc-Ser(*t*-Bu)-OH/Oxyma/DIC (1:1:3) after 0.5 h at rt, 50 μL of this mixture was diluted with MeCN (1.0 mL).

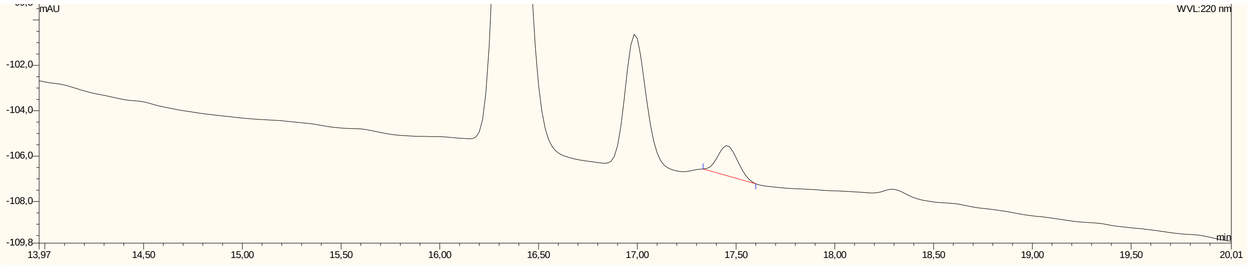

Figure S6. UV chromatogram zoom-in of a reaction mixture of Fmoc-Ser(*t*-Bu)-OH/Oxyma/DIC (1:1:3) after 0.5 h at rt, 50 μL of this mixture was diluted with MeCN (1.0 mL).

Table S3. Area (mAu^{x}min) for the integrated peak of oxadiazole **3** from the reaction mixture of Fmoc-Ser(*t*-Bu)-OH/Oxyma/DIC (1:1:3) after 0.5 h at rt, 50 μL of this mixture was diluted with MeCN (1.0 mL).

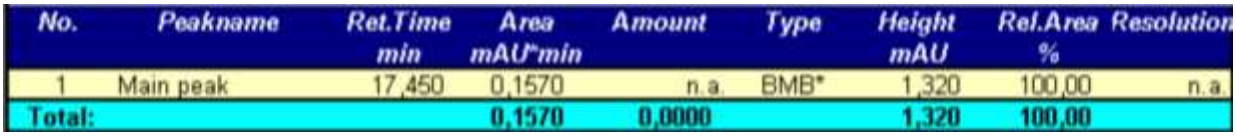

No.	Peakname	Ret.Time min	Area mAU*min	Amount	Type	Height mAU	Rel.Area %	Resolution
1	Main peak	17,450	0,1570	n.a.	BMB*	1,320	100,00	n.a.
Total:			0,1570	0,0000		1,320	100,00	

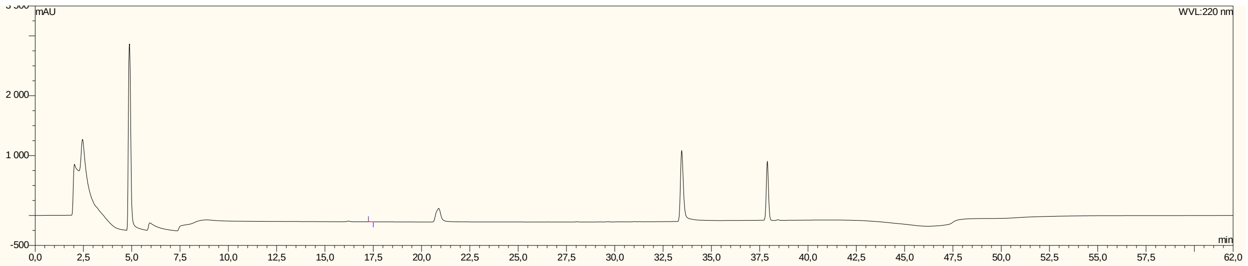

Figure S7. UV chromatogram overview of a reaction mixture of Fmoc-Ser(*t*-Bu)-OH/Oxyma/DIC (1:1:1) after 1.0 h at rt, 50 μL of this mixture was diluted with MeCN (1.0 mL).

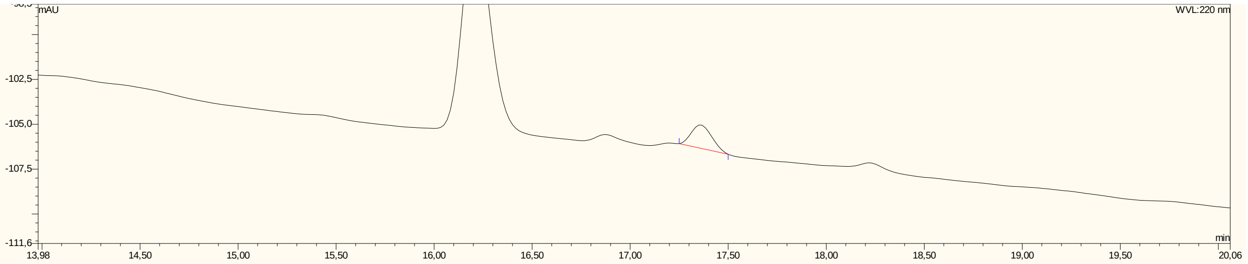

Figure S8. UV chromatogram zoom-in of a reaction mixture of Fmoc-Ser(*t*-Bu)-OH/Oxyma/DIC (1:1:1) after 1.0 h at rt, 50 μL of this mixture was diluted with MeCN (1.0 mL).

Table S4. Area (mAu^{x}min) for the integrated peak of oxadiazole **3** from the reaction mixture of Fmoc-Ser(*t*-Bu)-OH/Oxyma/DIC (1:1:1) after 1.0 h at rt, 50 μL of this mixture was diluted with MeCN (1.0 mL).

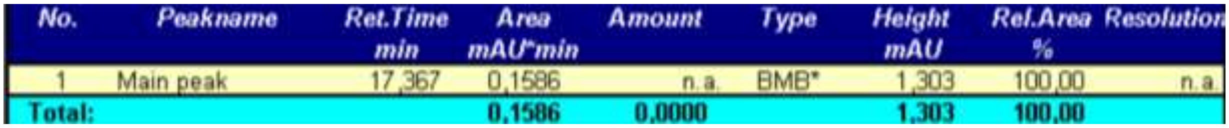

No.	Peakname	Ret.Time min	Area mAU*min	Amount	Type	Height mAU	Rel.Area %	Resolution
1	Main peak	17,367	0,1586	n.a.	BMB*	1,303	100,00	n.a.
Total:			0,1586	0,0000		1,303	100,00	

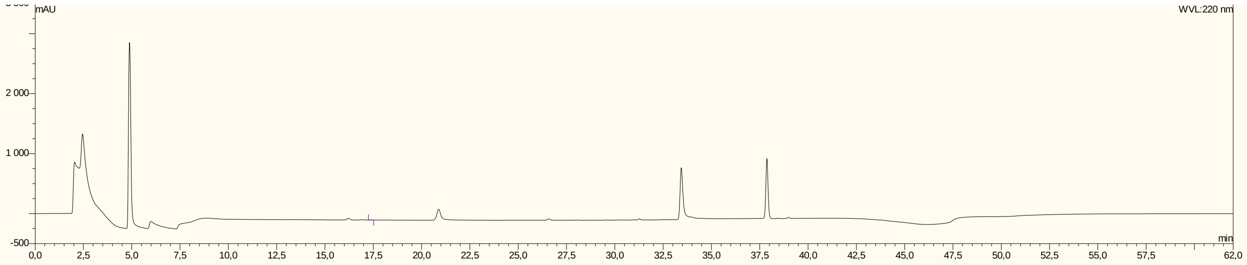

Figure S9. UV chromatogram overview of a reaction mixture of Fmoc-Ser(*t*-Bu)-OH/Oxyma/DIC (1:1:3) after 1.0 h at rt, 50 μL of this mixture was diluted with MeCN (1.0 mL).

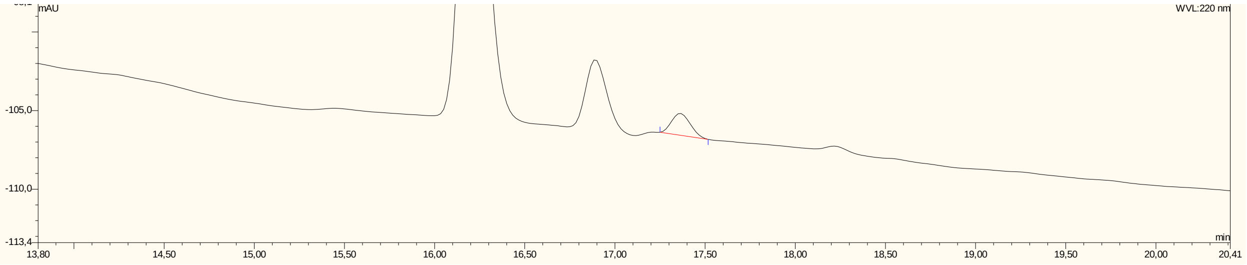

Figure S10. UV chromatogram zoom-in of a reaction mixture of Fmoc-Ser(*t*-Bu)-OH/Oxyma/DIC (1:1:3) after 1.0 h at rt, 50 μL of this mixture was diluted with MeCN (1.0 mL).

Table S5. Area (mAu^{x}min) for the integrated peak of oxadiazole **3** from the reaction mixture of Fmoc-Ser(*t*-Bu)-OH/Oxyma/DIC (1:1:3) after 1.0 h at rt, 50 μL of this mixture was diluted with MeCN (1.0 mL).

No.	Peakname	Ret.Time min	Area mAU*min	Amount	Type	Height mAU	Rel.Area %	Resolution
1	Main peak	17,367	0,1677	n.a.	BMB*	1,389	100,00	n.a.
Total:			0,1677	0,0000		1,389	100,00	

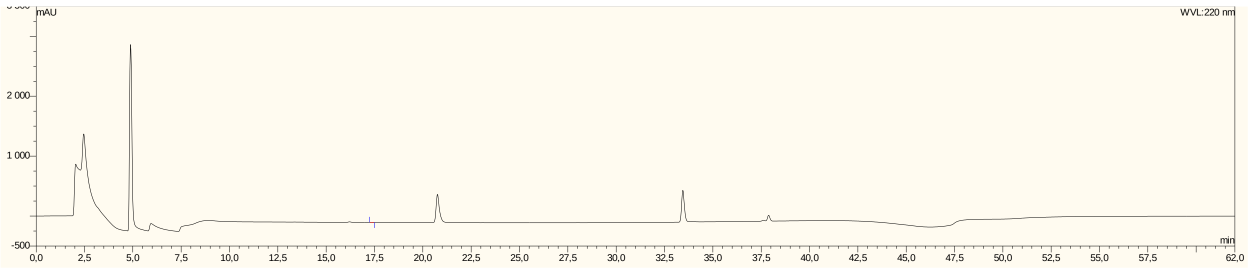

Figure S11. UV chromatogram overview of a reaction mixture supernate of 2 equiv Fmoc-Ser(*t*-Bu)-OH/Oxyma/DIC (1:1:1) with H-RMG AMS resin after 0.5 h at rt, 50 μL of this mixture was diluted with MeCN (1.0 mL).

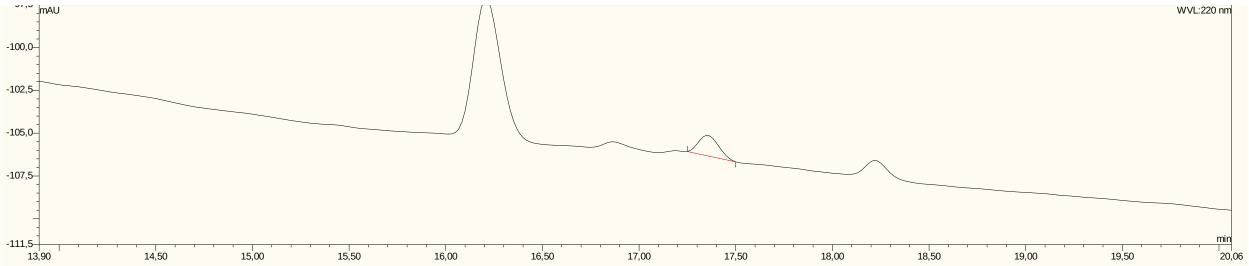

Figure S12. UV chromatogram zoom-in of a reaction mixture supernate of 2 equiv Fmoc-Ser(*t*-Bu)-OH/Oxyma/DIC (1:1:1) with H-RMG AMS resin after 0.5 h at rt, 50 μL of this mixture was diluted with MeCN (1.0 mL).

Table S6. Area (mAu^{x}min) for the integrated peak of oxadiazole **3** from the reaction mixture supernate of 2 equiv Fmoc-Ser(*t*-Bu)-OH/Oxyma/DIC (1:1:1) with H-RMG AMS resin after 0.5 h at rt, 50 μL of of this mixture was diluted with MeCN (1.0 mL).

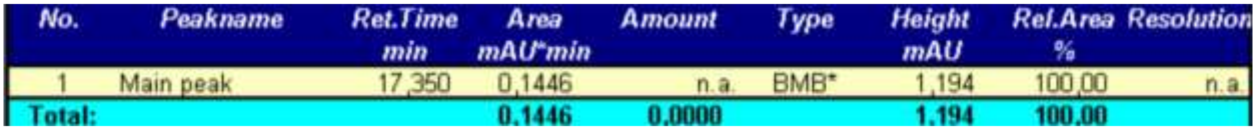

No.	Peakname	Ret.Time min	Area mAU*min	Amount	Type	Height mAU	Rel.Area %	Resolution
1	Main peak	17,350	0,1446	n.a.	BMB*	1,194	100,00	n.a.
Total:			0.1446	0.0000		1.194	100.00	

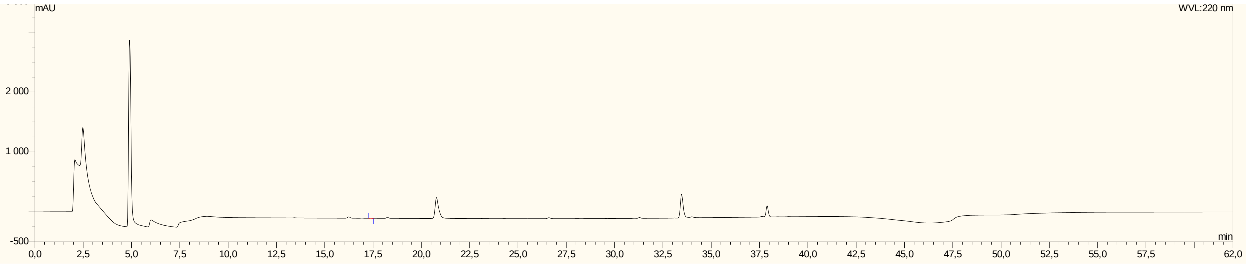

Figure S13. UV chromatogram overview of a reaction mixture supernate of 2 equiv Fmoc-Ser(*t*-Bu)-OH/Oxyma/DIC (1:1:3) with H-RMG AMS resin after 0.5 h at rt, 50 μL of of this mixture was diluted with MeCN (1.0 mL).

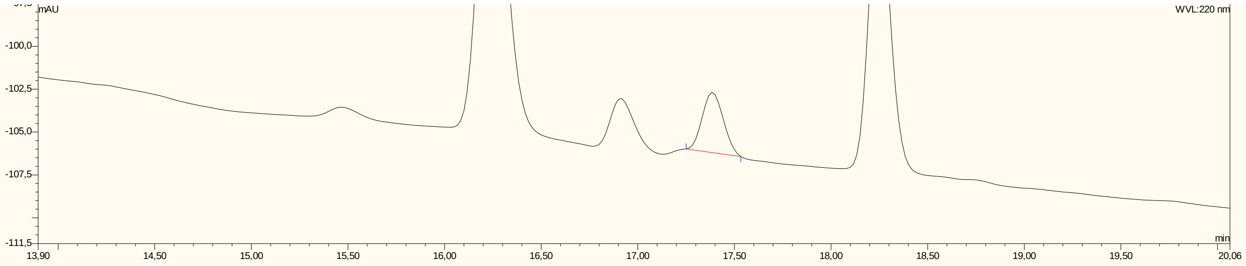

Figure S14. UV chromatogram zoom-in of a reaction mixture supernate of 2 equiv Fmoc-Ser(*t*-Bu)-OH/Oxyma/DIC (1:1:3) with H-RMG AMS resin after 0.5 h at rt, 50 μL of of this mixture was diluted with MeCN (1.0 mL).

Table S7. Area (mAu^{x}min) for the integrated peak of oxadiazole **3** from the reaction mixture supernate of 2 equiv Fmoc-Ser(*t*-Bu)-OH/Oxyma/DIC (1:1:3) with H-RMG AMS resin after 0.5 h at rt, 50 μL of of this mixture was diluted with MeCN (1.0 mL).

No.	Peakname	Ret.Time min	Area mAU*min	Amount	Type	Height mAU	Rel.Area %	Resolution
1	Main peak	17,383	0,4439	n.a.	BMB*	3,520	100,00	n.a.
Total:			**0,4439**	**0,0000**		**3,520**	**100,00**	

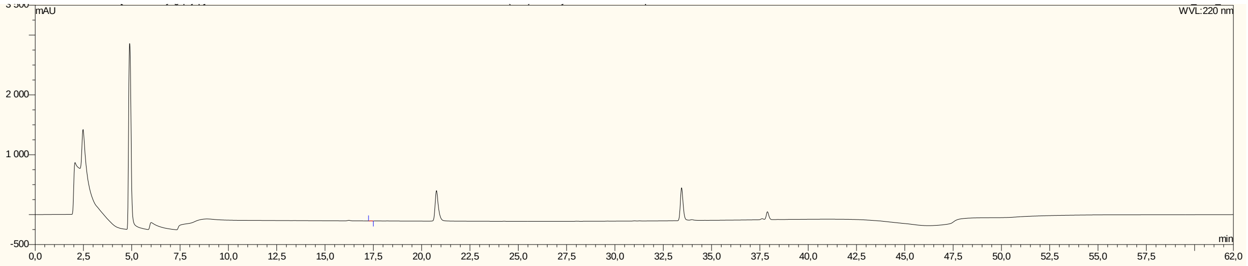

Figure S15. UV chromatogram overview of a reaction mixture supernate of 2 equiv Fmoc-Ser(*t*-Bu)-OH/Oxyma/DIC (1:1:1) with H-RMG AMS resin after 2.5 h at rt, 50 μL of of this mixture was diluted with MeCN (1.0 mL).

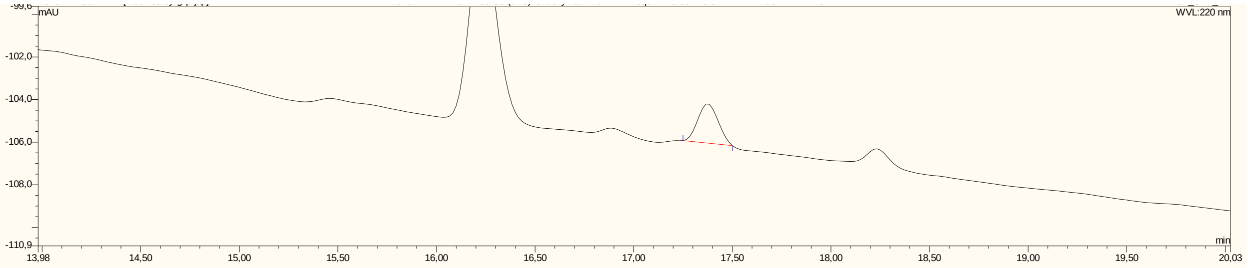

Figure S16. UV chromatogram zoom-in of a reaction mixture supernate of 2 equiv Fmoc-Ser(*t*-Bu)-OH/Oxyma/DIC (1:1:1) with H-RMG AMS resin after 2.5 h at rt, 50 μL of of this mixture was diluted with MeCN (1.0 mL).

Table S8. Area (mAu^{x}min) for the integrated peak of oxadiazole **3** from the reaction mixture supernate of 2 equiv Fmoc-Ser(*t*-Bu)-OH/Oxyma/DIC (1:1:1) with H-RMG AMS resin after 2.5 h at rt, 50 μL of of this mixture was diluted with MeCN (1.0 mL).

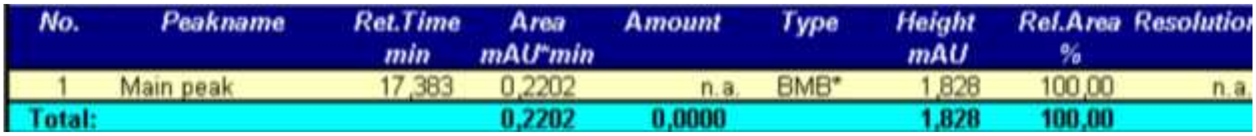

No.	Peakname	Ret.Time min	Area mAU*min	Amount	Type	Height mAU	Rel.Area %	Resolutio
1	Main peak	17,383	0,2202	n.a.	BMB*	1,828	100,00	n.a.
Total:			0,2202	0,0000		1,828	100,00	

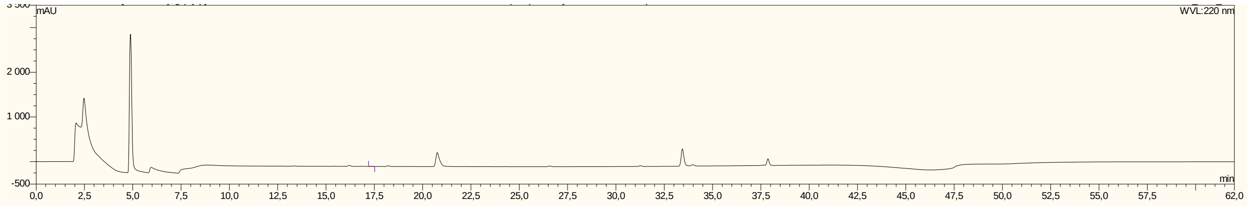

Figure S17. UV chromatogram overview of a reaction mixture supernate of 2 equiv Fmoc-Ser(*t*-Bu)-OH/Oxyma/DIC (1:1:3) with H-RMG AMS resin after 2.5 h at rt, 50 μL of of this mixture was diluted with MeCN (1.0 mL).

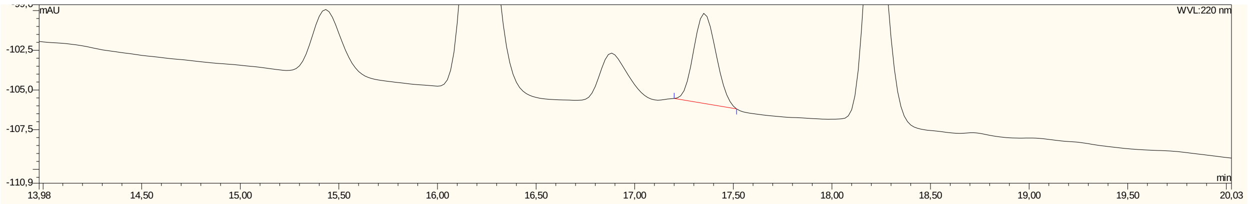

Figure S18. UV chromatogram zoom-in of a reaction mixture supernate of 2 equiv Fmoc-Ser(*t*-Bu)-OH/Oxyma/DIC (1:1:3) with H-RMG AMS resin after 2.5 h at rt, 50 μL of of this mixture was diluted with MeCN (1.0 mL).

Table S9. Area (mAu^{x}min) for the integrated peak of oxadiazole **3** from the reaction mixture supernate of 2 equiv Fmoc-Ser(*t*-Bu)-OH/Oxyma/DIC (1:1:3) with H-RMG AMS resin after 2.5 h at rt, 50 μL of of this mixture was diluted with MeCN (1.0 mL).

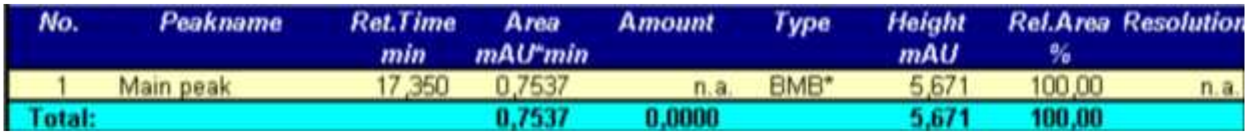

No.	Peakname	Ret.Time min	Area mAU*min	Amount	Type	Height mAU	Rel.Area %	Resolution
1	Main peak	17,350	0,7537	n.a.	BMB*	5,671	100,00	n.a.
Total:			0,7537	0,0000		5,671	100,00	

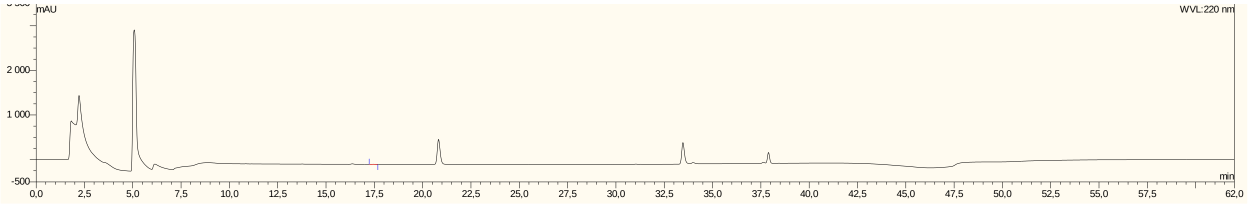

Figure S19. UV chromatogram overview of a reaction mixture supernate of 2 equiv Fmoc-Ser(*t*-Bu)-OH/Oxyma/DIC (1:1:1) with H-RMG AMS resin after 20 h at rt, 50 μL of of this mixture was diluted with MeCN (1.0 mL).

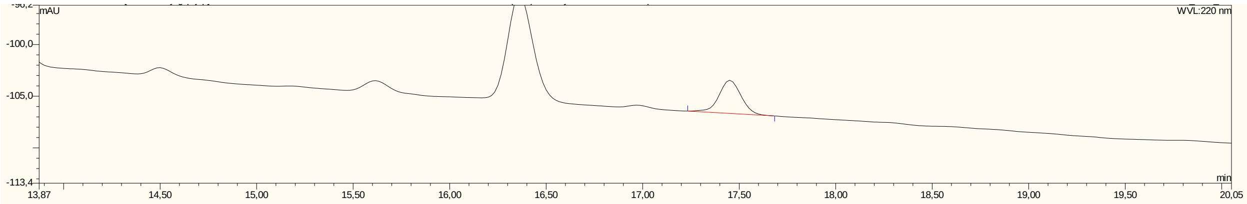

Figure S20. UV chromatogram zoom-in of a reaction mixture supernate of 2 equiv Fmoc-Ser(*t*-Bu)-OH/Oxyma/DIC (1:1:1) with H-RMG AMS resin after 20 h at rt, 50 μL of of this mixture was diluted with MeCN (1.0 mL).

Table S10. Area (mAu^{x}min) for the integrated peak of oxadiazole **3** from the reaction mixture supernate of 2 equiv Fmoc-Ser(*t*-Bu)-OH/Oxyma/DIC (1:1:1) with H-RMG AMS resin after 20 h at rt, 50 μL of of this mixture was diluted with MeCN (1.0 mL).

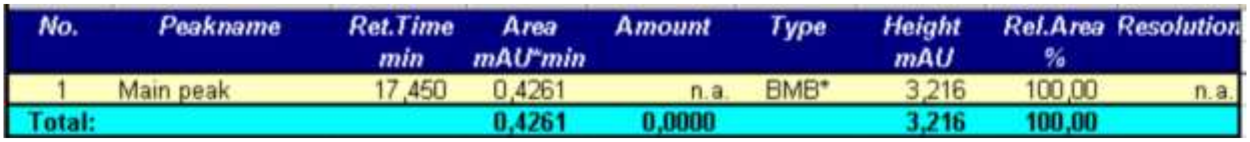

No.	Peakname	Ret.Time min	Area mAU*min	Amount	Type	Height mAU	Rel.Area %	Resolution
1	Main peak	17,450	0,4261	n.a.	BMB*	3,216	100,00	n.a.
Total:			0,4261	0,0000		3,216	100,00	

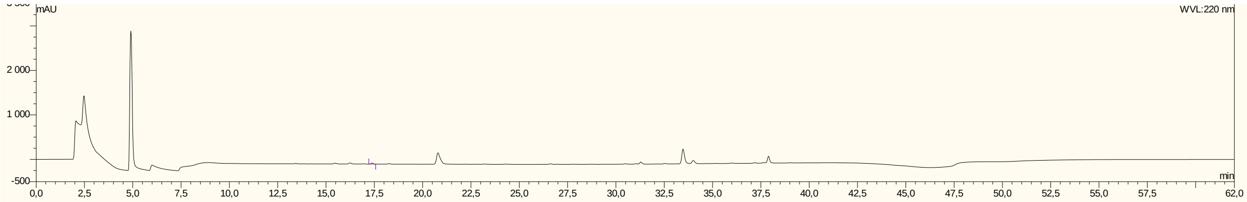

Figure S21. UV chromatogram overview of a reaction mixture supernate of 2 equiv Fmoc-Ser(*t*-Bu)-OH/Oxyma/DIC (1:1:3) with H-RMG AMS resin after 20 h at rt, 50 μL of of this mixture was diluted with MeCN (1.0 mL).

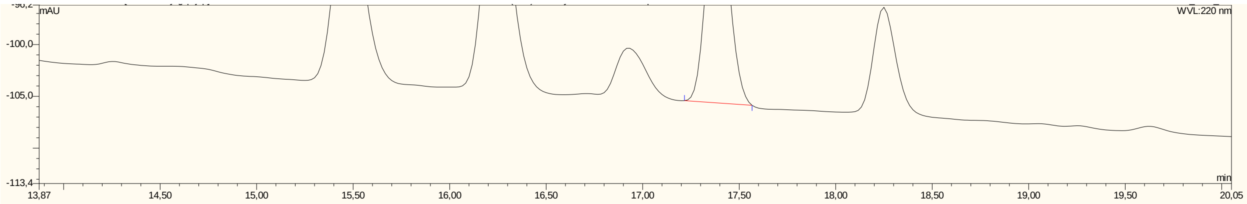

Figure S22. UV chromatogram zoom-in of a reaction mixture supernate of 2 equiv Fmoc-Ser(*t*-Bu)-OH/Oxyma/DIC (1:1:3) with H-RMG AMS resin after 20 h at rt, 50 μL of of this mixture was diluted with MeCN (1.0 mL).

Table S11. Area (mAu^{x}min) for the integrated peak of oxadiazole **3** from the reaction mixture supernate of 2 equiv Fmoc-Ser(*t*-Bu)-OH/Oxyma/DIC (1:1:3) with H-RMG AMS resin after 20 h at rt, 50 μL of of this mixture was diluted with MeCN (1.0 mL).

No.	Peakname	Ret.Time min	Area mAU*min	Amount	Type	Height mAU	Rel.Area %	Resolution
1	Main peak	17,383	2,9014	n.a.	BMB*	21,621	100,00	n.a.
Total:			**2,9014**	**0,0000**		**21,621**	**100,00**	

2.2 Determination of Oxyma to HCN conversions and total amounts of HCN formed per mol of an amidation reaction based on HPLC analyses of samples of Fmoc-Ser(*t*-Bu)-OH/DIC/Oxyma reaction mixtures containing oxadiazole 3.

The marker of HCN formation oxadiazole **3** was prepared as previously described.[3]

Oxyma→HCN conversions and amounts of HCN formed mol^{-1} of the coupling reaction were determined as follows:

1) Integrated areas of oxadiazole **3** (mAu^{x}min) present in the samples of run A (Fmoc-Ser(*t*-Bu-OH/Oxyma/DIC (1:1:1) and run B (Fmoc-Ser(*t*-Bu-OH/Oxyma/DIC (1:1:3) were determined by HPLC analyses (see section 2.1 of this ESI) and are summarized in Table S12.

2) Based on the determined areas of oxadiazole **3** in all samples of Fmoc-Ser(*t*-Bu-OH/Oxyma/DIC concentrations of **3** (gL^{-1}) in all samples of Fmoc-Ser(*t*-Bu-OH/Oxyma/DIC were determined (Table S12).

3) Based on i) the known volumes of Fmoc-Ser(*t*-Bu-OH/Oxyma/DIC reaction mixtures (20 mL) and Fmoc-Ser(*t*-Bu-OH/Oxyma/DIC+H-RMG AMS resin slurries (25 mL), ii) the determined concentrations of **3** and iii) assuming that **3** and HCN are formed in 1:1 ration(see Fig. 1) the total amounts of HCN formed (μmol) thoroughout the course of Run A and Run B experiments were determined (Table S12).

4) Based on the amounts of HCN formed and known amounts of Oxyma employed in Run A and Run B experiments (2 mmol), the Oxyma→HCN conversions were determined (Table S12).

5) Based on the amounts of HCN formed and known scale of Run A and Run B experiments (1 mmol), the amounts of HCN formed mol^{-1} of the coupling reaction were determined in mmol and mg HCN, respectively (Table S12).

Table S12. A summary of i) areas (mAu^{x}min) for the integrated peak of oxadiazole **3** throughout run A (Fmoc-Ser(*t*-Bu)-OH/Oxyma/DIC (1:1:1)) and run B (Fmoc-Ser(*t*-Bu)-OH/Oxyma/DIC (1:1:3) experiments; ii) concentrations of **3** throughout run A and Run B experiments; iii) Oxyma→HCN conversions throughout run A and Run B experiments; iv) amounts of HCN formed (mmol) mol^{-1} of the coupling experiment; v) amounts of HCN formed (mg) mol^{-1} of the coupling experiment.

Reaction time (h)	Run A: (mAuxmin) **3**	Run B: (mAuxmin) **3**	Run A: gL^{-1} **3**	Run B: gL^{-1} **3**	Run A: µmol **3**	Run B: µmol **3**	**Run A: %Oxyma->3**	**Run B: %Oxyma->3**	Run A: mmol HCN mol^{-1} AA coupling	Run B: mmol HCN mol^{-1} AA coupling	**Run A: mg HCN mol^{-1} AA coupling**	**Run B: mg HCN mol^{-1} AA coupling**
0,0 (preactivation)	0,00	0,00	0,00	0,00	0,00	0,00	**0,00**	**0,00**	0,00	0,00	**0,00**	**0,00**
0,5 (preactivation)	0,12	0,16	0,05	0,07	4,21	5,62	**0,21**	**0,28**	2,11	2,81	**56,96**	**75,95**
1,0 (preactivation)	0,16	0,17	0,07	0,07	5,62	5,97	**0,28**	**0,30**	2,81	2,99	**75,95**	**80,69**
0,5 (coupling)	0,18	0,55	0,08	0,23	7,90	24,15	**0,40**	**1,21**	3,95	12,07	**106,80**	**326,34**
2,5 (coupling)	0,28	0,94	0,12	0,40	12,29	41,27	**0,61**	**2,06**	6,15	20,63	**166,14**	**557,74**
20 (coupling)	0,54	3,62	0,23	1,53	23,71	158,93	**1,19**	**7,95**	11,85	79,46	**320,40**	**2147,90**

3. Details of the assessment of formation of linear and cyclic DIC/Oxyma adducts in the reaction of DIC with Oxyma with and without 10 mol% DITU in different solvents

The general protocol for the preparation of the requisite DIC/Oxyma solutions was as follows: 911 mg (6.4 mmol, 1.0 equiv) Oxyma was dissolved in a 10 x 10.0 mL of a given solvent (see below) at rt. To runs AT – ET (see below) 103 mg (0.64 mmol, 0.1 equiv) DITU was added and to all resulting solutions of runs A – E and AT – ET 1.0 mL DIC (7.8 mL, 1.2 equiv) was added. The resulting reaction mixtures were allowed to stand at rt for 17 days throughout which time 50 μL reaction aliquots were taken out, diluted with MeCN (1.0 mL) and analyzed by HPLC and LC-HRMS.

The ten experiments which were carried out:

1) Run A, DMF as solvent
2) Run B, NBP as solvent
3) Run C, NBP/EtOAc (1:1) as solvent
4) Run D, PC as solvent
5) Run E, PC/EtOAc (1:1) as solvent
6) Run AT, DMF as solvent, 10 mol% DITU
7) Run BT, NBP as solvent, 10 mol% DITU
8) Run CT, NBP/EtOAc (1:1) as solvent, 10 mol% DITU
9) Run DT, PC as solvent, 10 mol% DITU
10) Run ET, PC/EtOAc (1:1) as solvent, 10 mol% DITU

3.1 HPLC analysis of DIC/Oxyma solutions in different solvents with and without 10 mol% DITU

Experimental conditions as in section 2.1 of this ESI.

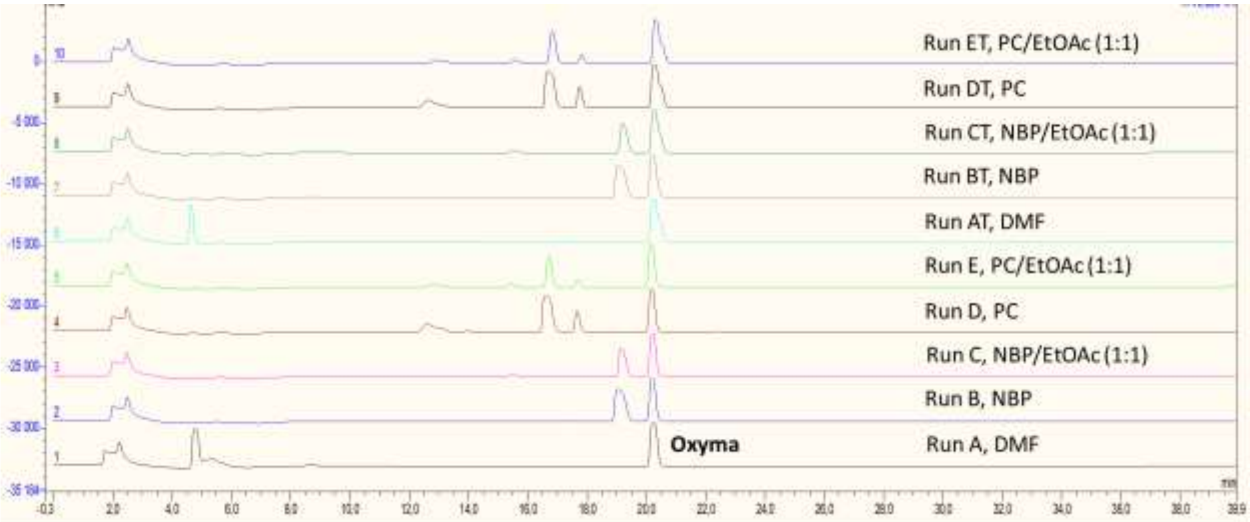

Figure S23. HPLC of Oxyma in five different solvents with and without 10 mol% DITU (t_0).

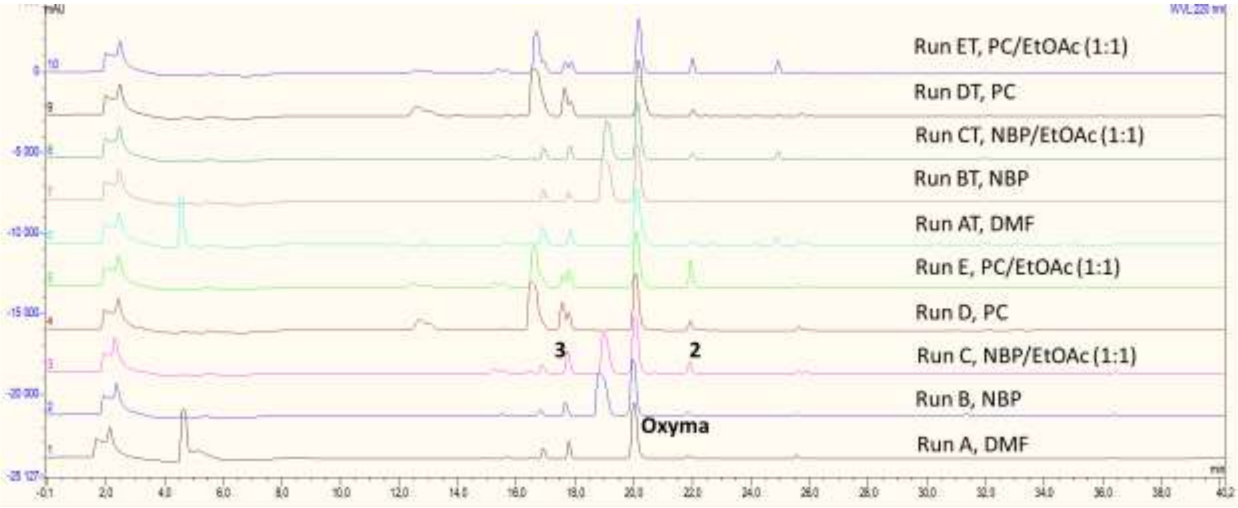

Figure S24. HPLC of Oxyma/DIC (1.0:1.2) mixtures with and without 10 mol% DITU in five different solvents after 5 hours at rt. Both linear (**2**) and cyclic (**3**) DIC/Oxyma adducts can be seen in all reaction mixtures in varying amounts. The presence of radical scavenger DITU in runs AT – ET did not prevent the formation of **2** and **3**.

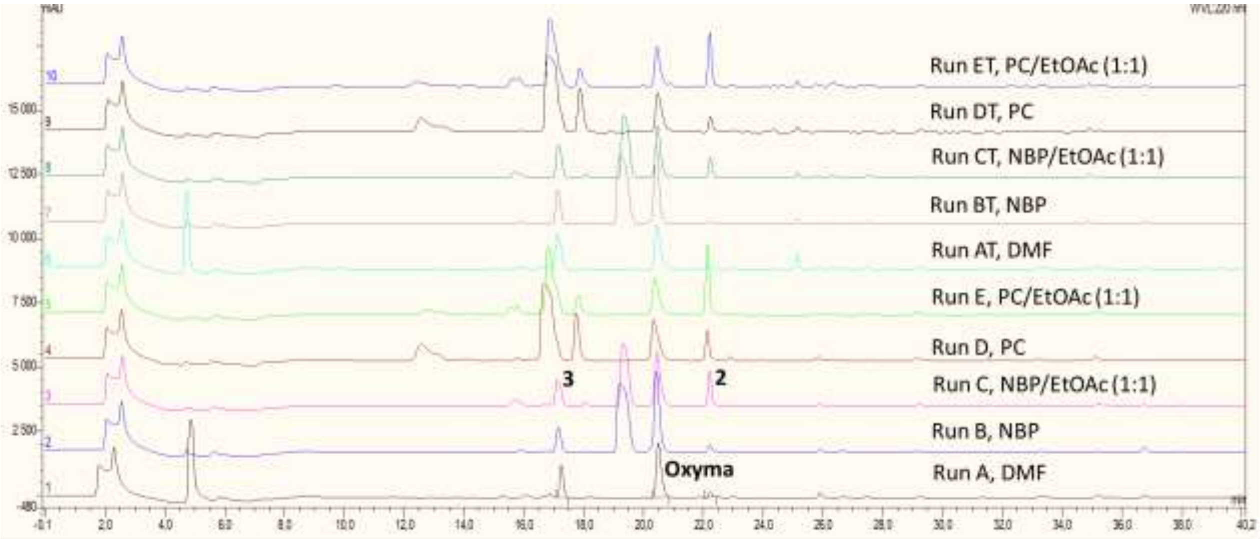

Figure S25. HPLC of Oxyma/DIC (1.0:1.2) mixtures with and without 10 mol% DITU in five different solvents after 4 days at rt. Both linear (**2**) and cyclic (**3**) DIC/Oxyma adducts can be seen in all reaction mixtures, in runs C – E and CT – ET the amount of the linear adduct **2** was significantly increased compared to A – B and AT – BT. The structures of **2** and **3** at this stage were confirmed by LC-HRMS, see section 3.2 of this ESI.

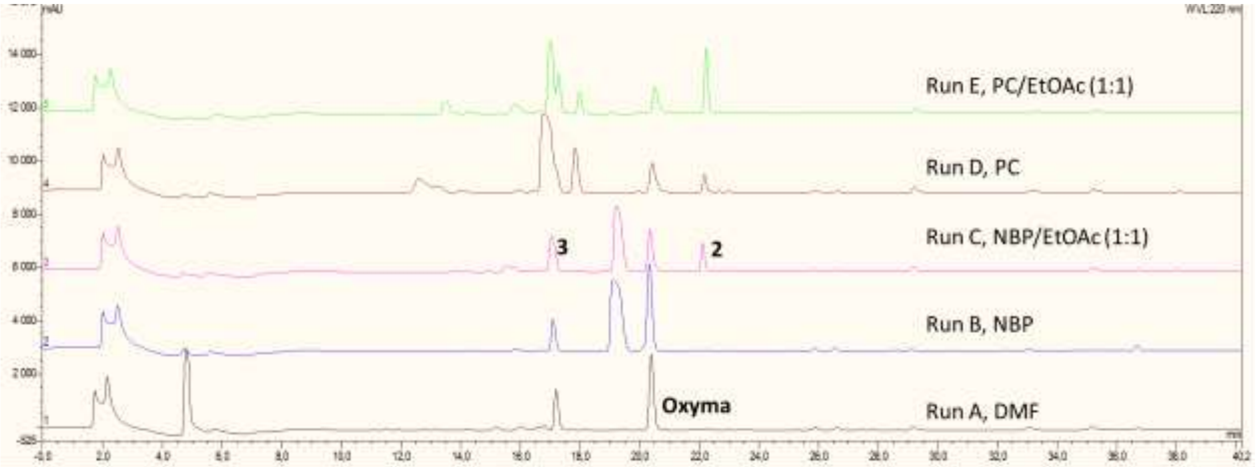

Figure S26. HPLC of Oxyma/DIC (1.0:1.2) mixtures in five different solvents after 17 days at rt. The linear DIC/Oxyma adduct **2** was still present to an appreciable extent in runs C – E while in runs A – B it was absent.

3.2 LC-HRMS analysis of DIC/Oxyma solutions in different solvents

Experimental conditions: column: Waters peptide CSH C18, 2.1x150mm, 1.7um, 130Å; column temperature: 30°C; injection volume: 1 µL; sampler temperature: 10°C; MS mode: positive 50-3200; DAD: 220 nm; data rate: 5Hz; detector cell: standard cell 1uL; flow: 0.2 ml/min; jet weaver: V380 mixer; mobile phase A: 0.1 % TFA in 90% water/MeCN, mobile phase B: 0.10 % TFA in 10% water/MeCN. Gradient (Time(min), %B): 0, 1; 1, 1; 30, 95; 32, 95; 32.1, 1; 42, 1. EIC (extracted ion chromatography)-MS analyses were carried out using a previously described methodology[4] in a following manner: upon performing the pertinent LC-HRMS selected extracted ion chromatograms (EICs) were obtained by inspecting the original chromatograms at appropriate m/z values, resulting in the EICs pertaining to the specific compounds investigated. To eliminate the risk that some of the peaks detected by EIC-MS were either other peptides and/or artefacts all peak assignments were a result of a two-step process:

1) an EIC-MS analysis was carried out searching for the most abundant mass of a given compound (z=+1) with the mass window of ±1 Da;

2) the mass spectra for the EIC-MS peaks thus obtained were inspected manually one by one and only the peaks for which the mass spectra were in full agreement with the expected mass spectrum of a given compound were included as the actual compounds. The peaks that were identified as hits in the initial screening round but subsequently did not fit with the expected mass spectrum were disregarded.

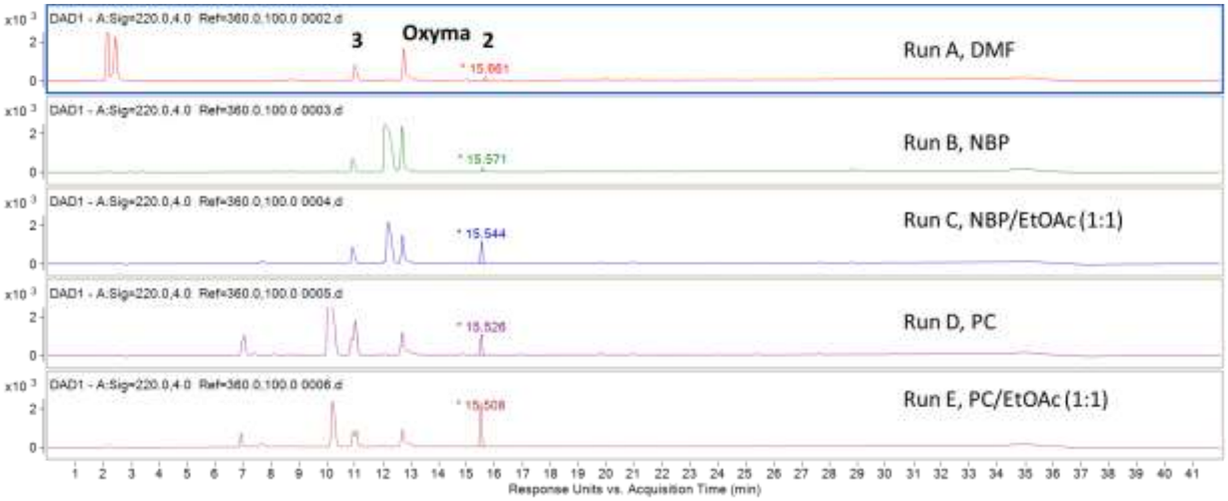

Figure S27. LC-HRMS (UV chromatogram overview) of Oxyma/DIC (1.0:1.2) mixtures in five different solvents after 4 days at rt.

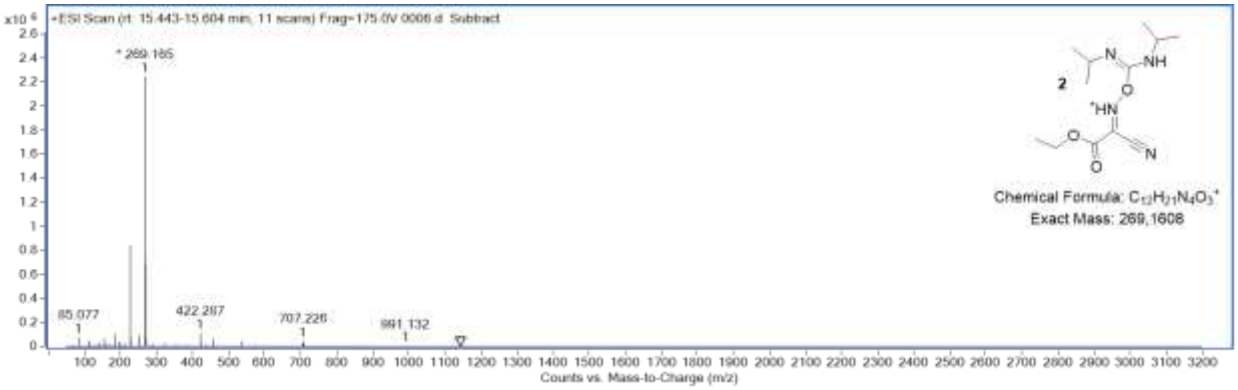

Figure S28. MS spectrum [M+H] of linear DIC/Oxyma adduct **2** detected in Oxyma/DIC (1.0:1.2) mixture in DMF after 4 days at rt.

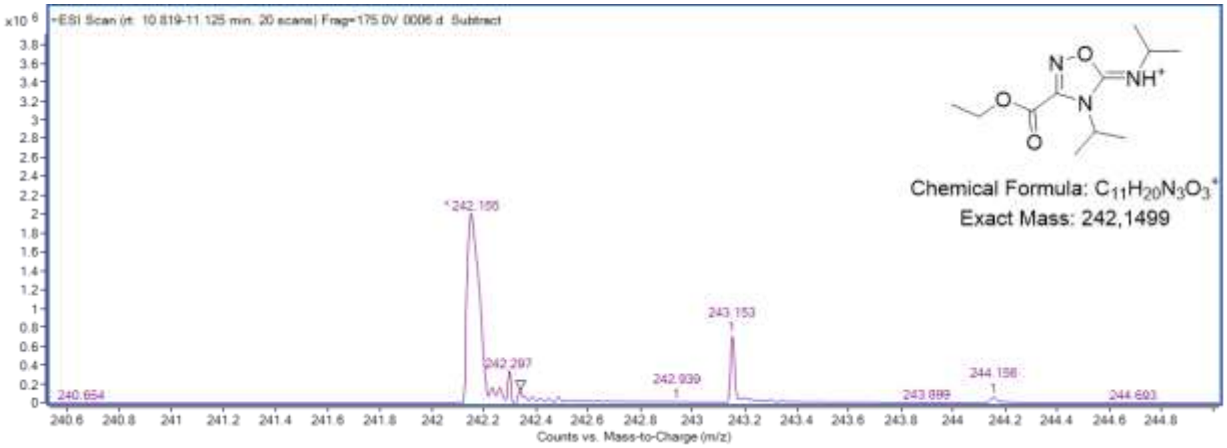

Figure S29. MS spectrum [M+H] of oxadiazole **3** detected in Oxyma/DIC (1.0:1.2) mixture in DMF after 4 days at rt.

Table S13. EIC-MS analysis of contents of linear DIC/Oxyma adduct **2** and oxadiazole **3** in Oxyma/DIC (1.0:1.2) mixtures in five different solvents after 4 days at rt (see Figure 2 for the corresponding chart).

Solvent	Quantification channel EIC	
	269.2 (**2**)	242.1 (**3**)
	Area (counts*min)	
DMF	14023022	71039476
NBP	13603308	66322408
NBP/EtOAc (1:1)	26735545	72034529
PC	25642669	69060166
PC/EtOAc (1:1)	34460762	57347695

4. Assessment of HCN formation during DIC/Oxyma mediated coupling of 2.0 equiv Fmoc-Ser(*t*-Bu)-OH with H-RMG resin in different solvents

8 x 1 mmol of dry H-RMG AMS resin was prepared as described in section 2 of this ESI. The dried H-RMG AMS resins were swollen in solvents as specified for each reaction and drained. The amounts of residual solvent in the swollen and drained resins were determined to be ~5 mL. Next, in eight reactions vessels, 8 x 766.9 mg (2.0 mmol, 1.0 equiv) of Fmoc-Ser(*t*-Bu)-OH and 284.2 mg (2.0 mmol, 1.0 equiv) of Oxyma were dissolved in 20 mL of solvents as specified for each reaction. Next, the resulting Fmoc-Ser(*t*-Bu)-OH/Oxyma mixtures were added to the washed and drained batches of H-RMG AMS resins prepared above. To the resulting slurries of Fmoc-Ser(*t*-Bu)-OH/Oxyma with H-RMG AMS resins DIC was added in the following manner:

experiment R1, DMF, 313.2 μL DIC (2.0 mmol, 1.0 equiv)
experiment R2, DMF, 939 μL DIC (6.0 mmol, 3.0 equiv)
experiment R3, NBP, 313.2 μL DIC (2.0 mmol, 1.0 equiv)
experiment R4, NBP, 939 μL DIC (6.0 mmol, 3.0 equiv)
experiment R5, NBP/EtOAc (1:1), 313.2 μL DIC (2.0 mmol, 1.0 equiv)
experiment R6, NBP/EtOAc (1:1), 939 μL DIC (6.0 mmol, 3.0 equiv)
experiment R7, NBP/EtOAc (1:4), 313.2 μL DIC (2.0 mmol, 1.0 equiv)
experiment R8, NBP/EtOAc (1:4), 939 μL DIC (6.0 mmol, 3.0 equiv)

and the resulting reaction mixtures were shaken at rt (300 rpm) for 20 h. Conversions of the amidation reactions were followed by a qualitative (ninhydrin) color test.[2] Upon completion of all eight reactions (20 h), 50 μL reaction aliquots were taken out and quenched with 0.5 % TFA/MeCN (1.0 mL). The samples thus obtained were analysed by HPLC for the content of oxadiazole **3** using the method described in section 2 of this ESI. As some of the solvents used in these experiments coeluted with **3** during the HPLC analyses using the experimental conditions reported in section 2 of this ESI, an EIC MS for the detection of **3** was employed instead (see section 4.1 of this ESI) based on which Oxyma to HCN conversions during these DIC/Oxyma mediated reactions were determined.

4.1 LC-HRMS analysis of Oxyma to HCN conversions during Fmoc-Ser(*t*-Bu)-OH + H-RMG AMS resin amidation reactions

Experimental conditions: column: Waters peptide CSH C18, 2.1x150mm, 1.7um, 130Å; column temperature: 30°C; injection volume: 0.4 µL; sampler temperature: 10°C; MS mode: Full scan; DAD: 220 nm; data rate: 5Hz; detector cell: standard cell 11µL; flow: 0.1 ml/min; jet weaver: V200 mixer; mobile phase A: 0.1 % TFA in water, mobile phase B: 0.10 % TFA in MeCN. Gradient (Time(min), %B): 0, 15; 40, 25; 48, 95; 54, 95; 55, 15; 62, 15. EIC (extracted ion chromatography) - MS analyses were carried out as previously described.[4] A methodology for determining %Oxyma→HCN conversions based on determining concentration of **3** was used, see section 2 of this ESI.

Table S14. A summary of integrated EIC areas, concentrations of **3** (gL^{-1}), amounts of **3** formed and %Oxyma→HCN conversions after reaction time 20 h for experiments R1 – R8.

Solvent	Fmoc-Ser(t-Bu)-OH/Oxyma/DIC (1:1:**X**)	Rt (min), quantification channel EIC 242,15	Area (counts*min) quantification channel EIC	gL^{-1} **3**	µmol **3**	%Oxyma->HCN
DMF	1:1:**1**	16,936	3217592	0,14278	14,7933	0,7397
DMF	1:1:**3**	16,926	38447402	1,70608	176,7669	8,8383
NBP	1:1:**1**	16,868	1969508	0,08740	9,0551	0,4528
NBP	1:1:**3**	16,868	27756109	1,23166	127,6123	6,3806
NBP/EtOAc (1:1)	1:1:**1**	16,902	878422	0,03898	4,0387	0,2019
NBP/EtOAc (1:1)	1:1:**3**	16,872	49872540	2,21307	229,2955	11,4648
NBP/EtOAc (1:4)	1:1:**1**	16,901	370573	0,01644	1,7038	0,0852
NBP/EtOAc (1:4)	1:1:**3**	16,849	98067042	4,35167	450,8759	22,5438

Table S15. A summary of %Oxyma→HCN conversions after reaction time 20 h for experiments R1 – R8.

Fmoc-Ser(t-Bu)-OH/Oxyma/DIC (1:1:**X**)	Solvent			
	DMF	NBP	NBP/EtOAc (1:1)	NBP/EtOAc (1:4)
	Oxyma→HCN conversion (%)			
1:1:**1**	0,7397	0,4528	0,2019	0,0852
1:1:**3**	8,8383	6,3806	11,4648	22,5438

5. Assessment of HCN formation and amide bond formation kinetics during DIC/Oxyma mediated coupling of 1.3 equiv Fmoc-Ser(*t*-Bu)-OH with H-RMG resin in different solvents

Conversions of the amidation reactions were followed by determining the Fmoc content of the Fmoc-Ser(*t*-Bu)-RMG AMS resins as follows: resin aliquots (ca 50 – 100 mg) were taken out at specified times, washed thoroughly by DMF, *i*-PrOH and Et_2O and dried to constant weight in vacuo before determining the amidation conversions as described in section 5.1 of this ESI. At specified times throughout the amidation reactions, 20 μL reaction aliquots were taken out and quenched with 0.5 % TFA/MeCN (1.0 mL). The samples thus obtained were analysed by LC-HRMS for the content of oxadiazole **3** using the method described in section 4 of this ESI. EIC MS analyses for the detection of **3** were used (see section 5.2 of this ESI) based on which Oxyma to HCN conversions were determined.

5.1 HPLC analysis of conversion during Fmoc-Ser(*t*-Bu)-OH + H-RMG AMS resin amidation reactions

Using the samples of Fmoc-Ser(*t*-Bu)-RMG AMS resins isolated as described in the section 5 of this ESI. The Fmoc content determinations were carried out using a previously reported protocol[1] based on a literature method which utilizes the quantification of dibenzofulvene (DBF) liberated from the Fmoc containing resins by the action of the strong base 1,8-diazabicyclo[5.4. 0]undec-7-ene (DBU).[5] As a reference standard (100% conversion) we used a sample of a Fmoc-Ser(*t*-Bu)-RMG AMS resin for which full amidation conversion was attained. Following experimental conditions were used for all DBF quantifications: column: Phenomenex Kinetex C18 100Å 2.6µm 4.6x50mm; detection wavelength: 220 nm; column temperature: 45°C; injection volume: 1.0 µL; sampler temperature: 10°C; flow: 1.0 ml/min; mobile phase A: 0.1 % TFA in water, mobile phase B: 0.08 % TFA in 90% MeCN/10 %water. Gradient (Time(min), %B): 0, 1; 10, 100; 13, 100; 14, 100; 19, 1; 20, 1.

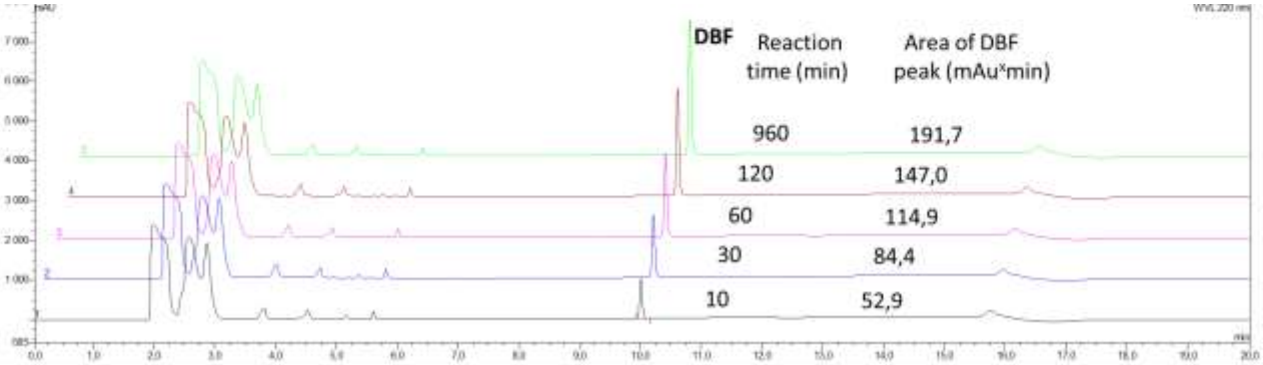

Figure S30. Integrated areas (mAu^{x}min) of DBF peak from determinations of conversions of Fmoc-Ser(*t*-Bu)-OH/Oxyma/DIC/H-RMG-AMS resin amidation reactions in DMF.

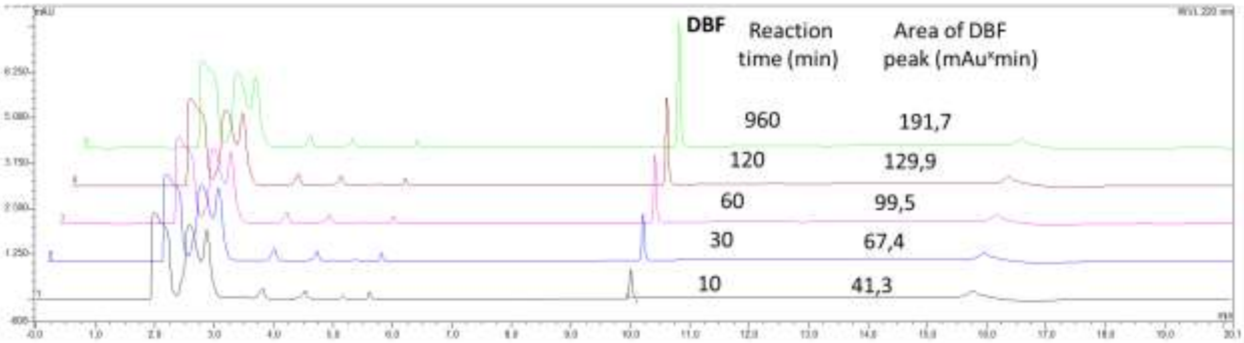

Figure S31. Integrated areas (mAu^{x}min) of DBF peak from determinations of conversions of Fmoc-Ser(*t*-Bu)-OH/Oxyma/DIC/H-RMG-AMS resin amidation reactions in NBP.

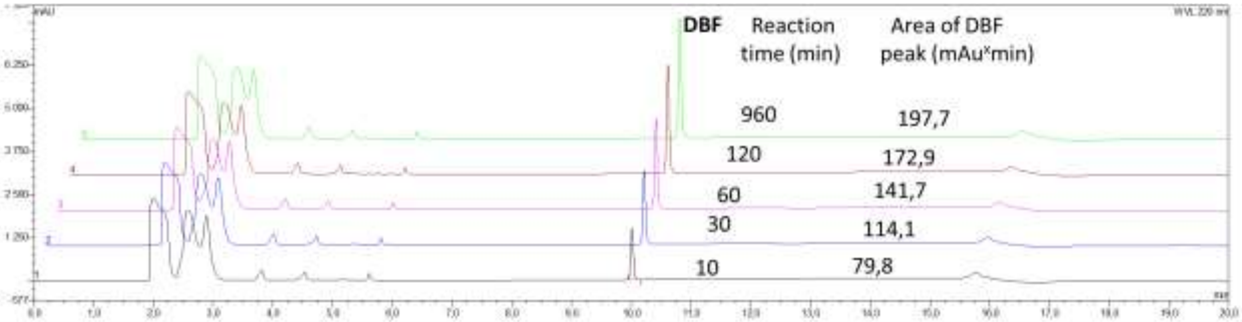

Figure S32. Integrated areas (mAu^{x}min) of DBF peak from determinations of conversions of Fmoc-Ser(*t*-Bu)-OH/Oxyma/DIC/H-RMG-AMS resin amidation reactions in NBP/EtOAc (1:1).

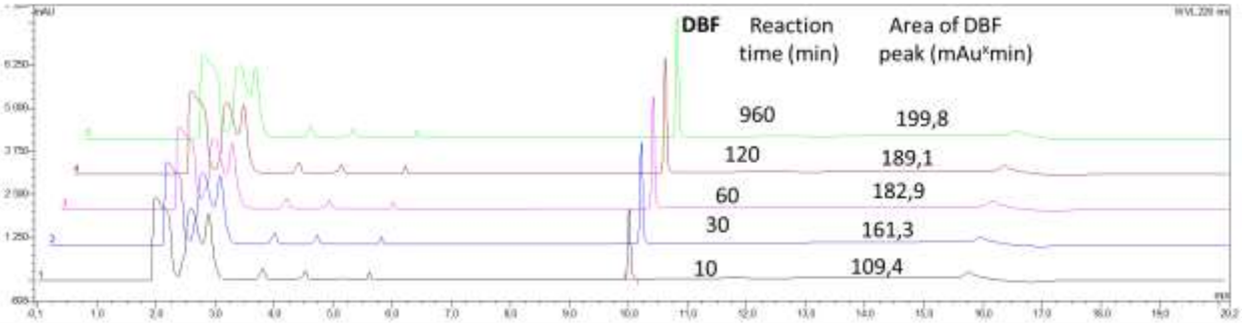

Figure S33. Integrated areas (mAu^{x}min) of DBF peak from determinations of conversions of Fmoc-Ser(*t*-Bu)-OH/Oxyma/DIC/H-RMG-AMS resin amidation reactions in NBP/EtOAc (1:4).

Table S16. A summary of integrated areas (mAu^{x}min) of DBF peak from determinations of conversions of Fmoc-Ser(*t*-Bu)-OH/Oxyma/DIC/H-RMG-AMS resin amidation reactions in DMF, NBP, NBP/EtOAc (1:1) and NBP/EtOAc (1:4).

Reaction time (min)	Solvent			
	DMF	NBP	NBP/EtOAc (1:1)	NBP/EtOAc (1:4)
	Integrated areas (mAu^{x}min) of DBF peak			
0	0,0	0,0	0,0	0,0
10	52,9	41,3	79,8	109,4
30	84,4	67,4	114,1	161,3
60	114,9	99,5	141,7	182,9
120	147,0	129,9	172,9	189,1
960	191,7	191,7	197,7	199,8

Table S17. A summary of conversions during Fmoc-Ser(*t*-Bu)-OH/Oxyma/DIC/H-RMG-AMS resin amidation reactions in DMF, NBP, NBP/EtOAc (1:1) and NBP/EtOAc (1:4).

Reaction time (min)	Solvent			
	DMF	NBP	NBP/EtOAc (1:1)	NBP/EtOAc (1:4)
	Amidation conversion (%)			
0	0,0	0,0	0,0	0,0
10	26,5	20,7	39,9	54,7
30	42,2	33,7	57,1	80,7
60	57,5	49,8	70,9	91,5
120	73,5	65,0	86,5	94,6
960	95,9	95,9	98,9	99,9

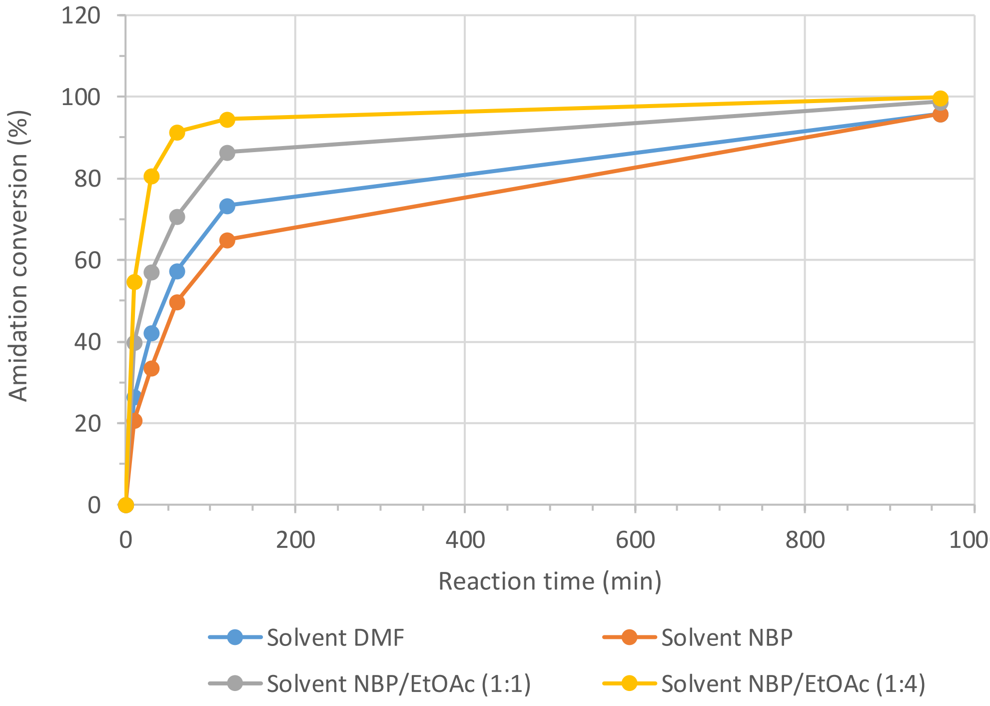

Figure S34. Schematic representation of conversions during Fmoc-Ser(*t*-Bu)-OH/Oxyma/DIC/H-RMG-AMS resin amidation reactions in DMF, NBP, NBP/EtOAc (1:1) and NBP/EtOAc (1:4).

5.2 LC-HRMS analysis of Oxyma to HCN conversion during Fmoc-Ser(*t*-Bu)-OH + H-RMG AMS resin amidation reactions

Experimental conditions: column: Waters peptide CSH C18, 2.1x150mm, 1.7μm, 130Å; column temperature: 30°C; injection volume: 0.4 μL; sampler temperature: 10°C; MS mode: Full scan; DAD: 220 nm; data rate: 5Hz; detector cell: standard cell 11μL; flow: 0.1 ml/min; jet weaver: V200 mixer; mobile phase A: 0.1 % TFA in water, mobile phase B: 0.10 % TFA in MeCN. Gradient (Time(min), %B): 0, 15; 40, 25; 48, 95; 54, 95; 55, 15; 62, 15. EIC-MS analyses were carried out as previously described.[4] A methodology for determining %Oxyma→HCN conversions based on determining concentration of **3** was used, see section 2 of this ESI.

Table S18. A summary of integrated EIC areas, **3** concentrations (gL^{-1}), amounts of **3** formed and %Oxyma→HCN conversions during experiments R1 – R4.

Solvent	Reaction time (min)	Rt (min), quantification channel EIC 242,15	Area (counts*min) quantification channel EIC 242,15	gL^{-1} **3**	μmol **3**	%Oxyma->HCN
DMF	10	17,280	13069	0,002780	0,2880	0,0222
NBP	10	17,274	6231	0,001326	0,1373	0,0106
NBP/EtOAc (1:1)	10	17,271	4758	0,001012	0,1049	0,0081
NBP/EtOAc (1:4)	10	17,299	5537	0,001178	0,1220	0,0094
DMF	30	17,259	19191	0,004082	0,4230	0,0325
NBP	30	17,249	10939	0,002327	0,2411	0,0185
NBP/EtOAc (1:1)	30	17,285	9465	0,002013	0,2086	0,0160
NBP/EtOAc (1:4)	30	17,287	8106	0,001724	0,1786	0,0137
DMF	60	17,282	41323	0,008790	0,9108	0,0701
NBP	60	17,269	19632	0,004176	0,4327	0,0333
NBP/EtOAc (1:1)	60	17,268	13710	0,002916	0,3022	0,0232
NBP/EtOAc (1:4)	60	17,248	12241	0,002604	0,2698	0,0208
DMF	120	17,266	89789	0,019100	1,9790	0,1522
NBP	120	17,254	45285	0,009633	0,9981	0,0768
NBP/EtOAc (1:1)	120	17,279	29201	0,006212	0,6436	0,0495
NBP/EtOAc (1:4)	120	17,345	17345	0,003690	0,3823	0,0294
DMF	960	17,323	577535	0,122855	12,7289	0,9791
NBP	960	17,293	255907	0,054437	5,6402	0,4339
NBP/EtOAc (1:1)	960	17,317	87195	0,018548	1,9218	0,1478
NBP/EtOAc (1:4)	960	17,349	37293	0,007933	0,8219	0,0632

Table S19. A summary of %Oxyma→HCN conversions during experiments R1 – R4.

Reaction time (min)	Solvent			
	DMF	NBP	NBP/EtOAc (1:1)	NBP/EtOAc (1:4)
	Oxyma→HCN conversion (%)			
0	0,0000	0,0000	0,0000	0,0000
10	0,0222	0,0106	0,0081	0,0094
30	0,0325	0,0185	0,0160	0,0137
60	0,0701	0,0333	0,0232	0,0208
120	0,1522	0,0768	0,0495	0,0294
960	0,9791	0,4339	0,1478	0,0632

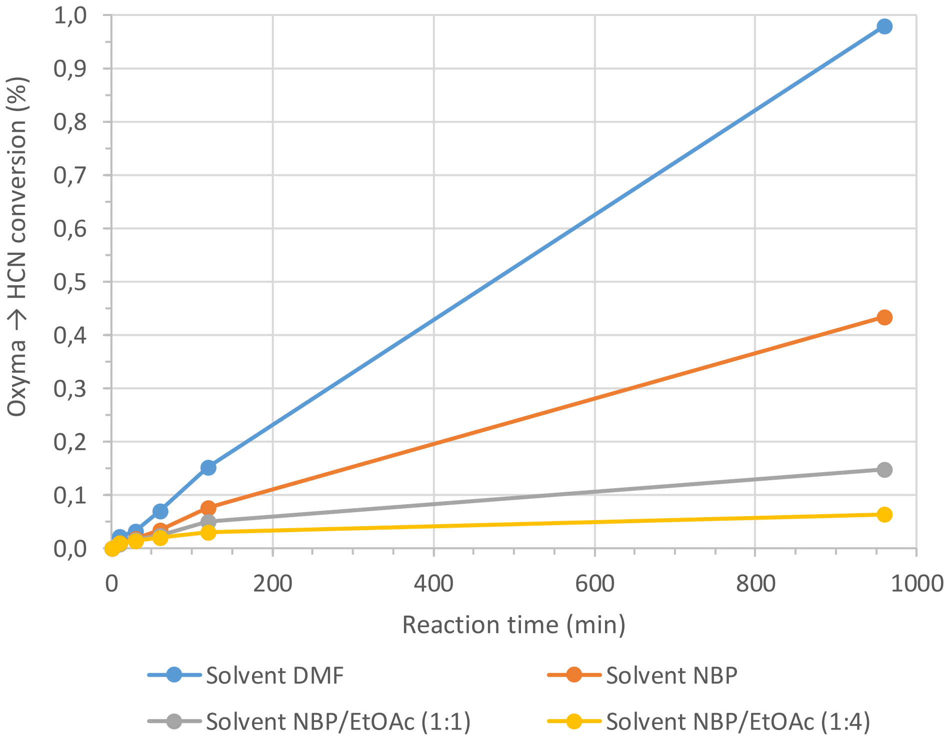

Figure S35. A schematic representation of %Oxyma→HCN conversions during experiments R1 – R4.

6. Assessment of HCN formation and amide bond formation kinetics during DIC/Oxyma mediated coupling of 1.0 equiv Fmoc-Ser(*t*-Bu)-OH with (S)-(-)-1-phenylethylamine in different solvents

For all four reactions 20 μL were taken out and quenched with 0.5 % TFA/MeCN (1.0 mL) at 0, 10, 30, 60, 120 and 960 min. Conversions of the amidation reactions at these timepoints were determined by HPLC (see section 6.1 of this ESI) and the contents of oxadiazole **3** used for the calculations of conversion of Oxyma to HCN were determined by LC-HRMS (see section 6.2 of this ESI).

6.1 HPLC analysis of conversions of the Fmoc-Ser(*t*-Bu)-OH + (S)-(-)-1-phenylethylamine amidation reactions

Experimental conditions used in the section 5.1 of this ESI were employed. Following peaks were integrated: i) Fmoc-Ser(*t*-Bu)-OH (starting material), rt 9.0 min; ii) Fmoc-Ser(*t*-Bu)-S)-(-)-1-phenylethylamide (product of amidation reaction), rt 10.2 min.

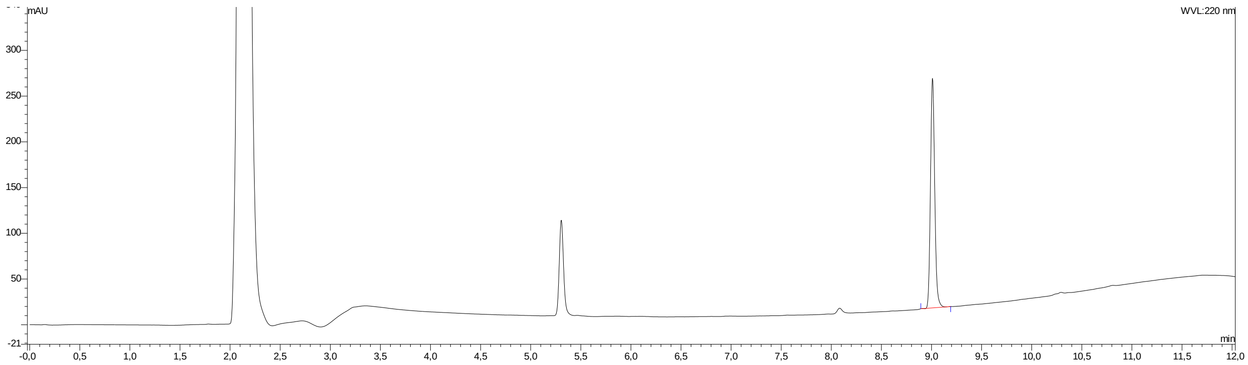

Figure S36. HPLC chromatogram of Fmoc-Ser(*t*-Bu)-OH/Oxyma/DIC/(S)-(-)-1-phenylethylamine amidation reaction in DMF at t=0 min (prior to DIC addition).

Table S20. Area% for the integrated peak.

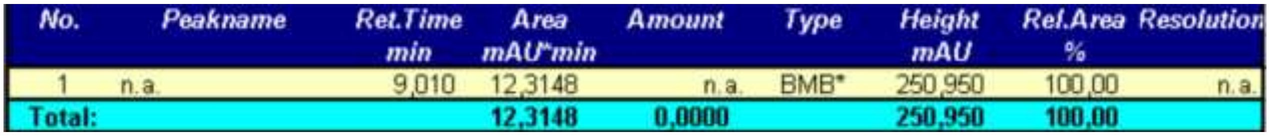

No.	Peakname	Ret.Time min	Area mAU*min	Amount	Type	Height mAU	Rel.Area %	Resolution
1	n.a.	9,010	12,3148	n.a.	BMB*	250,950	100,00	n.a.
Total:			12,3148	0,0000		250,950	100,00	

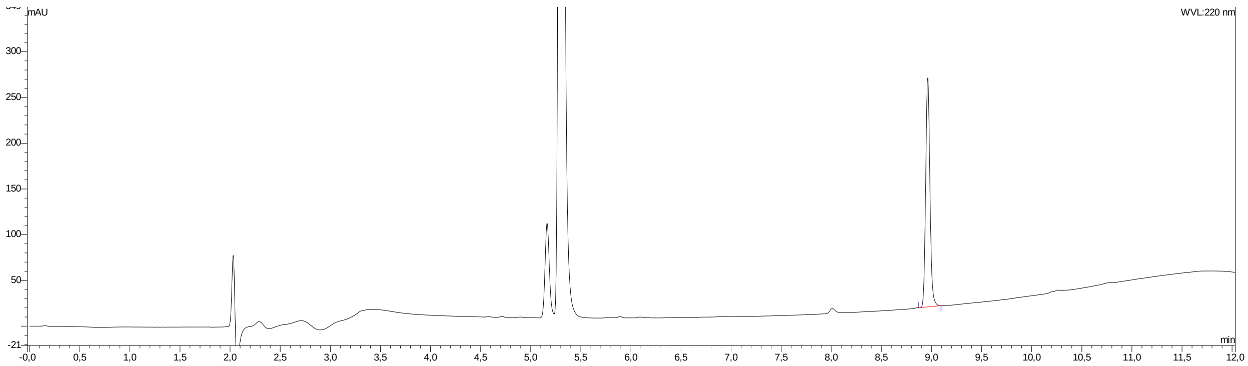

Figure S37. HPLC chromatogram of Fmoc-Ser(*t*-Bu)-OH/Oxyma/DIC/(S)-(-)-1-phenylethylamine amidation reaction in NBP at t=0 min (prior to DIC addition).

Table S21. Area% for the integrated peak.

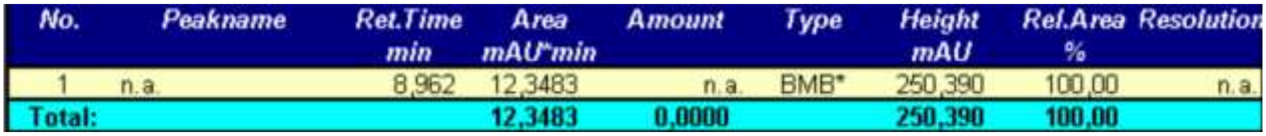

No.	Peakname	Ret.Time min	Area mAU*min	Amount	Type	Height mAU	Rel.Area %	Resolutio
1	n.a.	8,962	12,3483	n.a.	BMB*	250,390	100,00	n.a.
Total:			**12,3483**	**0,0000**		**250,390**	**100,00**	

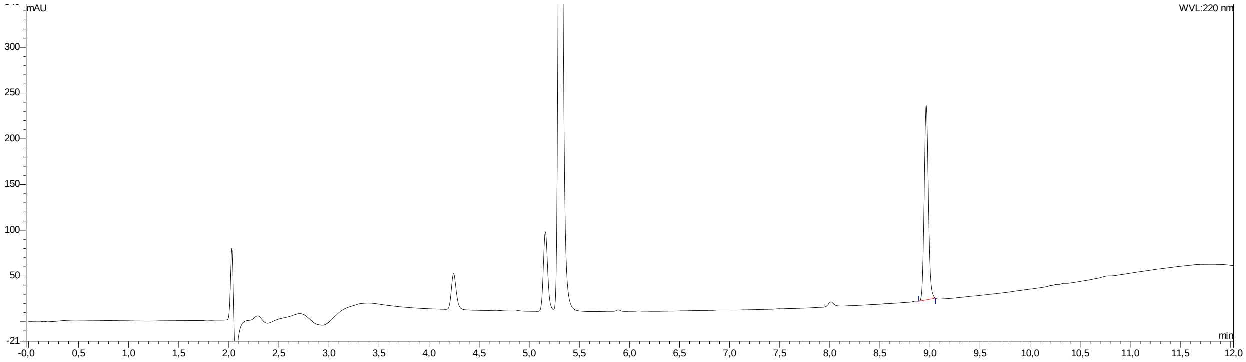

Figure S38. HPLC chromatogram of Fmoc-Ser(*t*-Bu)-OH/Oxyma/DIC/(S)-(-)-1-phenylethylamine amidation reaction in NBP/EtOAc (1:1) at t=0 min (prior to DIC addition).

Table S22. Area% for the integrated peak.

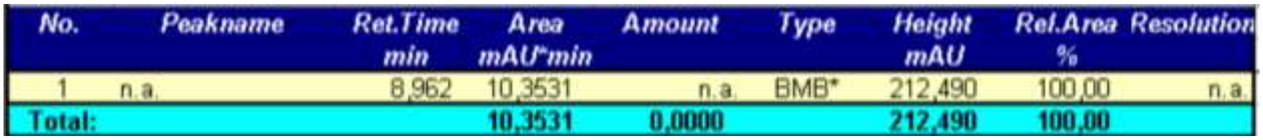

No.	Peakname	Ret.Time min	Area mAU*min	Amount	Type	Height mAU	Rel.Area %	Resolution
1	n.a.	8,962	10,3531	n.a.	BMB*	212,490	100,00	n.a.
Total:			**10,3531**	**0,0000**		**212,490**	**100,00**	

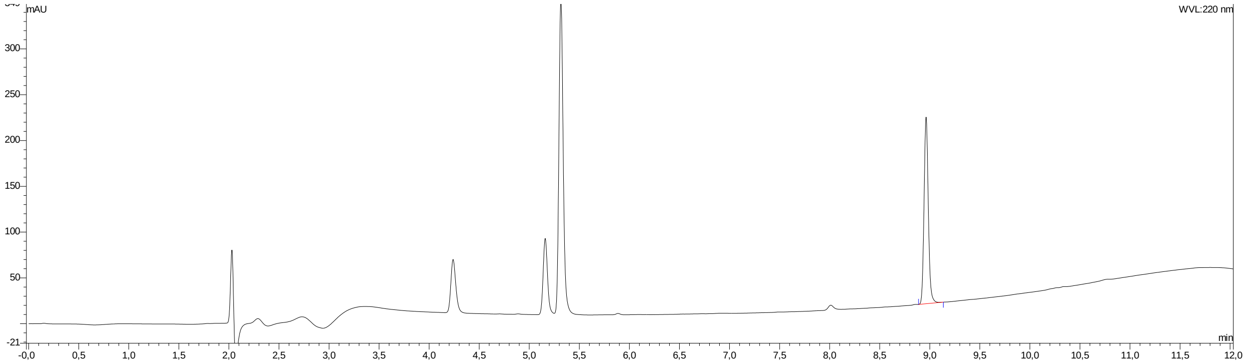

Figure S39. HPLC chromatogram of Fmoc-Ser(*t*-Bu)-OH/Oxyma/DIC/(S)-(-)-1-phenylethylamine amidation reaction in NBP/EtOAc (1:4) at t=0 min (prior to DIC addition).

Table S23. Area% (mAu^{x}min) for the integrated peaks.

No.	Peakname	Ret.Time min	Area mAU*min	Amount	Type	Height mAU	Rel.Area %	Resolution
1	n.a.	8,963	10,0501	n.a.	BMB*	203,762	100,00	n.a.
Total:			**10,0501**	**0,0000**		**203,762**	**100,00**	

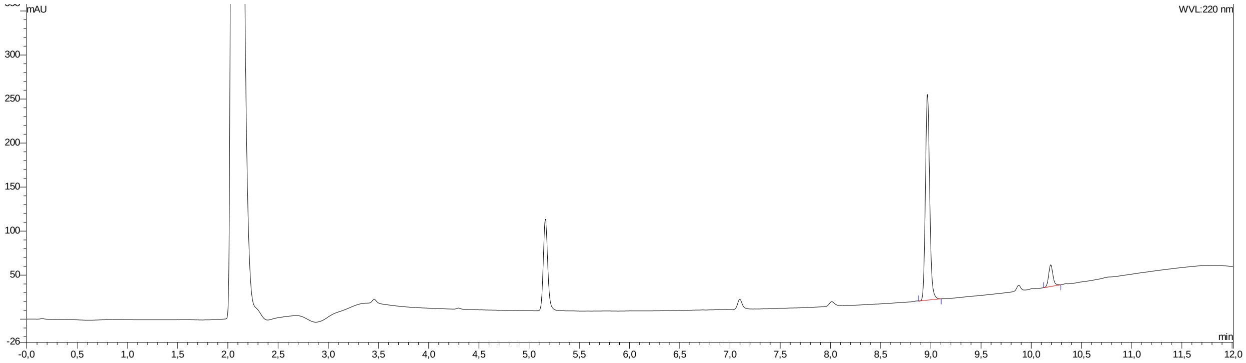

Figure S40. HPLC chromatogram of Fmoc-Ser(*t*-Bu)-OH/Oxyma/DIC/(S)-(-)-1-phenylethylamine amidation reaction in DMF at t=10 min.

Table S24. Area% for the integrated peaks.

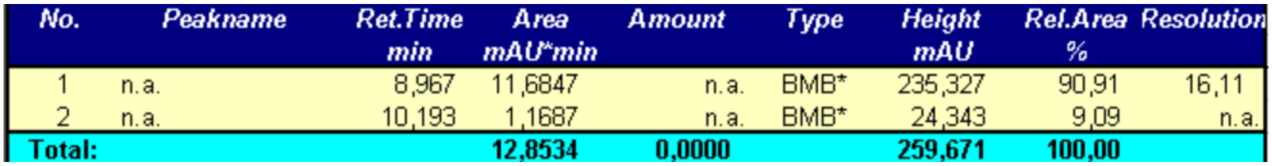

No.	Peakname	Ret.Time min	Area mAU*min	Amount	Type	Height mAU	Rel.Area %	Resolution
1	n.a.	8,967	11,6847	n.a.	BMB*	235,327	90,91	16,11
2	n.a.	10,193	1,1687	n.a.	BMB*	24,343	9,09	n.a.
Total:			**12,8534**	**0,0000**		**259,671**	**100,00**	

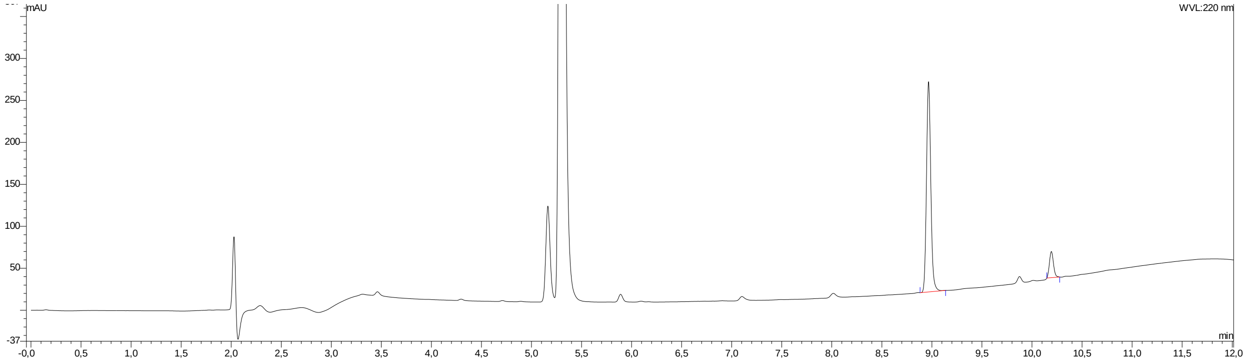

Figure S41. HPLC chromatogram of Fmoc-Ser(*t*-Bu)-OH/Oxyma/DIC/(S)-(-)-1-phenylethylamine amidation reaction in NBP at t=10 min.

Table S25. Area% for the integrated peaks.

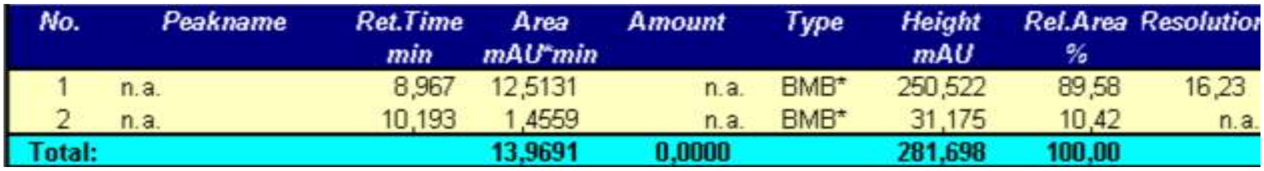

No.	Peakname	Ret.Time min	Area mAU*min	Amount	Type	Height mAU	Rel.Area %	Resolution
1	n.a.	8,967	12,5131	n.a.	BMB*	250,522	89,58	16,23
2	n.a.	10,193	1,4559	n.a.	BMB*	31,175	10,42	n.a.
Total:			13,9691	0,0000		281,698	100,00	

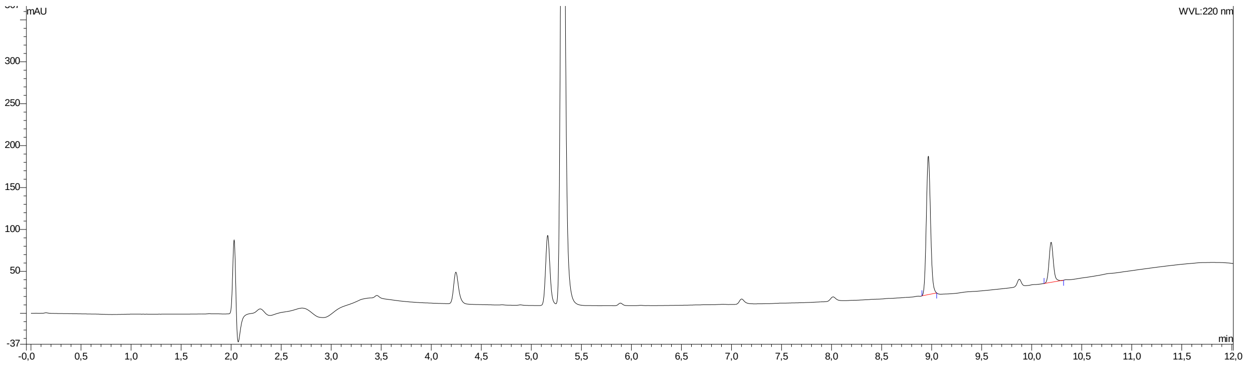

Figure S42. HPLC chromatogram of Fmoc-Ser(*t*-Bu)-OH/Oxyma/DIC/(S)-(-)-1-phenylethylamine amidation reaction in NBP/EtOAc (1:1) at t=10 min.

Table S26. Area% for the integrated peaks.

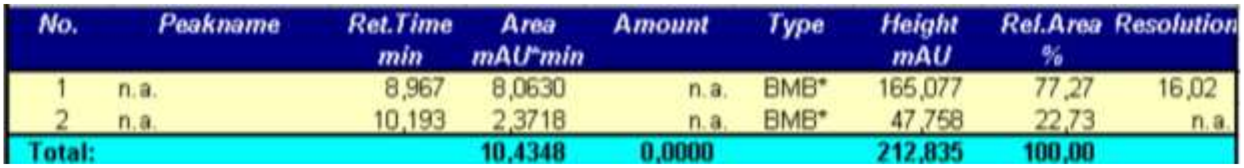

No.	Peakname	Ret.Time min	Area mAU*min	Amount	Type	Height mAU	Rel.Area %	Resolution
1	n.a.	8,967	8,0630	n.a.	BMB*	165,077	77,27	16,02
2	n.a.	10,193	2,3718	n.a.	BMB*	47,758	22,73	n.a.
Total:			10,4348	0,0000		212,835	100,00	

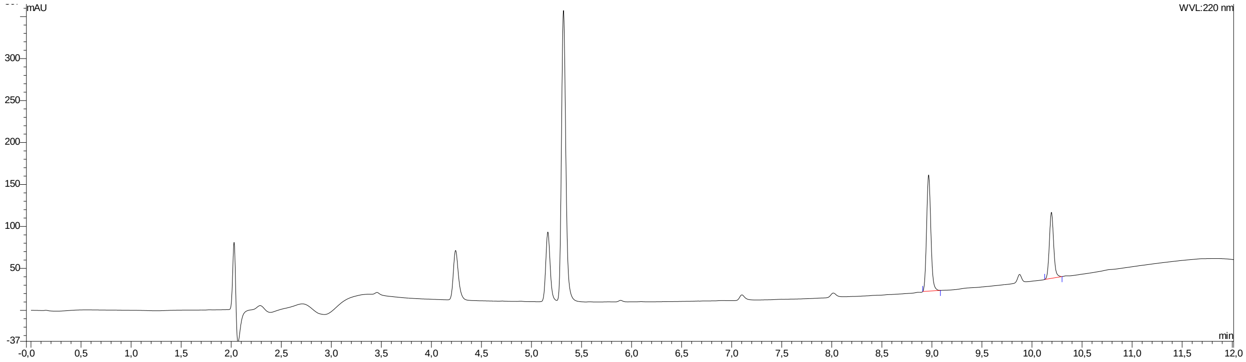

Figure S43. HPLC chromatogram of Fmoc-Ser(*t*-Bu)-OH/Oxyma/DIC/(S)-(-)-1-phenylethylamine amidation reaction in NBP/EtOAc (1:4) at t=10 min.

Table S27. Area% for the integrated peaks.

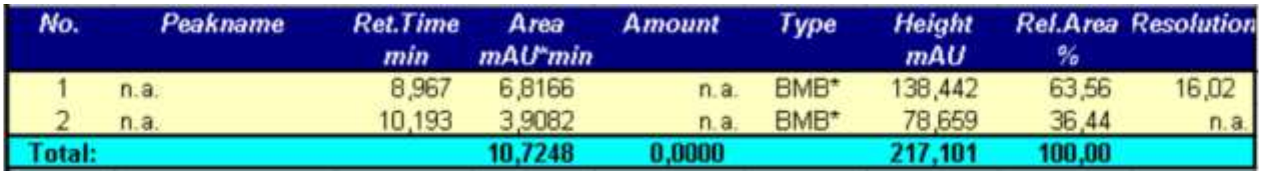

No.	Peakname	Ret.Time min	Area mAU*min	Amount	Type	Height mAU	Rel.Area %	Resolution
1	n.a.	8,967	6,8166	n.a.	BMB*	138,442	63,56	16,02
2	n.a.	10,193	3,9082	n.a.	BMB*	78,659	36,44	n.a.
Total:			10,7248	0,0000		217,101	100,00	

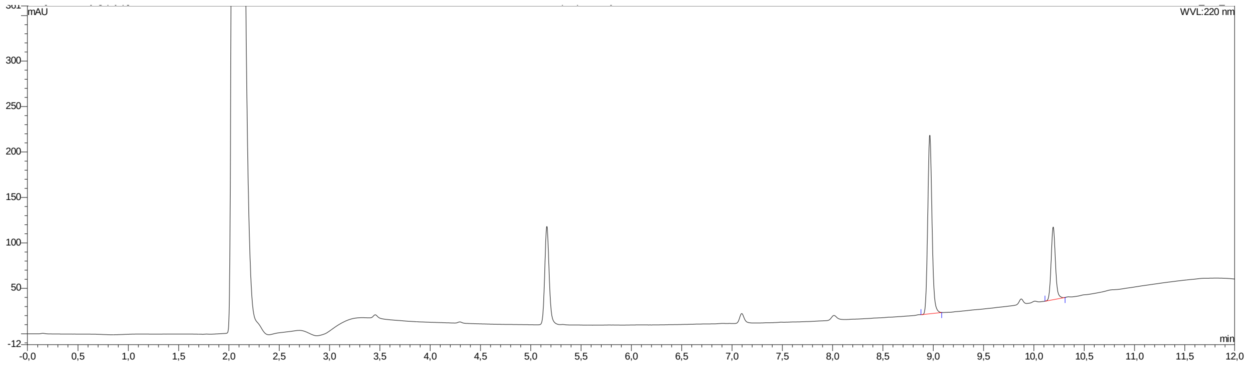

Figure S44. HPLC chromatogram of Fmoc-Ser(*t*-Bu)-OH/Oxyma/DIC/(S)-(-)-1-phenylethylamine amidation reaction in DMF at t=30 min.

Table S28. Area% for the integrated peaks.

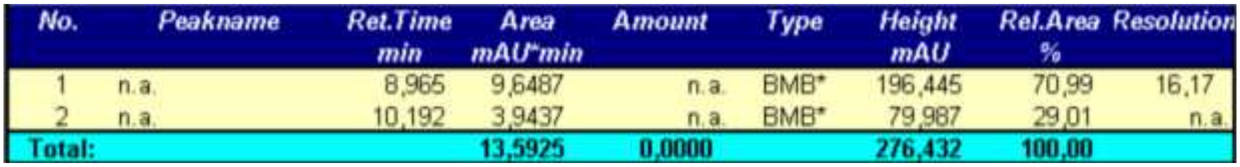

No.	Peakname	Ret.Time min	Area mAU*min	Amount	Type	Height mAU	Rel.Area %	Resolution
1	n.a.	8,965	9,6487	n.a.	BMB*	196,445	70,99	16,17
2	n.a.	10,192	3,9437	n.a.	BMB*	79,987	29,01	n.a.
Total:			13,5925	0,0000		276,432	100,00	

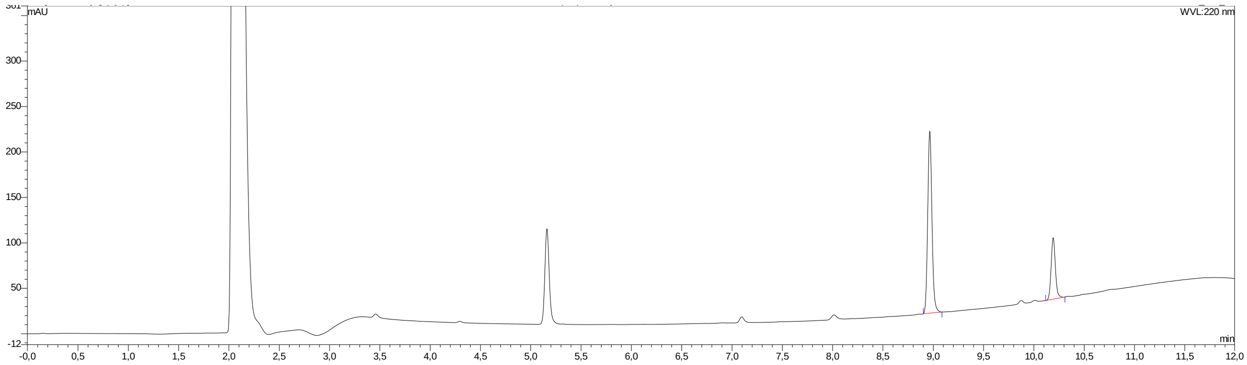

Figure S45. HPLC chromatogram of Fmoc-Ser(*t*-Bu)-OH/Oxyma/DIC/(S)-(-)-1-phenylethylamine amidation reaction in NBP at t=30 min.

Table S29. Area% for the integrated peaks.

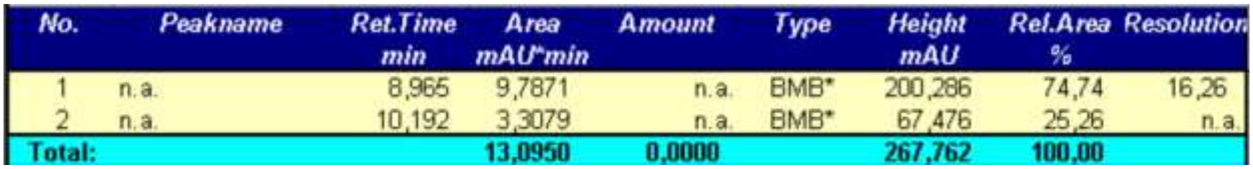

No.	Peakname	Ret.Time min	Area mAU*min	Amount	Type	Height mAU	Rel.Area %	Resolution
1	n.a.	8,965	9,7871	n.a.	BMB*	200,286	74,74	16,26
2	n.a.	10,192	3,3079	n.a.	BMB*	67,476	25,26	n.a.
Total:			13,0950	0,0000		267,762	100,00	

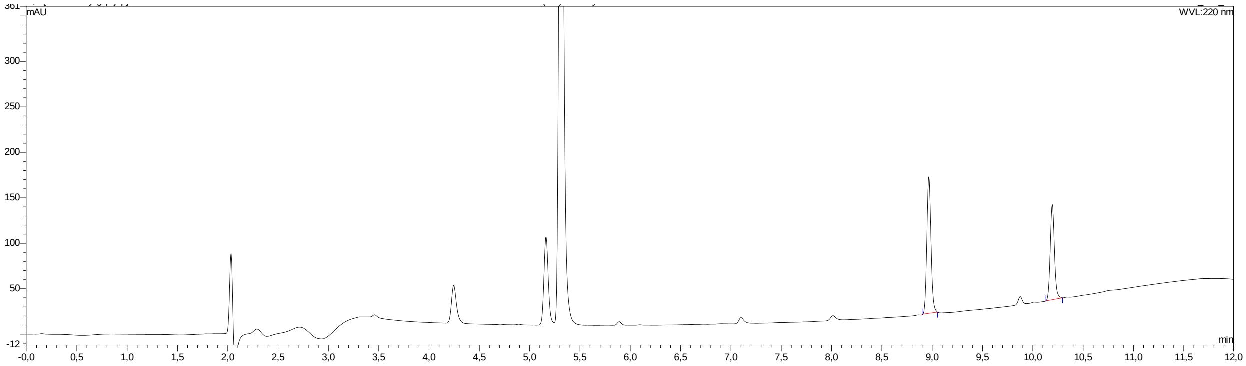

Figure S46. HPLC chromatogram of Fmoc-Ser(*t*-Bu)-OH/Oxyma/DIC/(S)-(-)-1-phenylethylamine amidation reaction in NBP/EtOAc (1:1) at t=30 min.

Table S30. Area% for the integrated peaks.

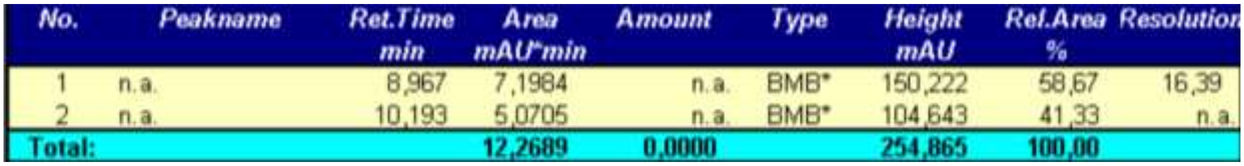

No.	Peakname	Ret.Time min	Area mAU*min	Amount	Type	Height mAU	Rel.Area %	Resolution
1	n.a.	8,967	7,1984	n.a.	BMB*	150,222	58,67	16,39
2	n.a.	10,193	5,0705	n.a.	BMB*	104,643	41,33	n.a.
Total:			12,2689	0,0000		254,865	100,00	

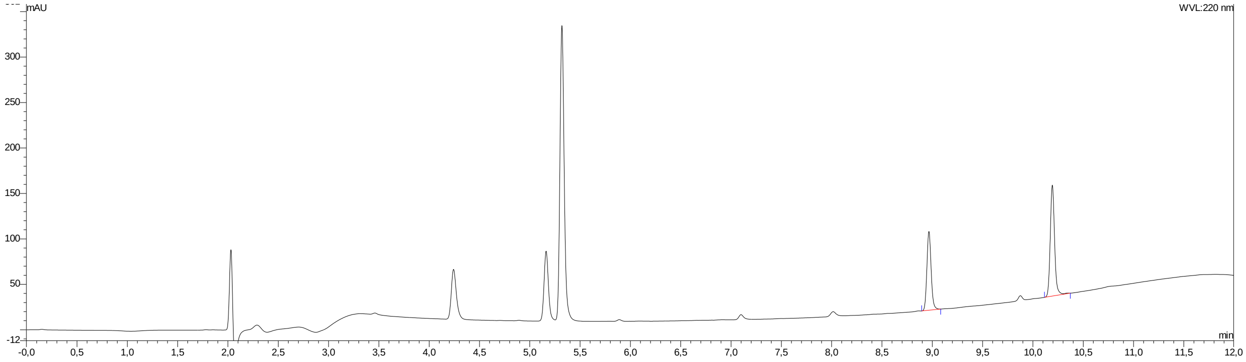

Figure S47. HPLC chromatogram of Fmoc-Ser(*t*-Bu)-OH/Oxyma/DIC/(S)-(-)-1-phenylethylamine amidation reaction in NBP/EtOAc (1:4) at t=30 min.

Table S31. Area% for the integrated peaks.

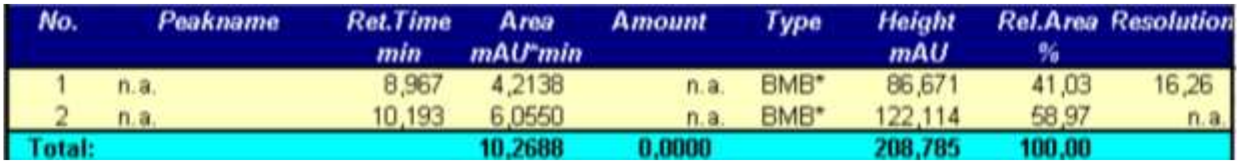

No.	Peakname	Ret.Time min	Area mAU*min	Amount	Type	Height mAU	Rel.Area %	Resolution
1	n.a.	8,967	4,2138	n.a.	BMB*	86,671	41,03	16,26
2	n.a.	10,193	6,0550	n.a.	BMB*	122,114	58,97	n.a.
Total:			**10,2688**	**0,0000**		**208,785**	**100,00**	

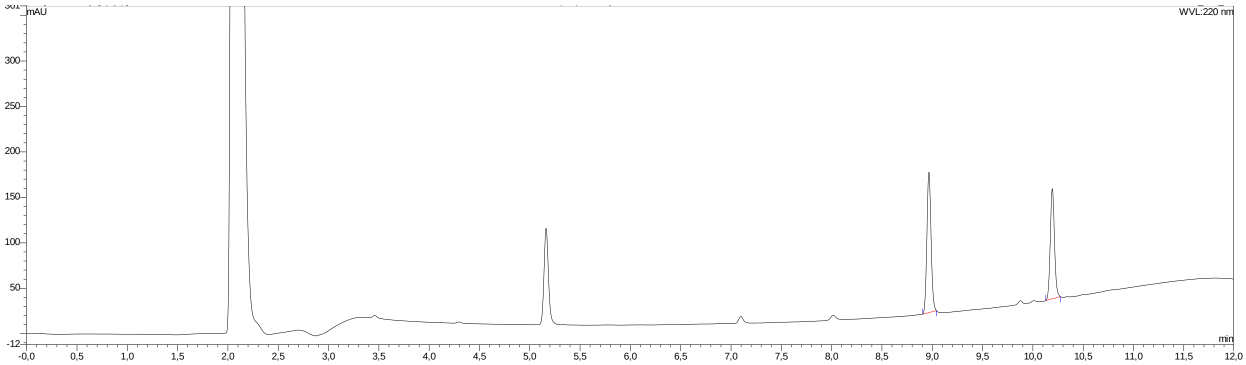

Figure S48. HPLC chromatogram of Fmoc-Ser(*t*-Bu)-OH/Oxyma/DIC/(S)-(-)-1-phenylethylamine amidation reaction in DMF at t=60 min.

Table S32. Area% for the integrated peaks.

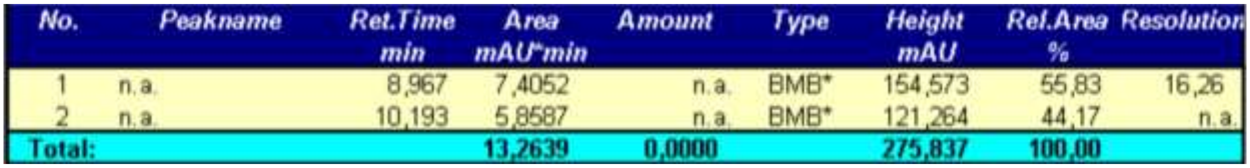

No.	Peakname	Ret.Time min	Area mAU*min	Amount	Type	Height mAU	Rel.Area %	Resolution
1	n.a.	8,967	7,4052	n.a.	BMB*	154,573	55,83	16,26
2	n.a.	10,193	5,8587	n.a.	BMB*	121,264	44,17	n.a.
Total:			**13,2639**	**0,0000**		**275,837**	**100,00**	

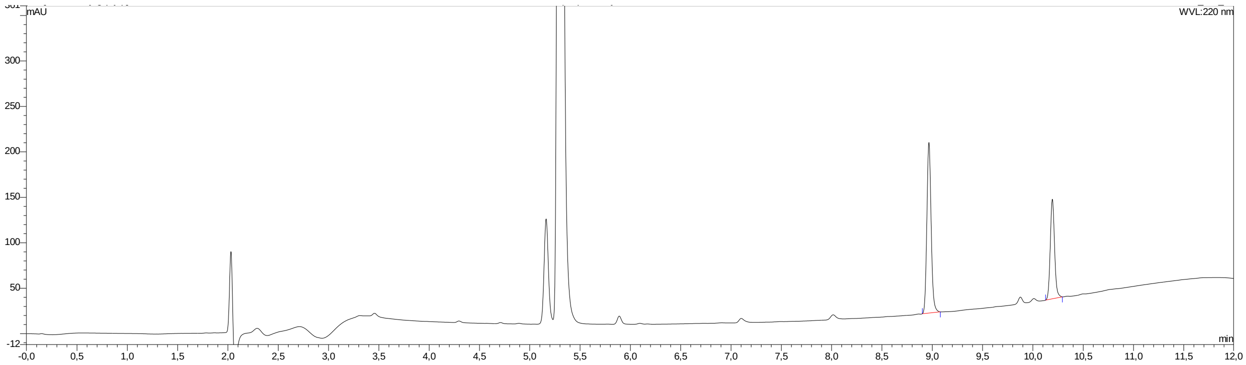

Figure S49. HPLC chromatogram of Fmoc-Ser(*t*-Bu)-OH/Oxyma/DIC/(S)-(-)-1-phenylethylamine amidation reaction in NBP at t=60 min.

Table S33. Area% for the integrated peaks.

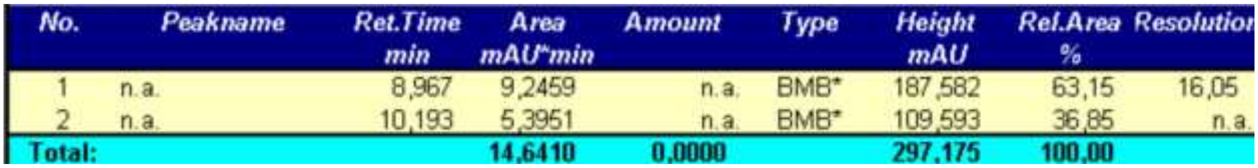

No.	Peakname	Ret.Time min	Area mAU*min	Amount	Type	Height mAU	Rel.Area %	Resolutio
1	n.a.	8,967	9,2459	n.a.	BMB*	187,582	63,15	16,05
2	n.a.	10,193	5,3951	n.a.	BMB*	109,593	36,85	n.a.
Total:			**14,6410**	**0,0000**		**297,175**	**100,00**	

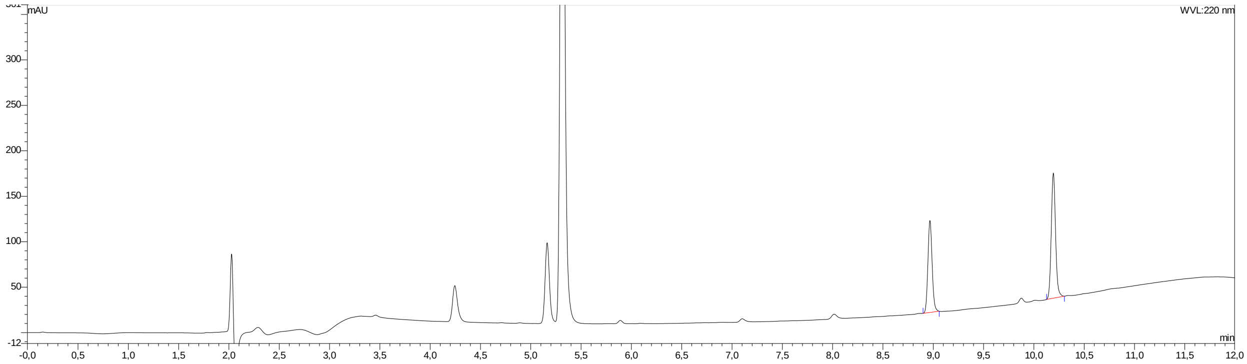

Figure S50. HPLC chromatogram of Fmoc-Ser(*t*-Bu)-OH/Oxyma/DIC/(S)-(-)-1-phenylethylamine amidation reaction in NBP/EtOAc (1:1) at t=60 min.

Table S34. Area% for the integrated peaks.

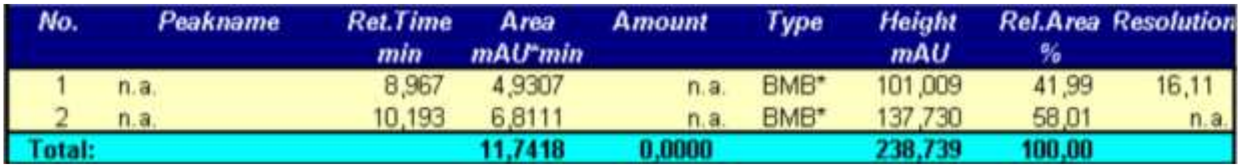

No.	Peakname	Ret.Time min	Area mAU*min	Amount	Type	Height mAU	Rel.Area %	Resolution
1	n.a.	8,967	4,9307	n.a.	BMB*	101,009	41,99	16,11
2	n.a.	10,193	6,8111	n.a.	BMB*	137,730	58,01	n.a.
Total:			**11,7418**	**0,0000**		**238,739**	**100,00**	

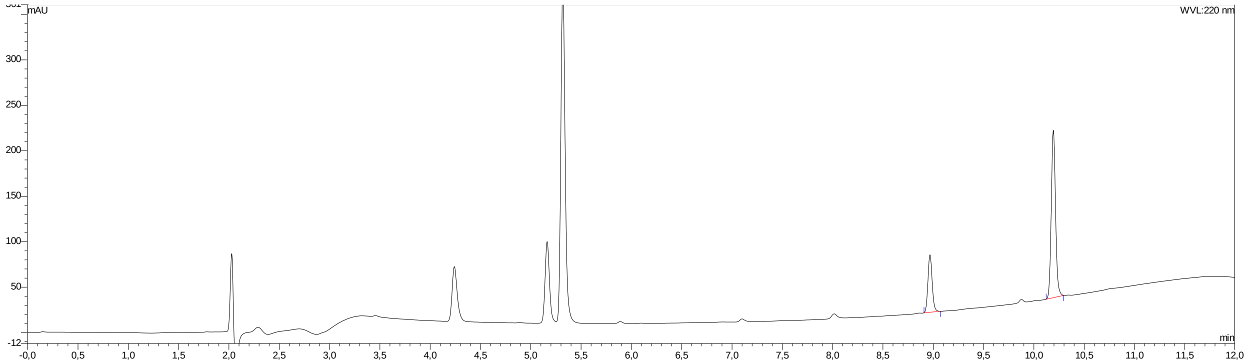

Figure S51. HPLC chromatogram of Fmoc-Ser(*t*-Bu)-OH/Oxyma/DIC/(S)-(-)-1-phenylethylamine amidation reaction in NBP/EtOAc (1:4) at t=60 min.

Table S35. Area% for the integrated peaks.

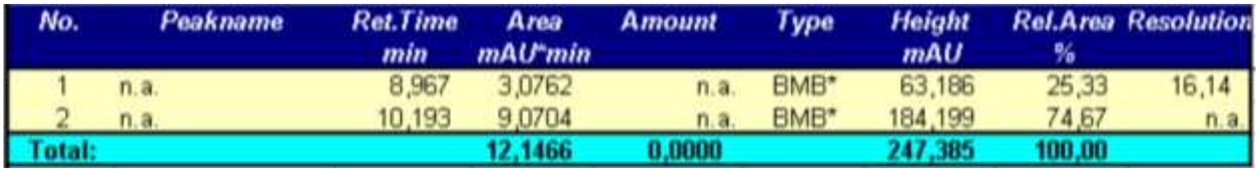

No.	Peakname	Ret.Time min	Area mAU*min	Amount	Type	Height mAU	Rel.Area %	Resolution
1	n.a.	8,967	3,0762	n.a.	BMB*	63,186	25,33	16,14
2	n.a.	10,193	9,0704	n.a.	BMB*	184,199	74,67	n.a.
Total:			12,1466	0,0000		247,385	100,00	

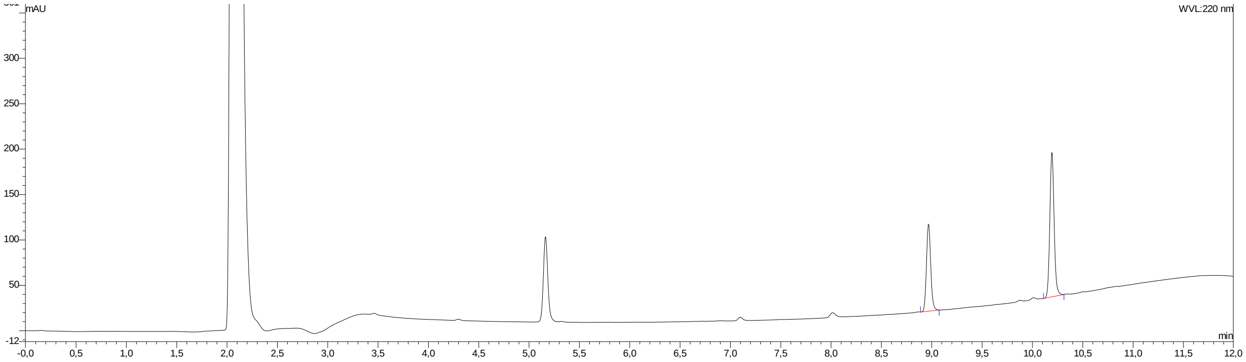

Figure S52. HPLC chromatogram of Fmoc-Ser(*t*-Bu)-OH/Oxyma/DIC/(S)-(-)-1-phenylethylamine amidation reaction in DMF at t=120 min.

Table S36. Area% for the integrated peaks.

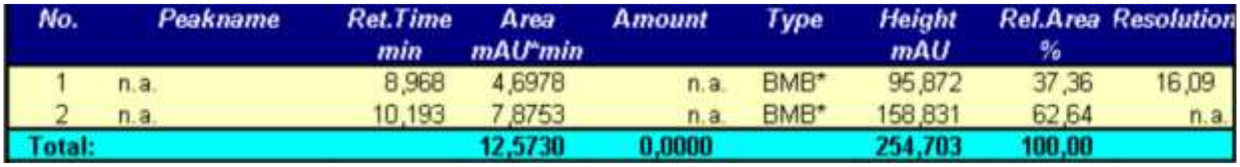

No.	Peakname	Ret.Time min	Area mAU*min	Amount	Type	Height mAU	Rel.Area %	Resolution
1	n.a.	8,968	4,6978	n.a.	BMB*	95,872	37,36	16,09
2	n.a.	10,193	7,8753	n.a.	BMB*	158,831	62,64	n.a.
Total:			12,5730	0,0000		254,703	100,00	

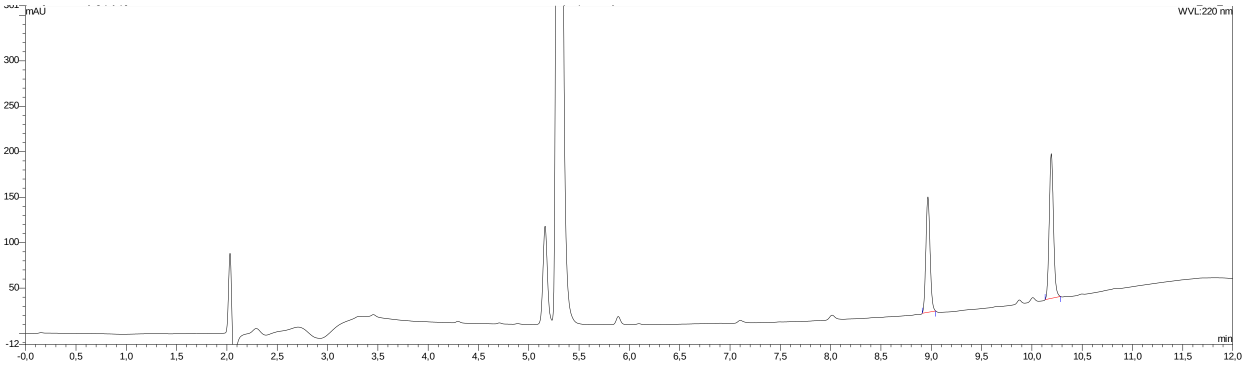

Figure S53. HPLC chromatogram of Fmoc-Ser(*t*-Bu)-OH/Oxyma/DIC/(S)-(-)-1-phenylethylamine amidation reaction in NBP at t=120 min.

Table S37. Area% for the integrated peaks.

No.	Peakname	Ret.Time min	Area mAU*min	Amount	Type	Height mAU	Rel.Area %	Resolution
1	n.a.	8,967	6,0834	n.a.	BMB*	126,860	43,90	16,17
2	n.a.	10,193	7,7737	n.a.	BMB*	159,110	56,10	n.a.
Total:			13,8571	0,0000		285,970	100,00	

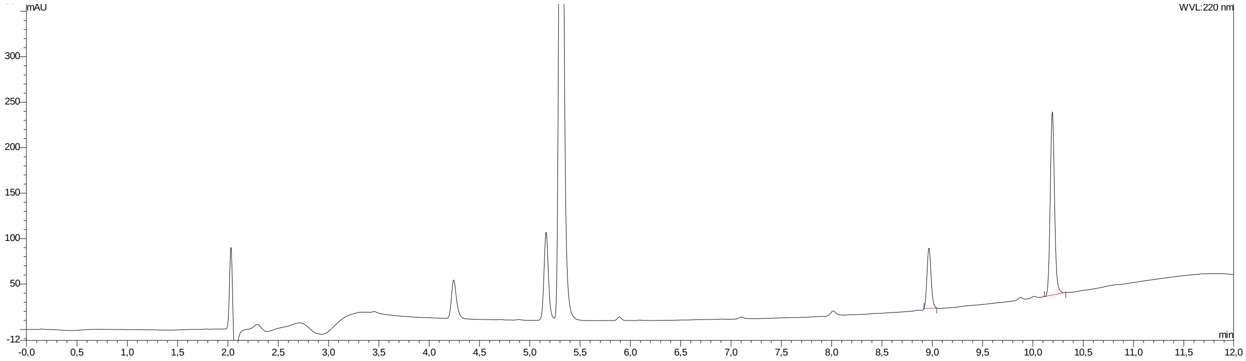

Figure S54. HPLC chromatogram of Fmoc-Ser(*t*-Bu)-OH/Oxyma/DIC/(S)-(-)-1-phenylethylamine amidation reaction in NBP/EtOAc (1:1) at t=120 min.

Table S38. Area% for the integrated peaks.

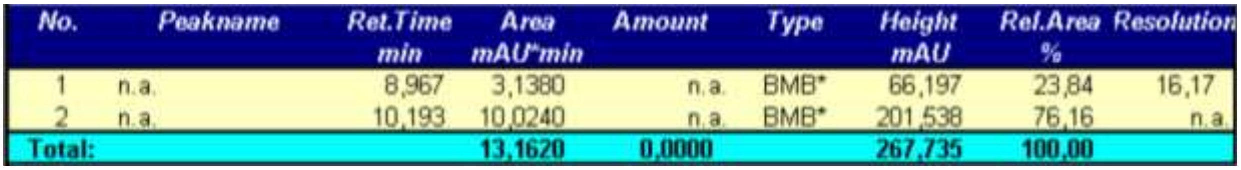

No.	Peakname	Ret.Time min	Area mAU*min	Amount	Type	Height mAU	Rel.Area %	Resolution
1	n.a.	8,967	3,1380	n.a.	BMB*	66,197	23,84	16,17
2	n.a.	10,193	10,0240	n.a.	BMB*	201,538	76,16	n.a.
Total:			13,1620	0,0000		267,735	100,00	

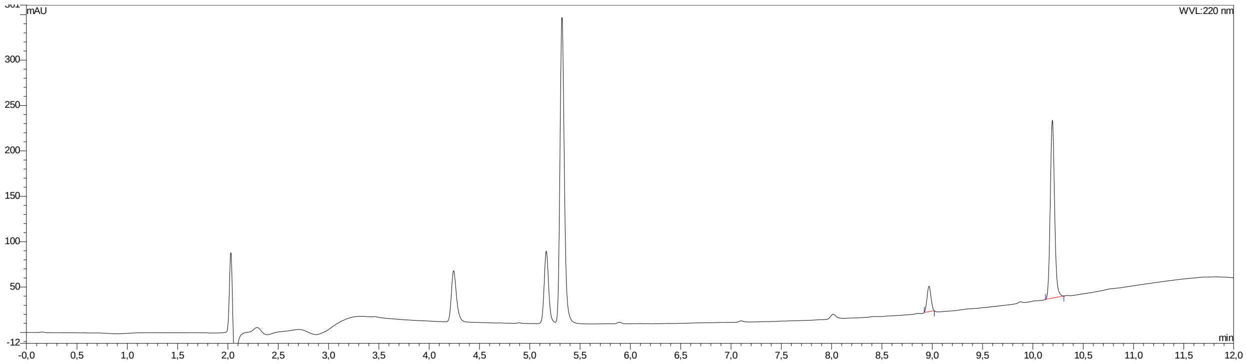

Figure S55. HPLC chromatogram of Fmoc-Ser(*t*-Bu)-OH/Oxyma/DIC/(S)-(-)-1-phenylethylamine amidation reaction in NBP/EtOAc (1:4) at t=120 min.

Table S39. Area% for the integrated peaks.

No.	Peakname	Ret.Time min	Area mAU*min	Amount	Type	Height mAU	Rel.Area %	Resolution
1	n.a.	8,967	1,2687	n.a.	BMB*	27,944	11,52	16,26
2	n.a.	10,193	9,7475	n.a.	BMB*	195,935	88,48	n.a.
Total:			11,0162	0,0000		223,879	100,00	

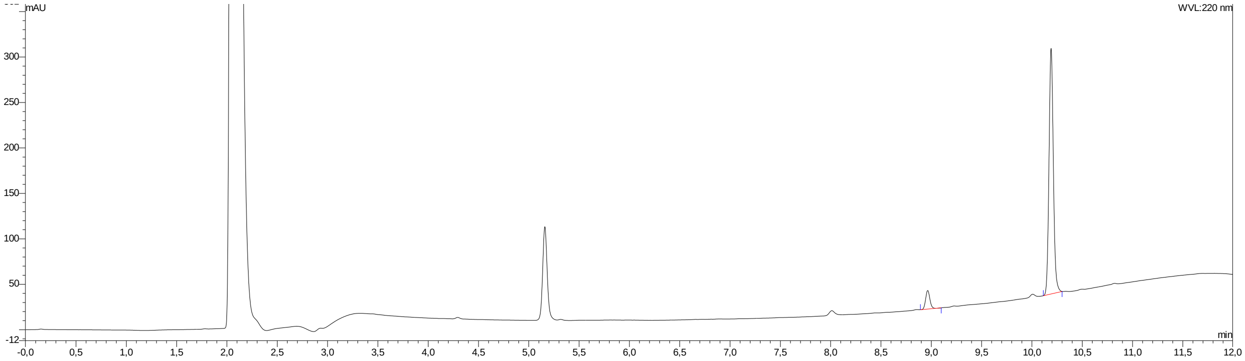

Figure S56. HPLC chromatogram of Fmoc-Ser(*t*-Bu)-OH/Oxyma/DIC/(S)-(-)-1-phenylethylamine amidation reaction in DMF at t=960 min.

Table S40. Area% for the integrated peaks.

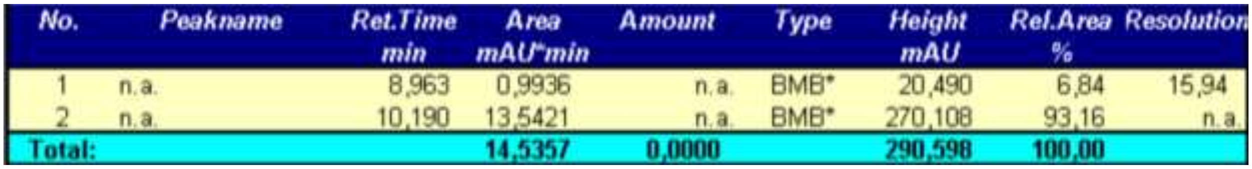

No.	Peakname	Ret.Time min	Area mAU*min	Amount	Type	Height mAU	Rel.Area %	Resolution
1	n.a.	8,963	0,9936	n.a.	BMB*	20,490	6,84	15,94
2	n.a.	10,190	13,5421	n.a.	BMB*	270,108	93,16	n.a.
Total:			14,5357	0,0000		290,598	100,00	

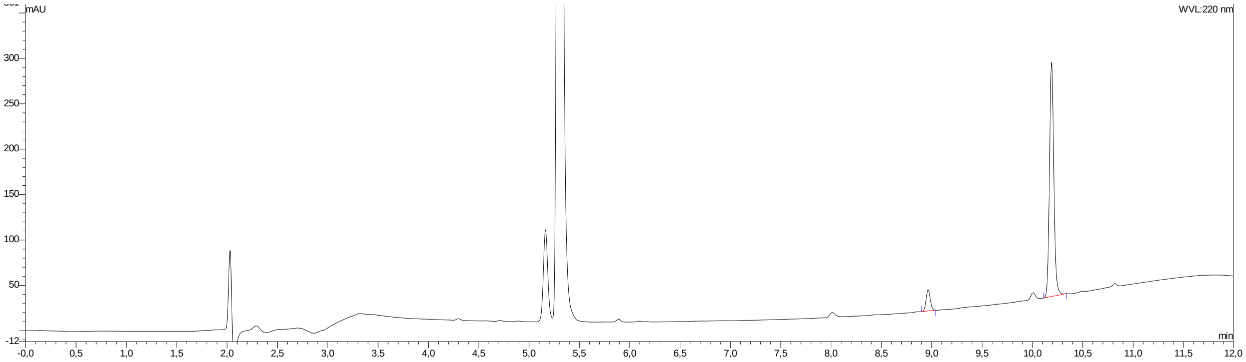

Figure S57. HPLC chromatogram of Fmoc-Ser(*t*-Bu)-OH/Oxyma/DIC/(S)-(-)-1-phenylethylamine amidation reaction in NBP at t=960 min.

Table S41. Area% for the integrated peaks.

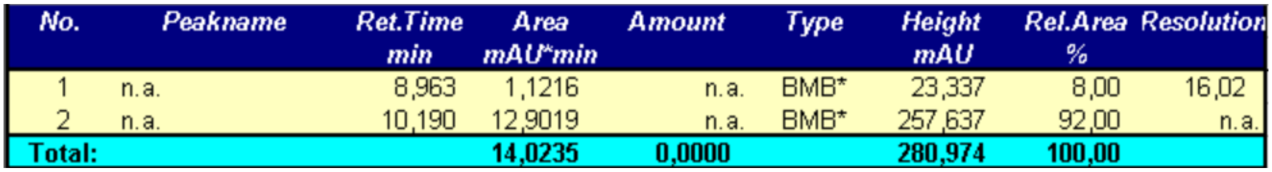

No.	Peakname	Ret.Time min	Area mAU*min	Amount	Type	Height mAU	Rel.Area %	Resolution
1	n.a.	8,963	1,1216	n.a.	BMB*	23,337	8,00	16,02
2	n.a.	10,190	12,9019	n.a.	BMB*	257,637	92,00	n.a.
Total:			**14,0235**	**0,0000**		**280,974**	**100,00**	

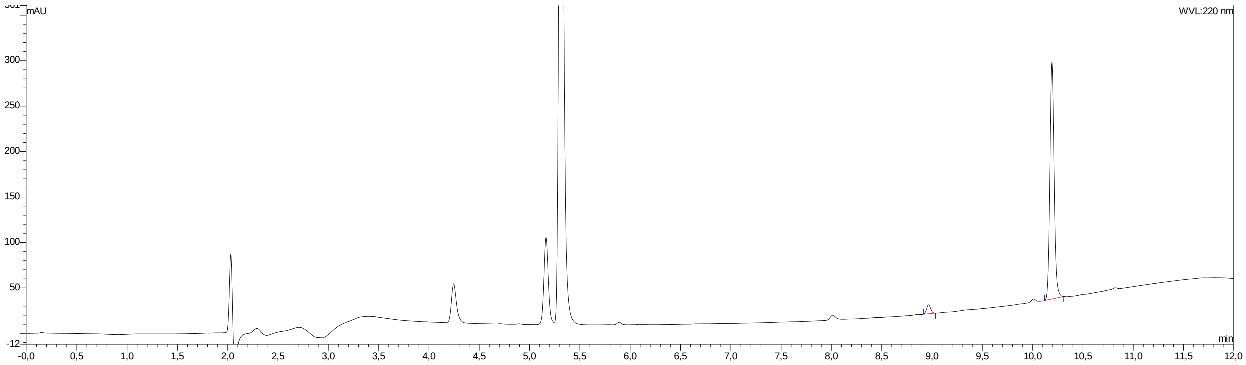

Figure S58. HPLC chromatogram of Fmoc-Ser(*t*-Bu)-OH/Oxyma/DIC/(S)-(-)-1-phenylethylamine amidation reaction in NBP/EtOAc (1:1) at t=960 min.

Table S42. Area% for the integrated peaks.

No.	Peakname	Ret.Time min	Area mAU*min	Amount	Type	Height mAU	Rel.Area %	Resolution
1	n.a.	8,965	0,4639	n.a.	BMB*	9,847	3,46	16,20
2	n.a.	10,192	12,9604	n.a.	BMB*	260,915	96,54	n.a.
Total:			**13,4243**	**0,0000**		**270,762**	**100,00**	

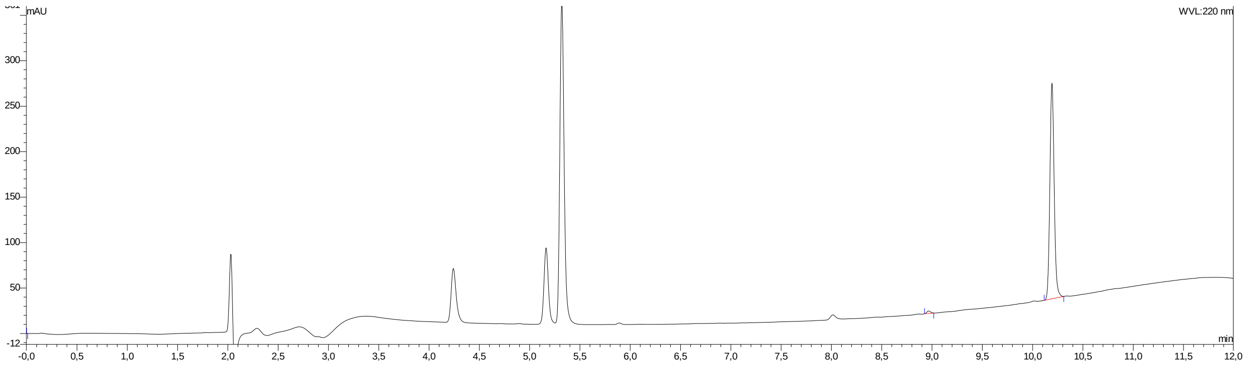

Figure S59. HPLC chromatogram of Fmoc-Ser(*t*-Bu)-OH/Oxyma/DIC/(S)-(-)-1-phenylethylamine amidation reaction in NBP/EtOAc (1:4) at t=960 min.

Table S43. Area% for the integrated peaks.

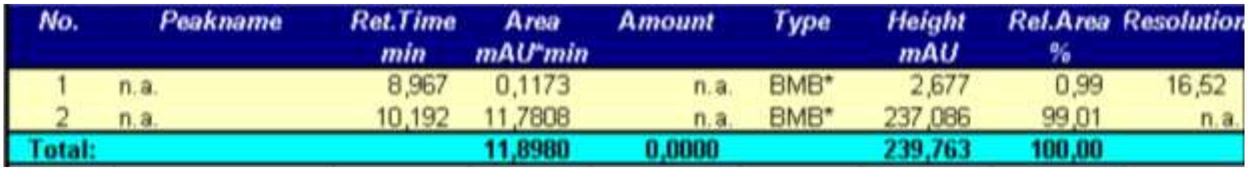

No.	Peakname	Ret.Time min	Area mAU*min	Amount	Type	Height mAU	Rel.Area %	Resolution
1	n.a.	8,967	0,1173	n.a.	BMB*	2,677	0,99	16,52
2	n.a.	10,192	11,7808	n.a.	BMB*	237,086	99,01	n.a.
Total:			11,8980	0,0000		239,763	100,00	

Table S44. A summary of conversions during Fmoc-Ser(*t*-Bu)-OH/Oxyma/DIC/(S)-(-)-1-phenylethylamine amidation reactions in DMF, NBP, NBP/EtOAc (1:1) and NBP/EtOAc (1:4).

Reaction time (min)	Solvent			
	DMF	NBP	NBP/EtOAc (1:1)	NBP/EtOAc (1:4)
	Amidation conversion (%)			
0	0,0	0,0	0,0	0,0
10	9,1	10,4	22,7	36,4
30	29,0	25,3	41,3	59,0
60	44,2	36,9	58,0	74,7
120	62,6	56,1	76,2	88,5
960	93,2	92,0	96,5	99,0

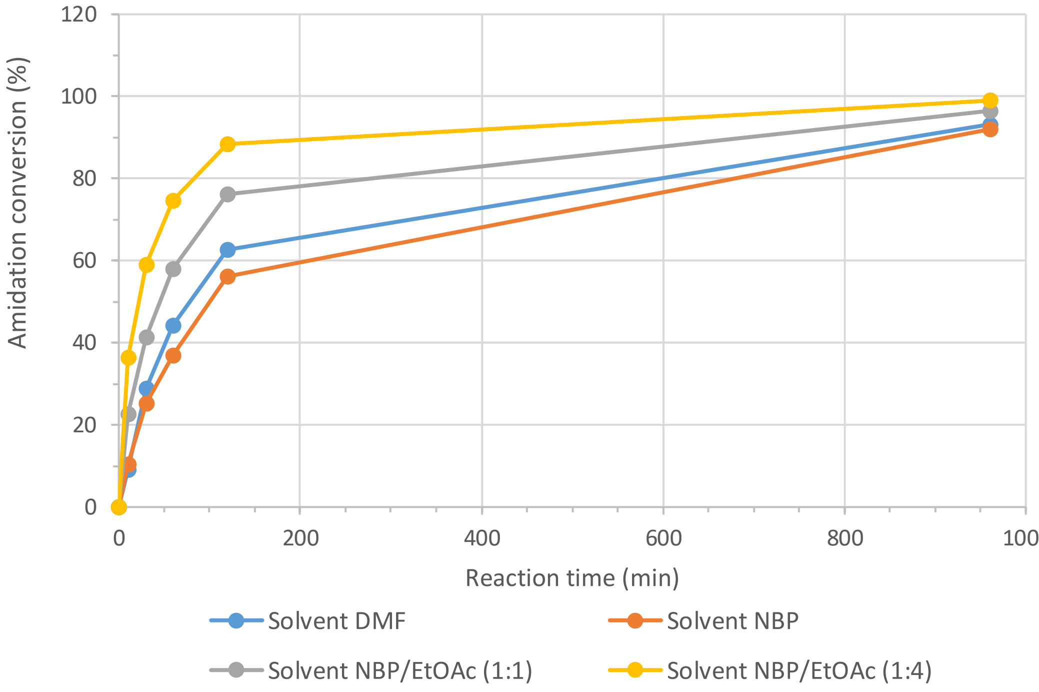

Figure S60. A schematic representation of conversions during Fmoc-Ser(*t*-Bu)-OH/Oxyma/DIC/(S)-(-)-1-phenylethylamine amidation reactions in DMF, NBP, NBP/EtOAc (1:1) and NBP/EtOAc (1:4).

6.2 LC-HRMS analysis of a product of Fmoc-Ser(*t*-Bu)-OH + (S)-(-)-1-phenylethylamine amidation reactions

Experimental conditions described in section 5.2 of this ESI were employed. A sample of the crude product from the amidation in NBP/EtOAc (1:1) after 1 h was analyzed, and the structures of Fmoc-Ser(*t*-Bu)-OH and Fmoc-Ser(*t*-Bu)-(S)-(-)-1-phenylethylamide (product of amidation reaction) were confirmed, see MS spectra in Figures S63 and S64, respectively.

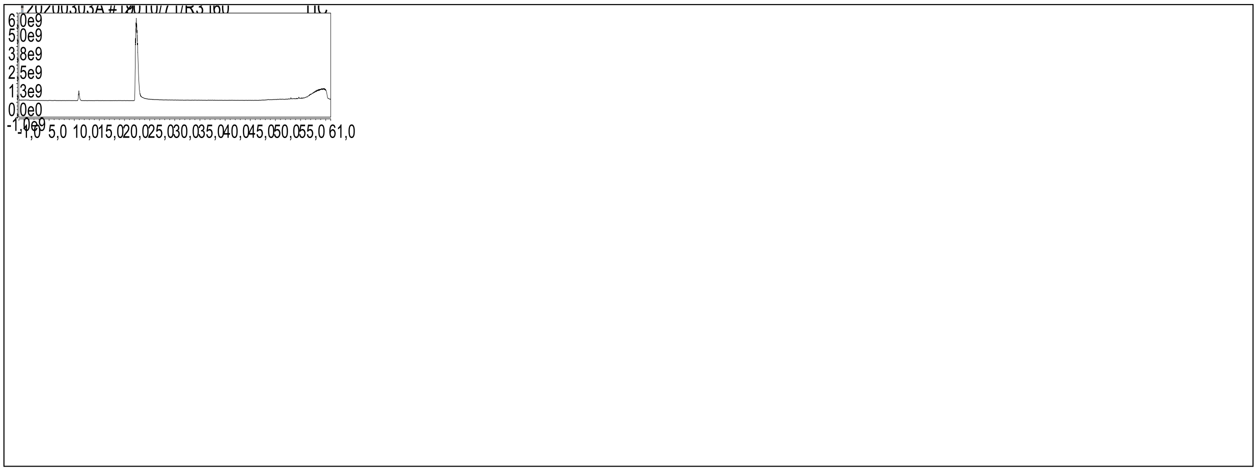

Figure S61. LC-HRMS, total ion count (TIC) overview of the crude product from the amidation in NBP/EtOAc (1:1) after 1 h, Fmoc-Ser(*t*-Bu)-OH (Rt 53.1 min) and Fmoc-Ser(*t*-Bu)-S)-(-)-1-phenylethylamide (Rt 54.7 min) are shown, for MS spectra of these compounds see Figures S63 and S64.

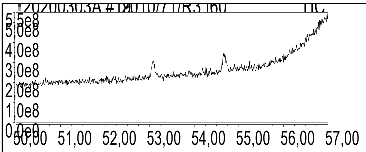

Figure S62. LC-HRMS, TIC zoom-in view of the crude product from the amidation in NBP/EtOAc (1:1) after 1 h, Fmoc-Ser(*t*-Bu)-OH (Rt 53.1 min) and Fmoc-Ser(*t*-Bu)-S)-(-)-1-phenylethylamide (Rt 54.7 min) are shown, for MS spectra of these compounds see Figures S63 and S64.

Table S45. EIC Area% for the integrated peaks in LC-HRMS (TIC) of the crude product from the amidation in NBP/EtOAc (1:1) after 1 h, Fmoc-Ser(*t*-Bu)-OH (Rt 53.1 min) and Fmoc-Ser(*t*-Bu)-(S)-(-)-1-phenylethylamide (Rt 54.7 min) are shown, for MS spectra of these compounds see Figures S63 and S64.

Peak Name	Retention Time (min)	Area (counts*min)	Area (%)
EIC 384,18	53,0736	1981521,4257	28,0
EIC 487,26	54,6695	5096596,5907	72,0
n.d.	n.d.	7078118,0163	100,0

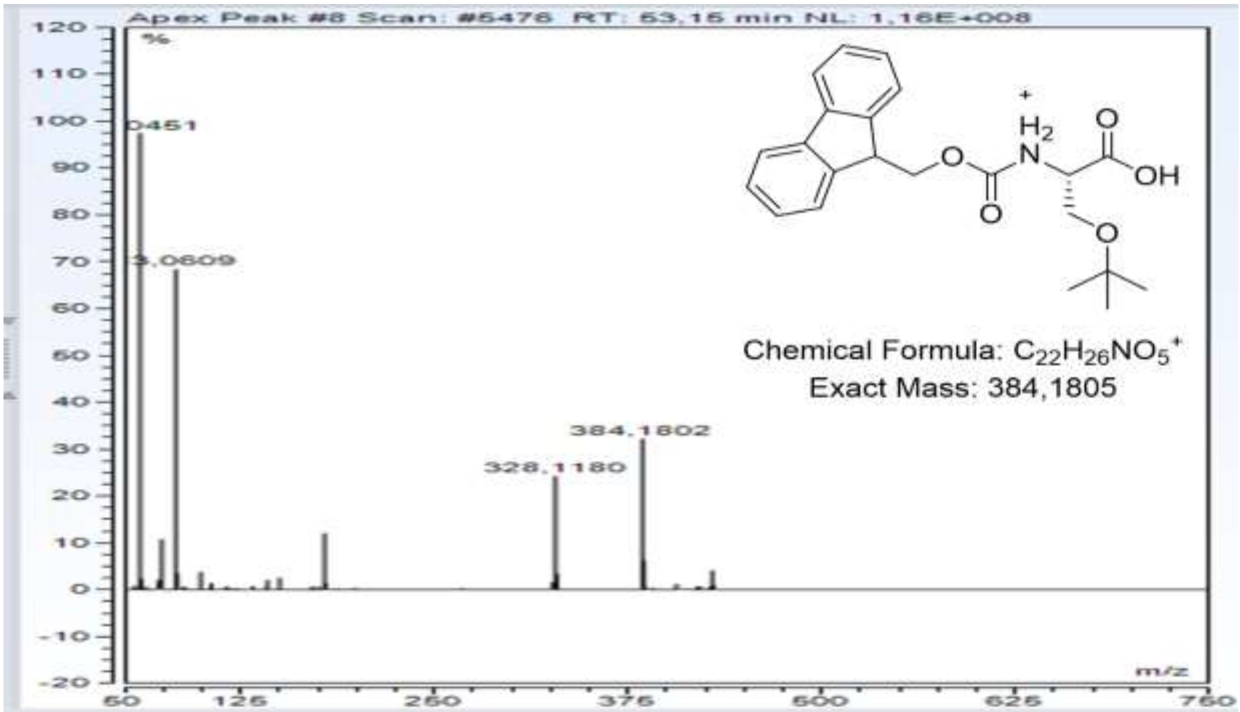

Figure S63. MS spectrum [M+H] of Fmoc-Ser(*t*-Bu)-OH detected in the crude product from the amidation in NBP/EtOAc (1:1) after 1 h.

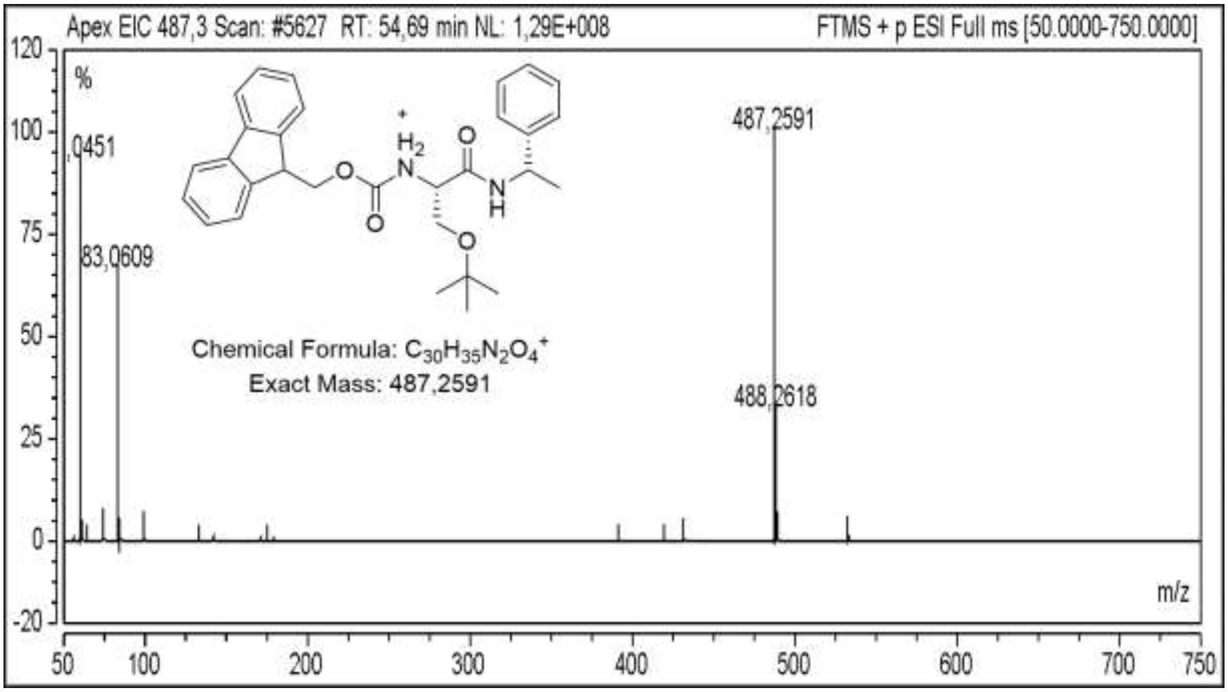

Figure S64. MS spectrum [M+H] of Fmoc-Ser(t-Bu)-S)-(-)-1-phenylethylamide detected in the crude product from the amidation in NBP/EtOAc (1:1) after 1 h.

6.3 LC-HRMS analysis of Oxyma to HCN conversion during Fmoc-Ser(*t*-Bu)-OH + (S)-(-)-1-phenylethylamine amidation reactions

Experimental conditions described in section 5.2 of this ESI were employed. EIC-MS analyses were carried out as previously described.[4] A methodology for determining %Oxyma→HCN conversions based on determining concentration of **3** was used, see section 2 of this ESI.

Table S46. A summary of integrated EIC areas, concentrations of **3** (gL^{-1}), amounts of **3** formed and %Oxyma→HCN conversions during experiments R1 – R4.

Solvent	Reaction time (min)	Rt (min), quantification channel EIC 242,15	Area (counts*min) quantification channel EIC 242,15	gL^{-1} **3**	μmol **3**	%Oxyma->HCN
DMF	10	17,309	1192	0,000253	0,0105	0,0021
NBP	10	17,274	2173	0,000462	0,0192	0,0038
NBP/EtOAc (1:1)	10	17,279	1755	0,000373	0,0155	0,0031
NBP/EtOAc (1:4)	10	17,269	1786	0,000380	0,0157	0,0031
DMF	30	17,315	10280	0,002187	0,0906	0,0181
NBP	30	17,279	5931	0,001262	0,0523	0,0105
NBP/EtOAc (1:1)	30	17,276	5981	0,001272	0,0527	0,0105
NBP/EtOAc (1:4)	30	17,284	4993	0,001062	0,0440	0,0088
DMF	60	17,285	22186	0,004719	0,1956	0,0391
NBP	60	17,281	12894	0,002743	0,1137	0,0227
NBP/EtOAc (1:1)	60	17,286	9641	0,002051	0,0850	0,0170
NBP/EtOAc (1:4)	60	17,311	9836	0,002092	0,0867	0,0173
DMF	120	17,381	60702	0,012913	0,5352	0,1070
NBP	120	17,309	33723	0,007174	0,2973	0,0595
NBP/EtOAc (1:1)	120	17,312	23836	0,005070	0,2101	0,0420
NBP/EtOAc (1:4)	120	17,303	14514	0,003087	0,1280	0,0256
DMF	960	17,310	538200	0,114487	4,7448	0,9490
NBP	960	17,310	268818	0,057184	2,3699	0,4740
NBP/EtOAc (1:1)	960	17,282	99983	0,021269	0,8815	0,1763
NBP/EtOAc (1:4)	960	17,296	42294	0,008997	0,3729	0,0746

Table S47. A summary of %Oxyma→HCN conversions during experiments R1 – R4.

Reaction time (min)	Solvent			
	DMF	NBP	NBP/EtOAc (1:1)	NBP/EtOAc (1:4)
	Oxyma→HCN conversion (%)			
0	0,0000	0,0000	0,0000	0,0000
10	0,0021	0,0038	0,0031	0,0031
30	0,0181	0,0105	0,0105	0,0088
60	0,0391	0,0227	0,0170	0,0173
120	0,1070	0,0595	0,0420	0,0256
960	0,9490	0,4740	0,1763	0,0746

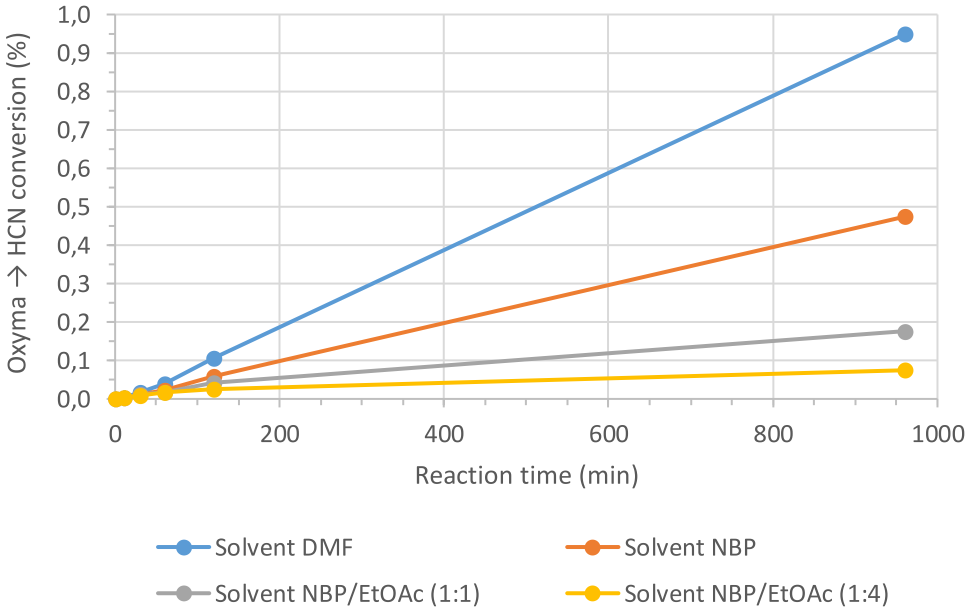

Figure S65. A schematic representation of %Oxyma→HCN conversions during experiments R1 – R4.

7. NMR analysis of HCN formation at different DIC/Oxyma concentrations

HCN is formed during the reaction between DIC and Oxyma. The goal of this section of the ESI was to study this reaction to better understand and minimize the formation of HCN. Two different parameters were studied: first, the influence of the concentration and secondly, the addition of an HCN scavenger, DMTS.

7.1 Assessment of HCN formation in 0.3 M DMF-d_7 solution of Oxyma and DIC

General procedure for Oxyma and DIC reaction.

A solution was prepared by dissolving Oxyma (7.2 mg, 0.051 mmol, 1.0 equiv) and caffeine (2.1 mg, 0.011 mmol, 0.22 equiv) in 170 µL of DMF-d_7. The solution was mixed by using an ultrasound bath. DIC (8.0 µL, 0.051 mmol, 1.0 equiv) was added to the solution. The latter was transferred into a 3 mm NMR tube and transferred to the spectrometer for monitoring at 20°C. 1D ^{1}H NMR acquisition was done after 1 h, 5 h, 10 h and 16 h.

Method used to calculate the ratio of HCN vs oxadiazole 3.

1)The calibration was done on the signal of Hb at 4.70 ppm (Figure S66), which corresponds to 1 proton.

2) Singlet at 6.21 ppm, corresponding to Ha, was integrated and it gives the ratio between **3** and HCN (Figure S67).

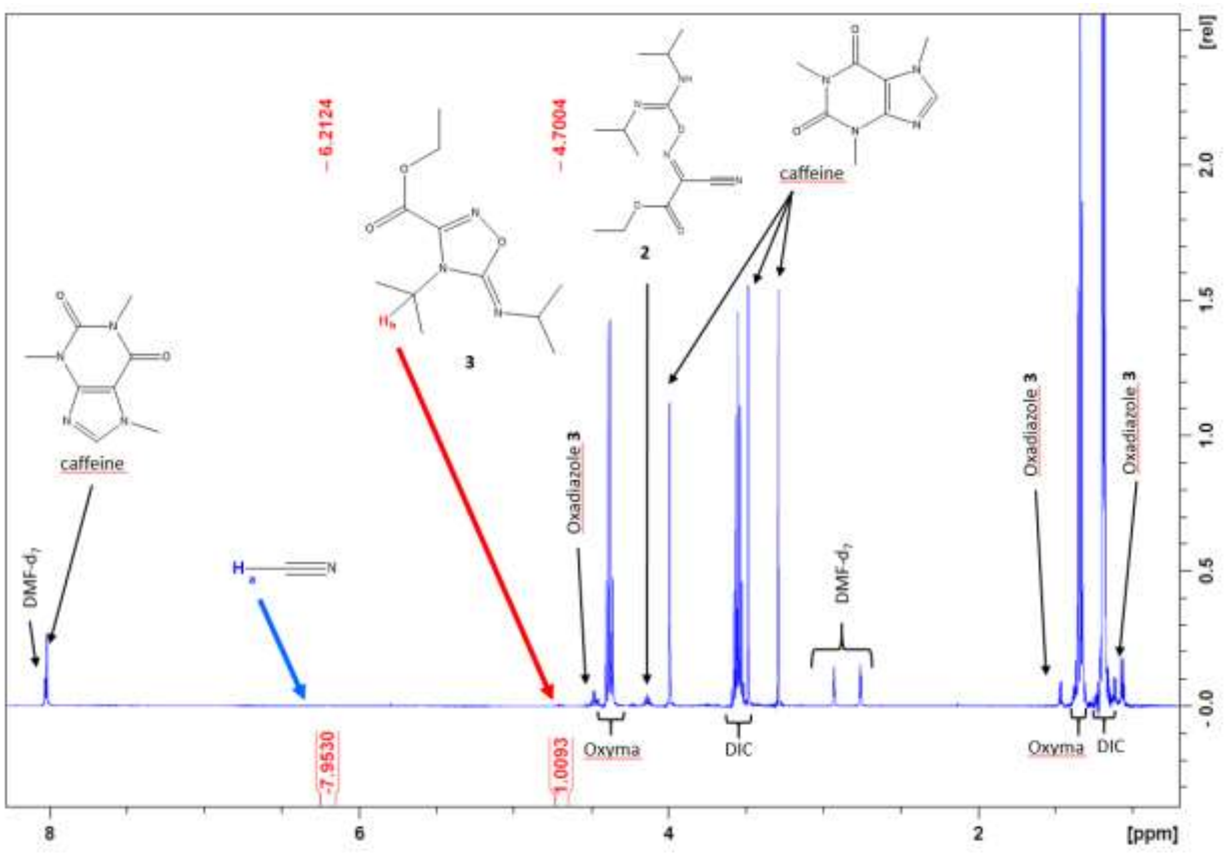

Figure S66. 1D ^1H NMR spectrum of DIC/Oxyma reaction at 0.3M after 1 h in DMF-d_7 (full spectrum).

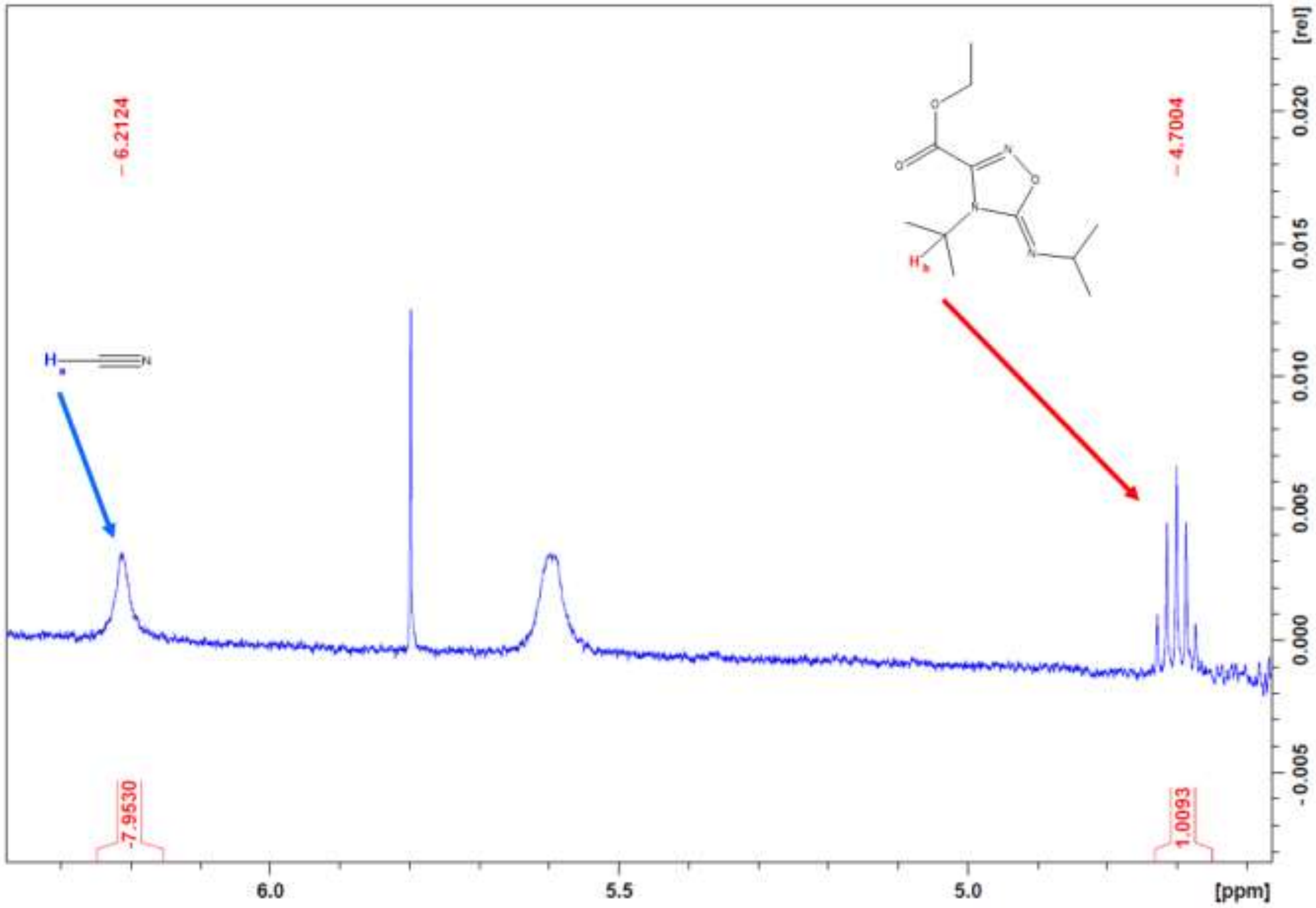

Figure S67. 1D ^{1}H NMR spectrum of DIC/Oxyma reaction at 0.3M after 1 h in DMF-d_7 (zoom-in).

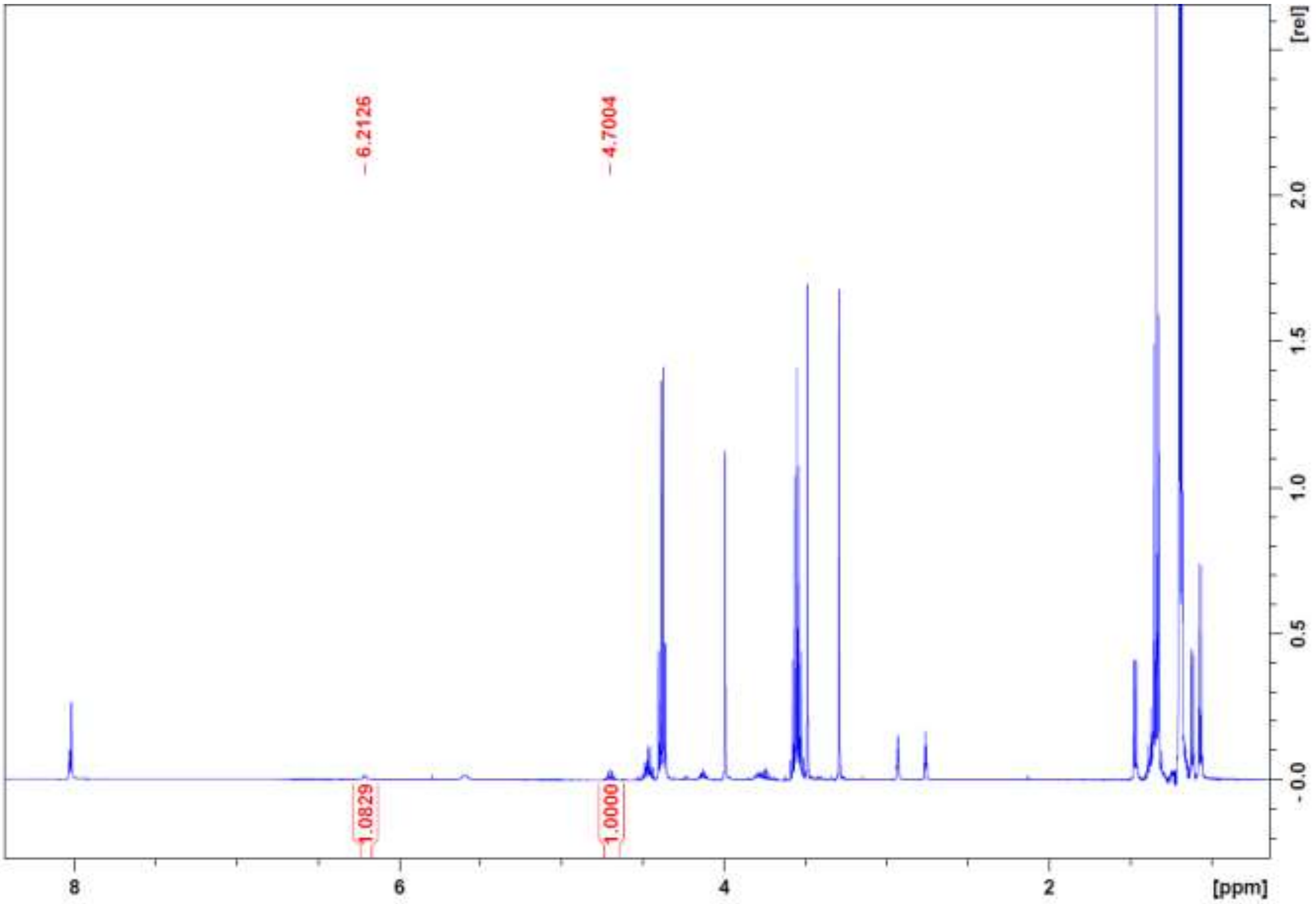

Figure S68. 1D ^{1}H NMR spectrum of DIC/Oxyma reaction at 0.3M after 5 h in DMF-d_7 (full spectrum).

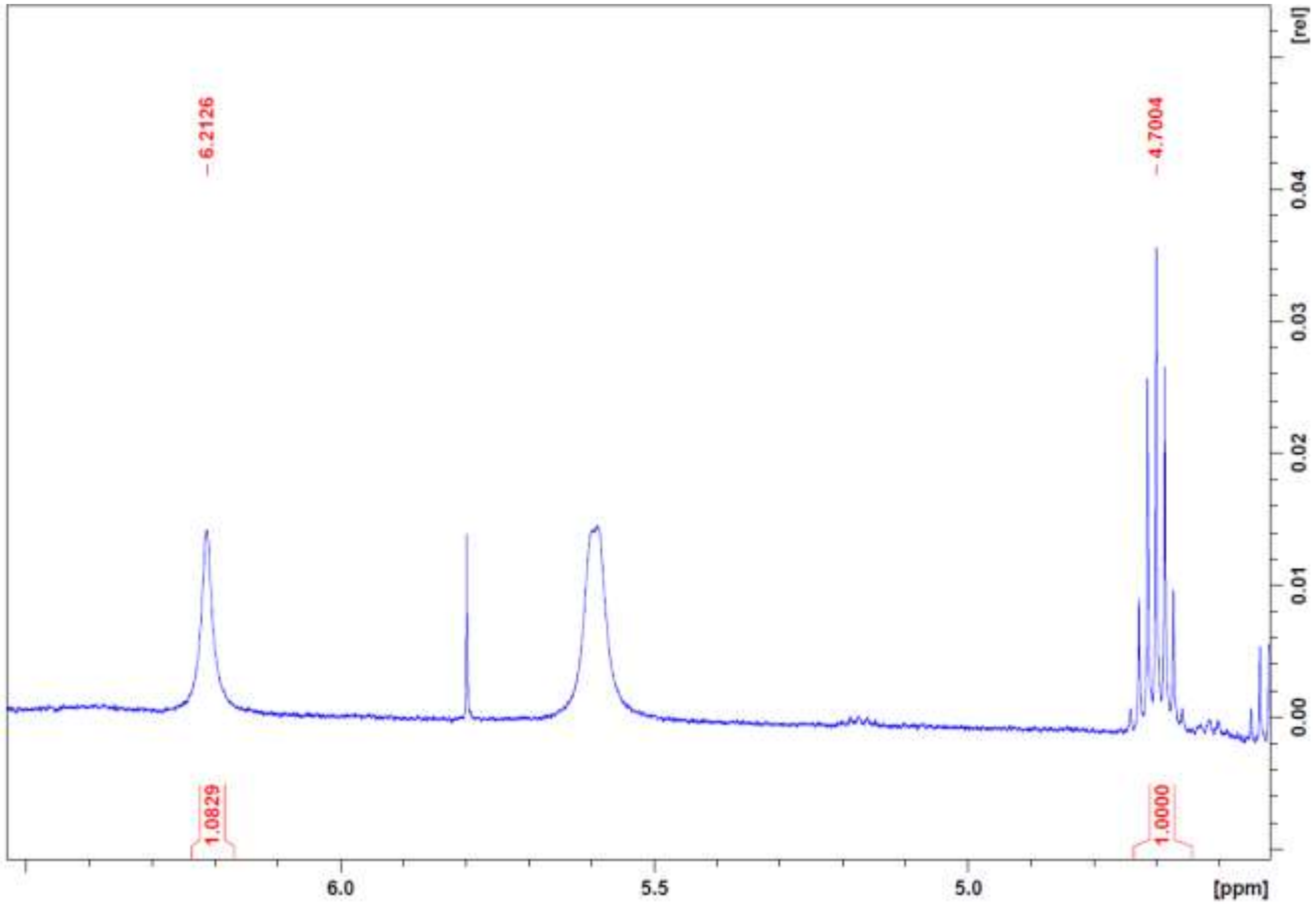

Figure S69. 1D ^{1}H NMR spectrum of DIC/Oxyma reaction at 0.3M after 5 h in DMF-d_7 (zoom-in).

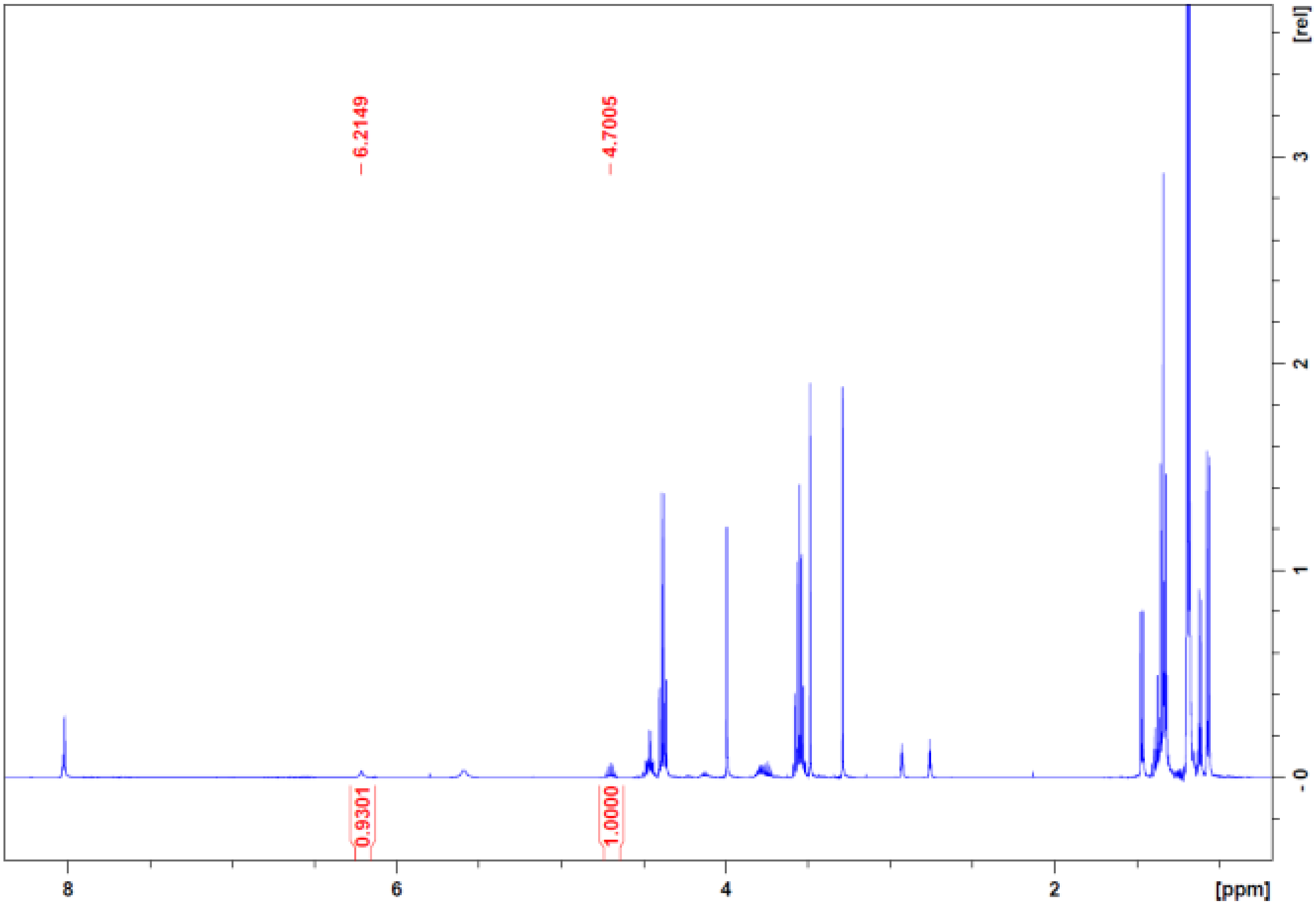

Figure S70. 1D ^{1}H NMR spectrum of DIC/Oxyma reaction at 0.3M after 10 h in DMF-d_7 (full spectrum).

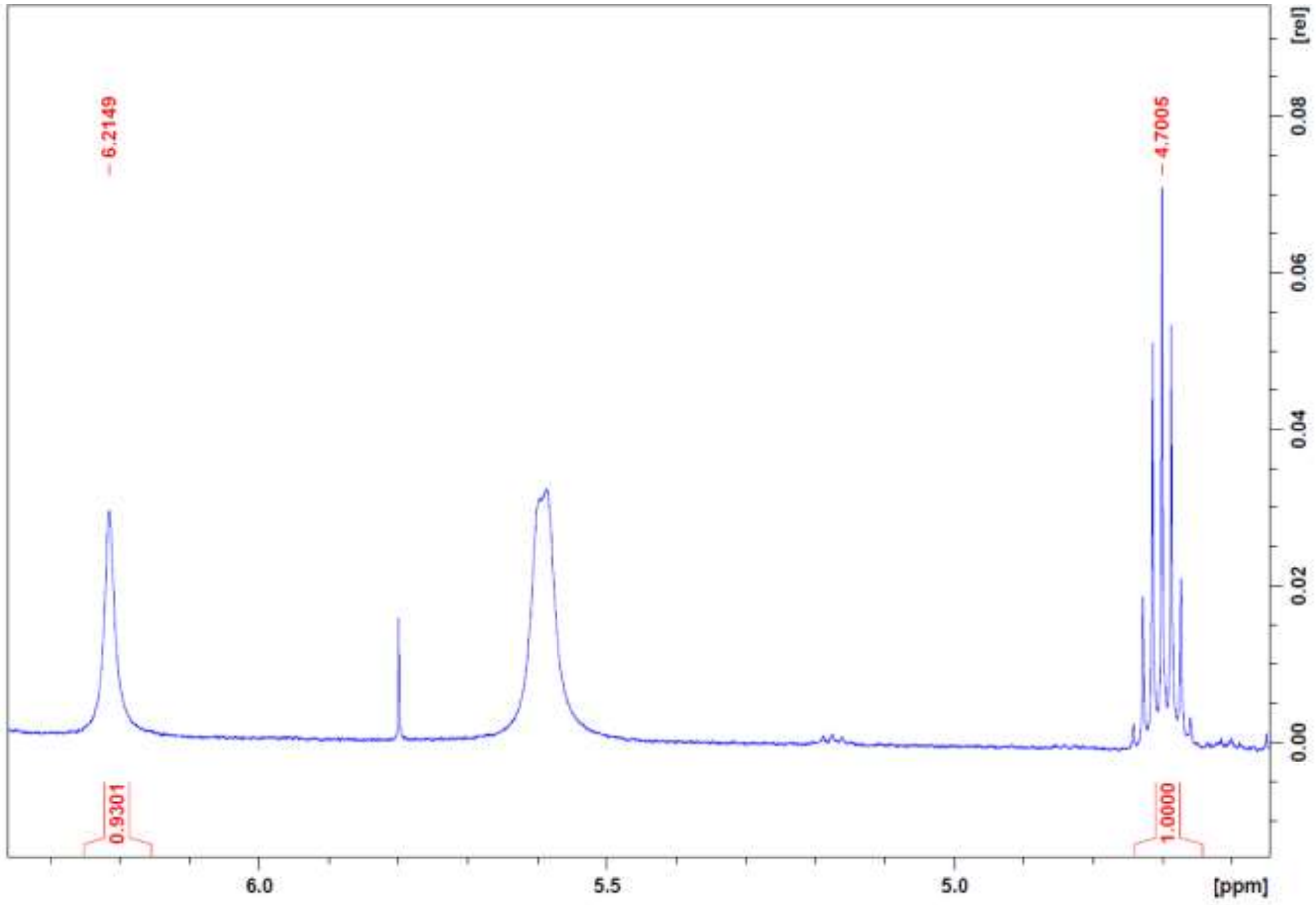

Figure S71. 1D ^{1}H NMR spectrum of DIC/Oxyma reaction at 0.3M after 10 h in DMF-d_7 (zoom-in).

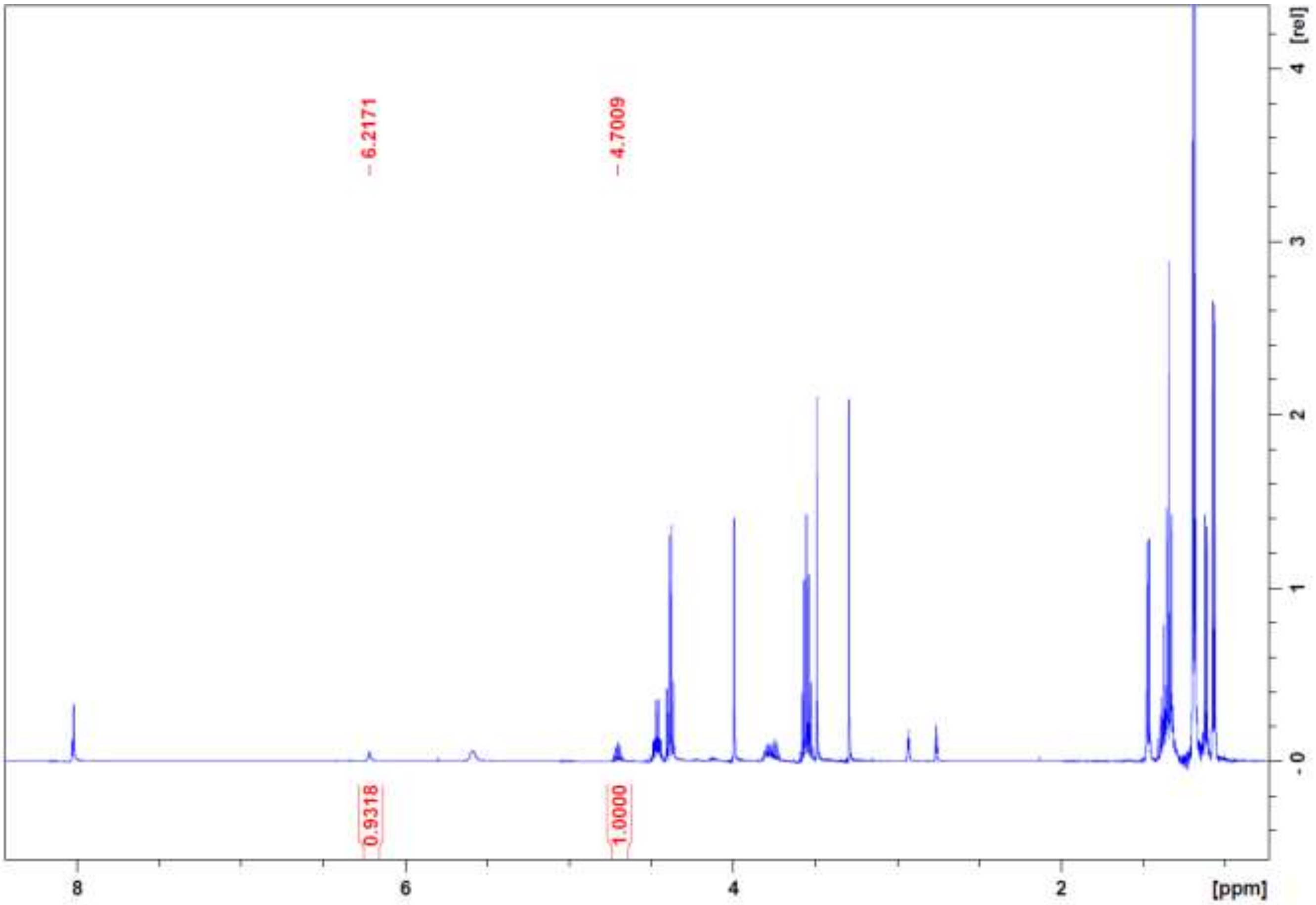

Figure S72. 1D ^{1}H NMR spectrum of DIC/Oxyma reaction at 0.3M after 16 h in DMF-d_7 (full spectrum).

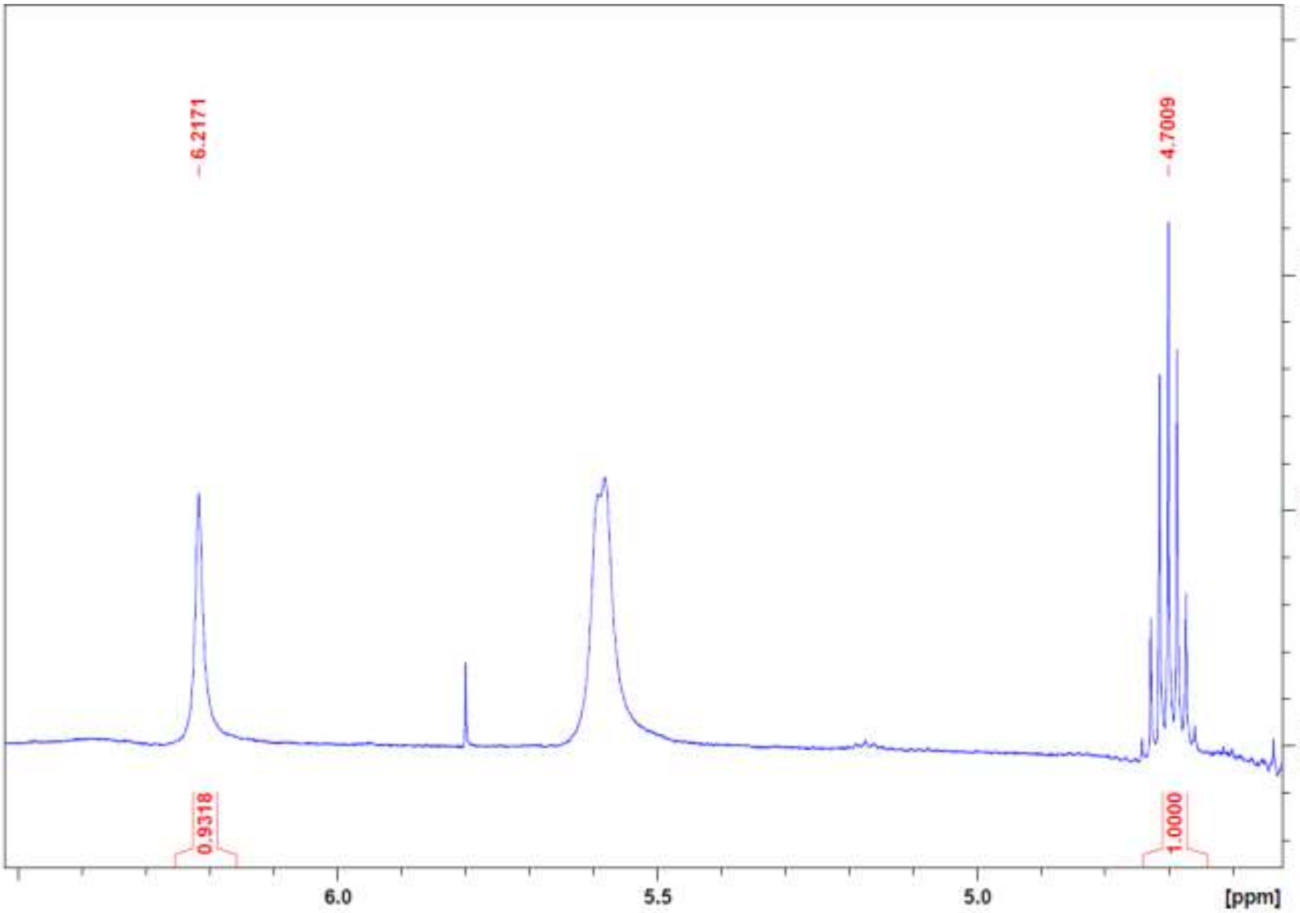

Figure S73. 1D ^{1}H NMR spectrum of DIC/Oxyma reaction at 0.3M after 16 h in DMF-d_7 (zoom-in).

7.2 Assessment of HCN formation in 0.4 M DMF-d_7 solution of Oxyma and DIC

The general procedure for the reactions of DIC and Oxyma in DMF-d_7 as described in the section 7.1 of this ESI was followed. The following amounts of starting materials were used: Oxyma (9.7 mg, 0.068 mmol, 1.0 equiv), caffeine (2.5 mg, 0.013 mmol, 0.19 equiv), DIC (10.7 µL, 0.068 mmol, 1.0 equiv).

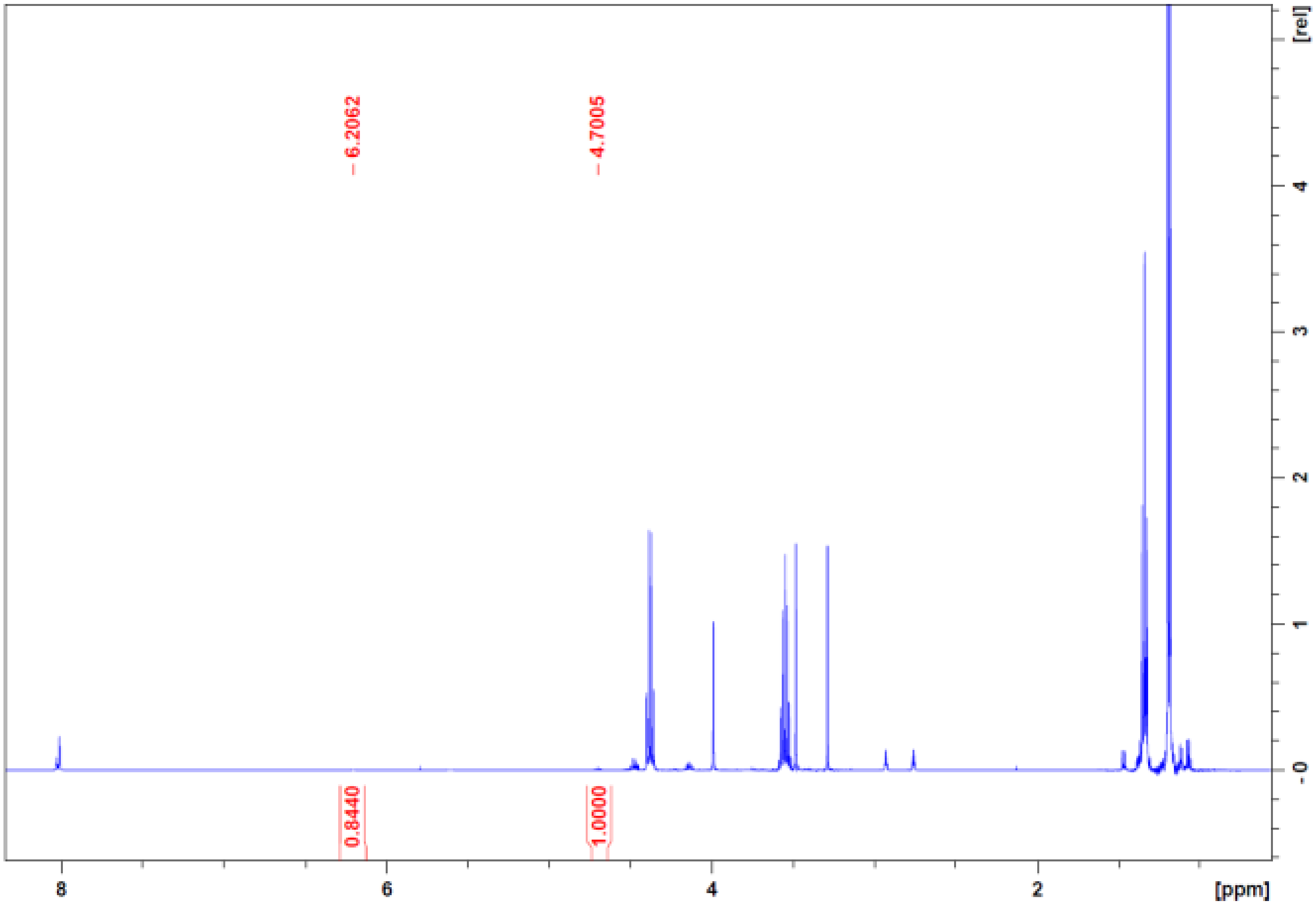

Figure S74. 1D ^{1}H NMR spectrum of DIC/Oxyma reaction at 0.4M after 1h in DMF-d_7 (full spectrum).

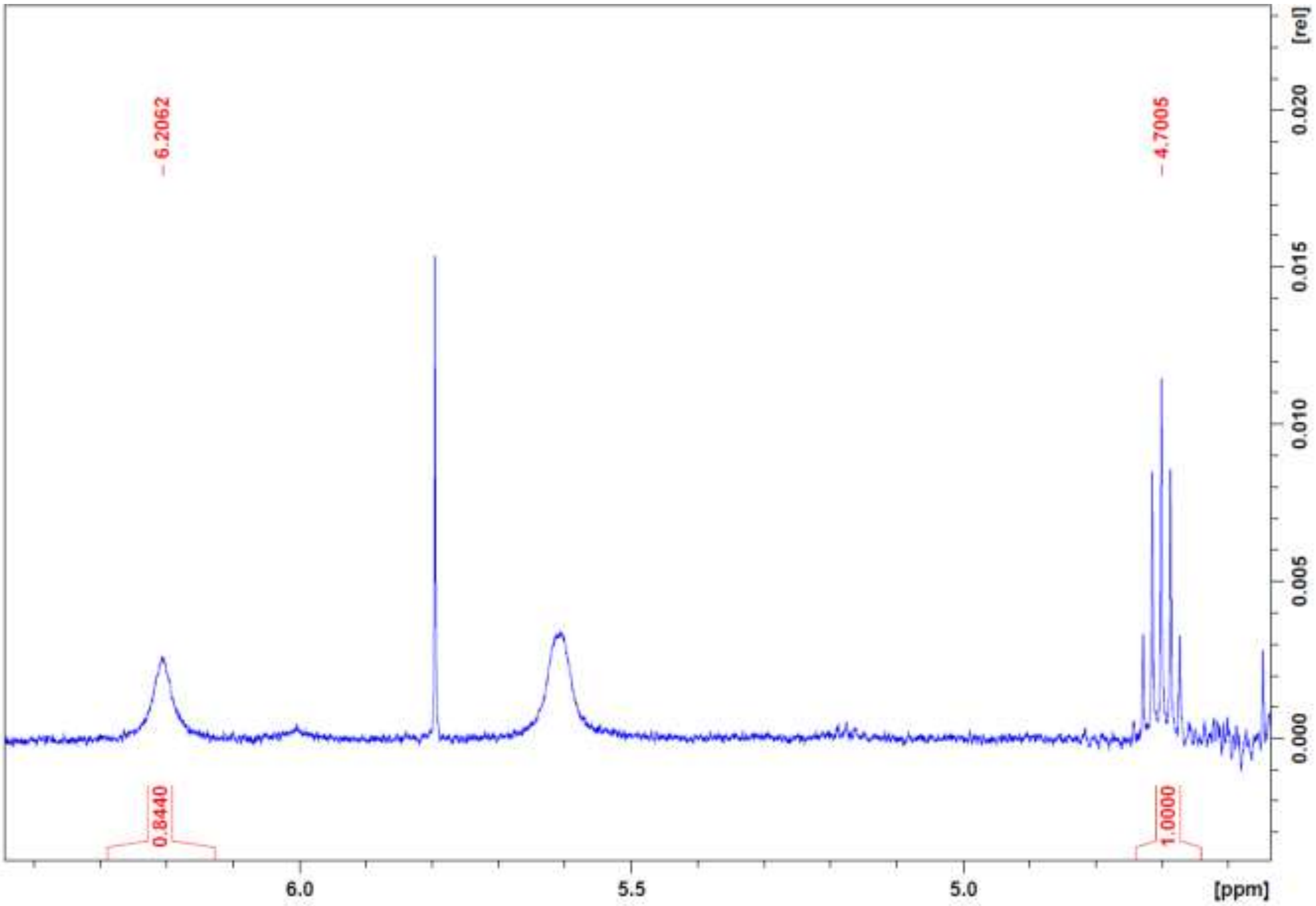

Figure S75. 1D ^{1}H NMR spectrum of DIC/Oxyma reaction at 0.4M after 1h in DMF-d_7 (zoom-in).

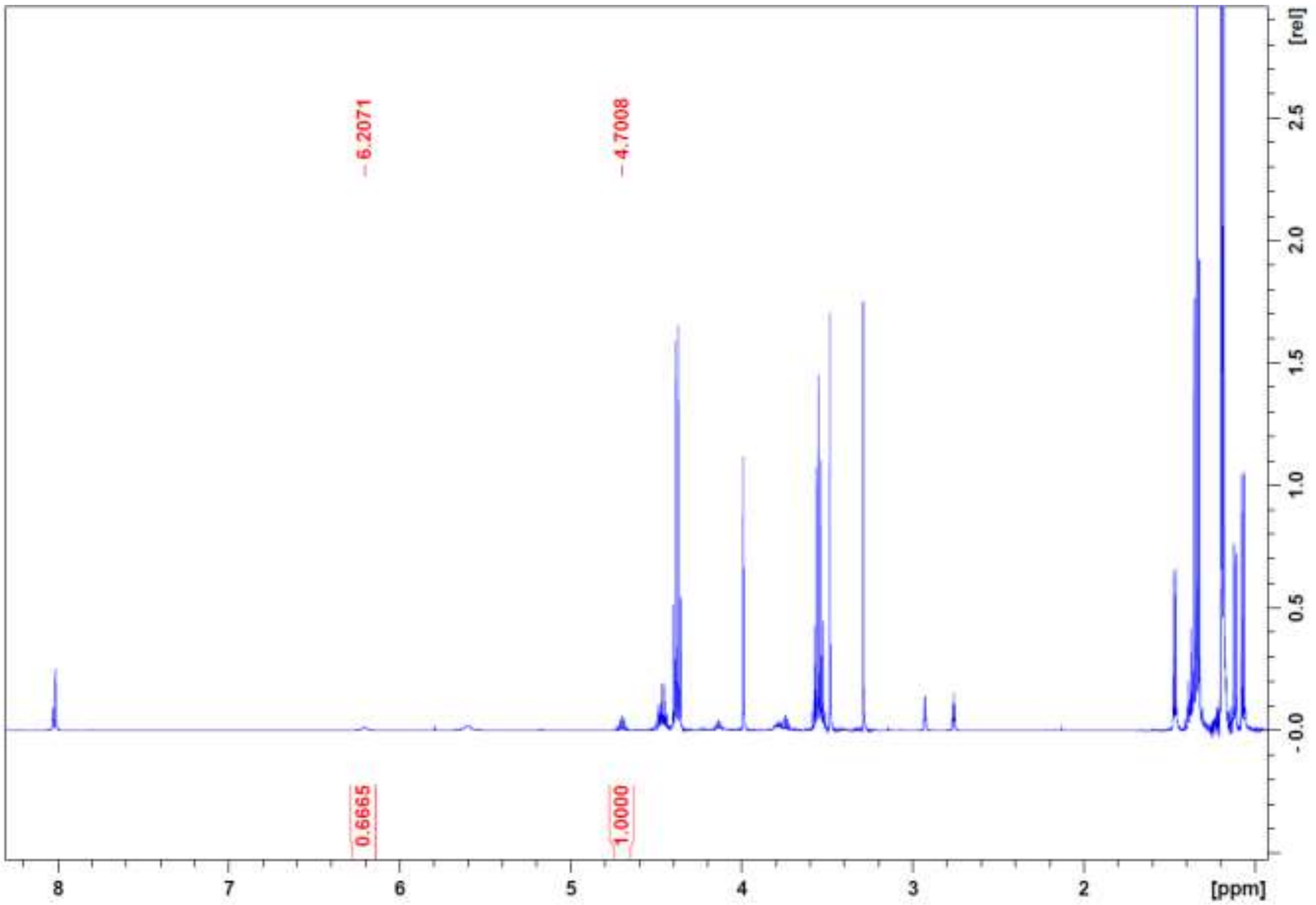

Figure S76. 1D ^{1}H NMR spectrum of DIC/Oxyma reaction at 0.4M after 5 h in DMF-d_7 (full spectrum).

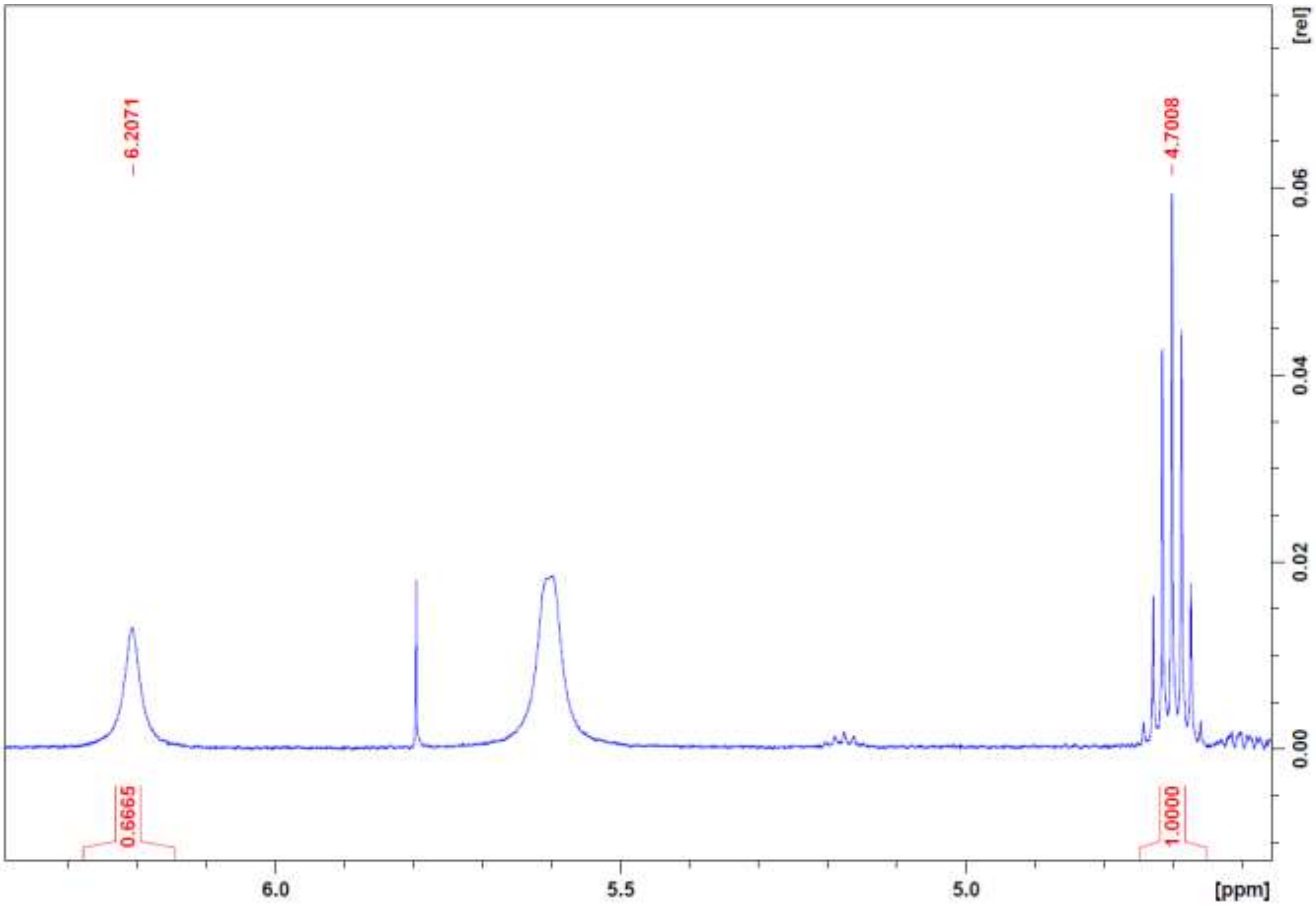

Figure S77. 1D ^{1}H NMR spectrum of DIC/Oxyma reaction at 0.4M after 5 h in DMF-d_7 (zoom-in).

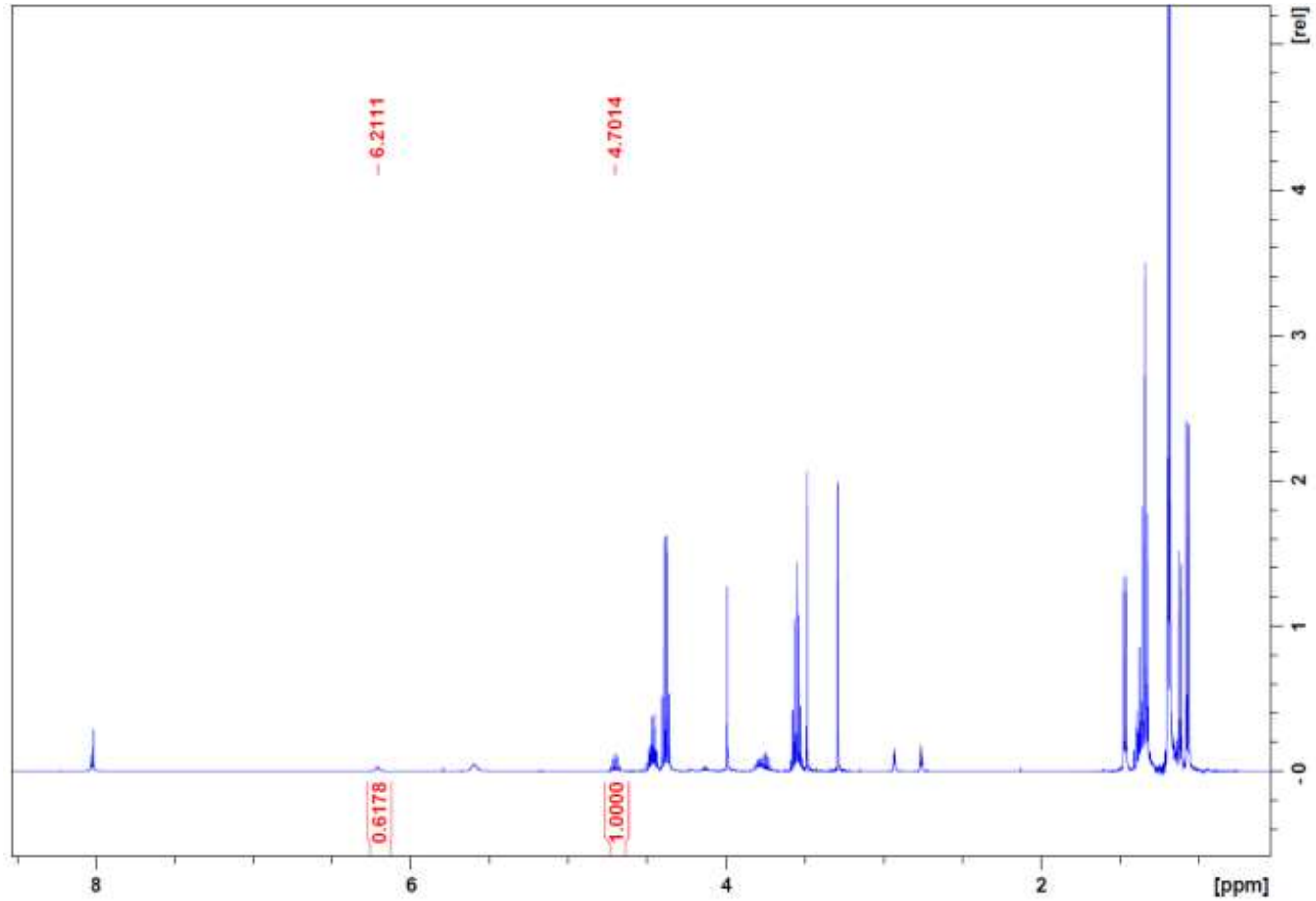

Figure S78. 1D ^{1}H NMR spectrum of DIC/Oxyma reaction at 0.4M after 10 h in DMF-d_7 (full spectrum).

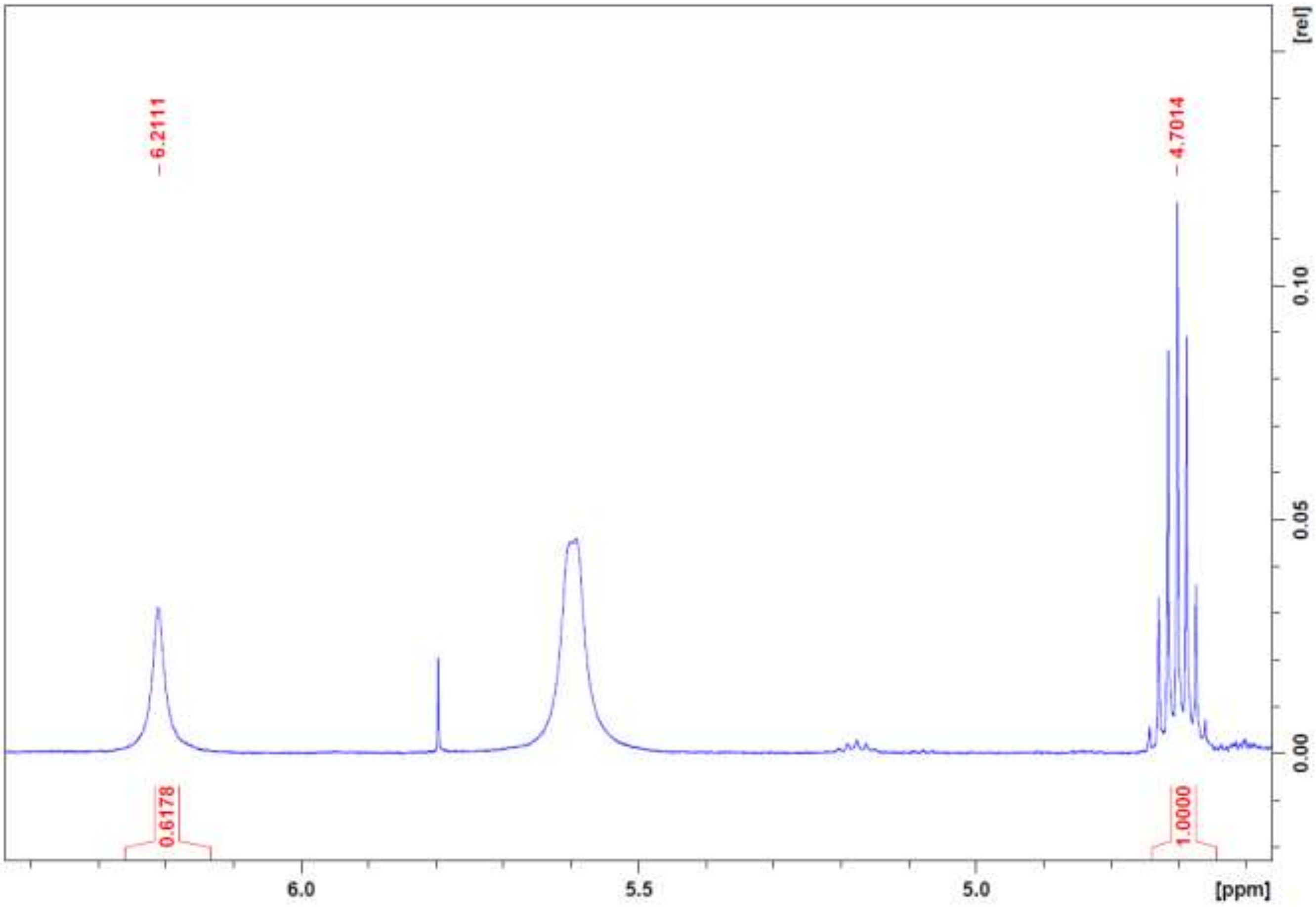

Figure S79. 1D ^{1}H NMR spectrum of DIC/Oxyma reaction at 0.4M after 10 h in DMF-d_7 (zoom-in).

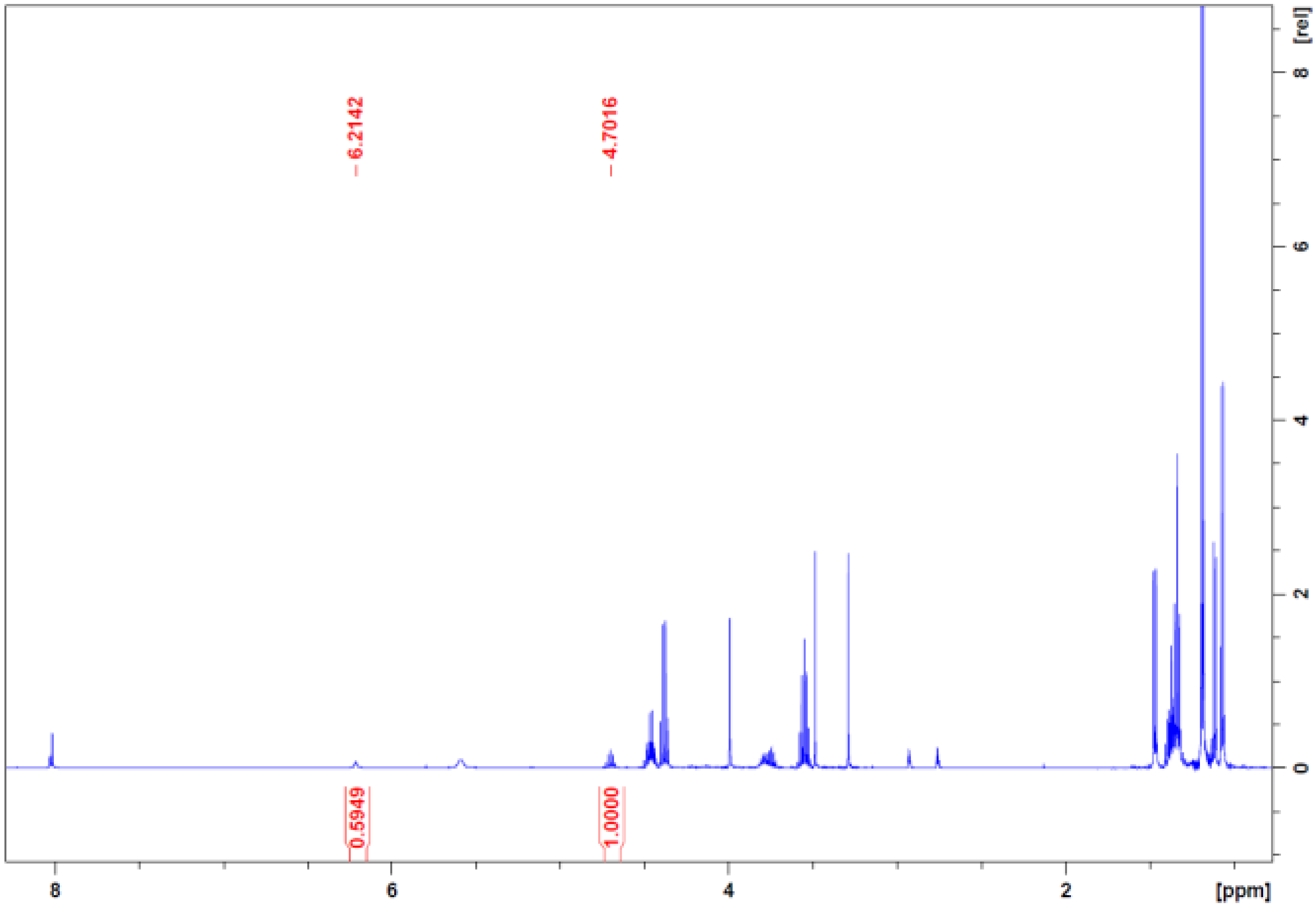

Figure S80. 1D ^{1}H NMR spectrum of DIC/Oxyma reaction at 0.4M after 16 h in DMF-d_7 (full spectrum).

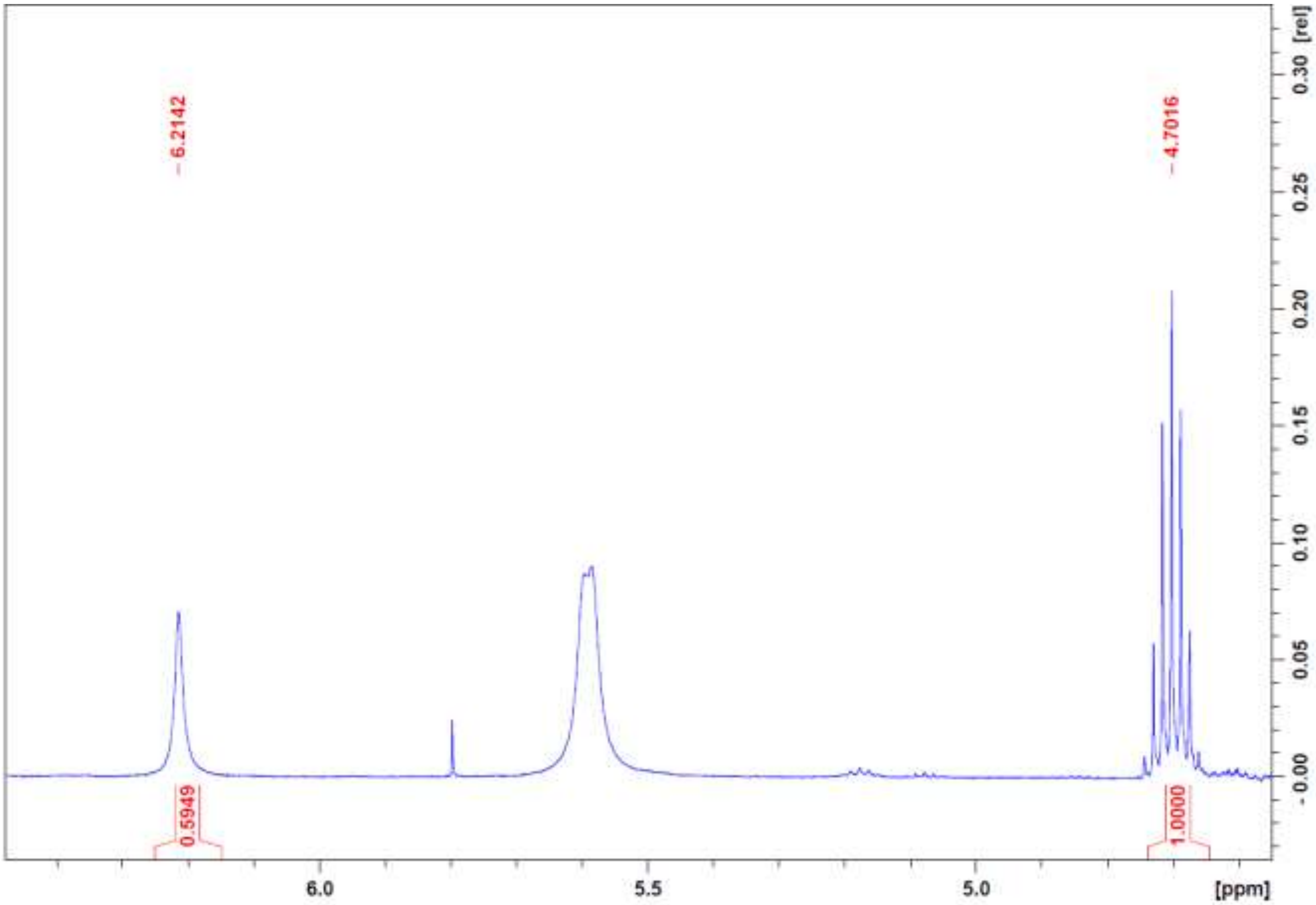

Figure S81. 1D ^{1}H NMR spectrum of DIC/Oxyma reaction at 0.4M after 16 h in DMF-d_7 (zoom-in).

7.3 Assessment of HCN formation in 0.5 M DMF-d_7 solution of Oxyma and DIC

The general procedure for the reactions of DIC and Oxyma in DMF-d_7 as described in the section 7.1 of this ESI was followed. The following amounts of starting materials were used: Oxyma (12.5 mg, 0.088 mmol, 1.03 equiv), caffeine (2.1 mg, 0.011 mmol, 0.13 equiv), DIC (13.3 µL, 0.085 mmol, 1.00 equiv).

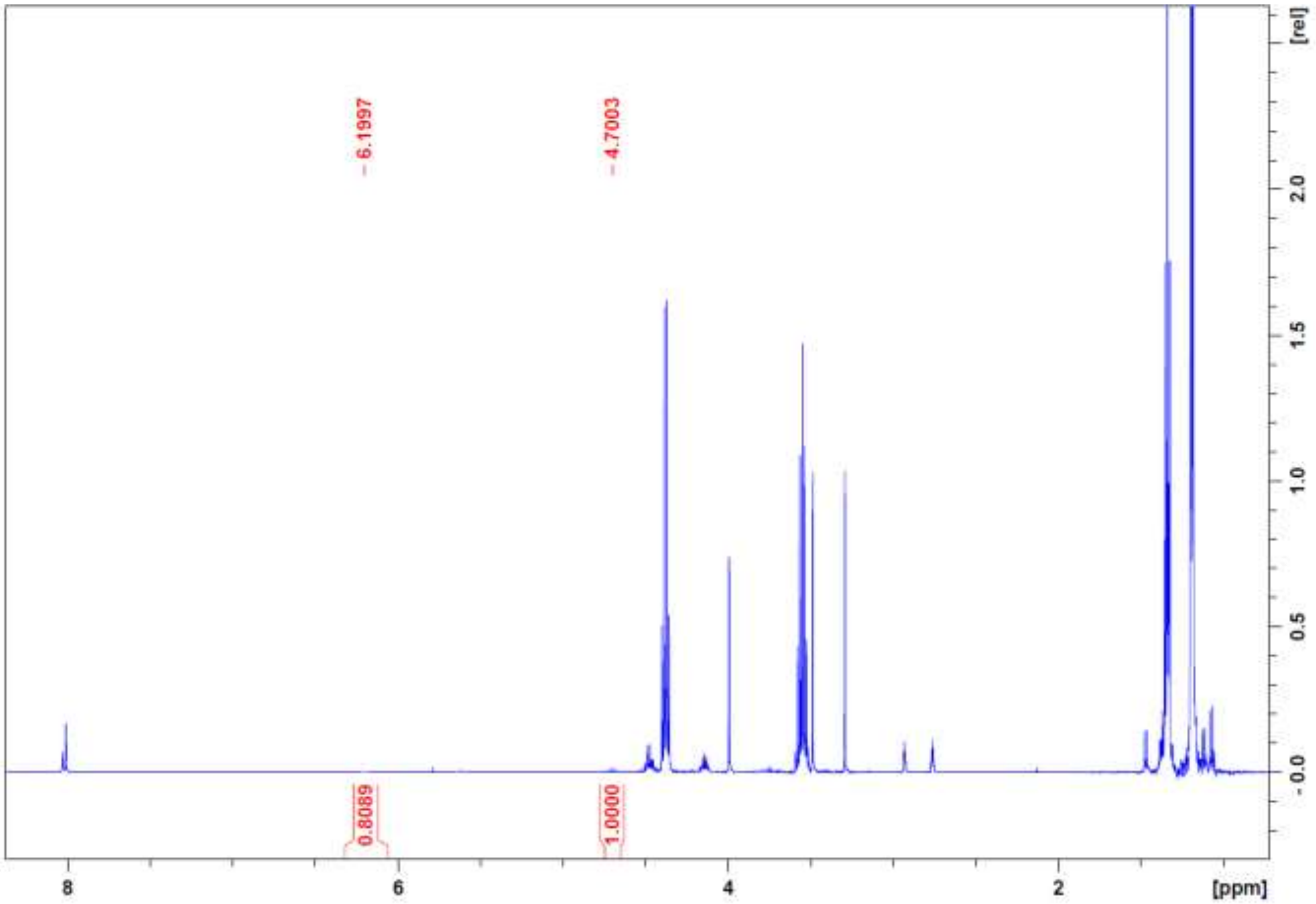

Figure S82. 1D ^{1}H NMR spectrum of DIC/Oxyma reaction at 0.5M after 1 h in DMF-d_7 (full spectrum).

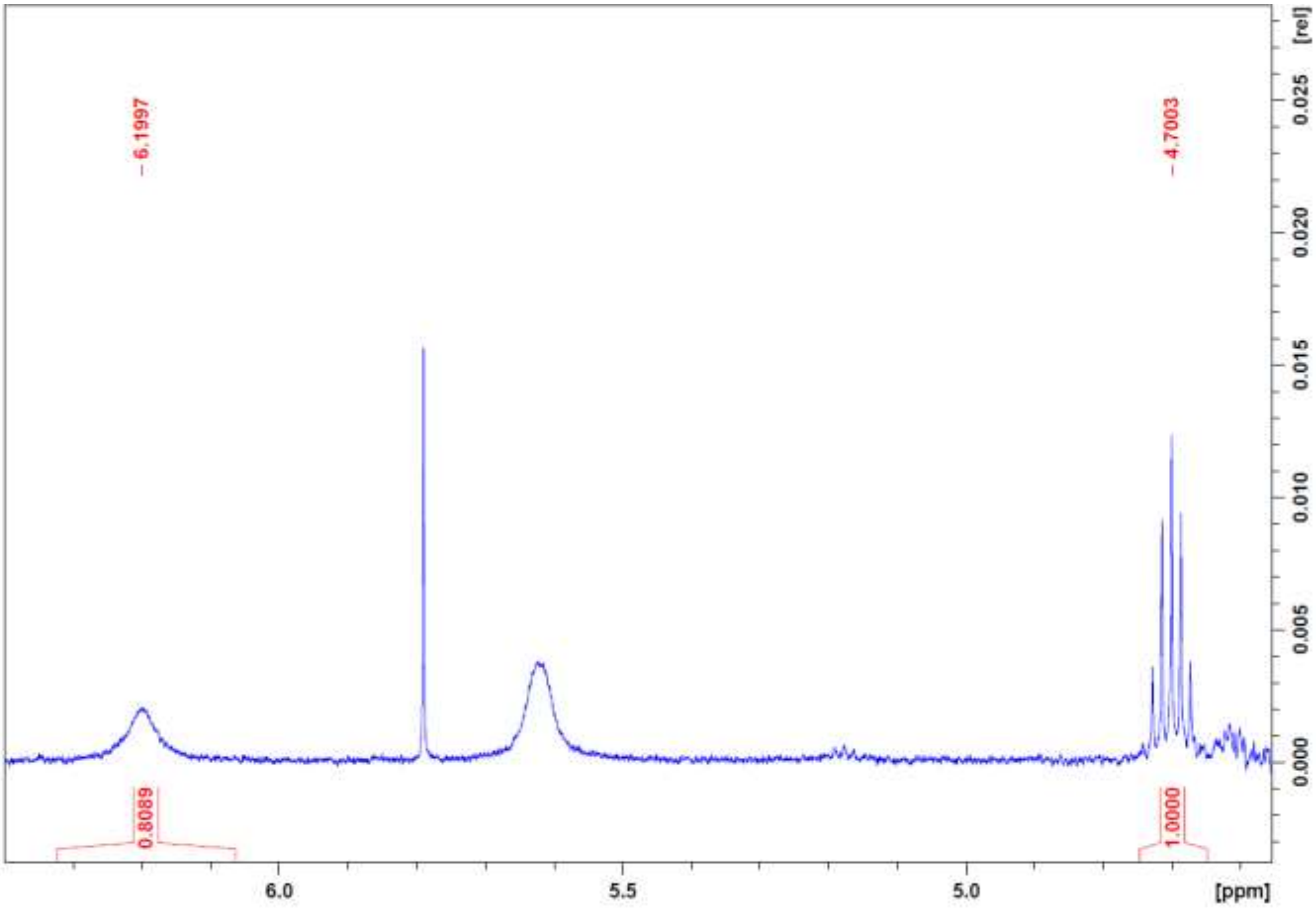

Figure S83. 1D ^{1}H NMR spectrum of DIC/Oxyma reaction at 0.5M after 1 h in DMF-d_7 (zoom-in).

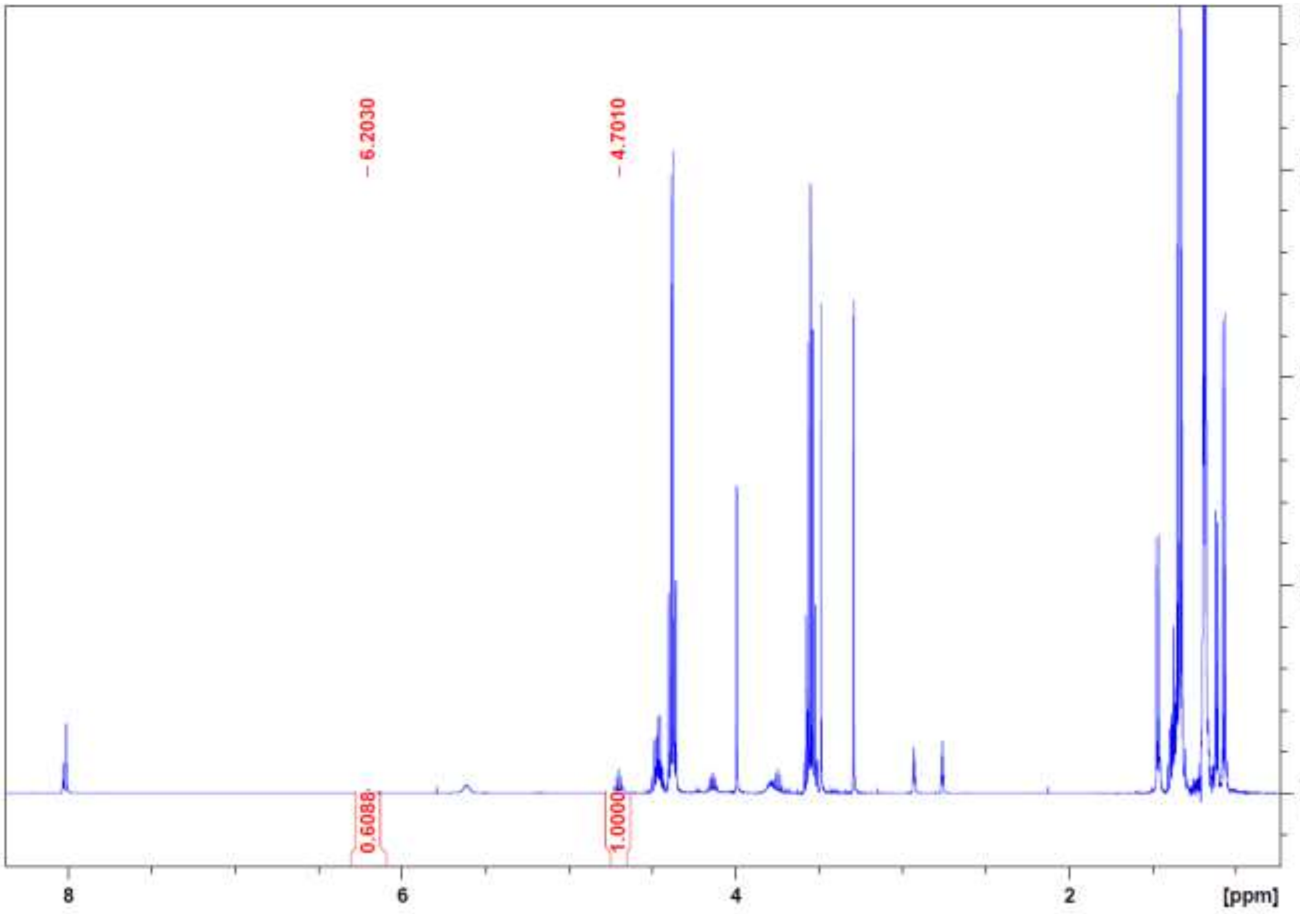

Figure S84. 1D ^{1}H NMR spectrum of DIC/Oxyma reaction at 0.5M after 5 h in DMF-d_7 (full spectrum).

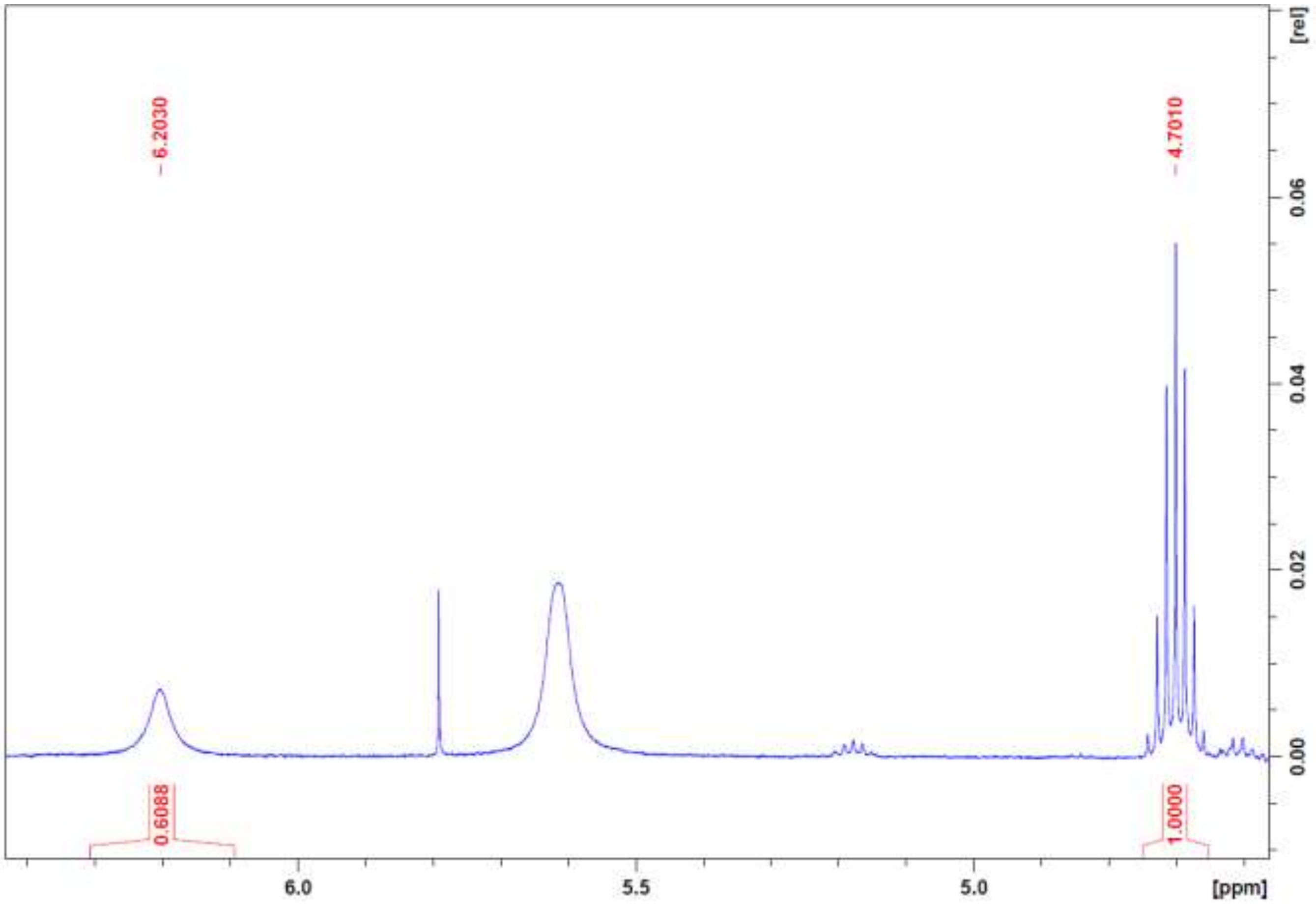

Figure S85. 1D ^{1}H NMR spectrum of DIC/Oxyma reaction at 0.5M after 5 h in DMF-d_7 (zoom-in).

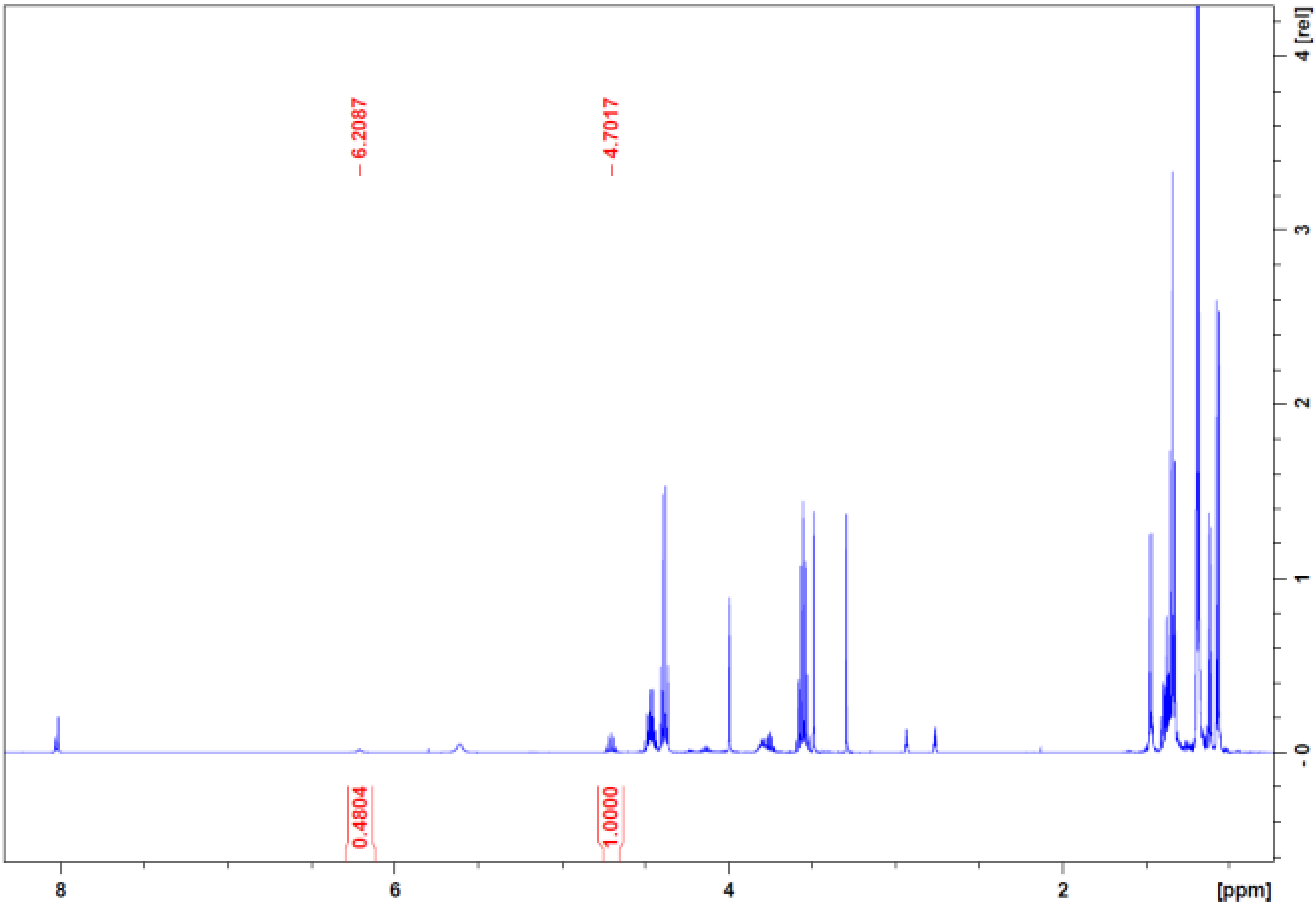

Figure S86. 1D ^{1}H NMR spectrum of DIC/Oxyma reaction at 0.5M after 10 h in DMF-d_7 (full spectrum).

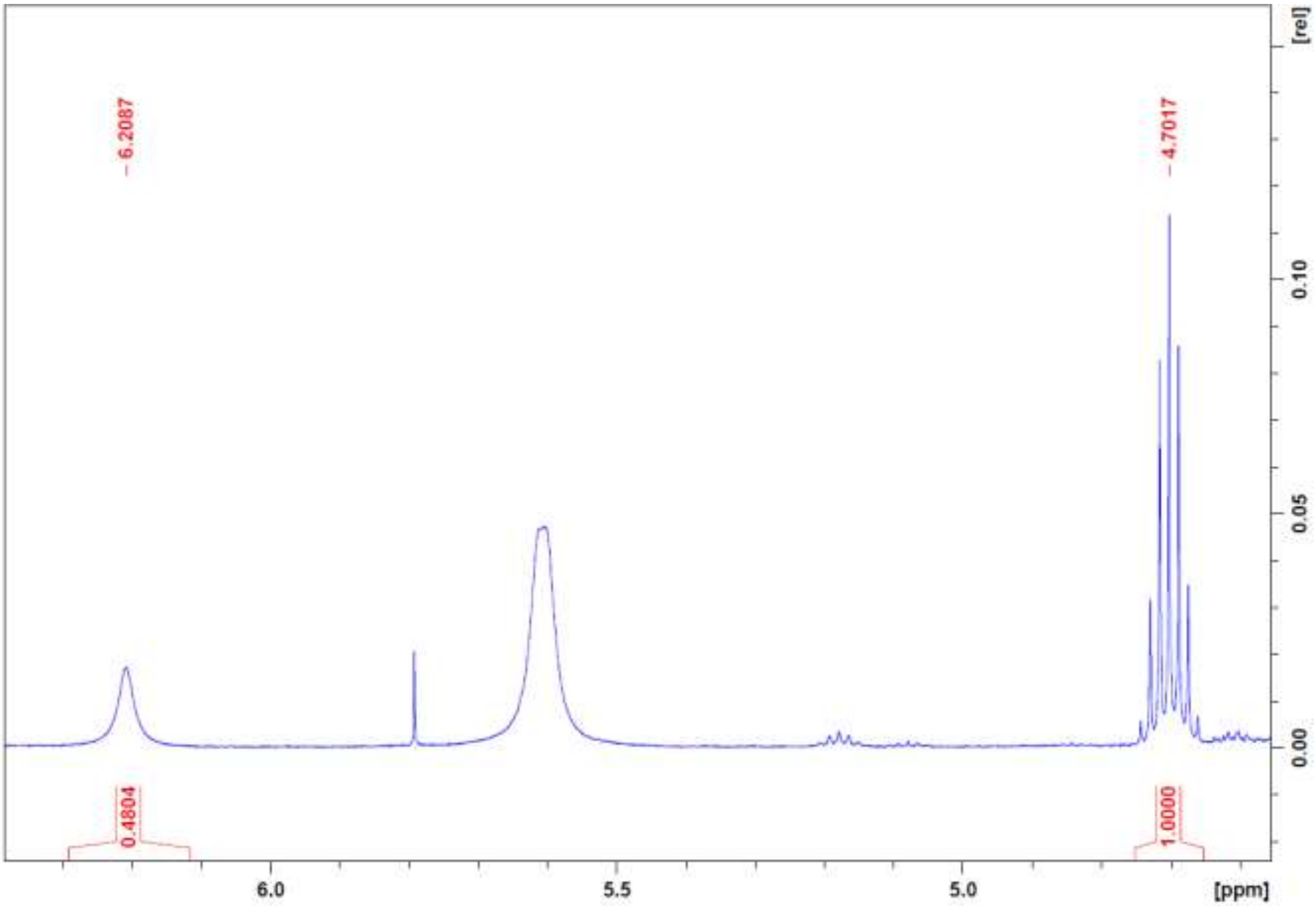

Figure S87. 1D ^{1}H NMR spectrum of DIC/Oxyma reaction at 0.5M after 10 h in DMF-d_7 (zoom-in).

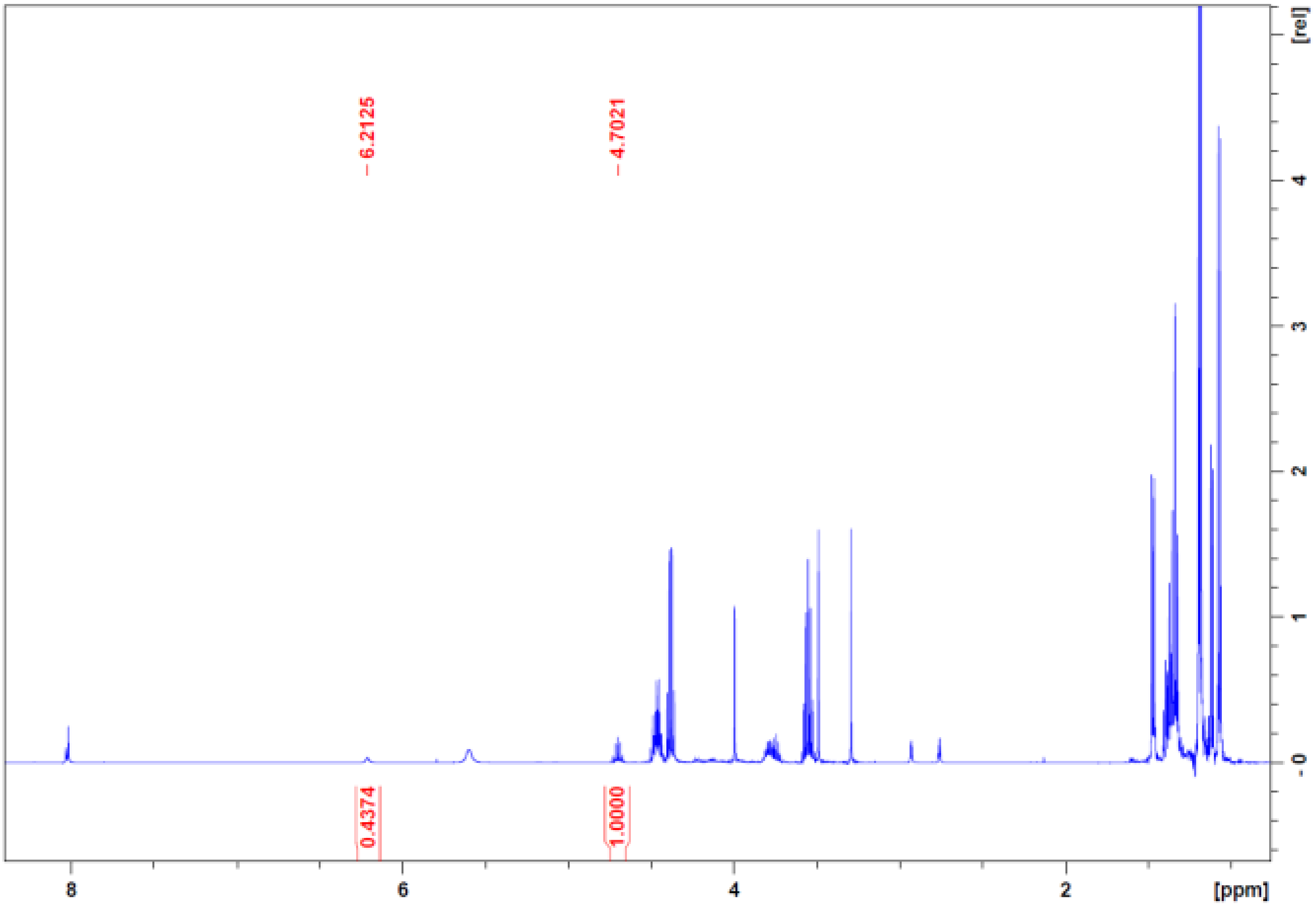

Figure S88. 1D ^{1}H NMR spectrum of DIC/Oxyma reaction at 0.5M after 16 h in DMF-d_7 (full spectrum).

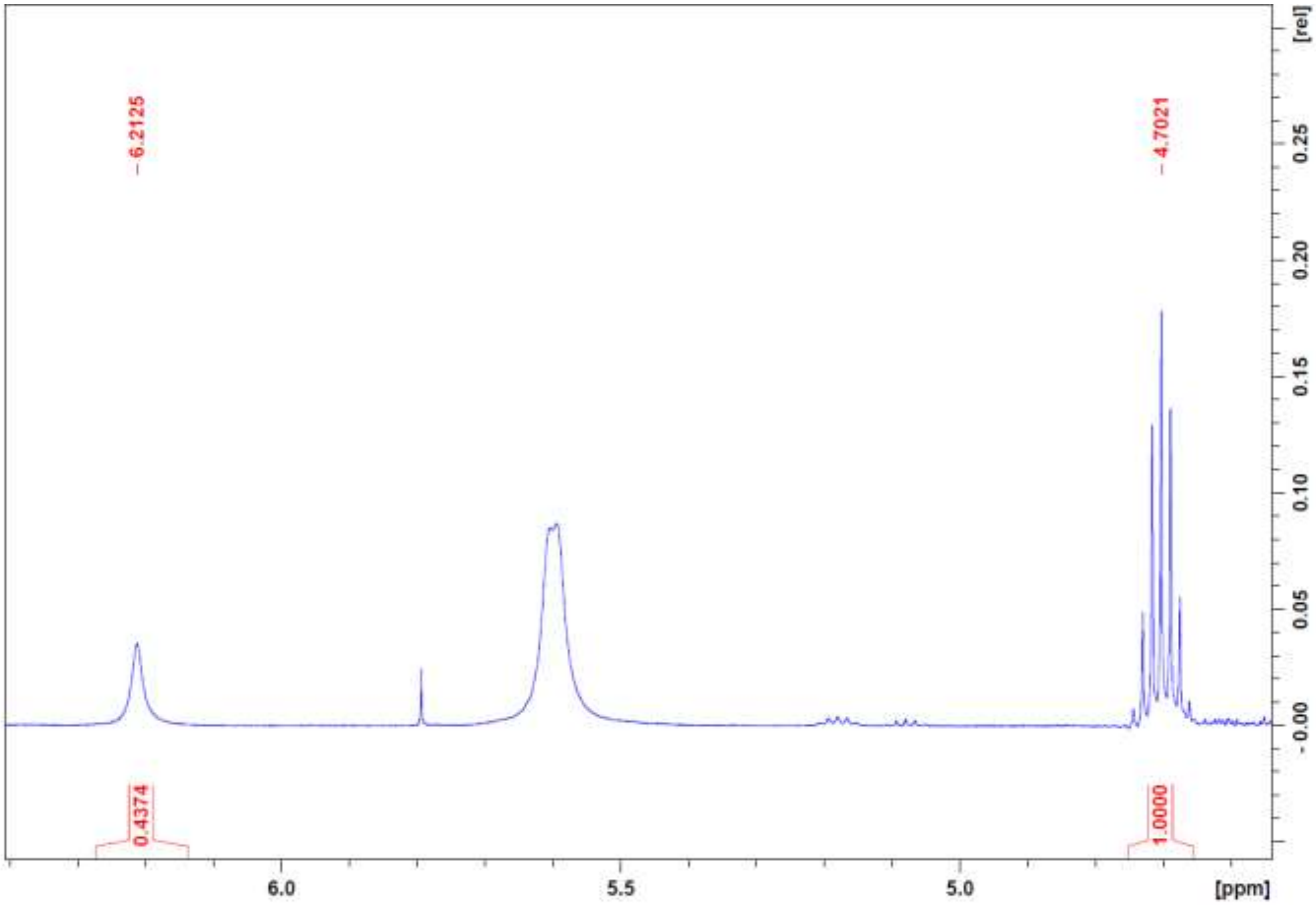

Figure S89. 1D ^{1}H NMR spectrum of DIC/Oxyma reaction at 0.5M after 16 h in DMF-d_7 (zoom-in).

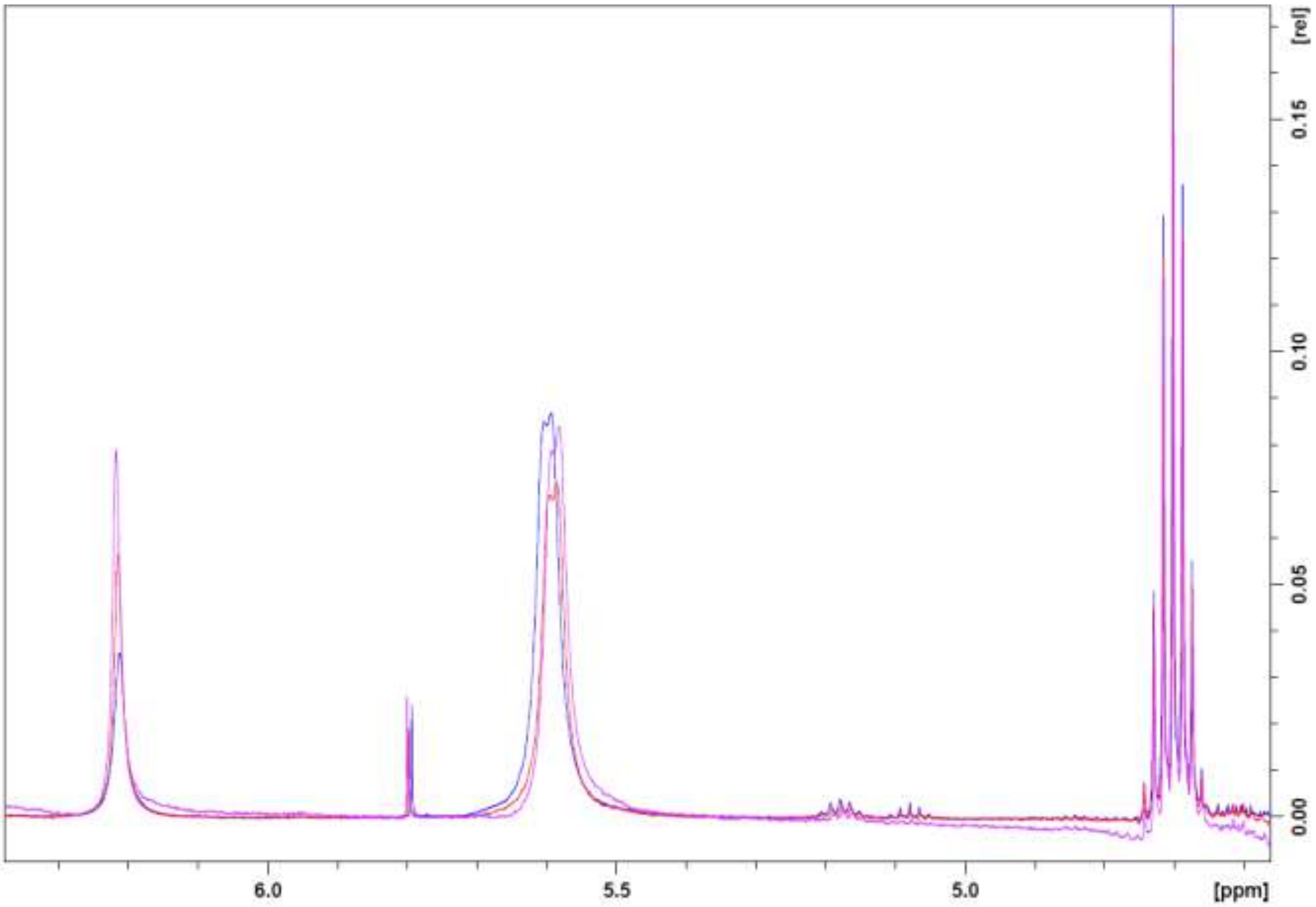

Figure S90. Overlay of 1D ^{1}H NMR spectra of DIC/Oxyma reaction at 0.5M (in blue), 0.4M (in red) and 0.3M (in purple) after 16 h in DMF-d_7 (zoom-in).

7.4 Assessment of HCN formation in 0.37M DMF-d_7 solution of Oxyma and DIC with 5 equiv DMTS

General Procedure for Oxyma and DIC reaction using DMTS

A solution was prepared by dissolving Oxyma (12.0 mg, 0.084 mmol, 1 equiv) and caffeine (2.3 mg, 0.012 mmol, 0.14 equiv) in 170 µL of DMF-d_7. The solution was mixed by using an ultrasound bath. DMTS (44.0 µL, 0.425 mmol, 5 equiv) and DIC (13.3 µL, 0.085 mmol, 1 equiv) were added to the solution. DMTS is carried out prior to addition of DIC. The latter was transferred into a 3mm NMR tube and transferred to the spectrometer for monitoring at 20°C. 1D ^{1}H NMR acquisition was done after 1 h, 5 h, 10 h and 16 h.

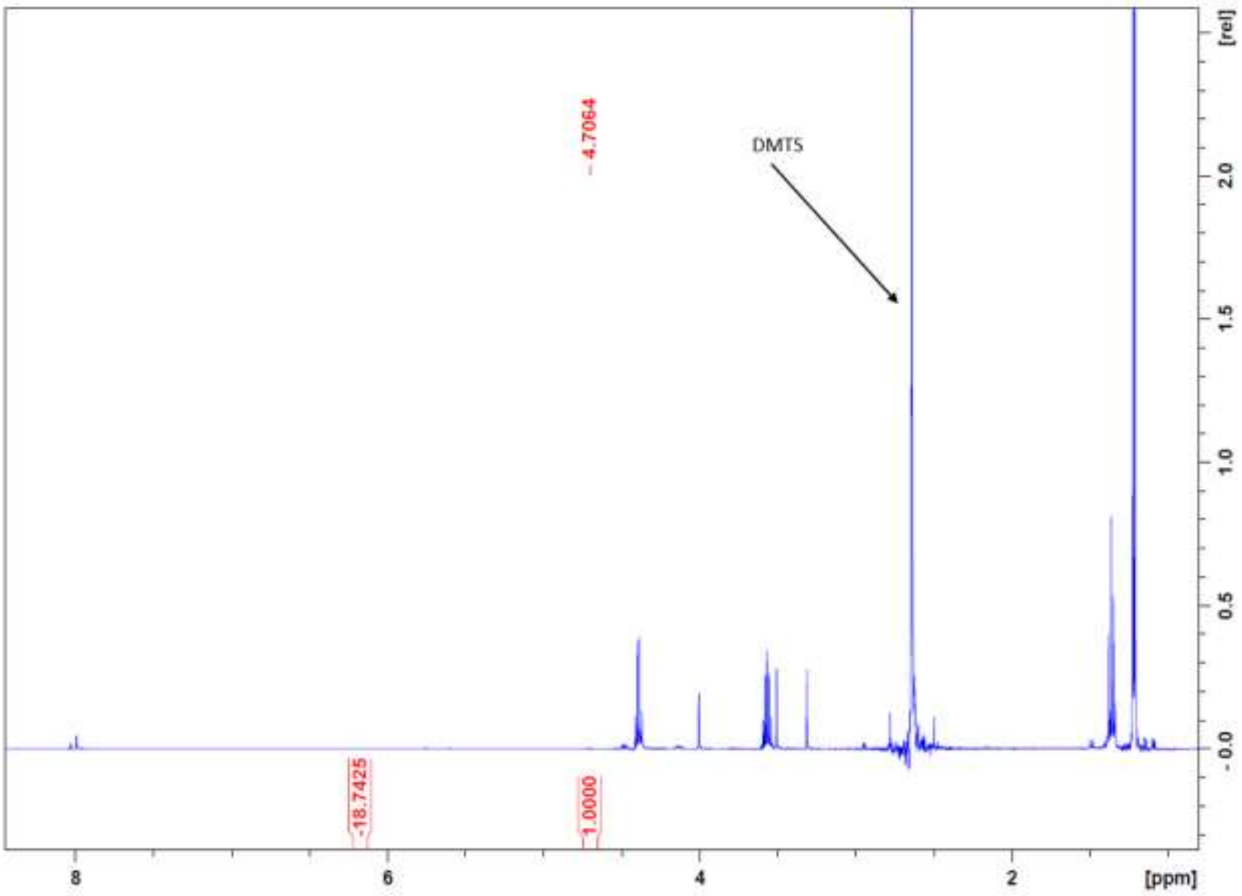

Figure S91. 1D ^{1}H NMR spectrum of DIC/Oxyma reaction with 5 equiv DMTS at 0.37M after 1h in DMF-d_7 (full spectrum).

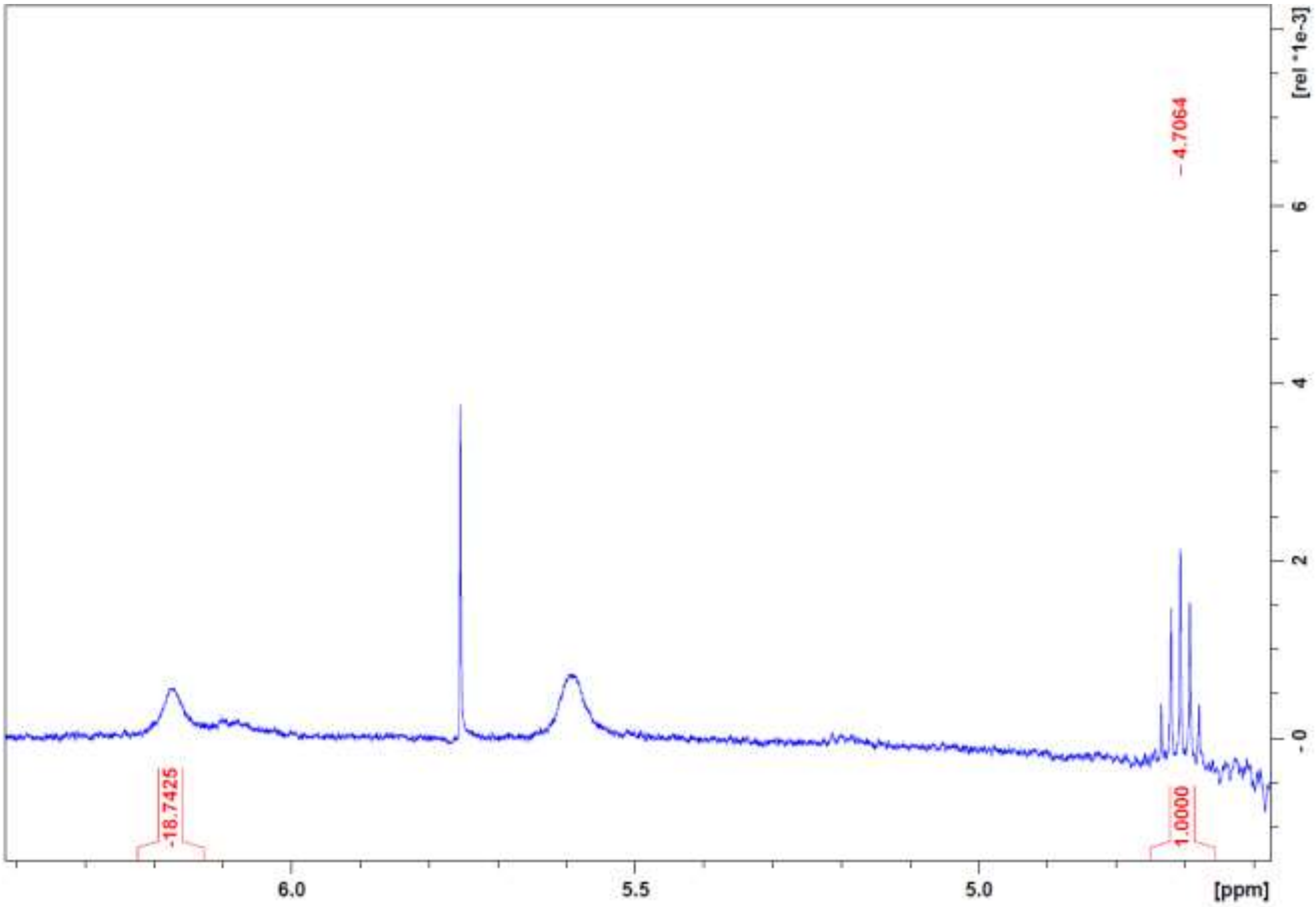

Figure S92. 1D ^{1}H NMR spectrum of DIC/Oxyma reaction with 5 equiv DMTS at 0.37M after 1 h in DMF-d_7 (zoom-in).

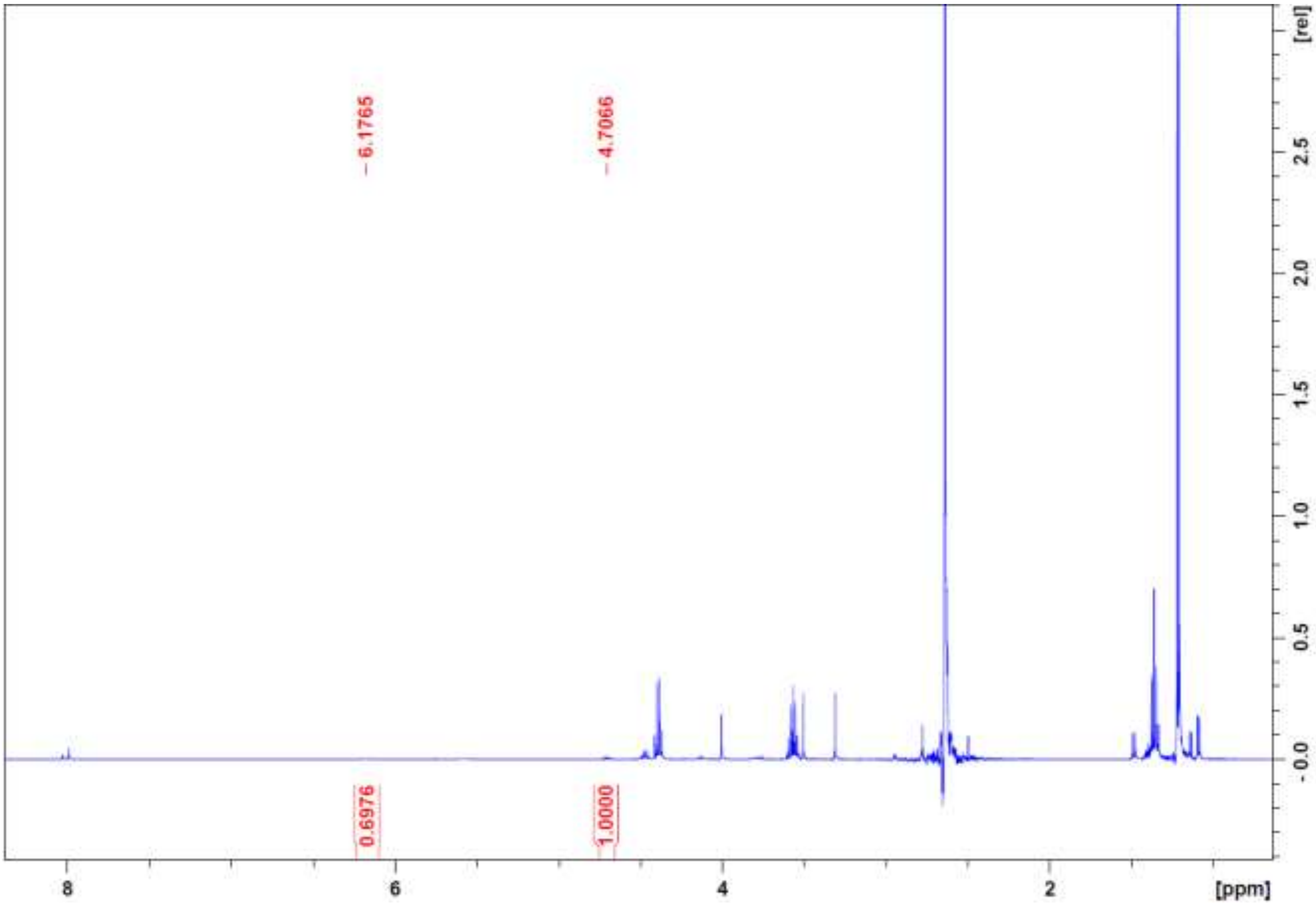

Figure S93. 1D ^{1}H NMR spectrum of DIC/Oxyma reaction with 5 equiv DMTS at 0.37M after 5 h in DMF-d_7 (full spectrum).

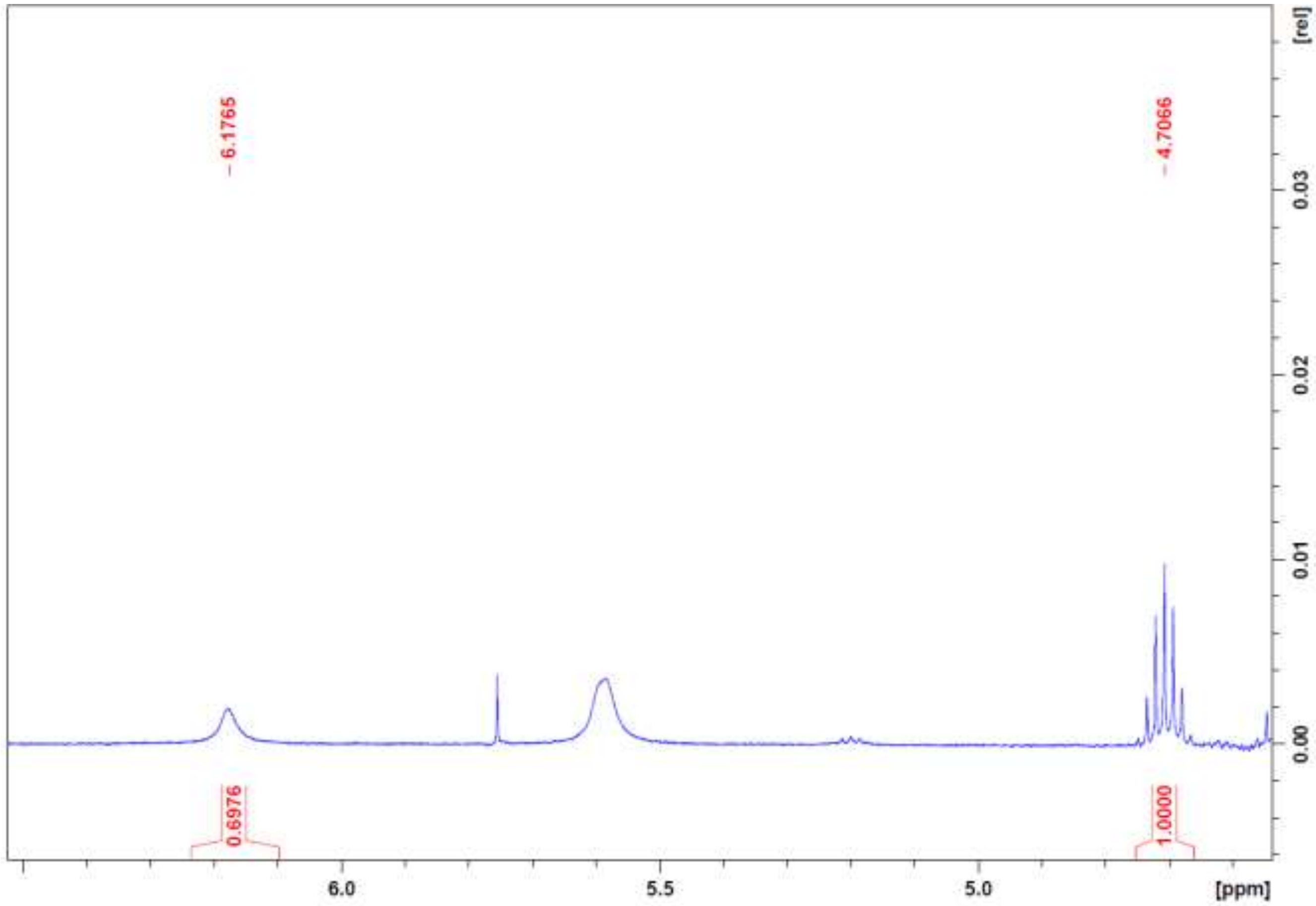

Figure S94. 1D ^{1}H NMR spectrum of DIC/Oxyma reaction with 5 equiv DMTS at 0.37M after 5 h in DMF-d_7 (zoom-in).

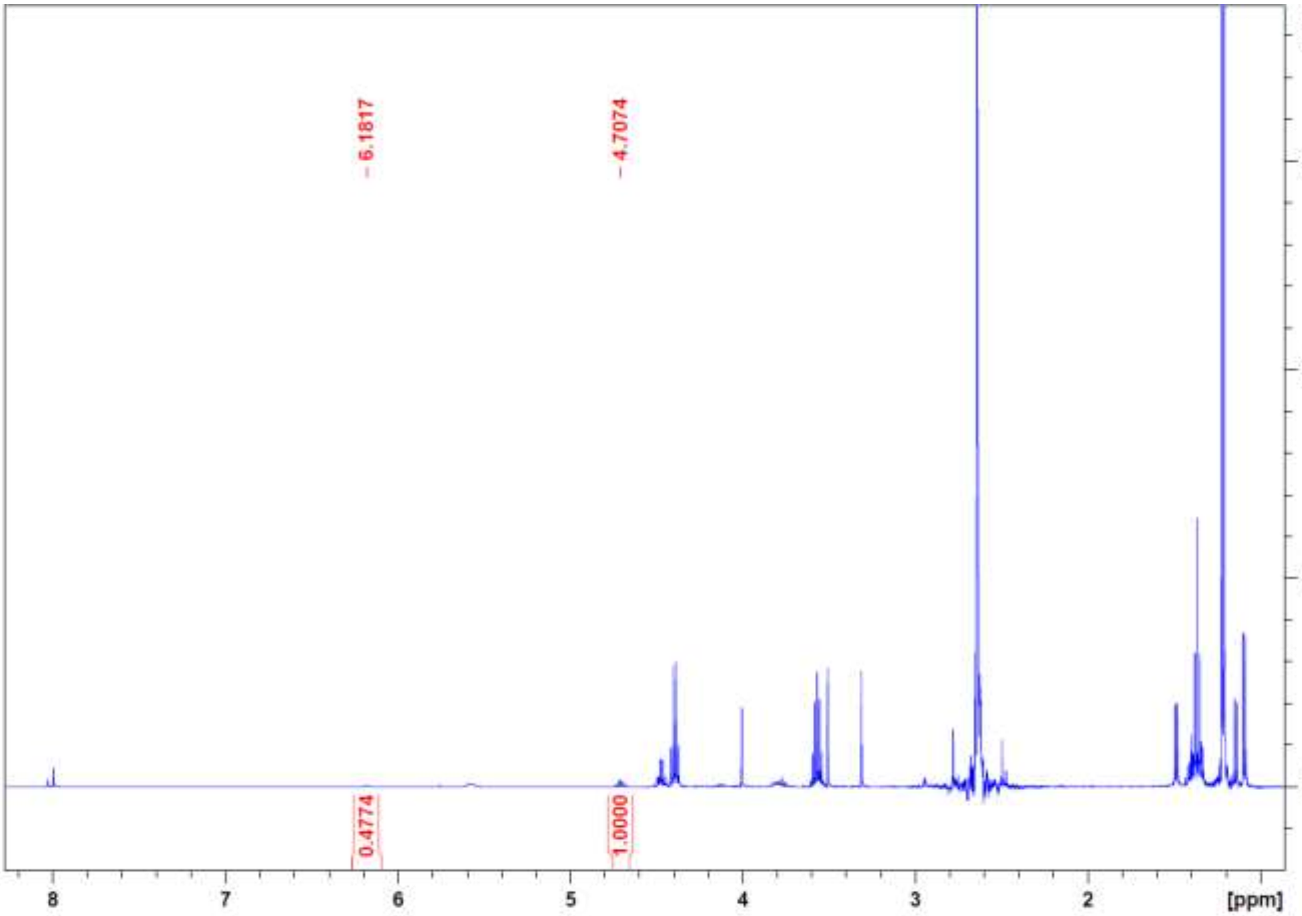

Figure S95. 1D ^{1}H NMR spectrum of DIC/Oxyma reaction with 5 equiv DMTS at 0.37M after 10 h in DMF-d_7 (full spectrum).

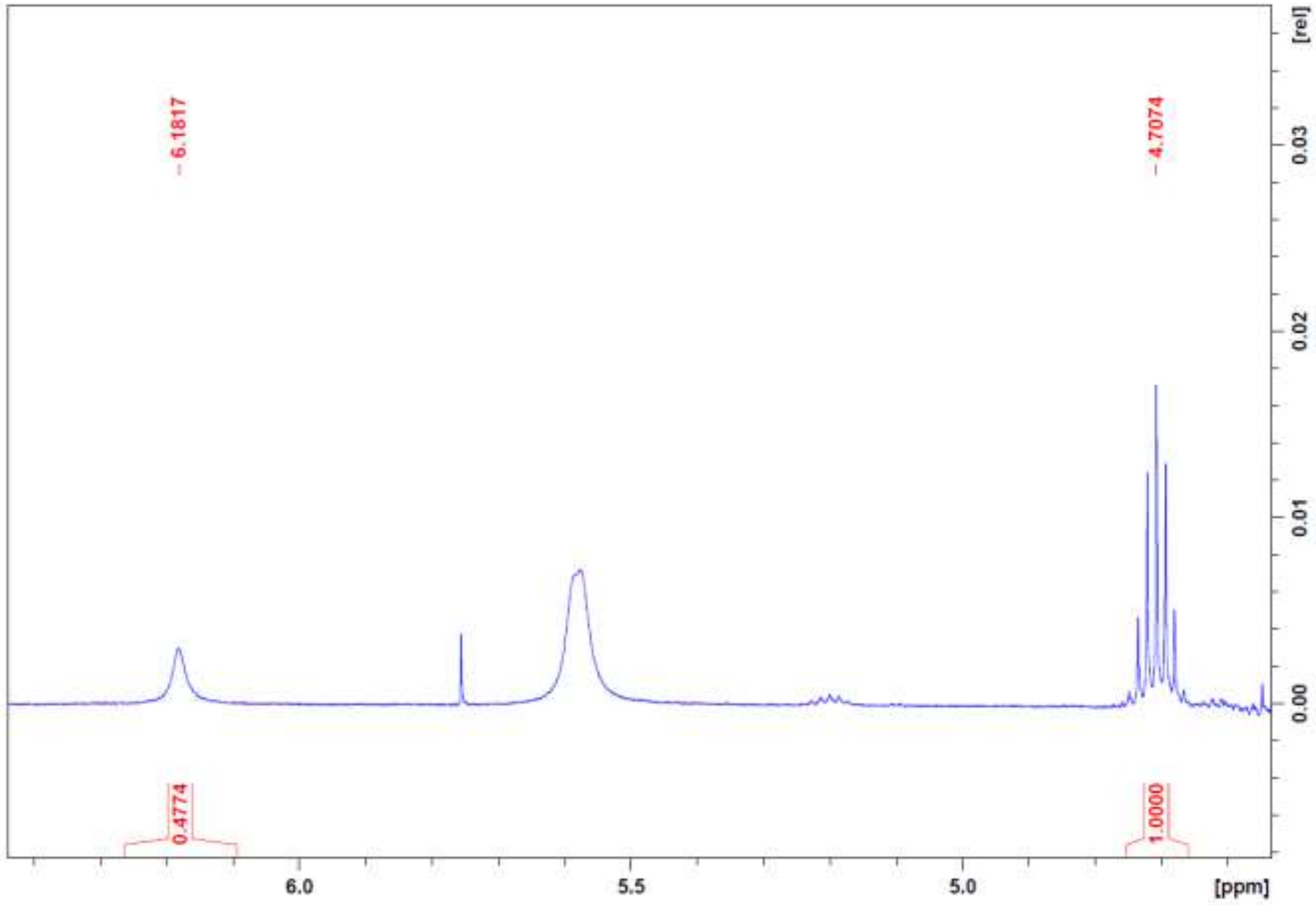

Figure S96. 1D ^{1}H NMR spectrum of DIC/Oxyma reaction with 5 equiv DMTS at 0.37M after 10 h in DMF-d_7 (zoom-in).

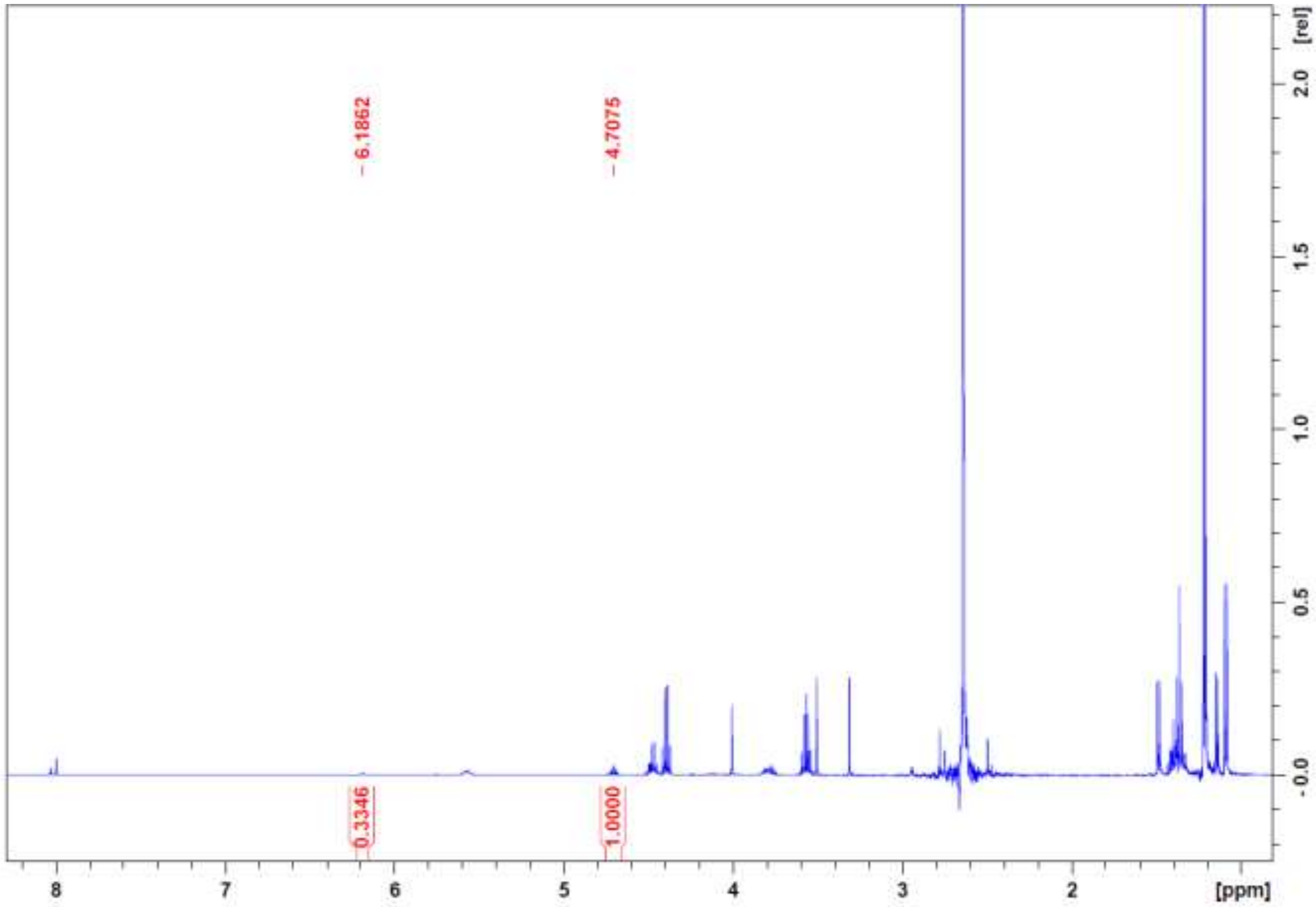

Figure S97. 1D ^{1}H NMR spectrum of DIC/Oxyma reaction with 5 equiv DMTS at 0.37M after 16 h in DMF-d$_7$ (full spectrum).

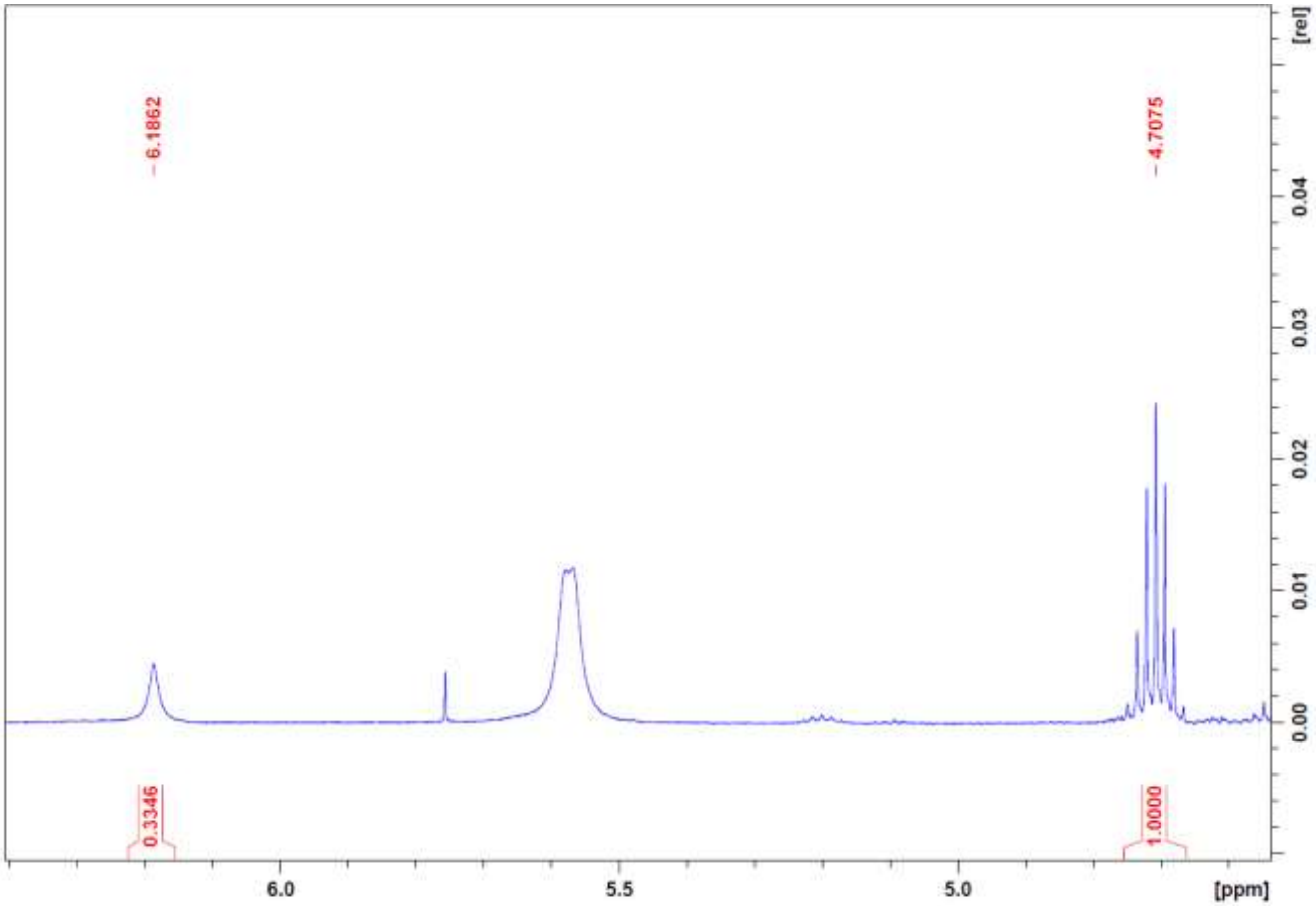

Figure S98. 1D ^{1}H NMR spectrum of DIC/Oxyma reaction with 5 equiv DMTS at 0.37M after 16 h in DMF-d_7 (zoom-in).

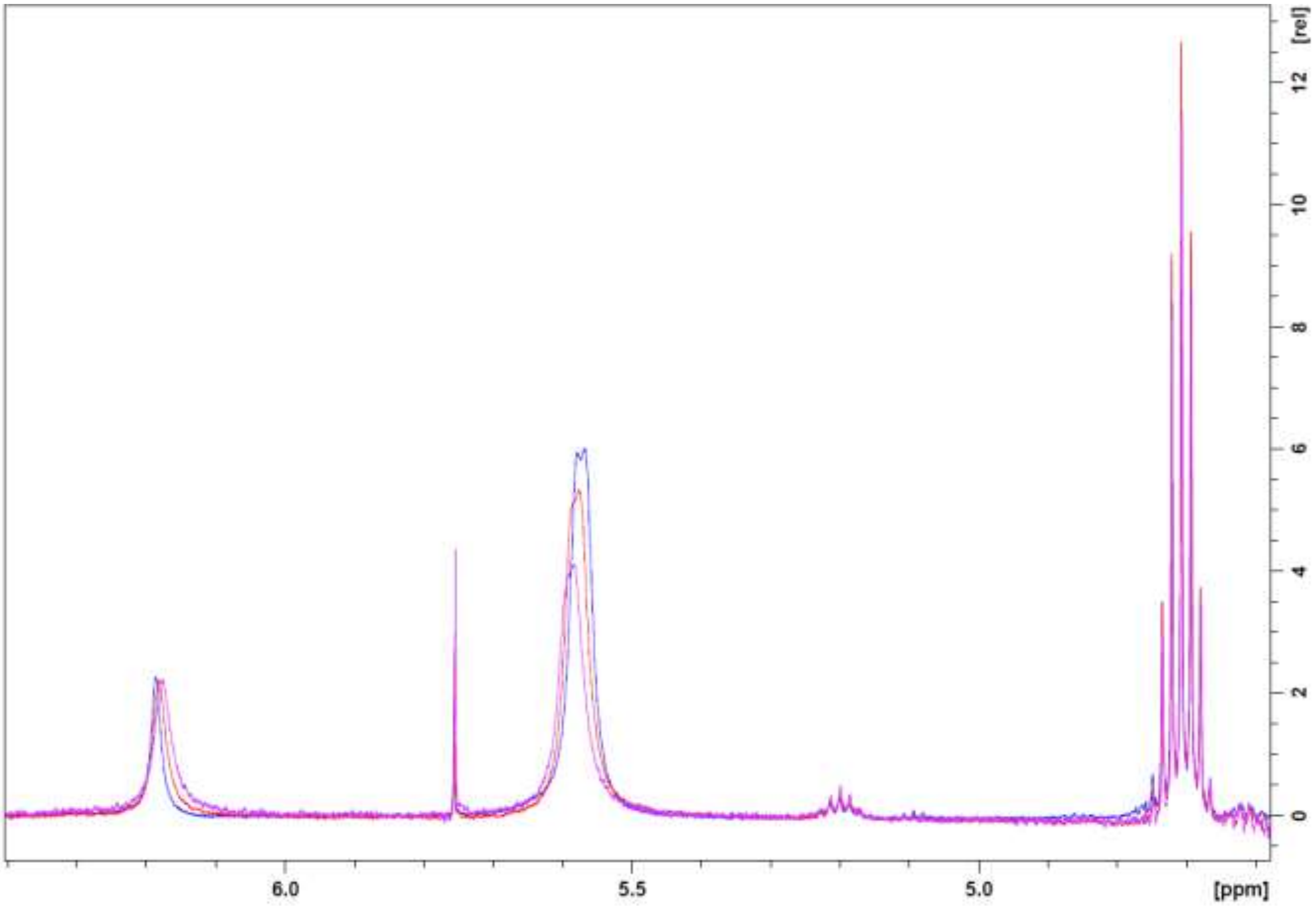

Figure S99. Overlap of 1D ^{1}H NMR spectra of DIC/Oxyma reaction with 5 equiv DMTS at 0.37M after 5 h (in purple), 10 h (in red) and 16 h (in blue) in DMF-d_7 (zoom-in).

7.5 Assessment of HCN formation in 0.32M DMF-d_7 solution of Oxyma and DIC with 10 equiv DMTS

The general procedure for the reactions of DIC and Oxyma using DMTS in DMF-d_7 as described in the section 7.4 of this ESI was followed. The following amounts of starting materials were used: Oxyma (12.4 mg, 0.087 mmol, 1.03 equiv), caffeine (1.9 mg, 0.010 mmol, 0.12 equiv), DMTS (89.6 µL, 0.85 mmol, 10 equiv), DIC (13.3 µL, 0.085 mmol, 1.0 equiv).

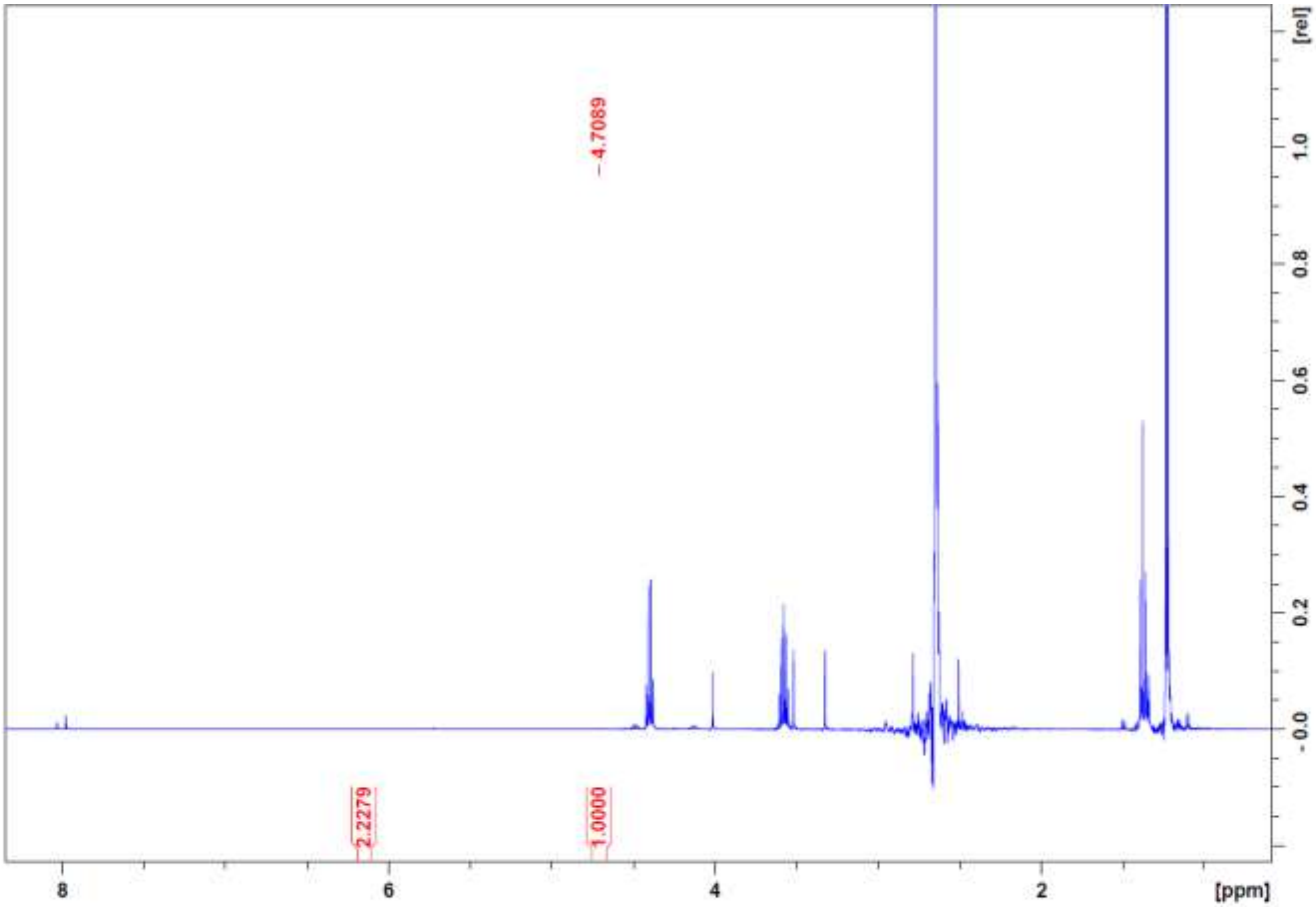

Figure S100. 1D ^{1}H NMR spectrum of DIC/Oxyma reaction with 10 equiv DMTS at 0.32M after 1 h in DMF-d_7 (full spectrum).

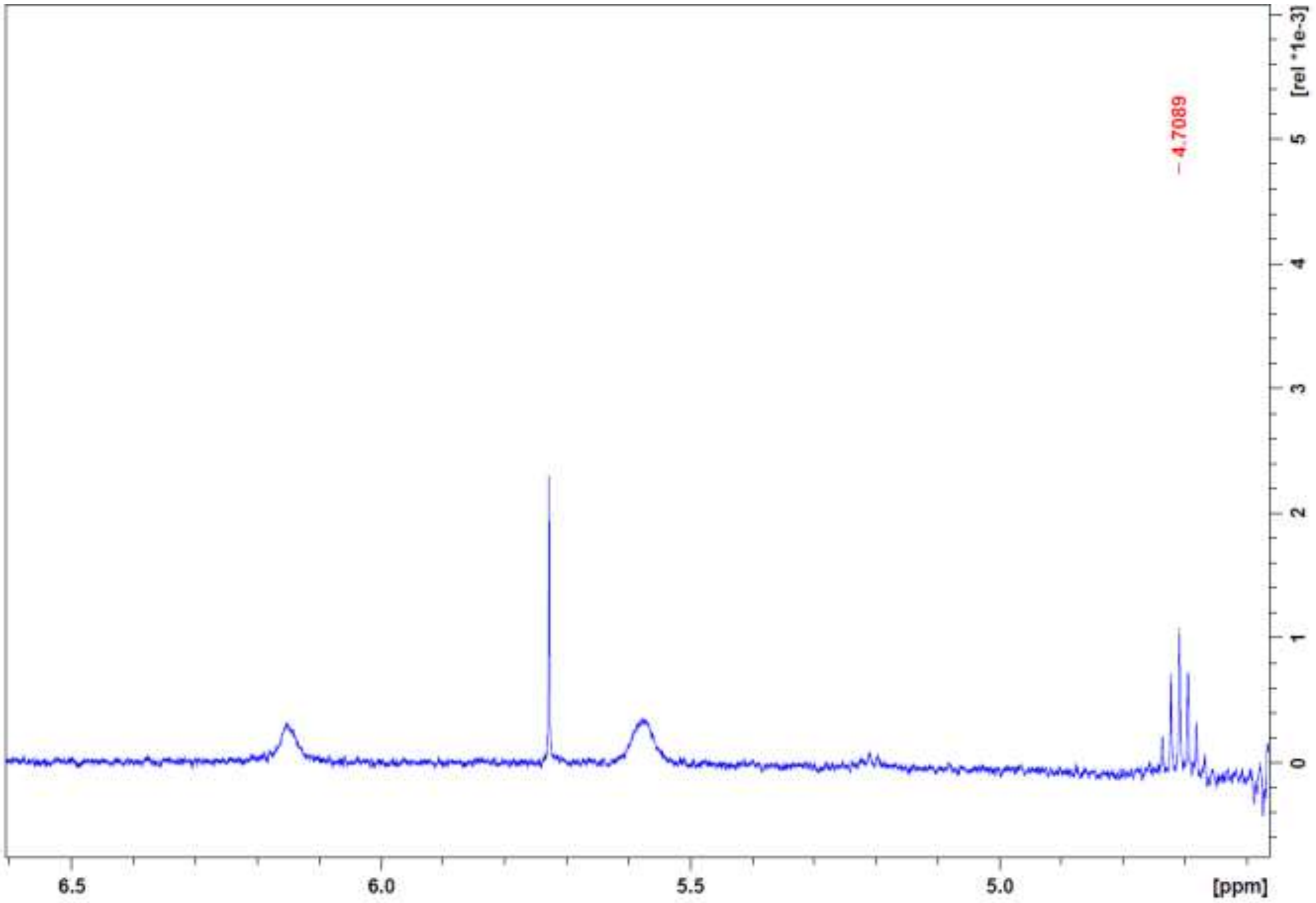

Figure S101. 1D ^{1}H NMR spectrum of DIC/Oxyma reaction with 10 equiv DMTS at 0.32M after 1 h in DMF-d$_7$ (zoom-in).

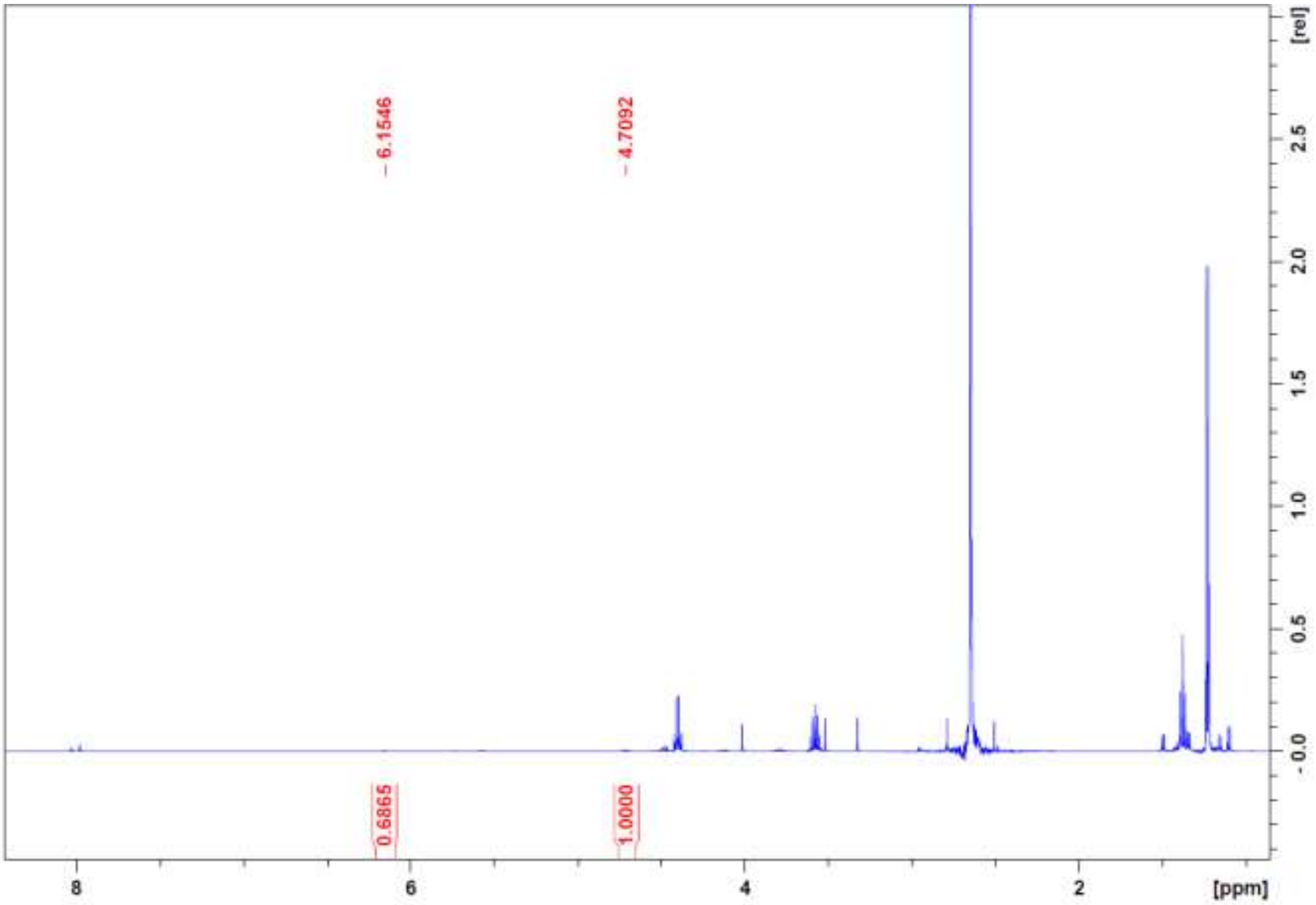

Figure S102. 1D ^{1}H NMR spectrum of DIC/Oxyma reaction with 10 equiv DMTS at 0.32M after 5 h in DMF-d_7 (full spectrum).

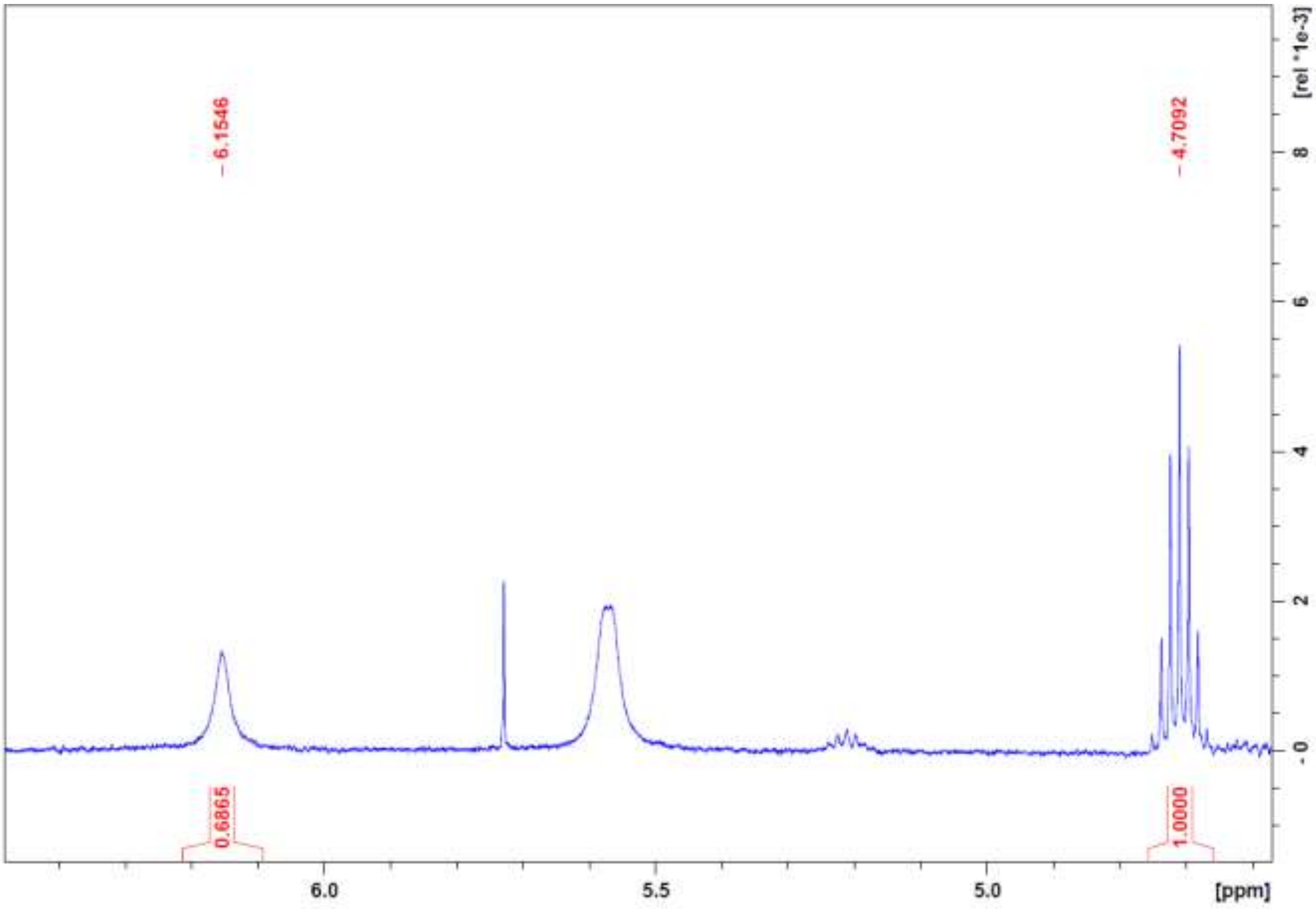

Figure S103. 1D ^{1}H NMR spectrum of DIC/Oxyma reaction with 10 equiv DMTS at 0.32 M after 5 h in DMF-d_7 (zoom-in).

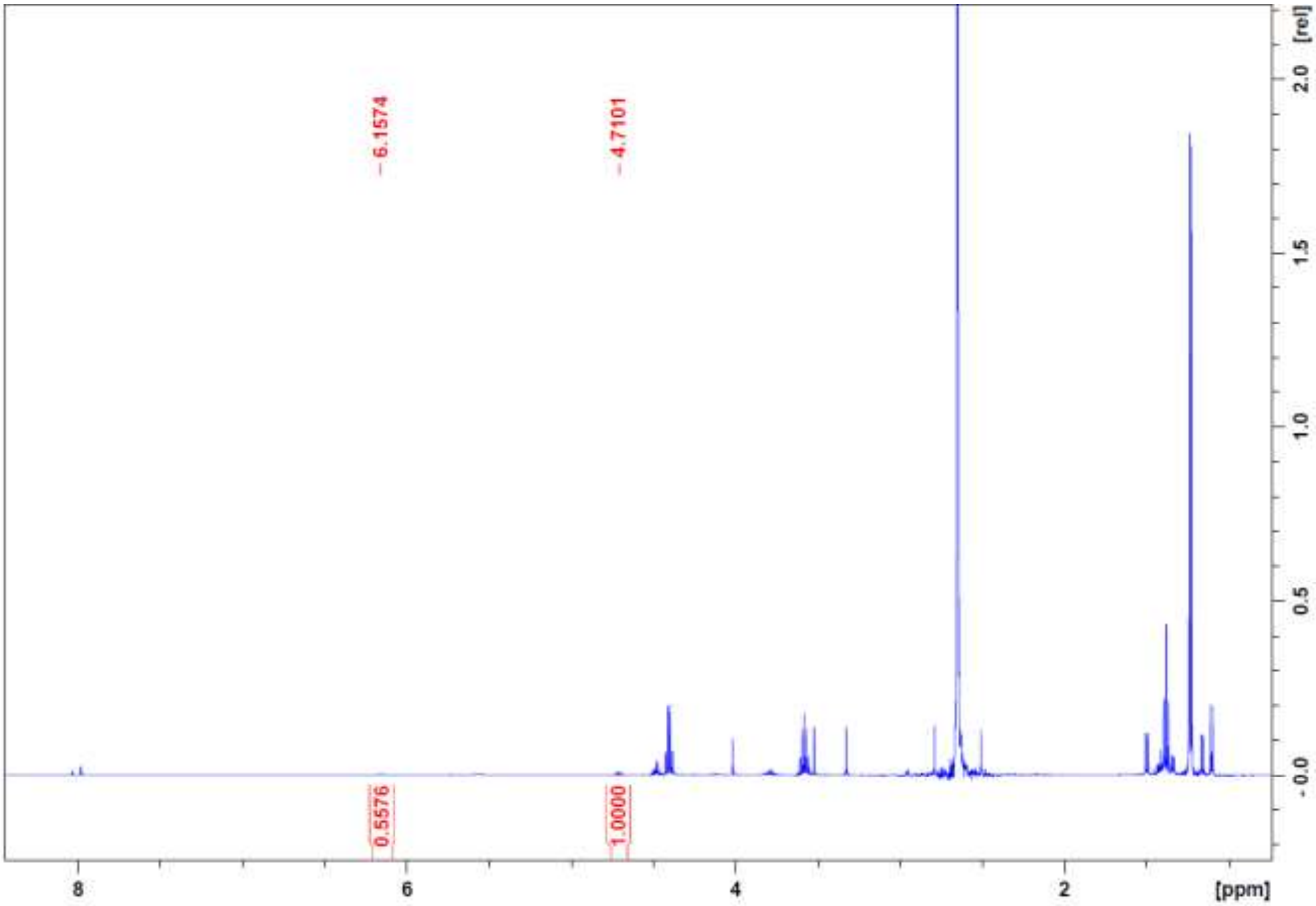

Figure S104. 1D ^{1}H NMR spectrum of DIC/Oxyma reaction with 10 equiv DMTS at 0.32M after 10 h in DMF-d_7 (full spectrum).

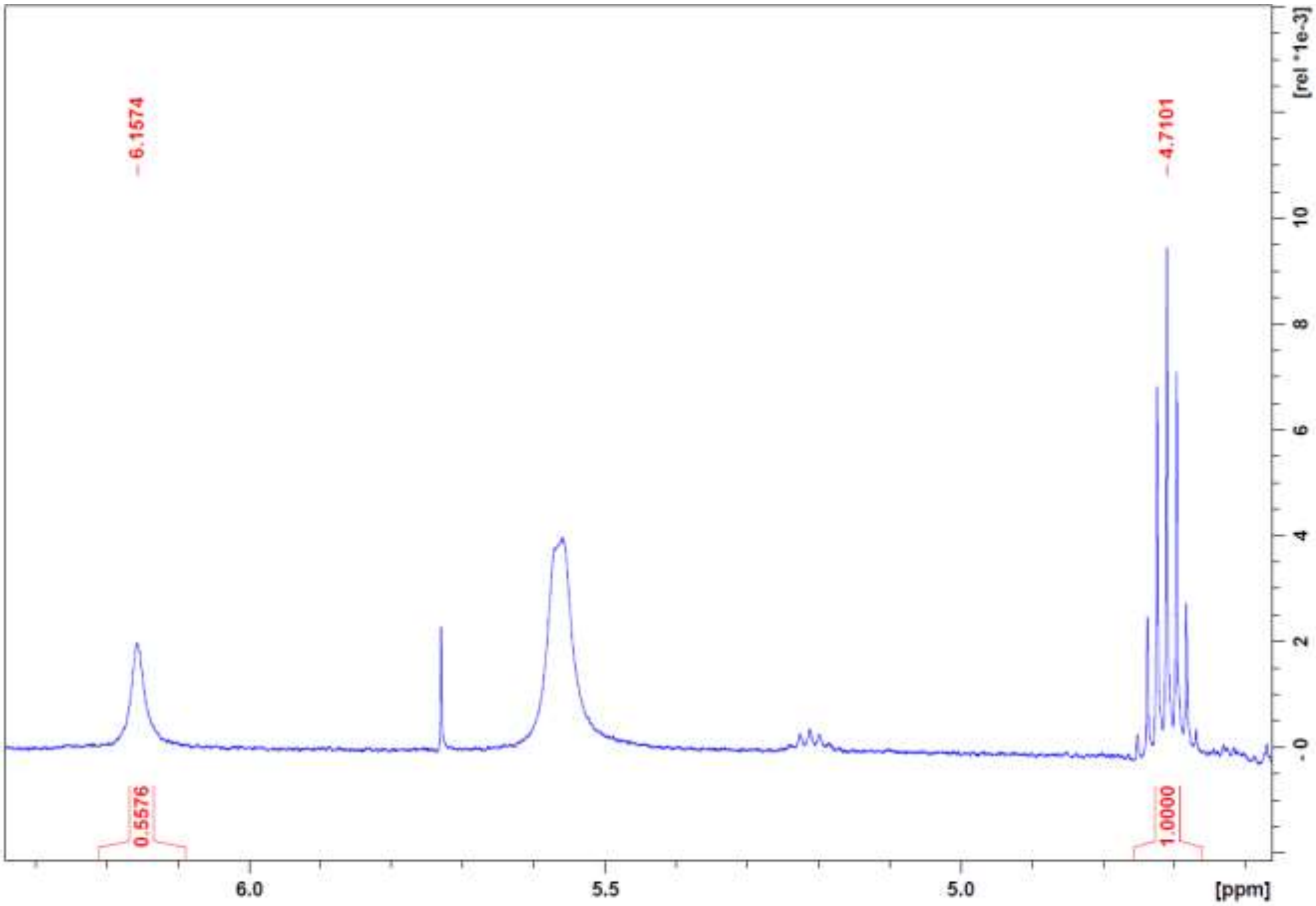

Figure S105. 1D ^{1}H NMR spectrum of DIC/Oxyma reaction with 10 equiv DMTS at 0.32M after 10 h in DMF-d_7 (zoom-in).

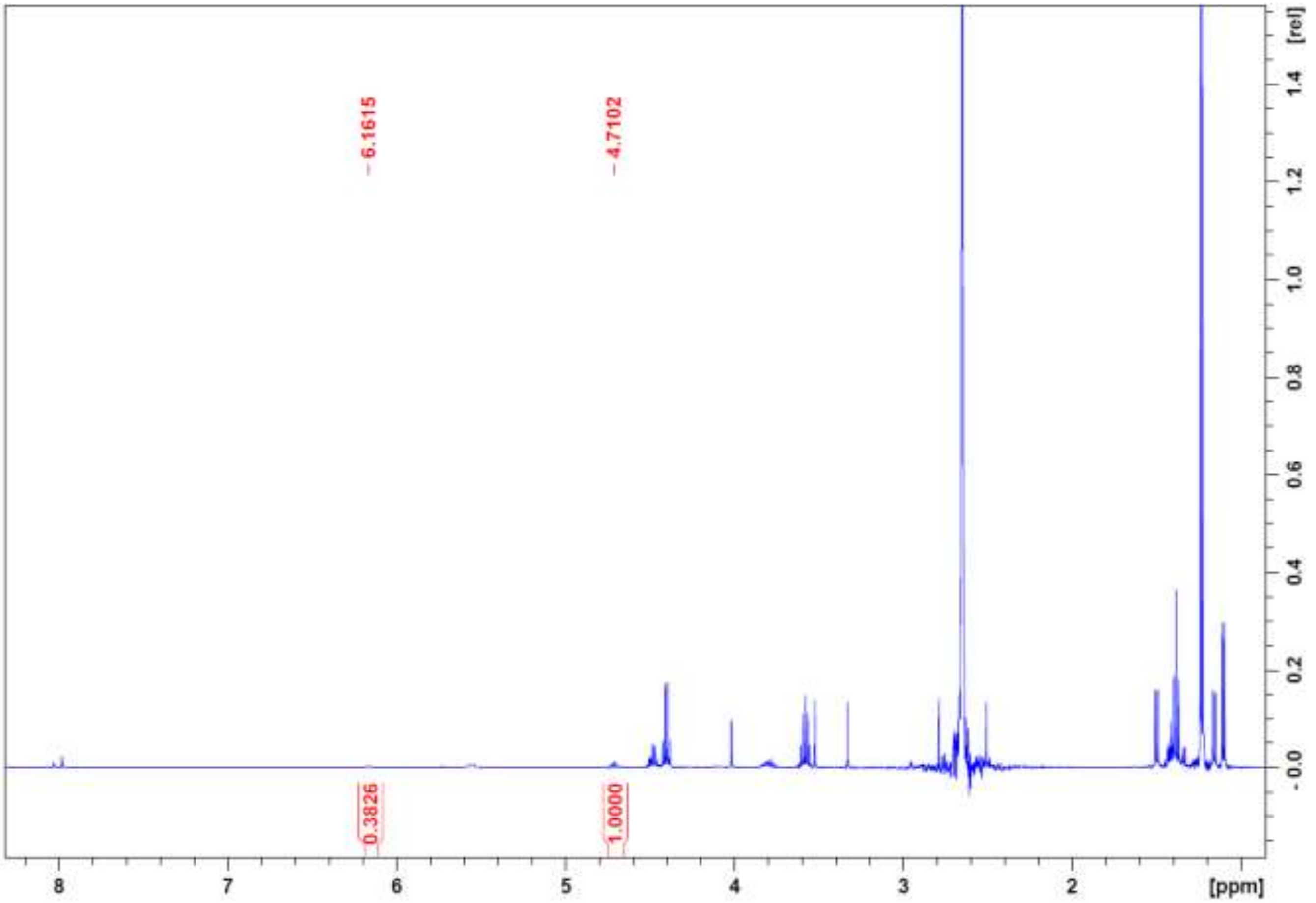

Figure S106. 1D ^{1}H NMR spectrum of DIC/Oxyma reaction with 10 equiv DMTS at 0.32M after 16 h in DMF-d_7 (full spectrum).

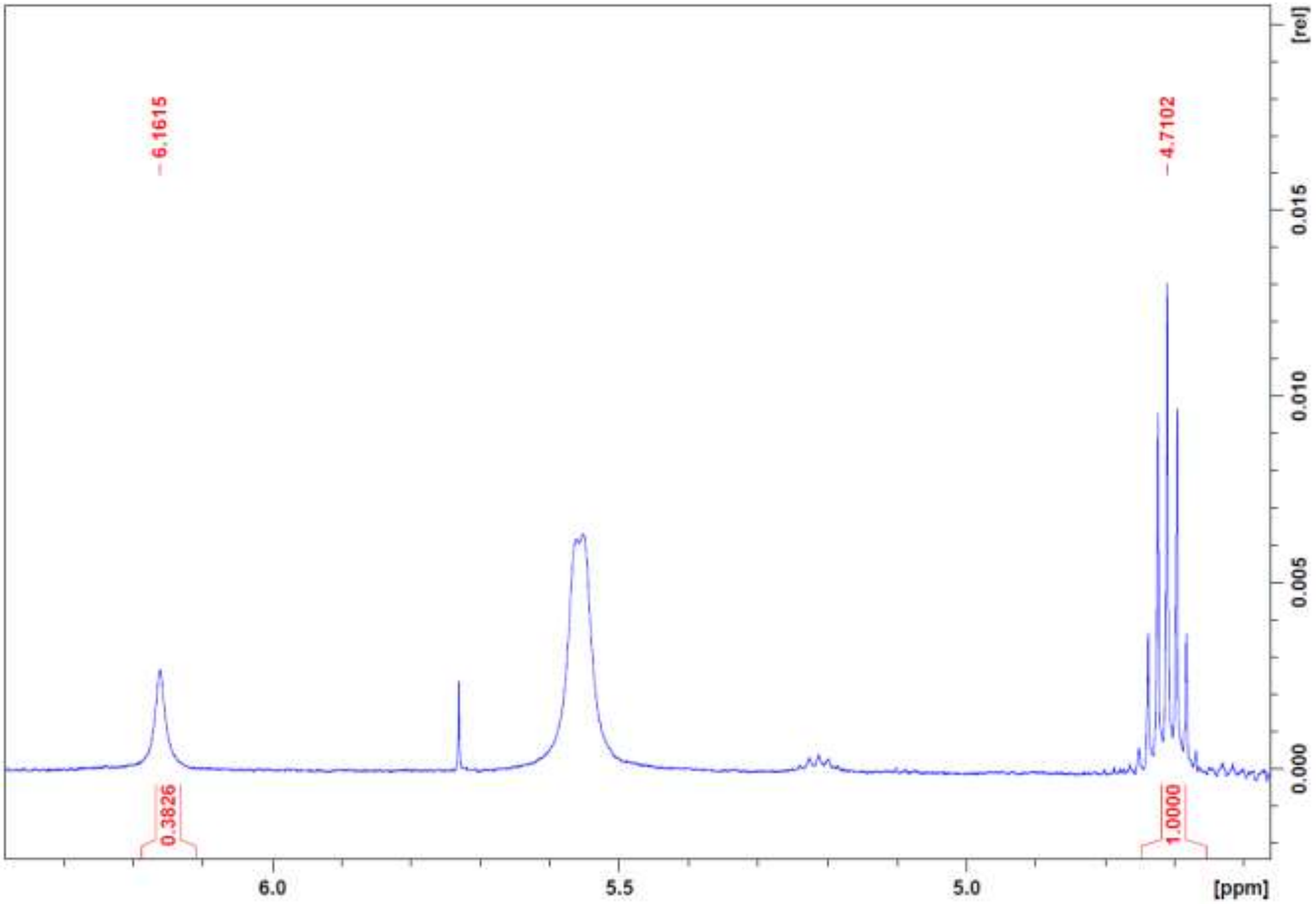

Figure S107. 1D ^{1}H NMR spectrum of DIC/Oxyma reaction with 10 equiv DMTS at 0.32M after 16 h in DMF-d_7 (zoom-in).

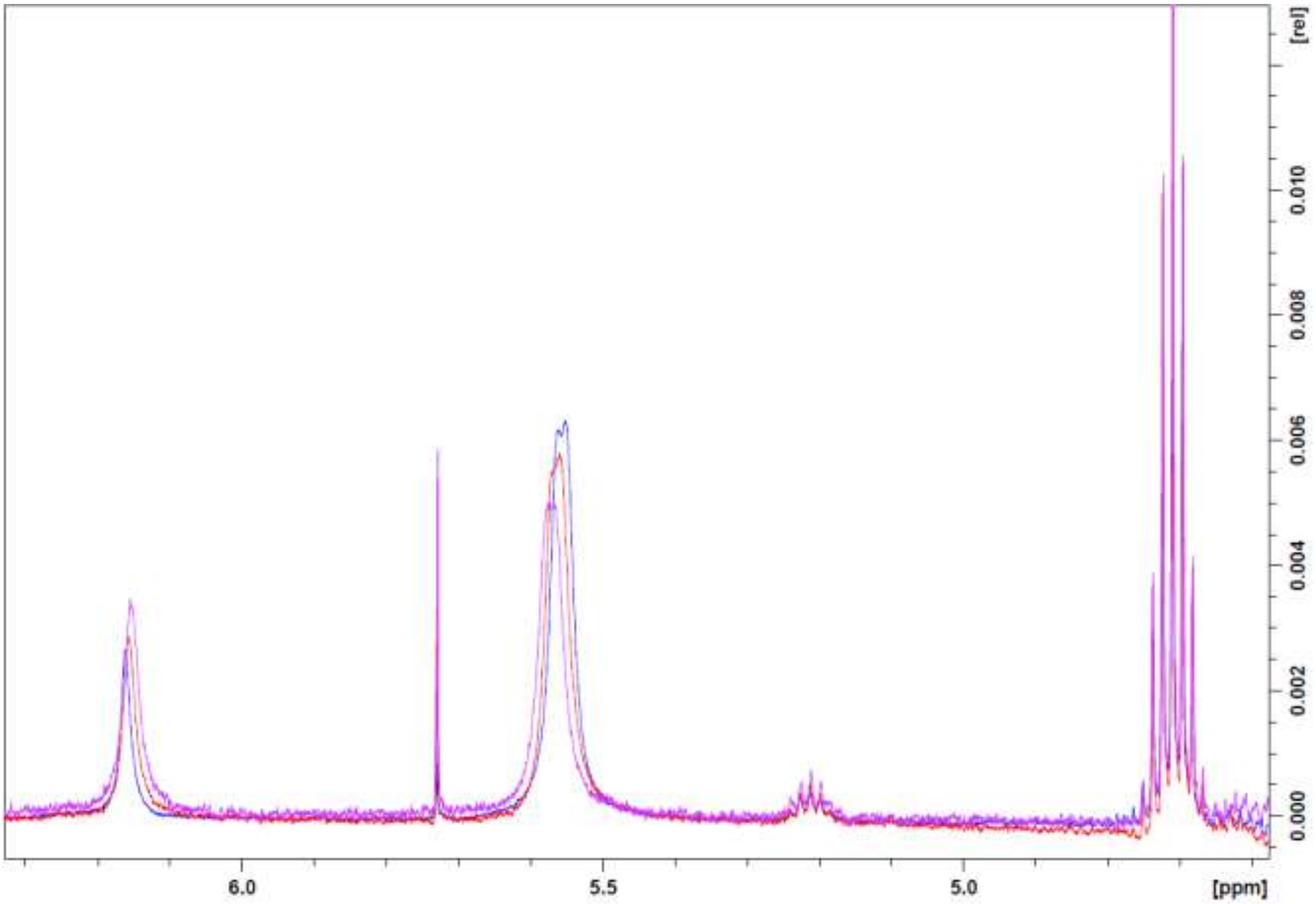

Figure S108. Overlay of 1D ^{1}H NMR spectra of DIC/Oxyma reaction with 10 equiv DMTS at 0.32M after 5 h (in purple), 10 h (in red) and 16 h (in blue) in DMF-d_7 (zoom-in).

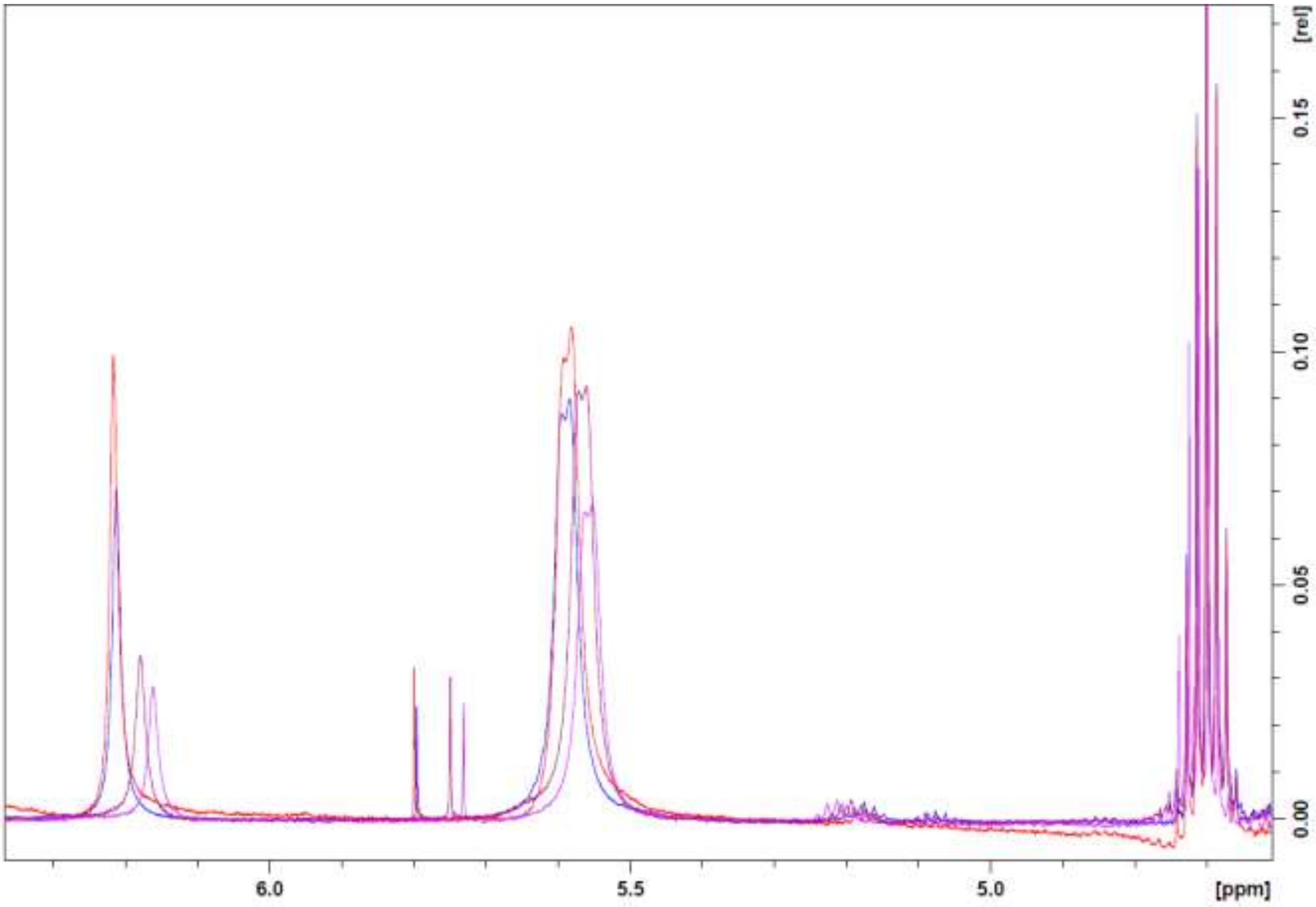

Figure S109. Overlay of 1D ^{1}H NMR spectra of DIC/Oxyma reaction after 16 h at 0.3M (in red), 0.4M (in blue), at 0.32M with 10 equiv of DMTS (in purple) and at 0.37M with 5 equiv of DMTS (in brown) in DMF-d_7 (zoom-in).

7.6 Summary of HCN formation during Oxyma/DIC reaction at different concentrations in DMF-d_7 with and without DMTS

This section summarize the results in sections 7.1 – 7.6.

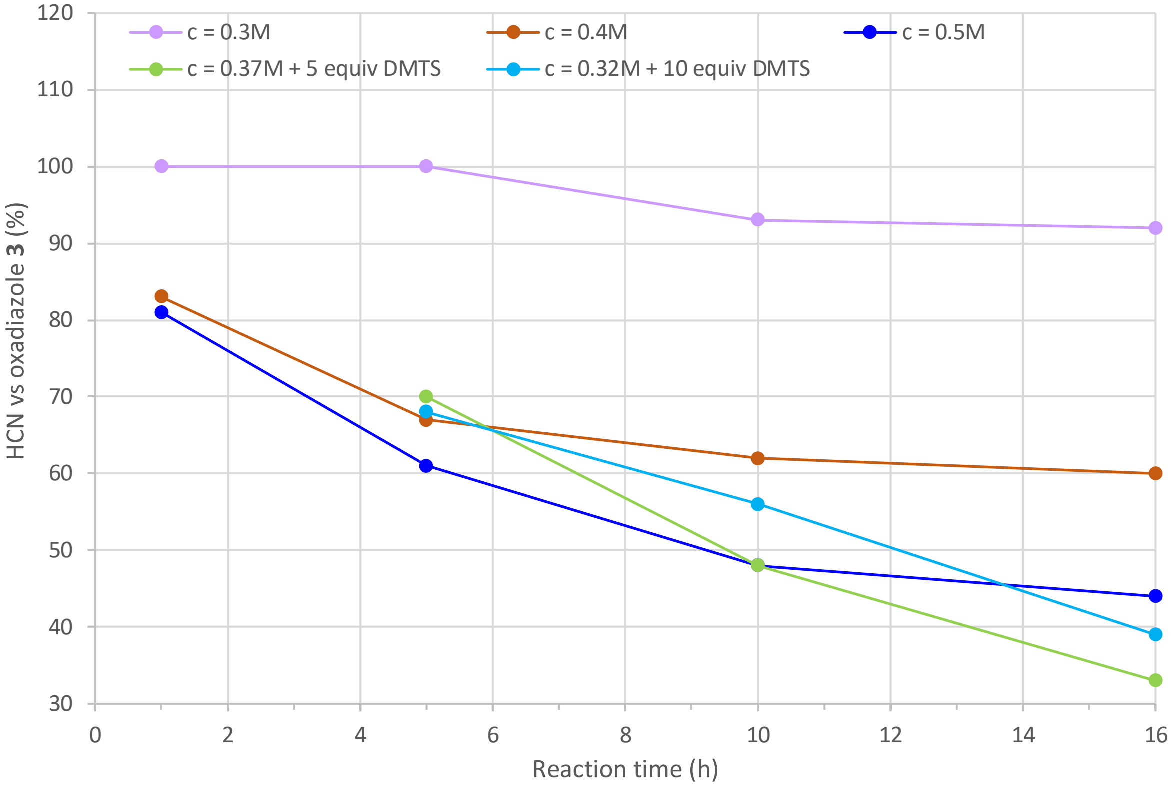

Figure S110. ^{1}H NMR assessment of the presence of HCN in DMF-d_7 solutions of DIC/Oxyma (1:1) with 0, 5, 10 equiv DMTS at different concentrations at rt.

Conclusion of the experiments summarized in Fig. S110: i) keeping the concentration low appears to be a good way to keep HCN formed in the solution and avoid the release in the gas phase; ii) of an HCN scavenger (DMTS) decreases significantly the amount of HCN in the solution. The use of this scavenger during DIC/Oxyma mediated amide bond formations is detailed in the ensuing sections of this ESI.

8. NMR analysis of different constituents of DIC/Oxyma mediated amide bond formations

8.1 Starting materials

In this section, NMR analyses are reported for the starting materials used in the DIC/Oxyma mediated amidation of Fmoc-Gly-OH and (S)-(-)-1-phenylethylamine, with and without DMTS (sections 8.1.1 – 8.1.2). The purpose of this investigation was to determine whether any of these materials reacts with DMTS to an appreciable extent and thereby could affect the course of the amidations in the presence of DMTS.

8.1.1 Starting materials without addition of DMTS

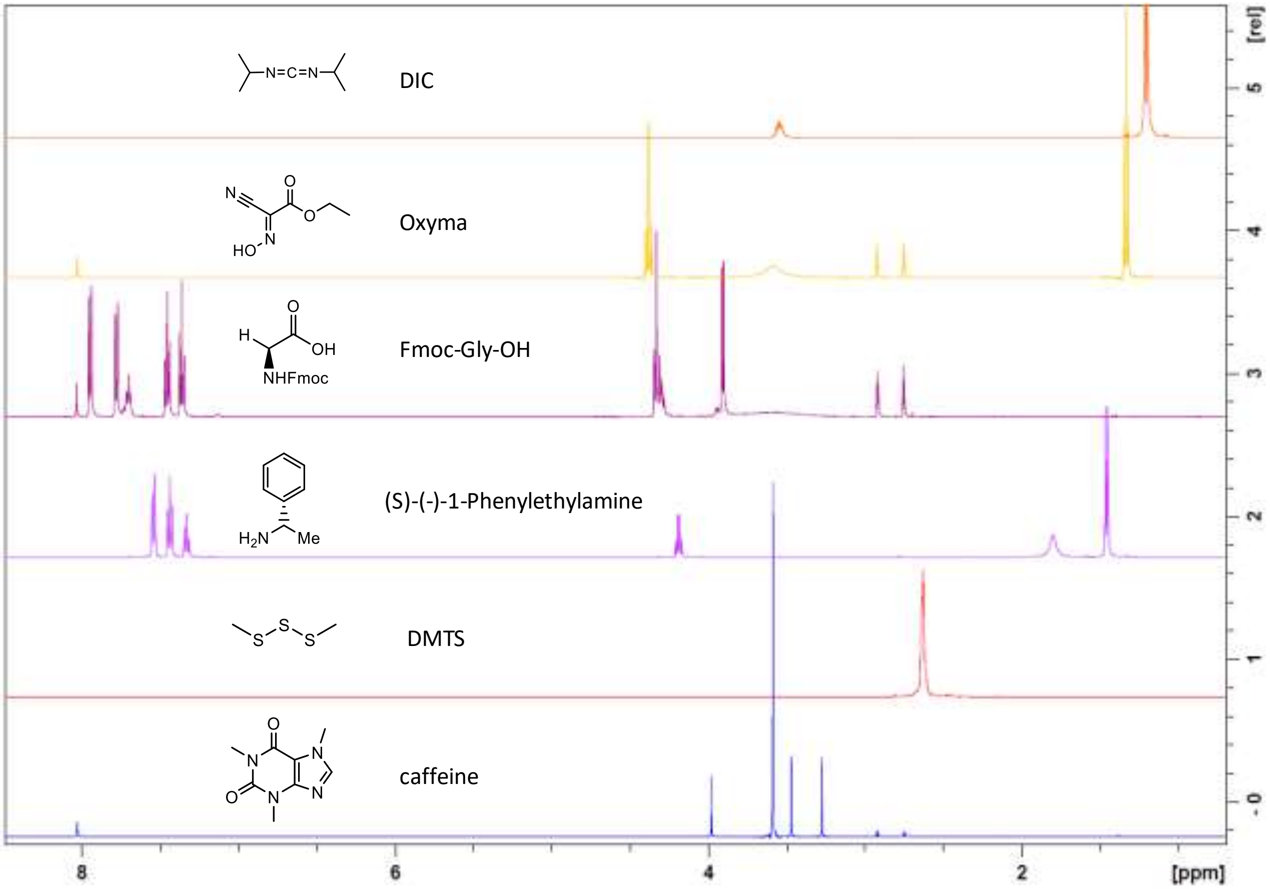

Figure S111. Overlay of 1D ^{1}H NMR spectra of starting materials and internal standard in DMF-d$_7$.

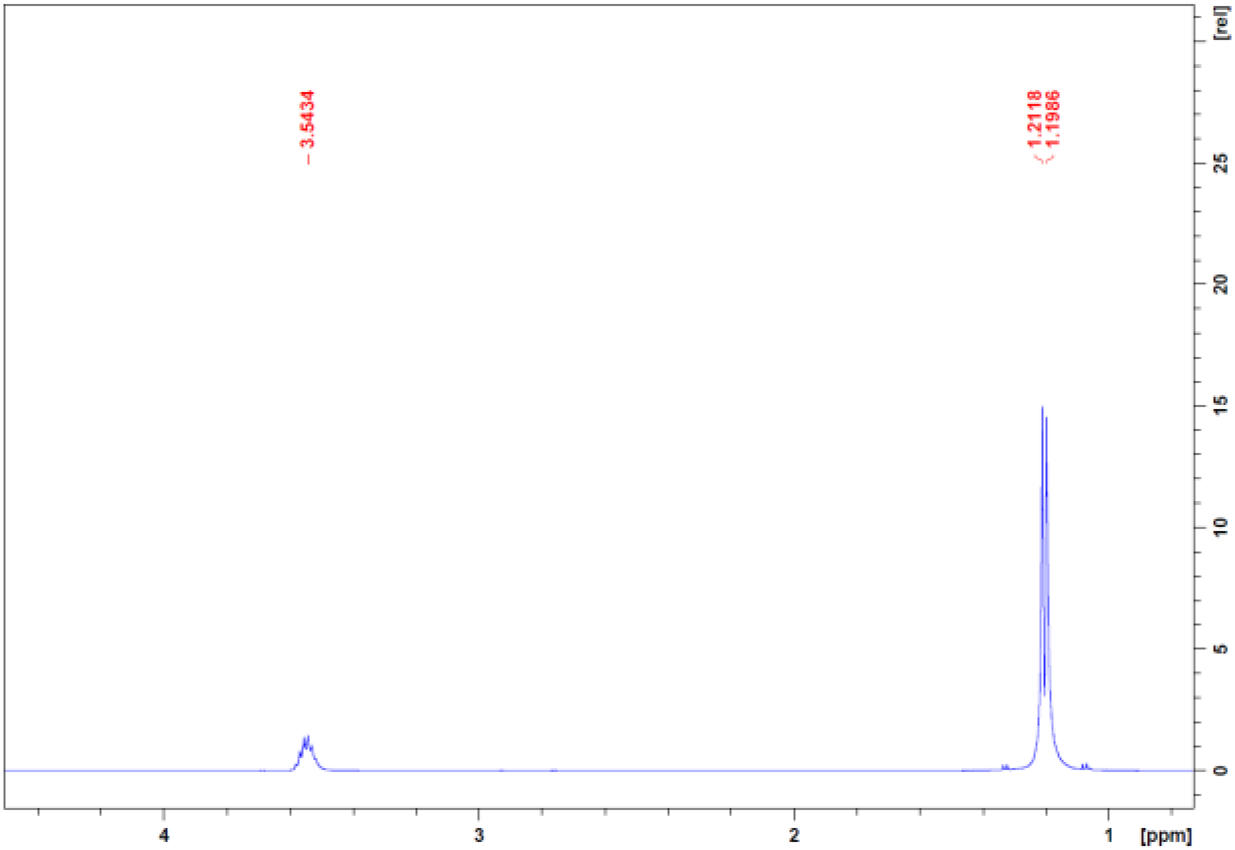

Figure S112. 1D ^{1}H NMR spectrum of DIC in DMF-d_7.

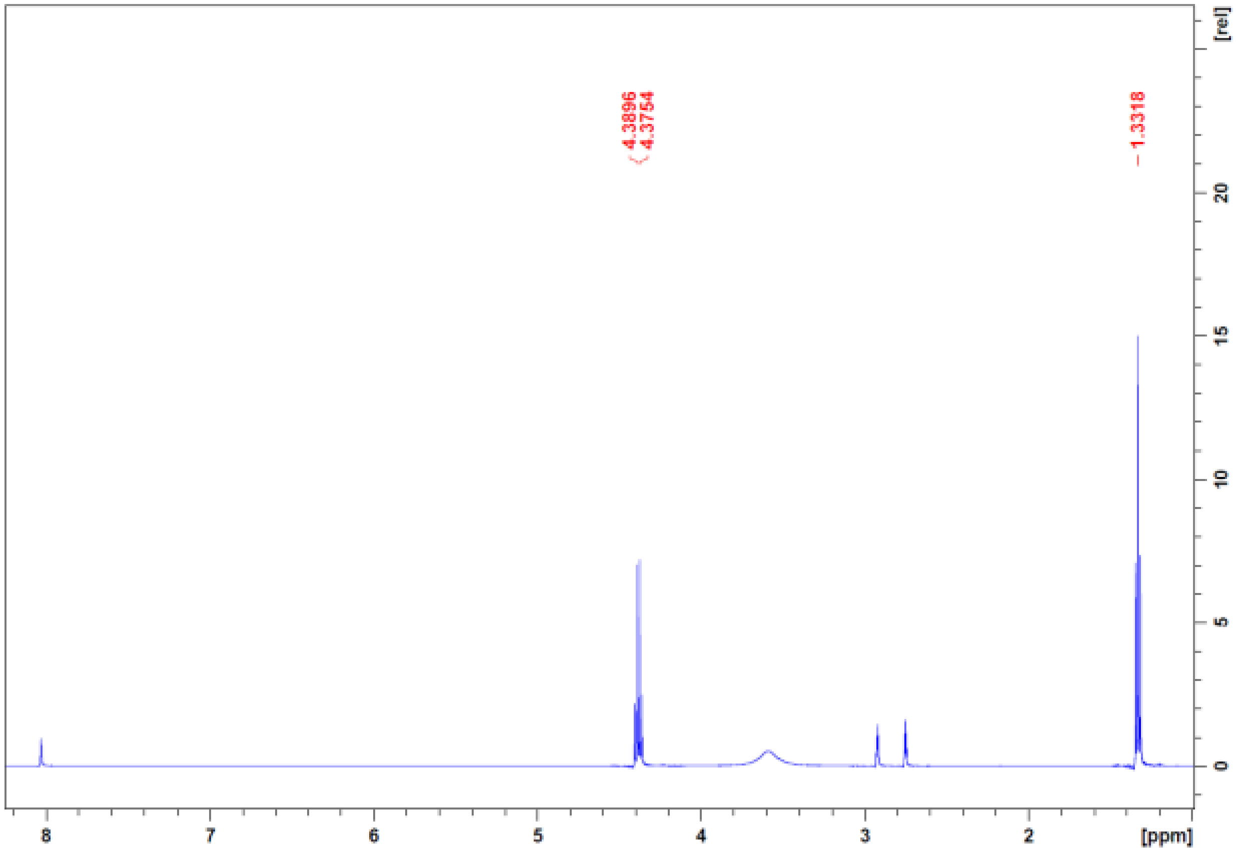

Figure S113. 1D ^{1}H NMR spectrum of Oxyma in DMF-d_7.

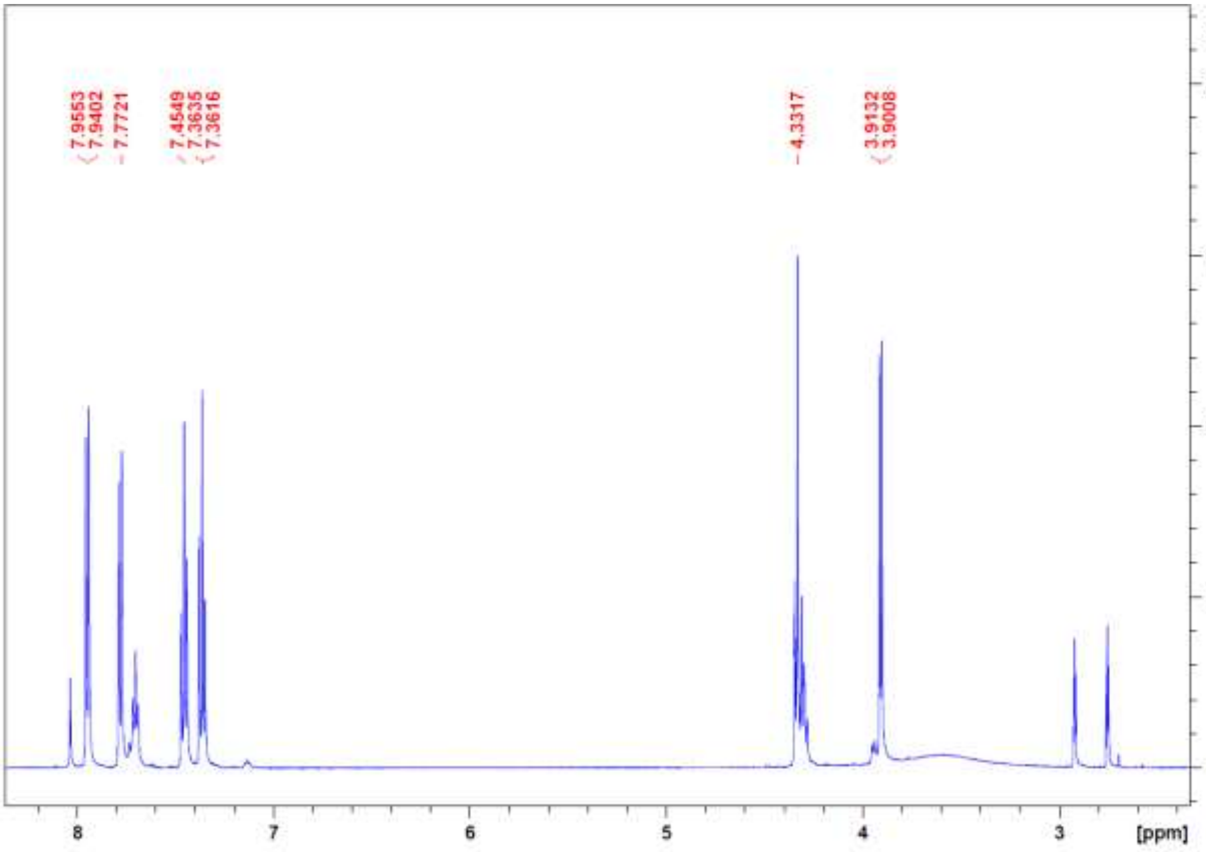

Figure S114. 1D ^{1}H NMR spectrum of Fmoc-Gly-OH in DMF-d_7.

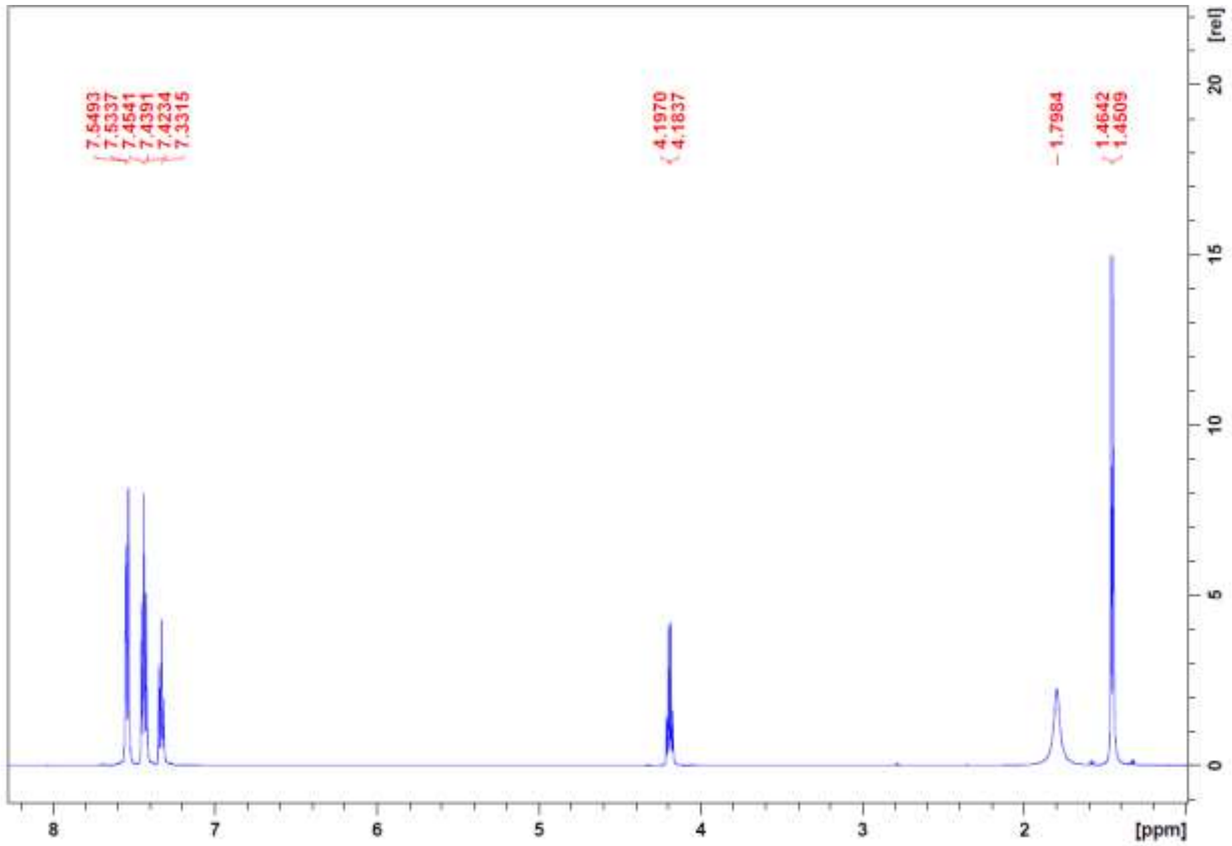

Figure S115. 1D ^{1}H NMR spectrum of (S)-(-)-1-phenylethylamine in DMF-d_7.

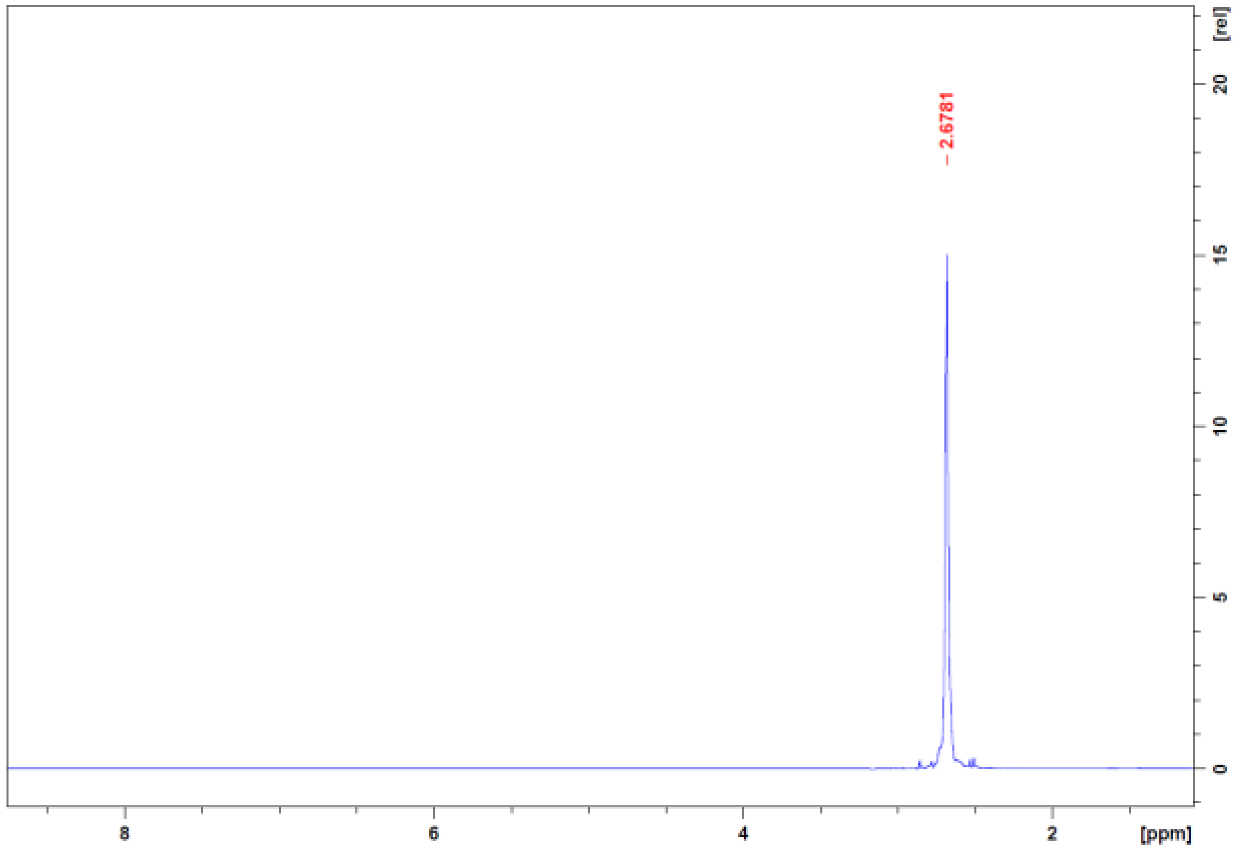

Figure S116. 1D ^{1}H NMR spectrum of DMTS in DMF-d_7.

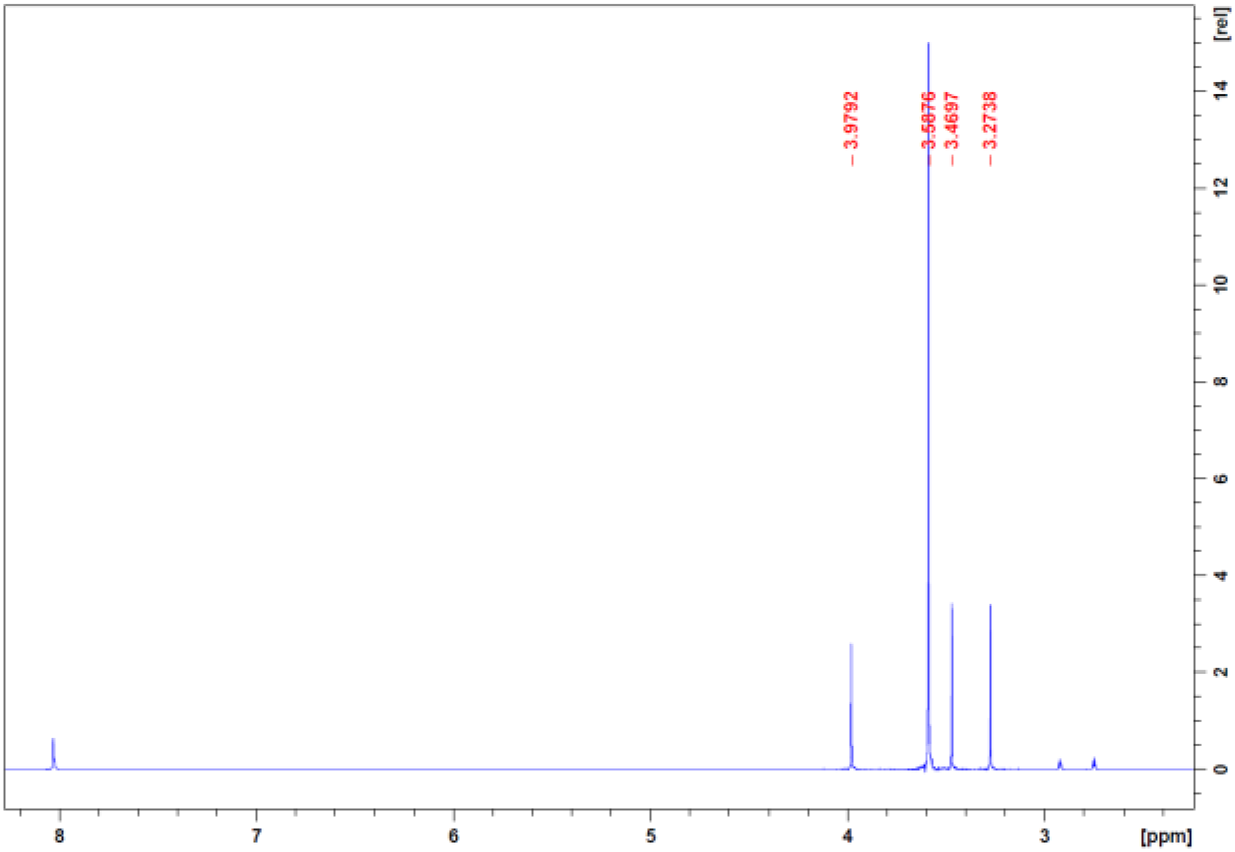

Figure S117. 1D ^{1}H NMR spectrum of caffeine in DMF-d_7.

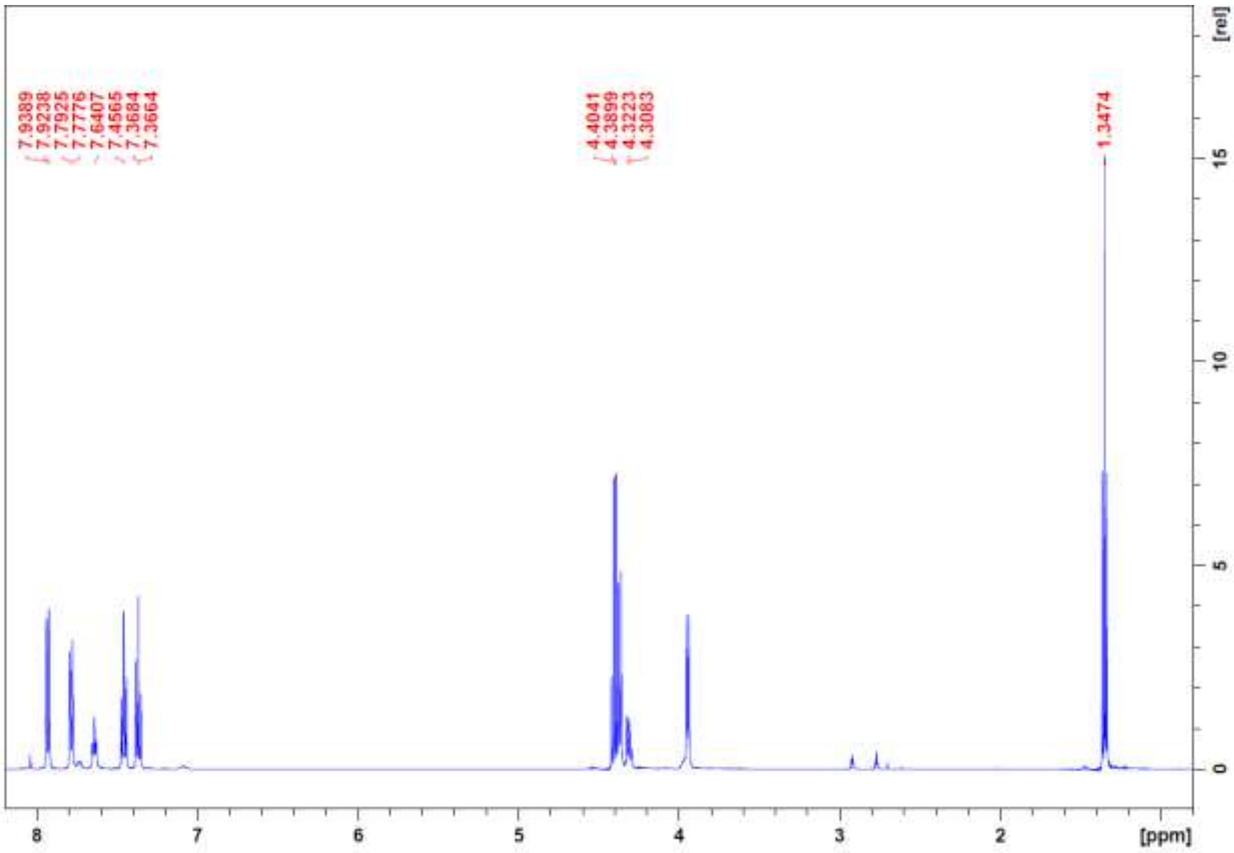

Figure S118. 1D ^{1}H NMR spectrum of Fmoc-Gly-OH with Oxyma in DMF-d$_7$.

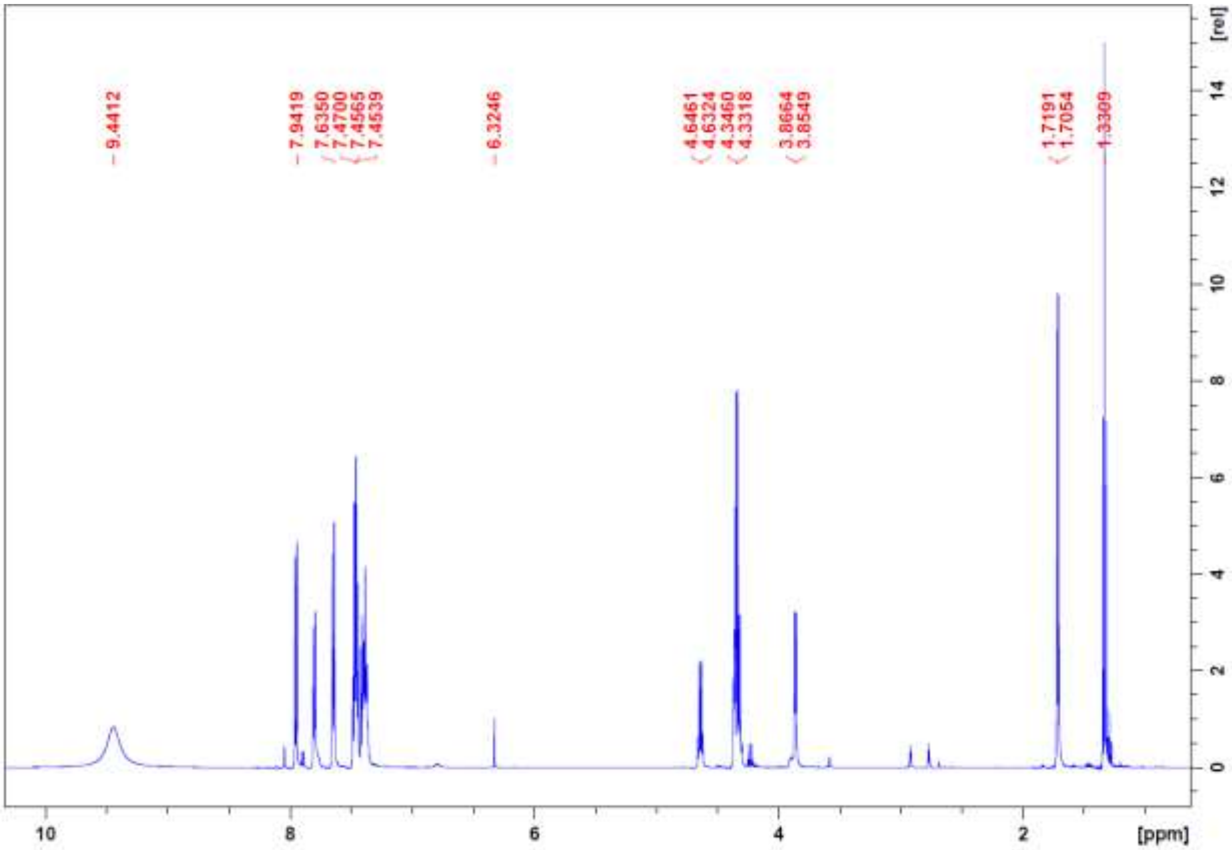

Figure S119. 1D ^{1}H NMR spectrum of Fmoc-Gly-OH with Oxyma and (S)-(-)-1-phenylethylamine in DMF-d_7.

8.1.2 Starting materials with addition of DMTS

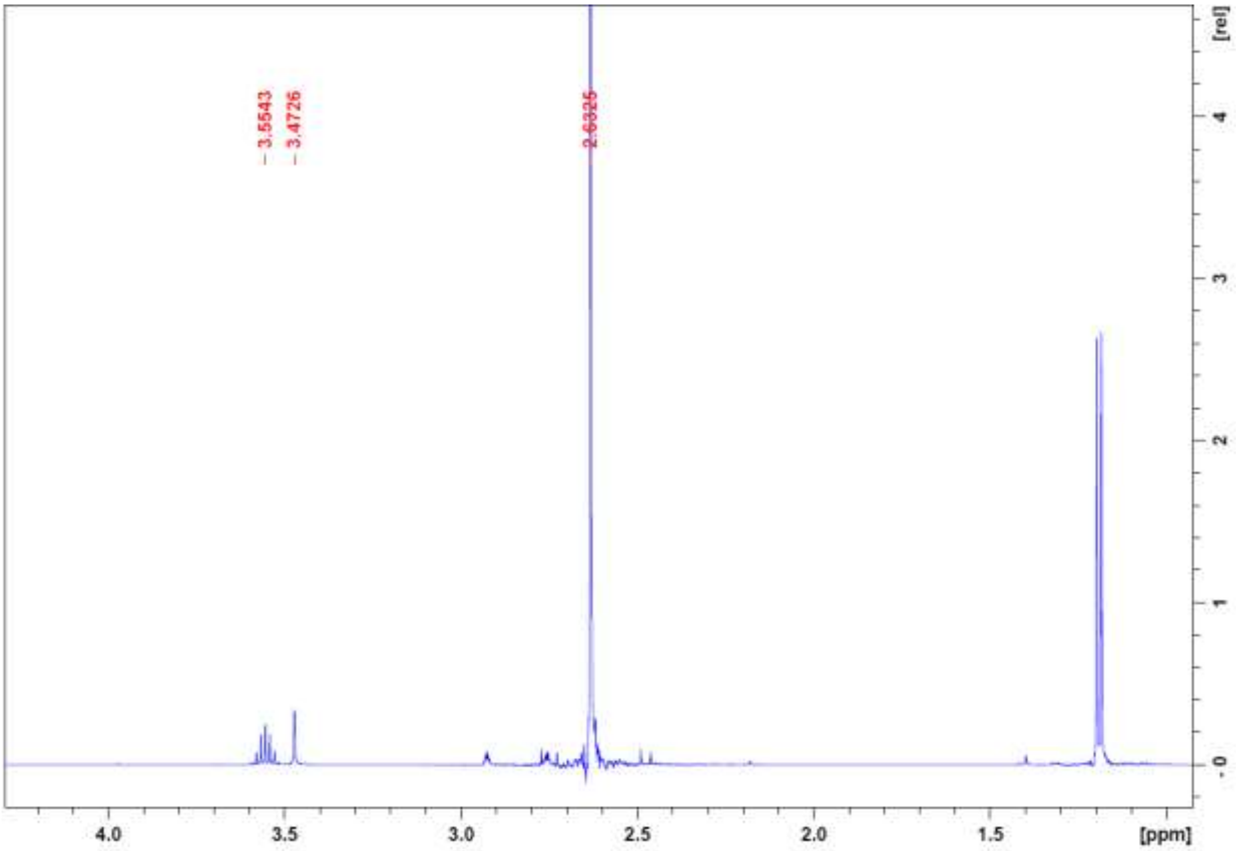

Figure S120. 1D ^{1}H NMR spectrum of DIC with 5 equiv DMTS in DMF-d_7.

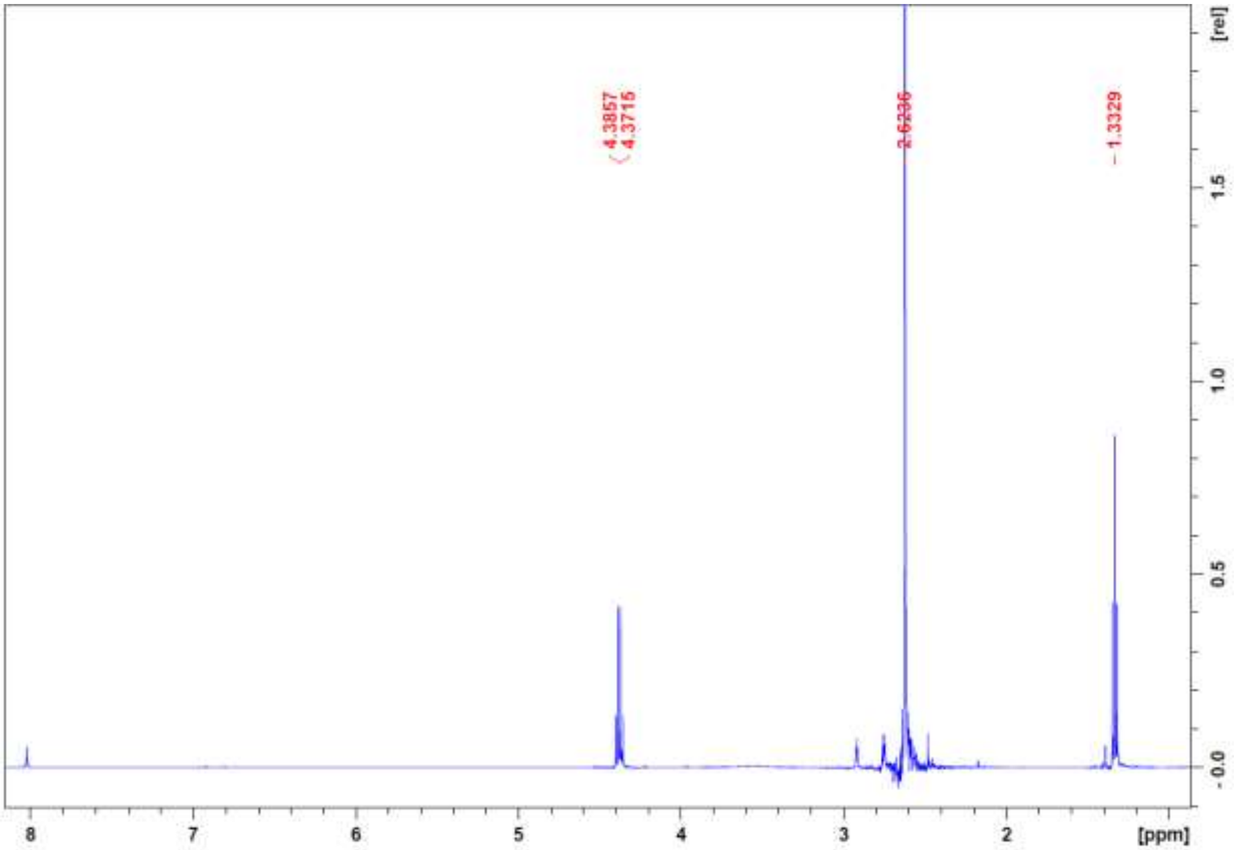

Figure S121. 1D ^{1}H NMR spectrum of Oxyma with 5 equiv DMTS in DMF-d_7.

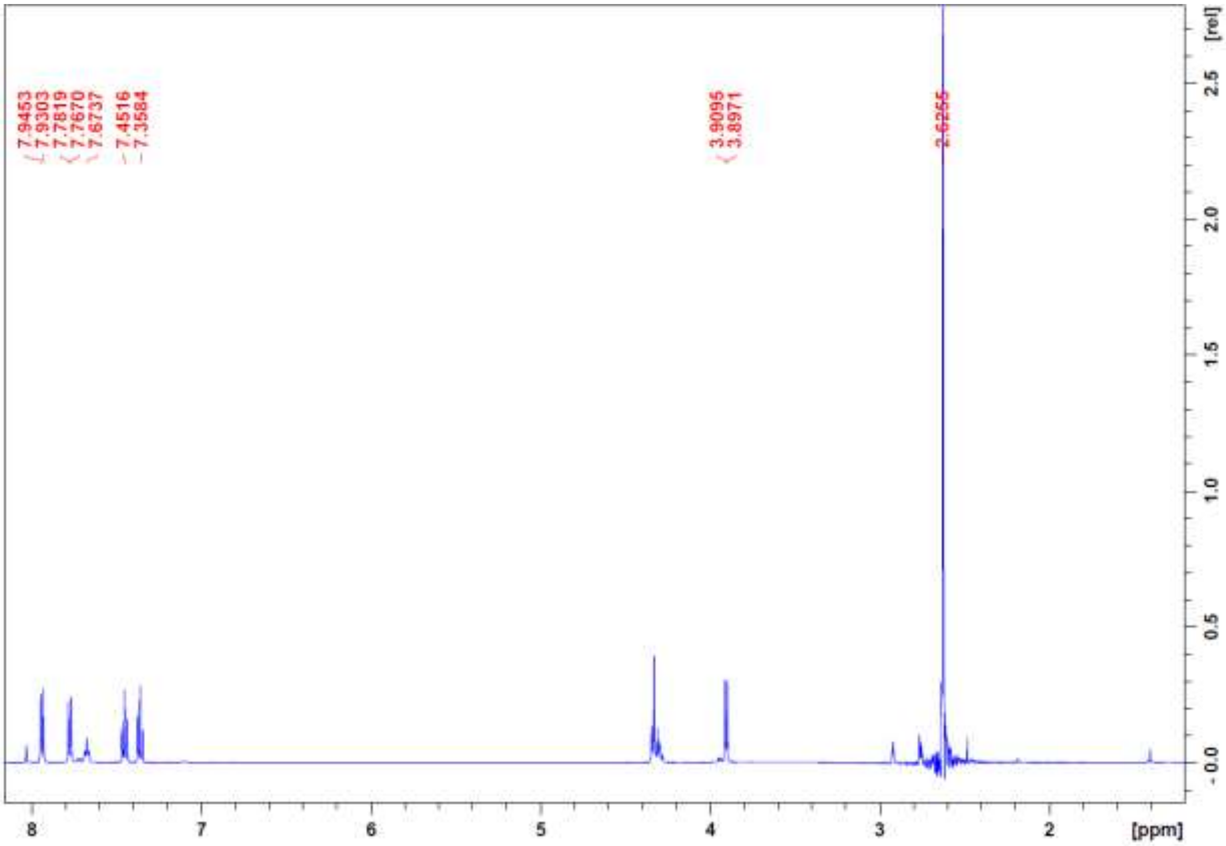

Figure S122. 1D ^{1}H NMR spectrum of Fmoc-Gly-OH with 5 equiv DMTS in DMF-d_7.

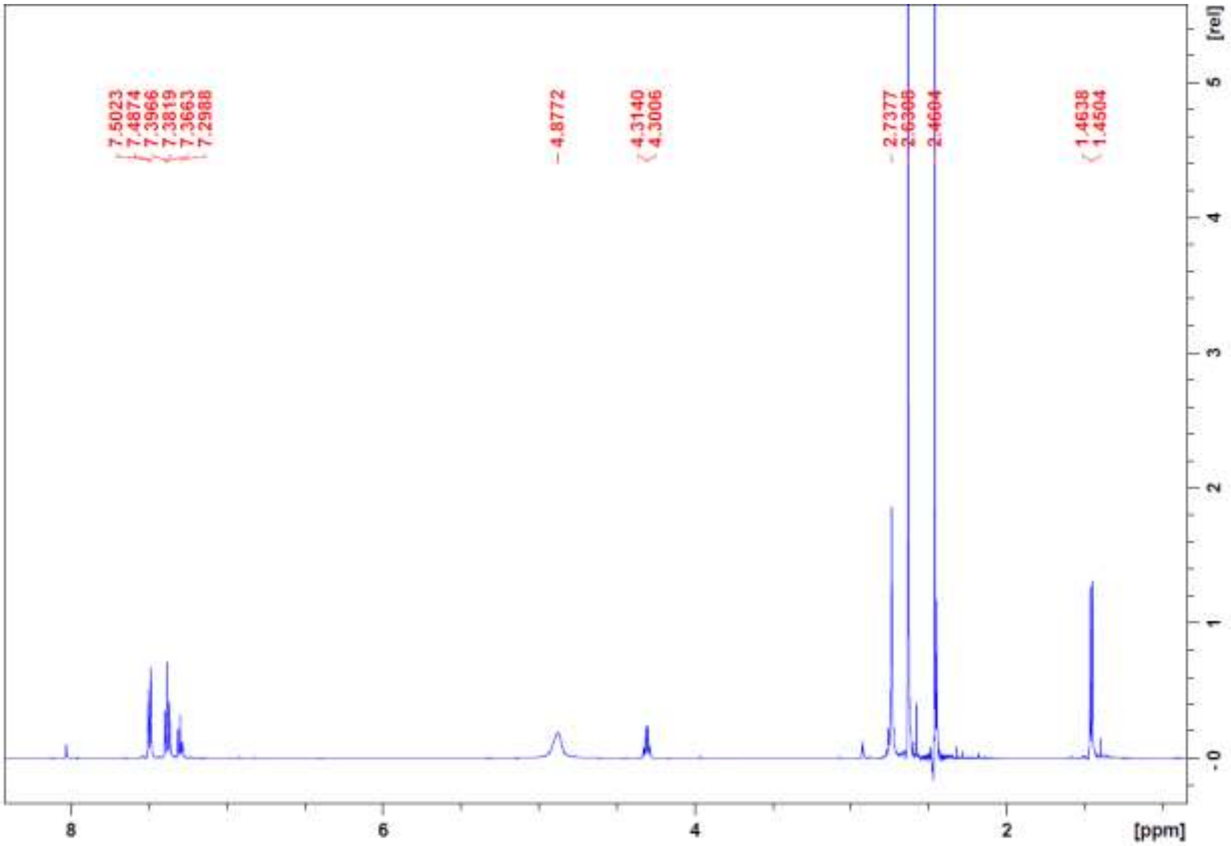

Figure S123. 1D ^{1}H NMR spectrum of (S)-(-)-1-phenylethylamine with 5 equiv DMTS in DMF-d_7.

8.2 Products

Considering that NMR was used to assess the DIC/Oxyma mediated reactions herein, ^{1}H NMR spectra of the different products was required.

All NMR spectra in section 8.2 of this ESI were recorded on a 400 MHz Brucker instrument.

Sample of **2**[3] was obtained as follows:

Oxyma (142.1 mg, 1 mmol, 1 equiv) was dissolved in 2 mL MeCN. DIC (156.6 µL, 1 mmol, 1 equiv) was added to the solution. The resulting mixture was stirred for 16 h at rt and concentrated under vacuum. The residue was purified by normal phase chromatography using silica gel as stationary phase employing Cyclohexane/EtOAc (10:1) → EtOAc to elute the product. 8.9 mg of a colorless oil was obtained.

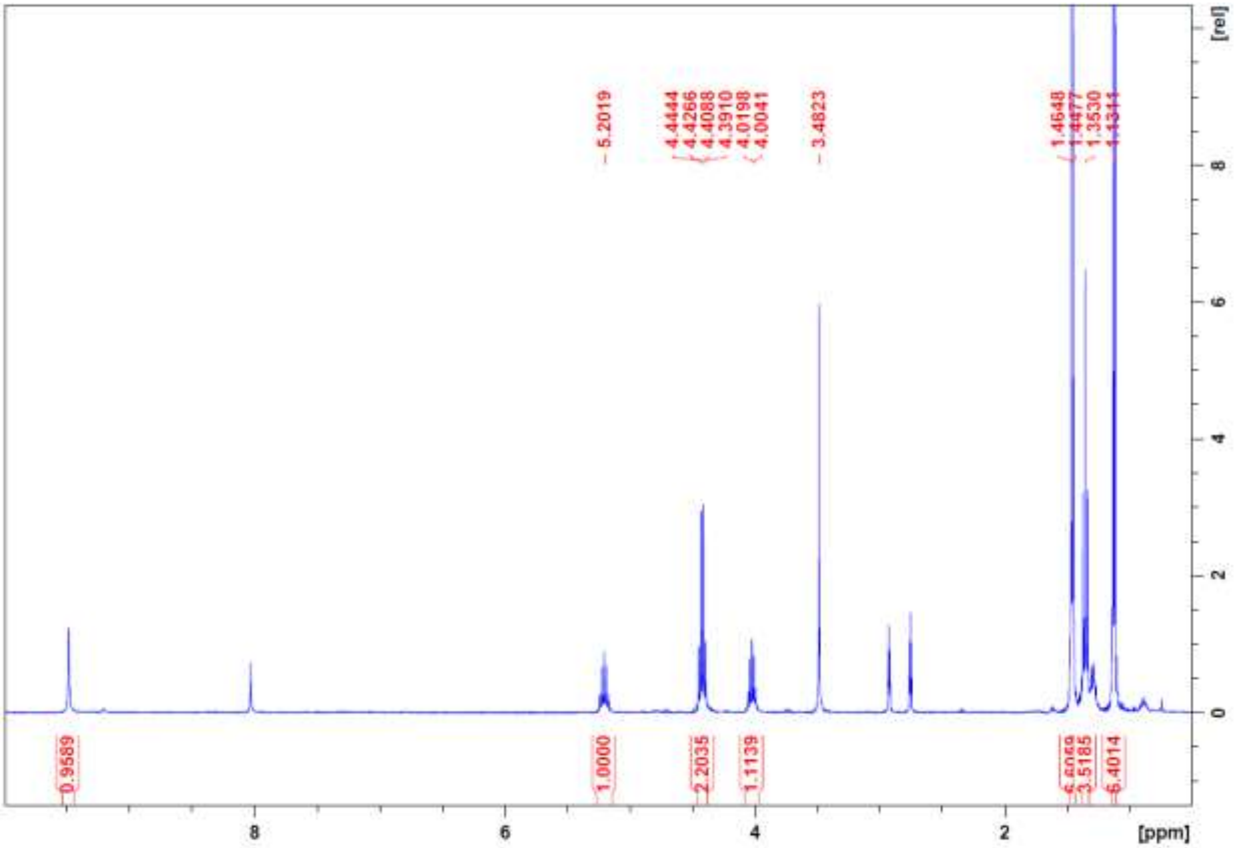

Figure S124. 1D ^{1}H NMR spectrum of **2** in DMF-d_7.

The ^{1}H NMR spectra of **2** and **3** were in keeping with those described by Mc Farland et al.[3]

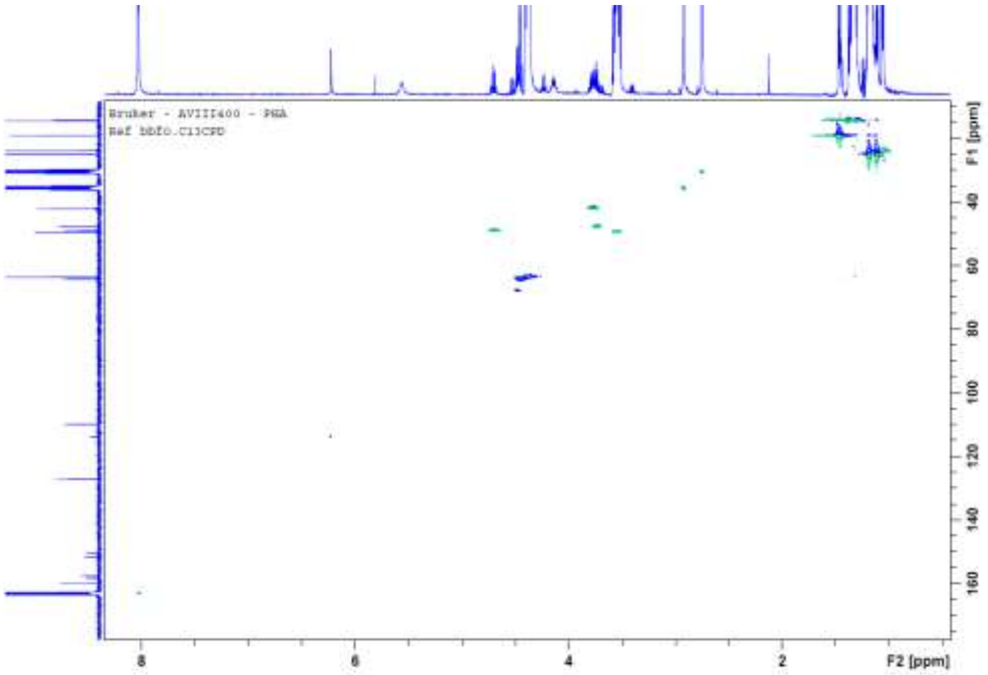

Figure S125. 2D HSQC NMR spectrum of DIC/Oxyma reaction in DMF-d$_7$: evidence of HCN presence in the solution, a correlation of H and C resonances in ^{1}H and ^{13}C was observed.

HCN. ^{1}H NMR (400 MHz, DMF-d$_7$): 6.21 ppm. ^{13}C NMR (400 MHz, DMF-d$_7$): 113.97 ppm.

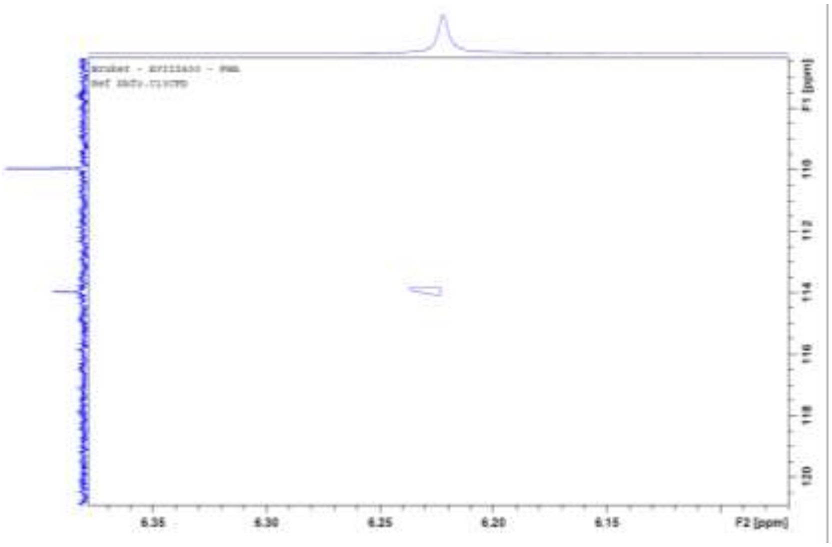

Figure S126. 2D HSQC NMR spectrum of DIC/Oxyma reaction in DMF-d$_7$ (zoom-in).

8.3 Reaction of Fmoc-Gly-OH, Oxyma and DIC in DMF-d_7 with and without DMTS

In this section, NMR assessment of HCN formation during the reaction of Fmoc-Gly-OH, Oxyma and DIC in DMF-d_7 with and without DMTS is delineated. The results pertaining to the reaction of Fmoc-Gly-OH, Oxyma and DIC without DMTS are described in section 8.3.1 and the results related to this reaction performed in the presence of DMTS are summarized in section 8.3.2. A summary of the results of both experiments is detailed in section 8.3.3.

8.3.1 Assessment of HCN formation during activation of Fmoc-Gly-OH using Oxyma/DIC in 0.1 M DMF-d_7

General Procedure for Fmoc-Gly-OH/Oxyma/DIC (1:1:1) reaction.

A stock solution was prepared by dissolving Oxyma (10.0 mg, 0.070 mmol, 1.03 equiv), Fmoc-Gly-OH (20.1 mg, 0.068 mmol, 1.00 equiv) and caffeine (8.2 mg, 0.042 mmol, 0.62 equiv) in 680 µL of DMF-d_7 and the solution was mixed by using an ultrasound bath until all starting materials were dissolved after which DIC (10.65 µL, 0.068 mmol, 1 equiv) was added to the stock solution. 2 x 170 µL (25% v/v of the solution i.e. ~ 0.017 mmol based on Fmoc-Gly-OH) of this stock solution was taken out and transferred to a separate reaction vessel. To this vessel, 5 equiv of DMTS (8.96 µL, 0.085 mmol, 5 equiv) was added and the resulting mixture was transferred to a 3 mm NMR tube. Resulting Fmoc-Gly-OH/Oxyma/DIC DMF-d_7 mixtures with and without DMTS were analysed by ^{1}H NMR at 1 h, 5 h, 10 h and 16 h and the contents of HCN at these time points were determined.

Protocol for the determination of HCN content.

1) Caffeine (2.05 mg, 0.0105 mmol, 0.155 equiv) present in each NMR tube was the reference standard, the singlet at 3.47 ppm (Figure S117) corresponds to 3 protons (CH_3).

2) The integration of the singlet at 6.23 ppm, which corresponds to the HCN proton, would be 1 if the amount of substance was 0.0105 mmol.

3) The integration of peaks in 1) and 2) enabled us to determine the amount of HCN formed from which the concentration of HCN was calculated.

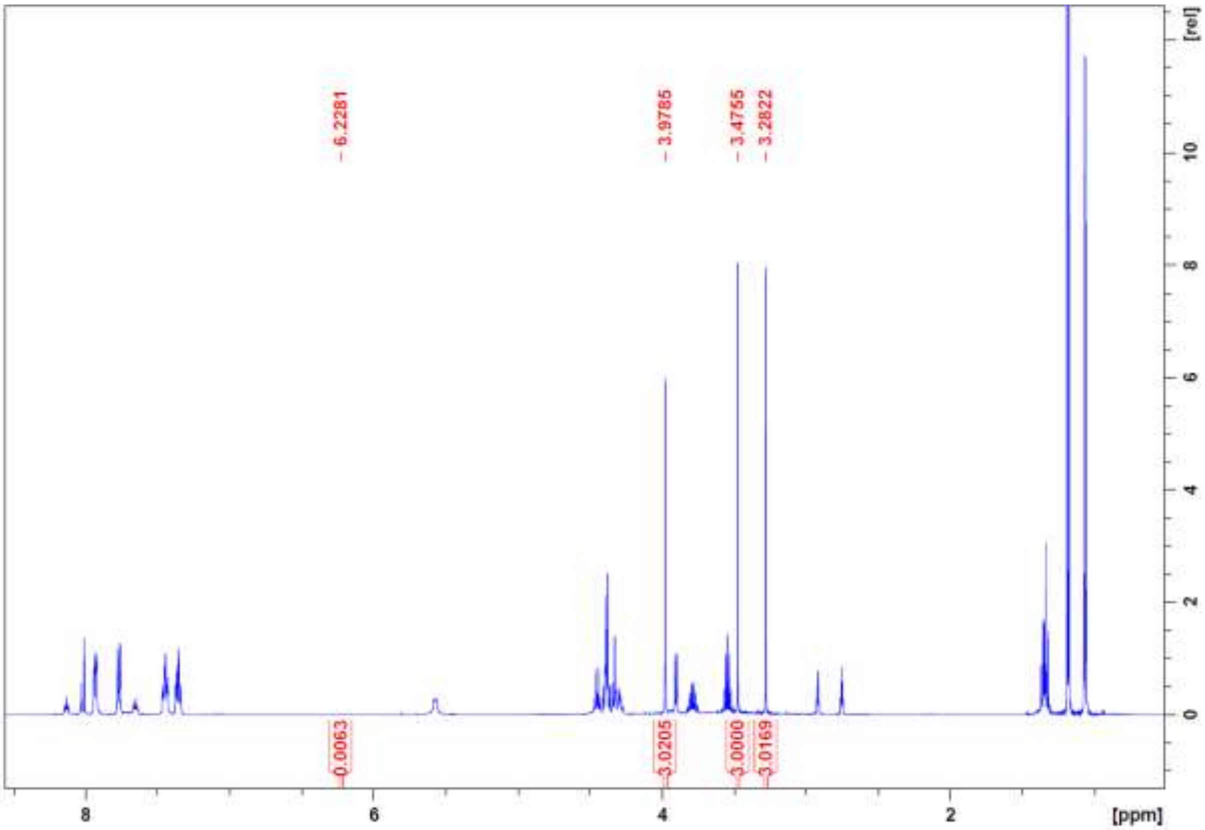

Figure S127. 1D ^{1}H NMR spectrum of Fmoc-Gly-OH/DIC/Oxyma (1:1:1) reaction at 0.1M after 1 h in DMF-d_7 (full spectrum).

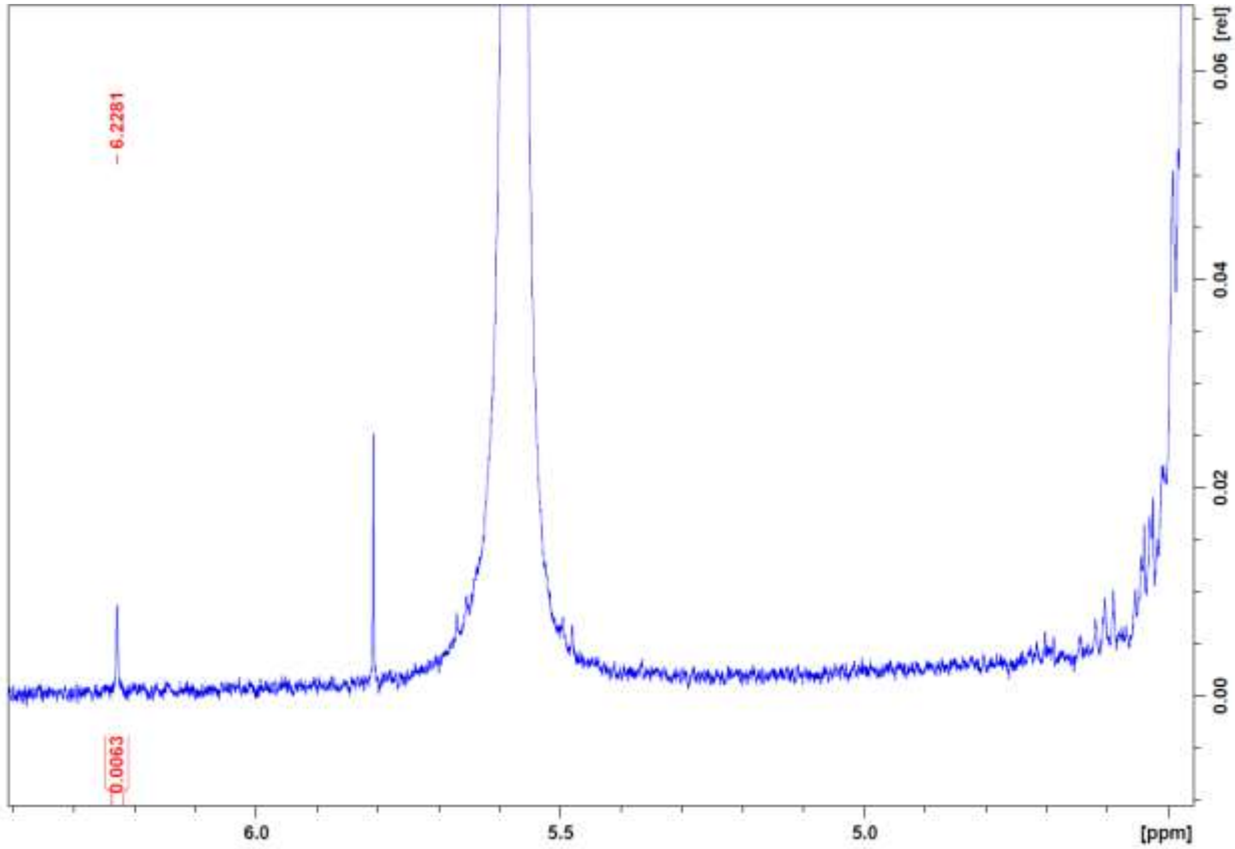

Figure S128. 1D ^{1}H NMR spectrum of Fmoc-Gly-OH/DIC/Oxyma (1:1:1) reaction at 0.1M after 1 h in DMF-d_7 (zoom-in).

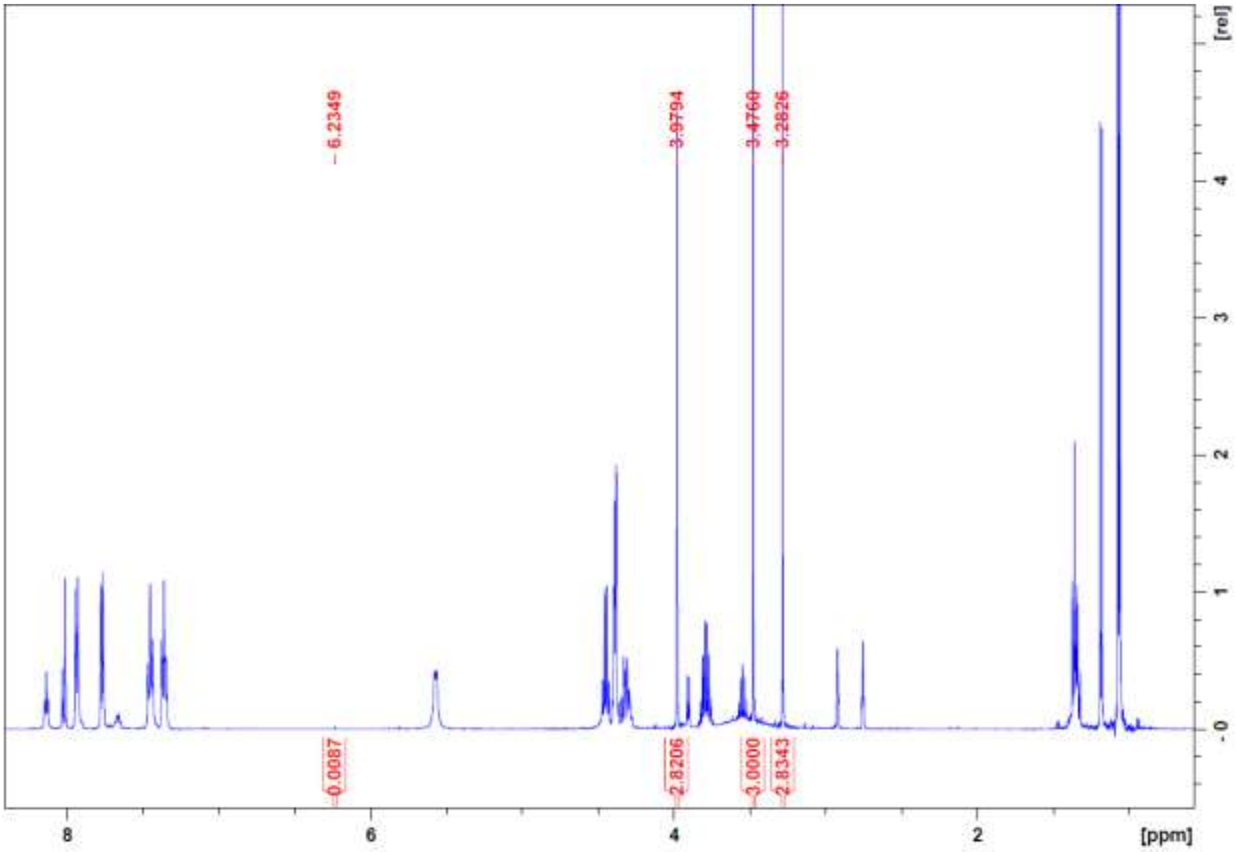

Figure S129. 1D ^{1}H NMR spectrum of Fmoc-Gly-OH/DIC/Oxyma (1:1:1) reaction at 0.1M after 5 h in DMF-d_7 (full spectrum).

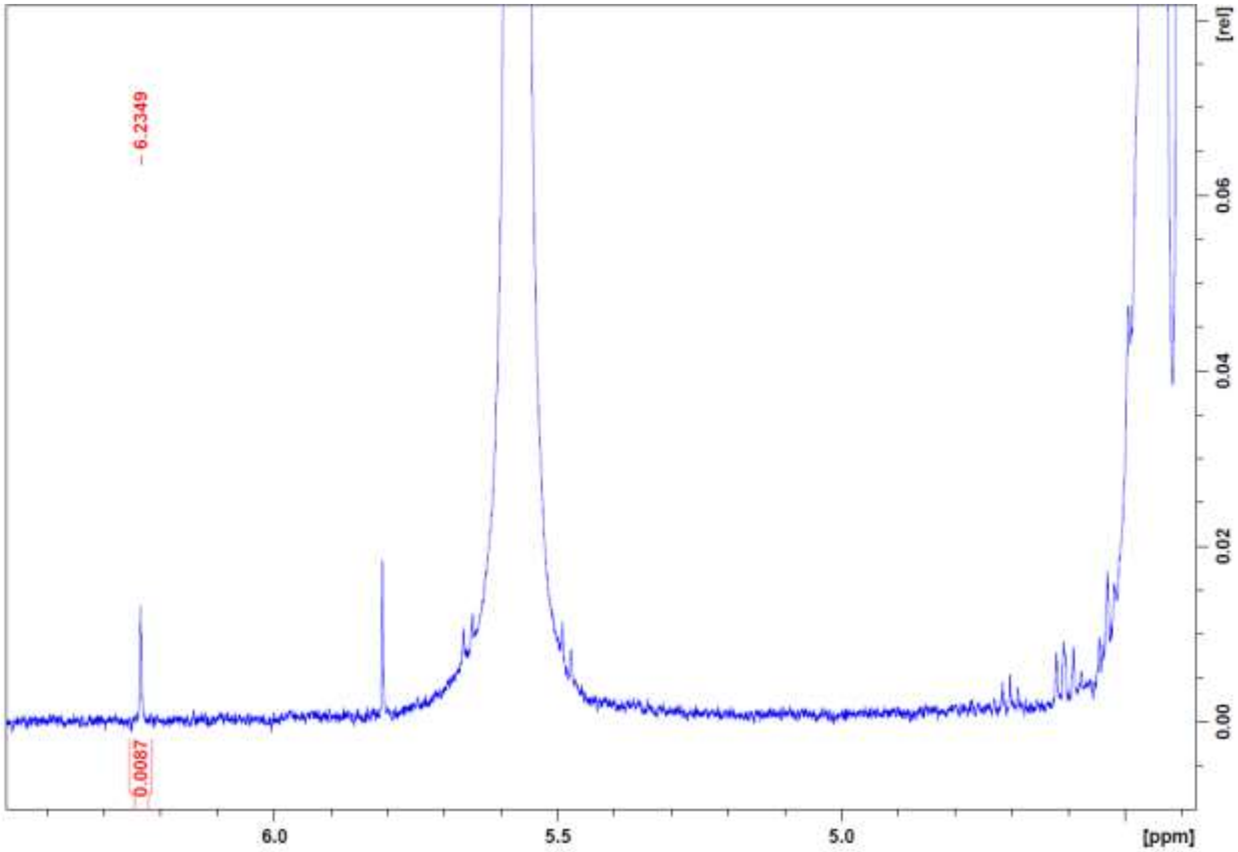

Figure S130. 1D ^{1}H NMR spectrum of Fmoc-Gly-OH/DIC/Oxyma (1:1:1) reaction at 0.1M after 5 h in DMF-d_7 (zoom-in).

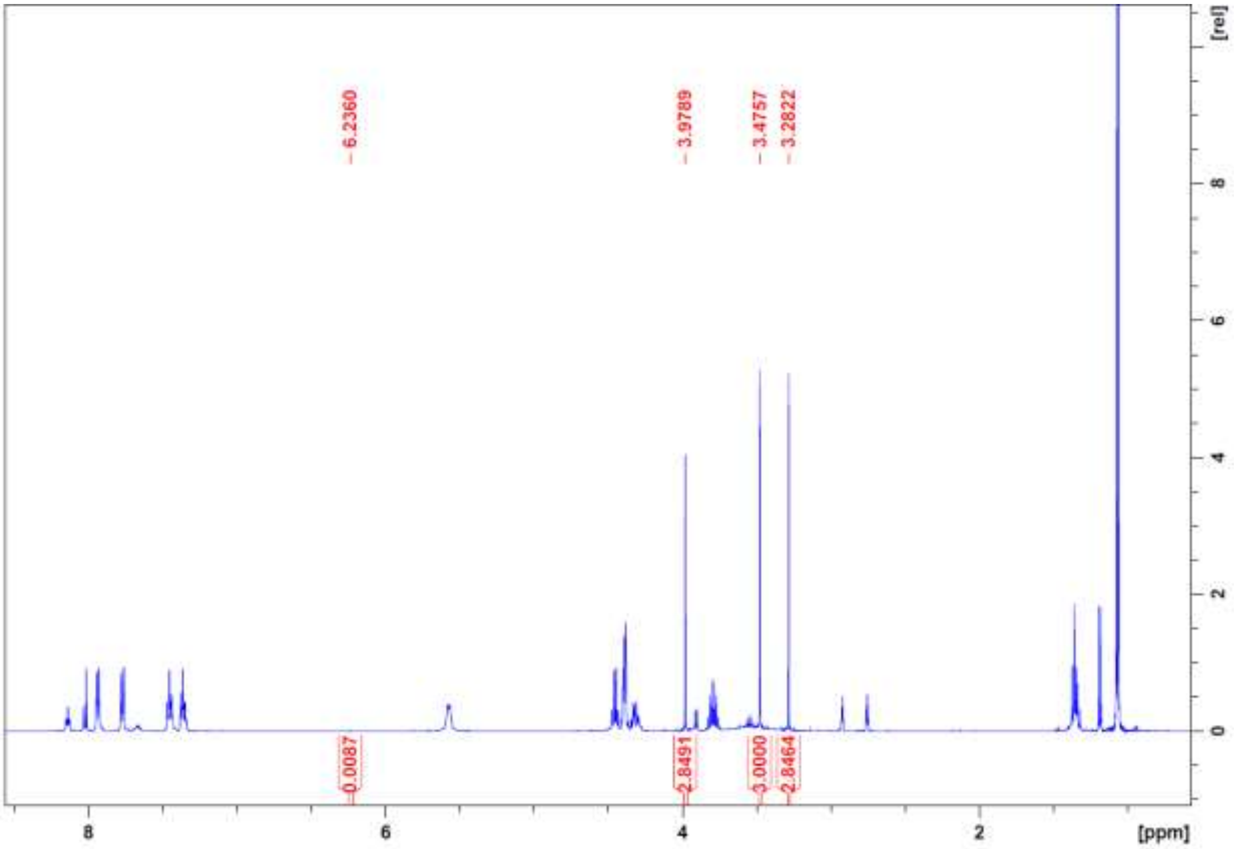

Figure S131. 1D ^{1}H NMR spectrum of Fmoc-Gly-OH/DIC/Oxyma (1:1:1) reaction at 0.1M after 10 h in DMF-d_7 (full spectrum).

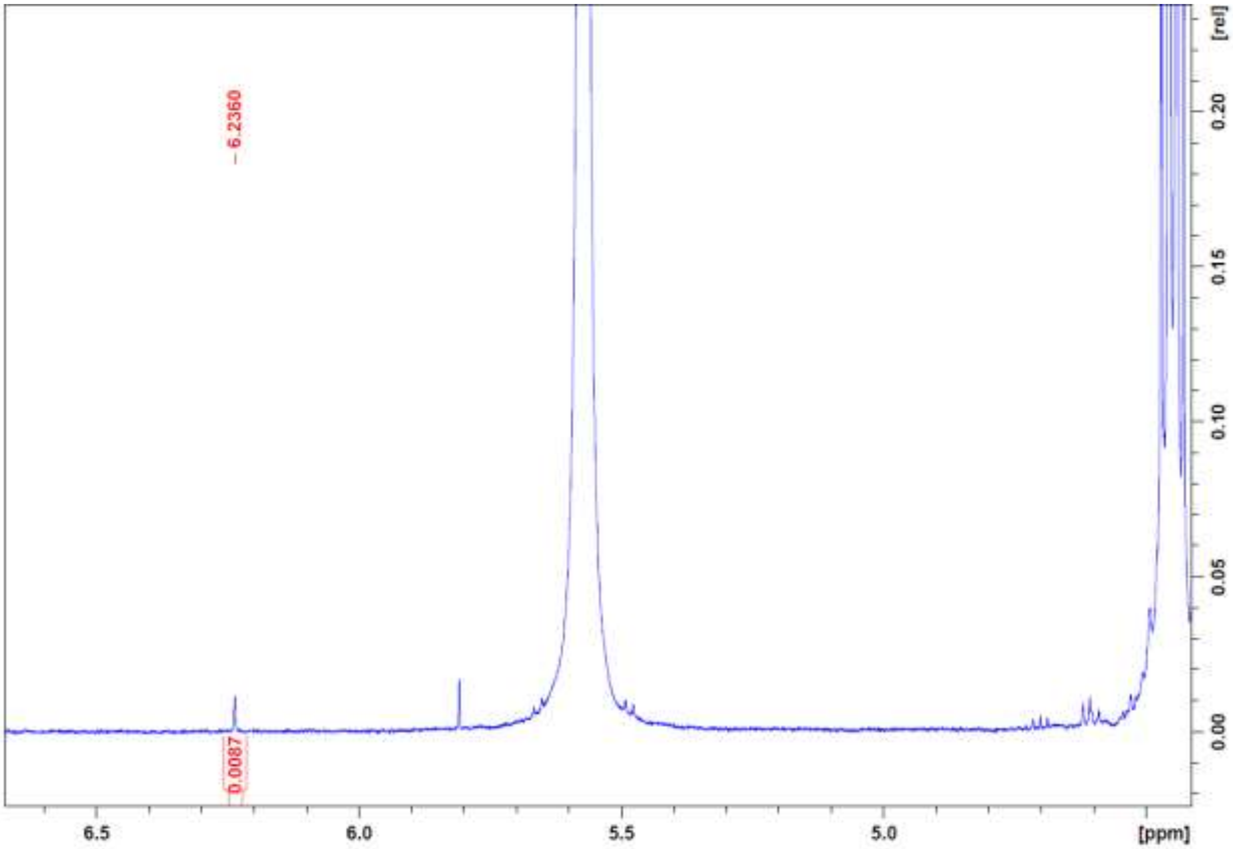

Figure S132. 1D ^{1}H NMR spectrum of Fmoc-Gly-OH/DIC/Oxyma (1:1:1) reaction at 0.1M after 10 h in DMF-d_7 (zoom-in).

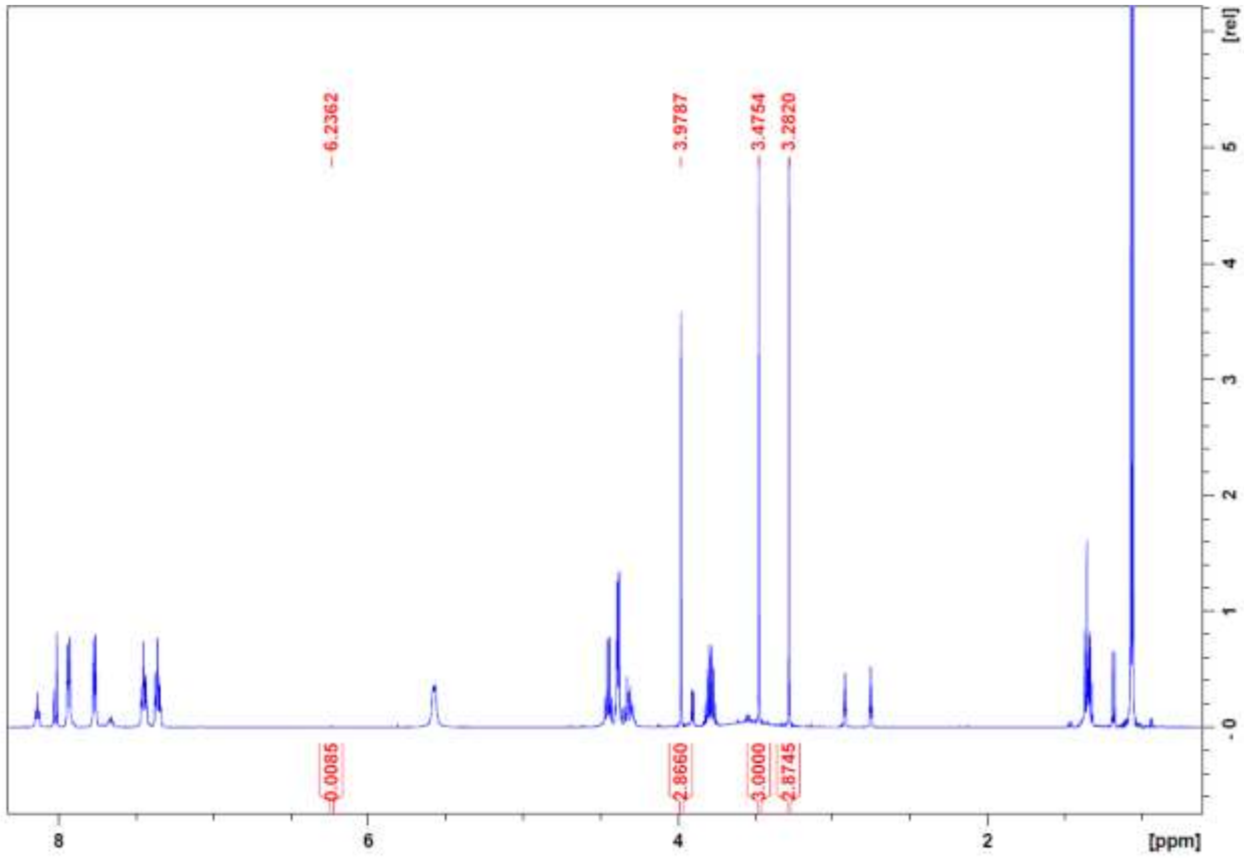

Figure S133. 1D ^{1}H NMR spectrum of Fmoc-Gly-OH/DIC/Oxyma (1:1:1) reaction at 0.1M after 16 h in DMF-d_7 (full spectrum).

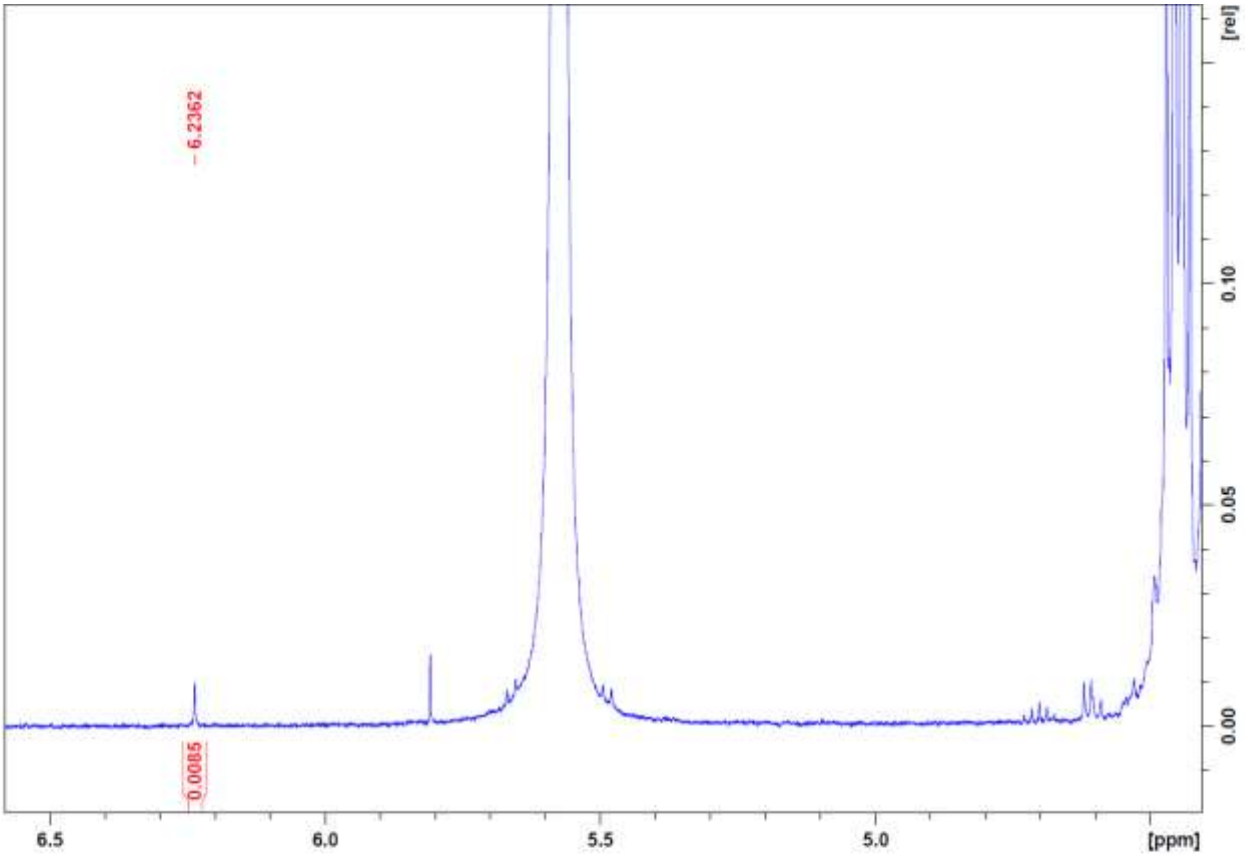

Figure S134. 1D ^{1}H NMR spectrum of Fmoc-Gly-OH/DIC/Oxyma (1:1:1) reaction at 0.1M after 16 h in DMF-d_7 (zoom-in).

8.3.2 Assessment of HCN formation during activation of Fmoc-Gly-OH using Oxyma/DIC with 5 equiv DMTS in 0.1 M DMF-d_7

The general procedure for the reactions of Fmoc-Gly-OH activation in DMF-d_7 as described in the section 8.3.1 of this ESI was followed.

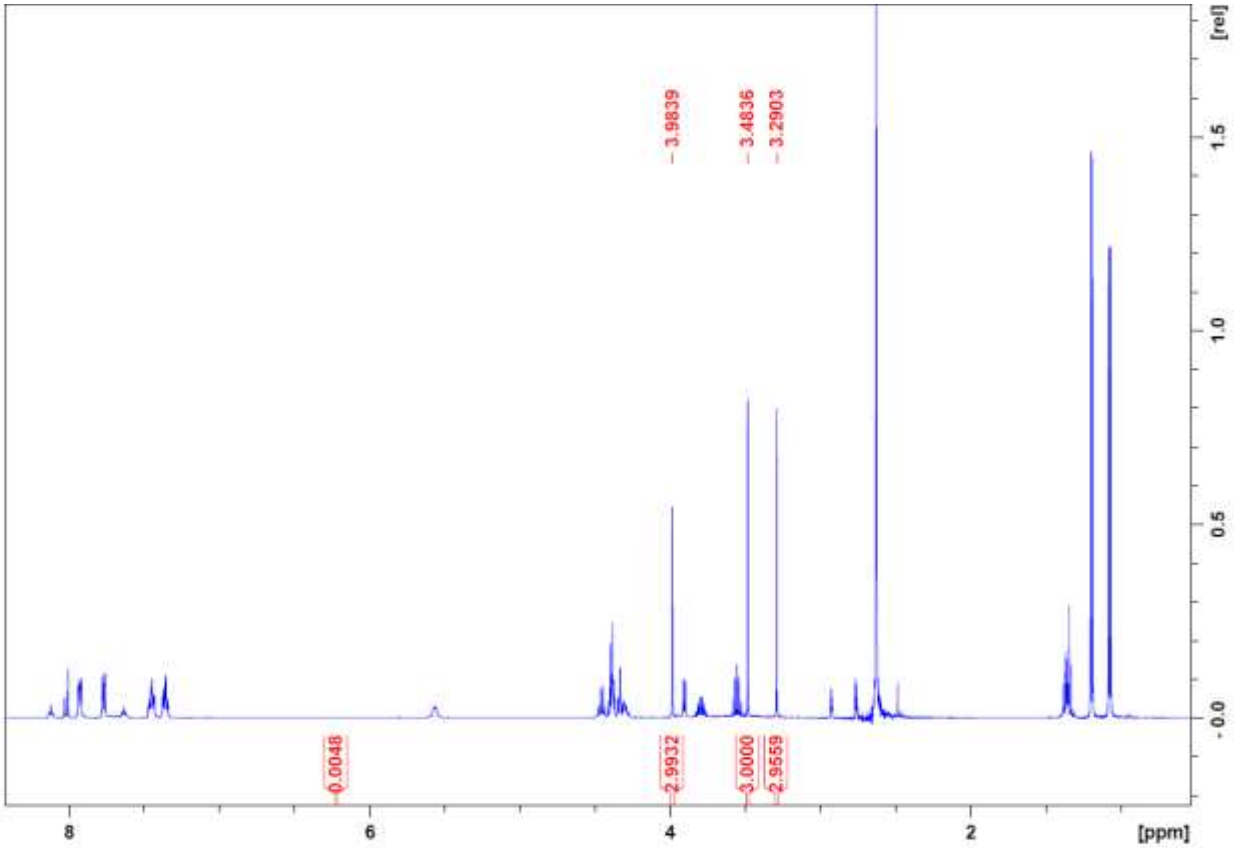

Figure S135. 1D ^{1}H NMR spectrum of Fmoc-Gly-OH/DIC/Oxyma (1:1:1) reaction with 5 equiv DMTS at 0.1M after 1 h in DMF-d_7 (full spectrum).

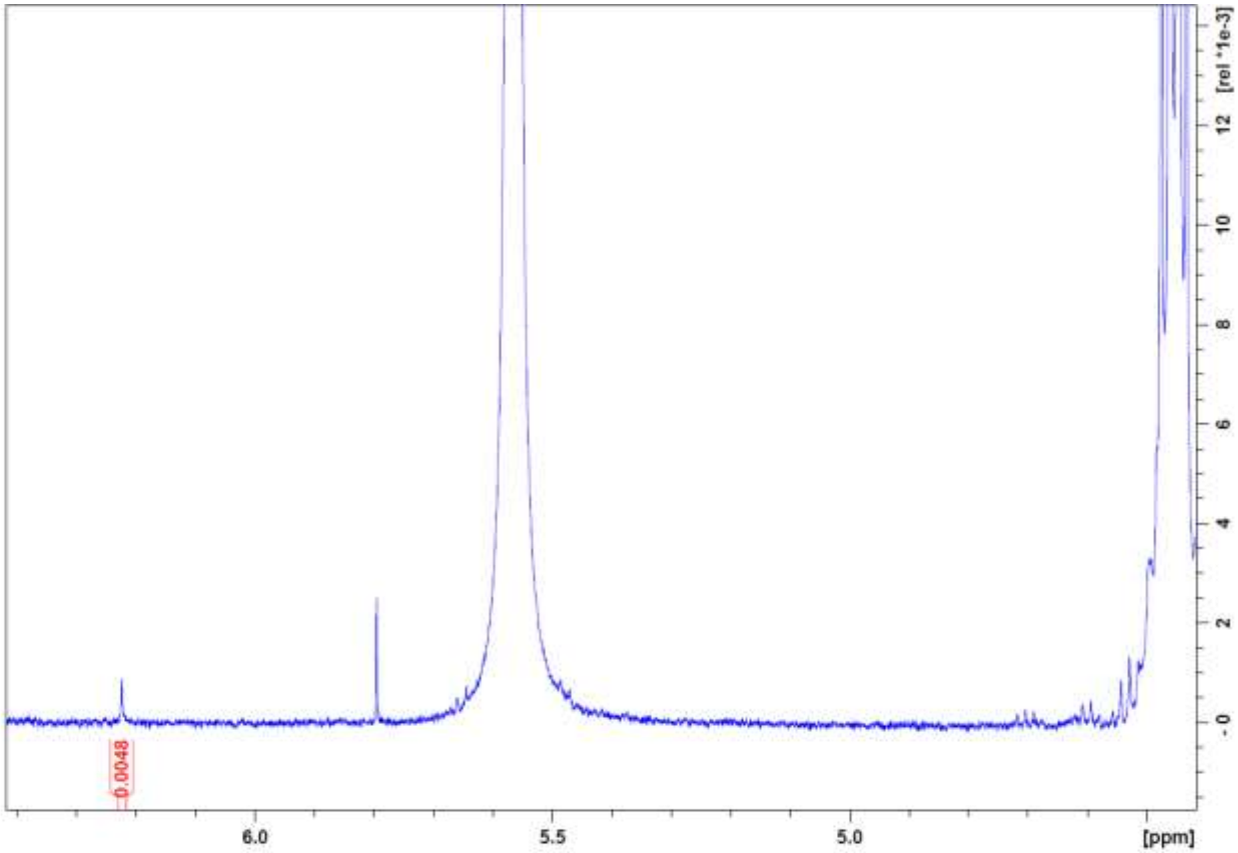

Figure S136. 1D ^{1}H NMR spectrum of Fmoc-Gly-OH/DIC/Oxyma (1:1:1) reaction with 5 equiv DMTS at 0.1M after 1 h in DMF-d_7 (zoom-in).

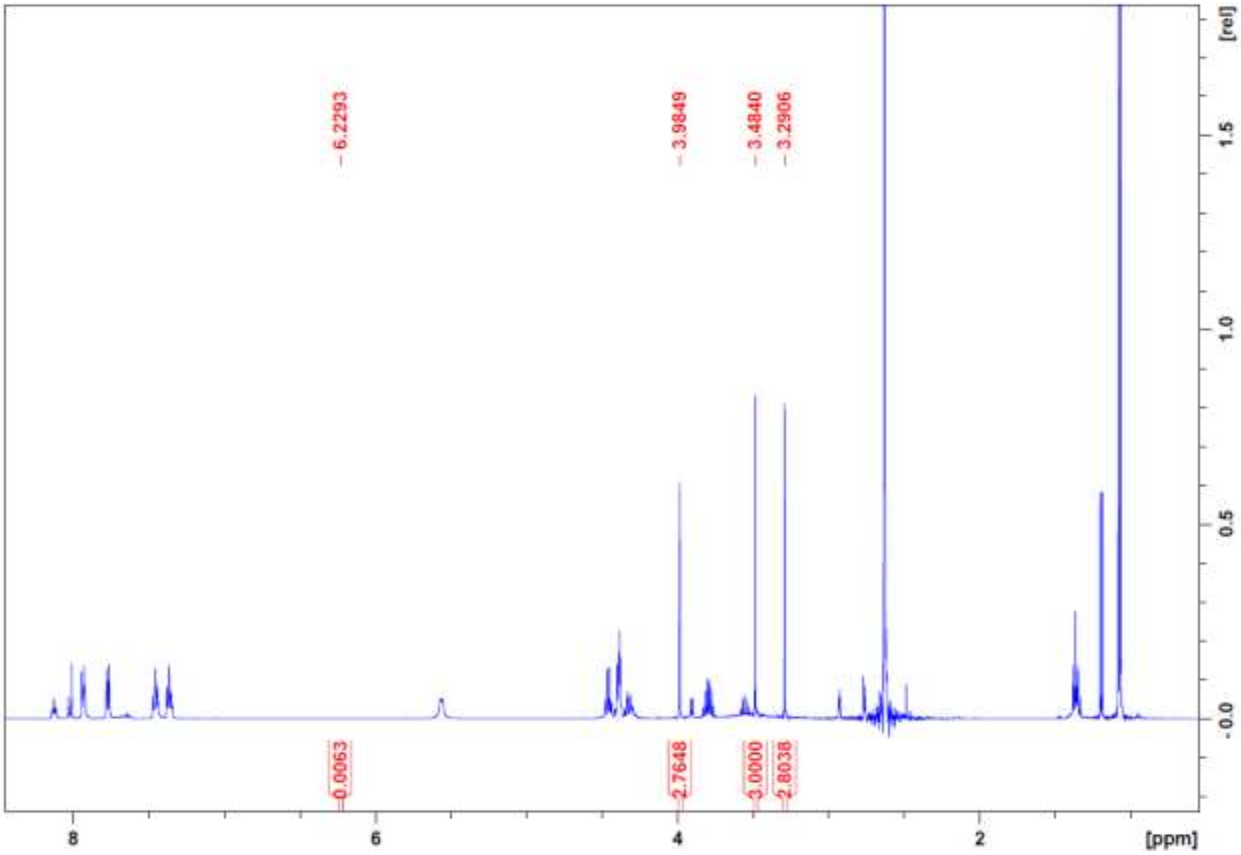

Figure S137. 1D ^{1}H NMR spectrum of Fmoc-Gly-OH/DIC/Oxyma (1:1:1) reaction with 5 equiv DMTS at 0.1M after 5 h in DMF-d_7 (full spectrum).

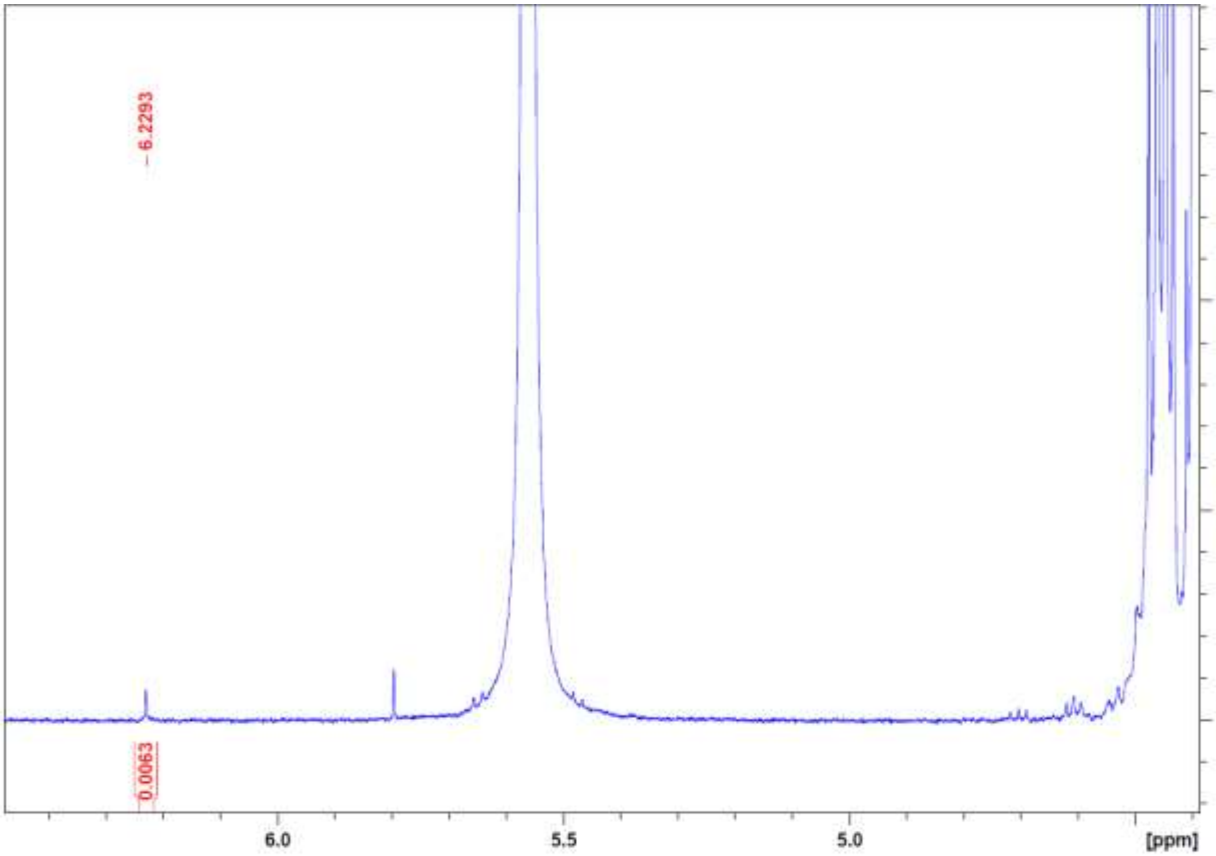

Figure S138. 1D ^{1}H NMR spectrum of Fmoc-Gly-OH/DIC/Oxyma (1:1:1) reaction with 5 equiv DMTS at 0.1M after 5 h in DMF-d$_7$ (zoom-in).

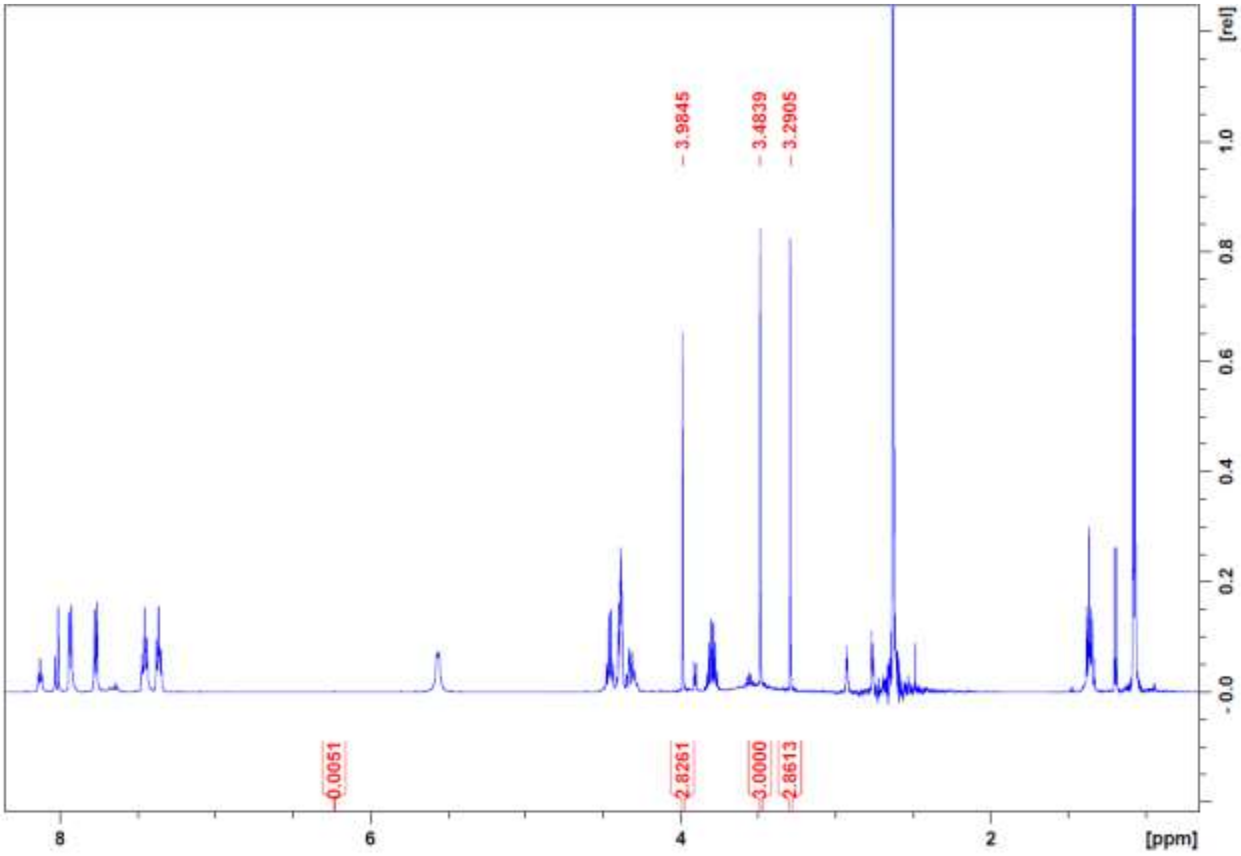

Figure S139. 1D ^{1}H NMR spectrum of Fmoc-Gly-OH/DIC/Oxyma (1:1:1) reaction with 5 equiv DMTS at 0.1M after 10 h in DMF-d_7 (full spectrum).

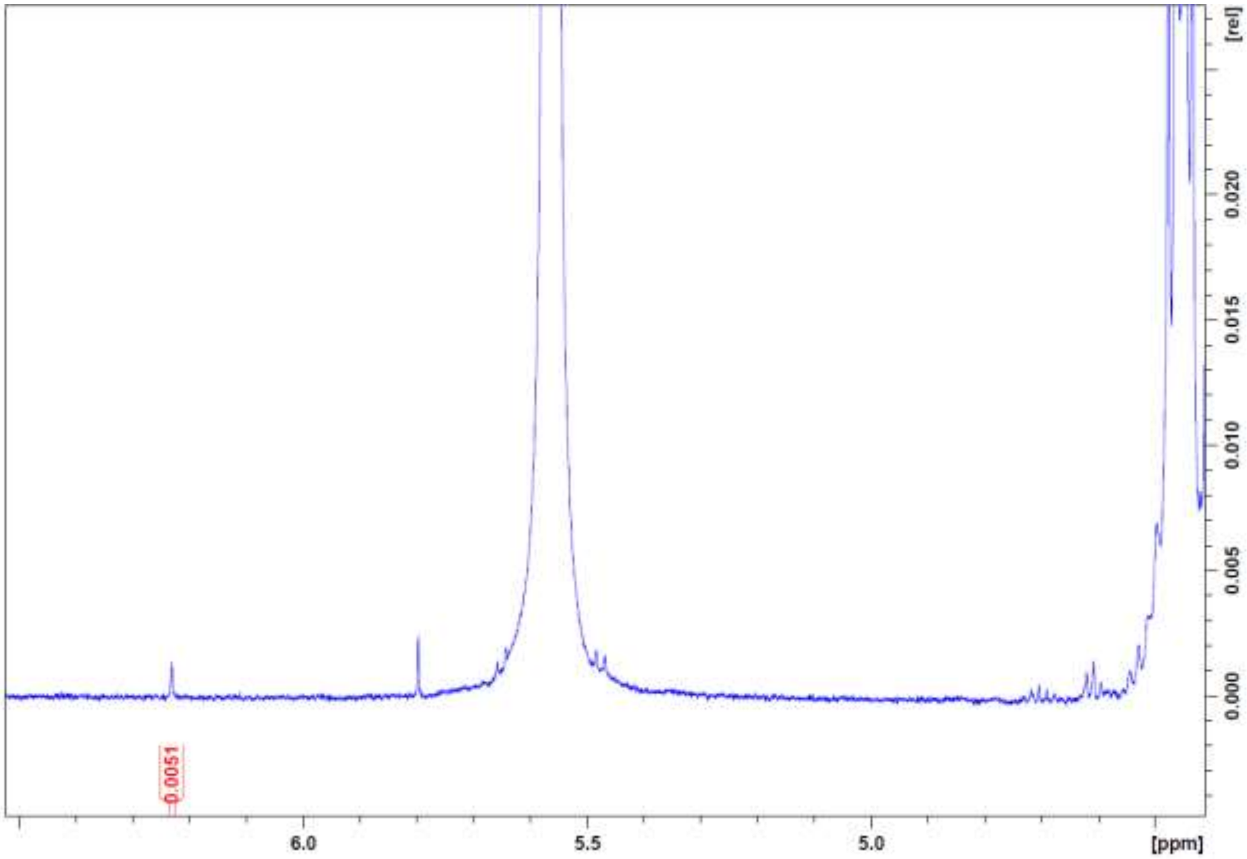

Figure S140. 1D ^{1}H NMR spectrum of Fmoc-Gly-OH/DIC/Oxyma (1:1:1) reaction with 5 equiv DMTS at 0.1M after 10 h in DMF-d_7 (zoom-in).

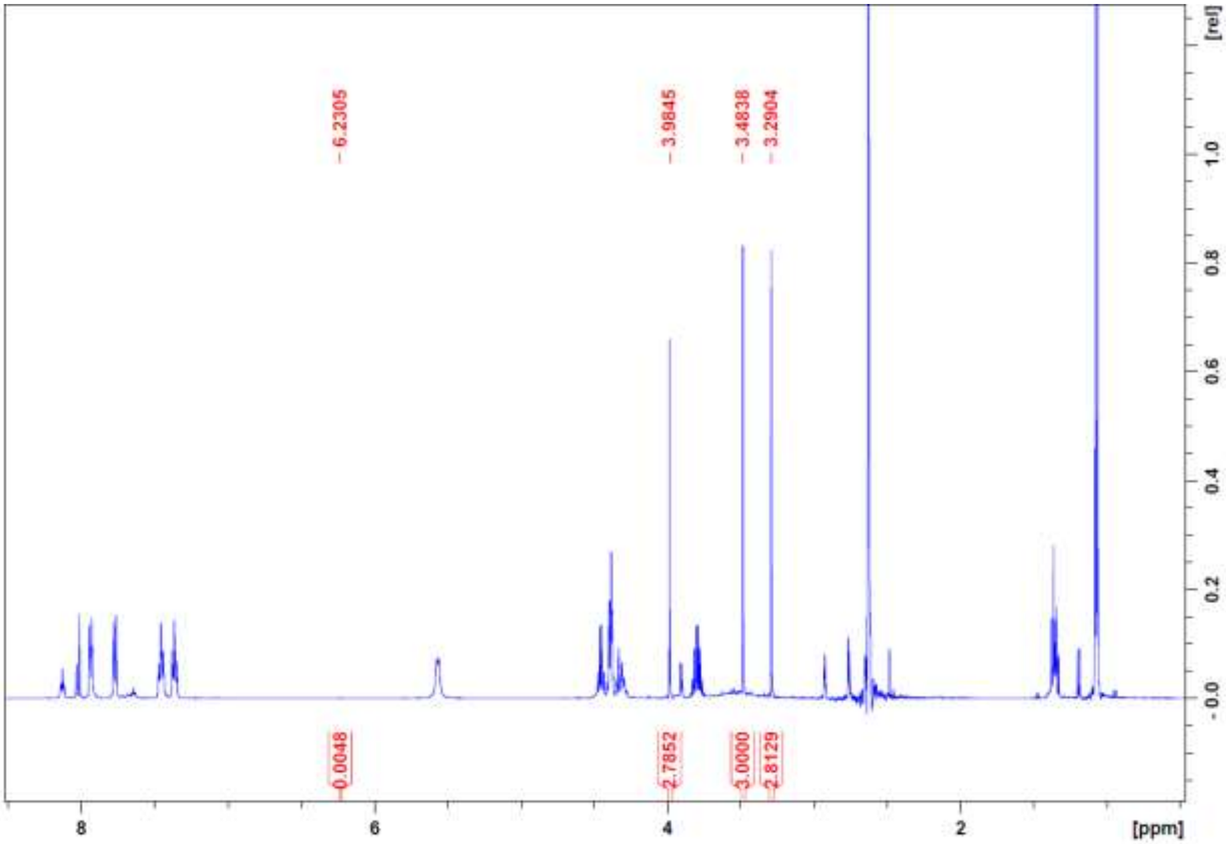

Figure S141. 1D ^{1}H NMR spectrum of Fmoc-Gly-OH/DIC/Oxyma (1:1:1) reaction with 5 equiv DMTS at 0.1M after 16 h in DMF-d_7 (full spectrum).

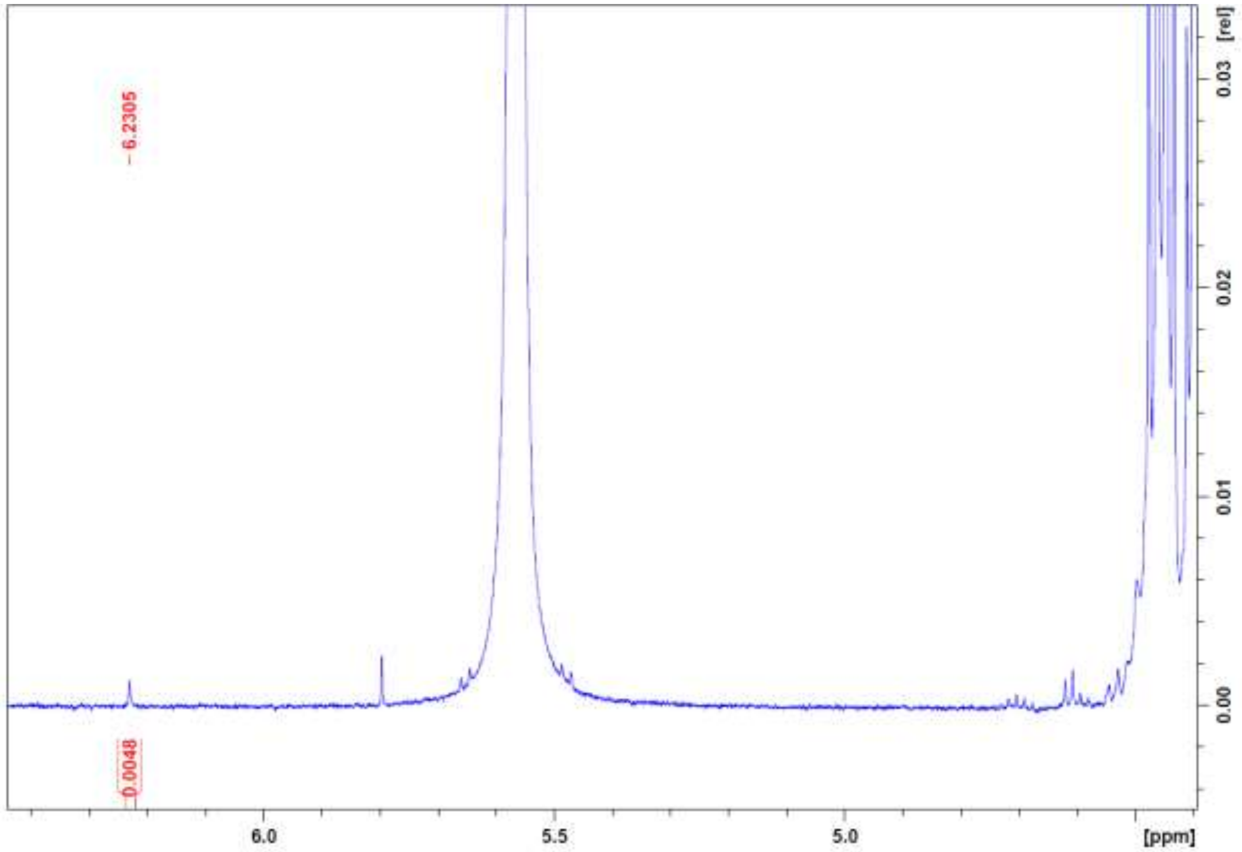

Figure S142. 1D ^{1}H NMR spectrum of Fmoc-Gly-OH/DIC/Oxyma (1:1:1) reaction with 5 equiv DMTS at 0.1M after 16 h in DMF-d_7 (zoom-in).

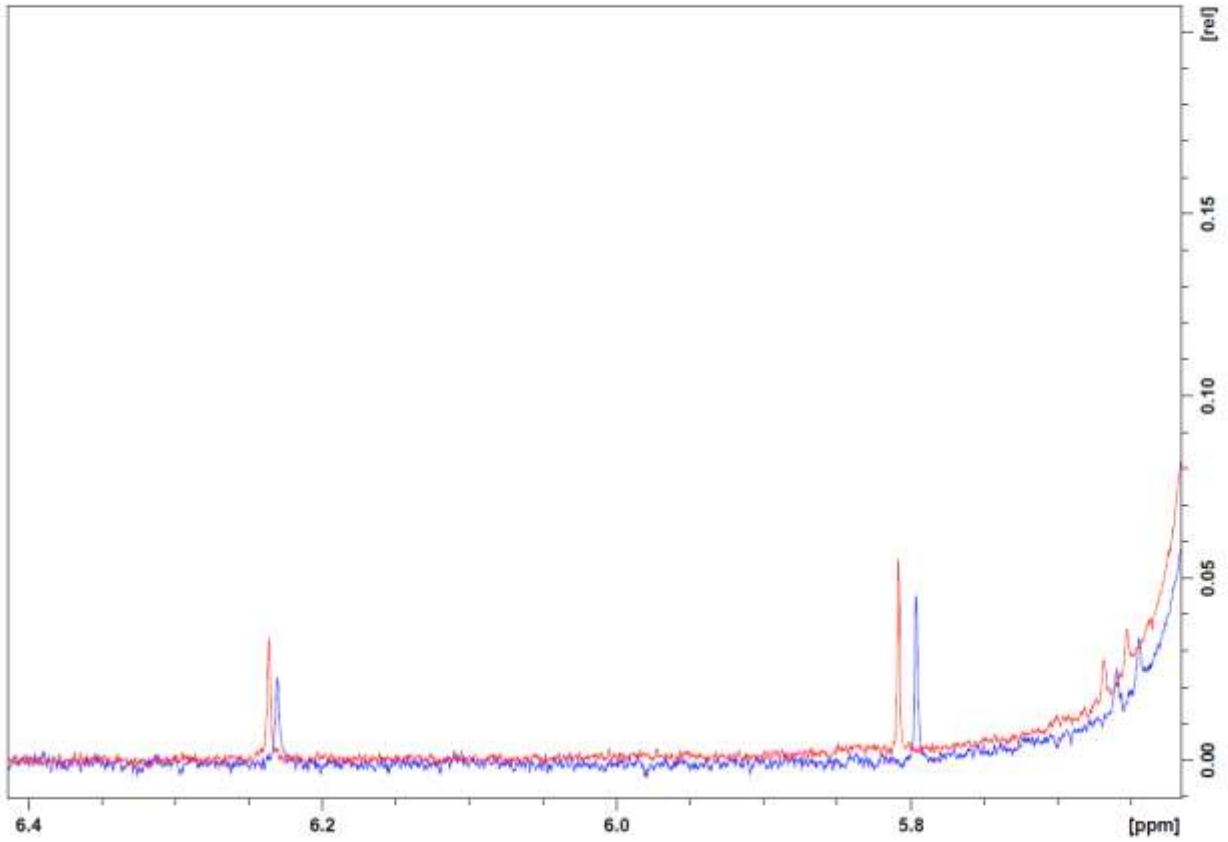

Figure S143. Overlap of 1D ^{1}H NMR spectra of Fmoc-Gly-OH/DIC/Oxyma (1:1:1) reaction without DMTS (in red) and with 5 equiv DMTS (in blue) after 16 h in DMF-d$_7$ (zoom-in).

8.3.3 Summary of HCN formation during activation of Fmoc-Gly-OH using Oxyma/DIC in 0.1 M DMF-d_7

This section summarize the results in sections 8.3.1 and 8.3.2.

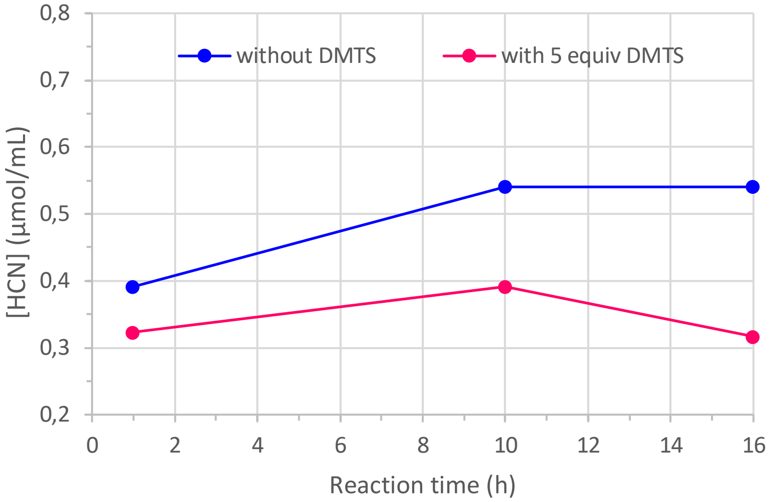

Figure S144. HCN concentration over time at rt in DMF-d_7 with and without 5 equiv DMTS. The concentration was calculated according to the method described in section 8.3.1.

Conclusion of the experiments summarized in Fig. S144: HCN concentration was lowered by using 5 equiv of DMTS during activation of Fmoc-Gly-OH with Oxyma/DIC. As the key step of peptide synthesis is not the activation of the AA but rather the amide bond formation itself, the impact of using DMTS as HCN scavenger during DIC/Oxyma mediated amide bond formation is described in the ensuing section of this ESI.

9. NMR analysis of HCN formation during amide bond formations mediated by DIC/Oxyma with and without DMTS

The impact of using DMTS as HCN scavenger in the reaction of DIC with Oxyma and during Fmoc-Gly-OH activation by DIC/Oxyma was described in sections 7 and 8 of this ESI, respectively. The aim of this section was to assess the amide bond formation using DMTS as an HCN scavenger. First, amidation reaction without DMTS was evaluated over time by ^{1}H NMR after which the same amide bond formation in the presence of 5 and 10 equiv of DMTS was evaluated.

9.1 Assessment of HCN formation during amide bond formation in 0.1 M DMF-d_7

General Procedure for amide bond formation.

A stock solution was prepared by dissolving Oxyma (10.1 mg, 0.071 mmol, 1.04 equiv), Fmoc-Gly-OH (20.3 mg, 0.068 mmol, 1 equiv) and caffeine (8.0 mg, 0.042 mmol, 0.62 equiv) in 680 µL of DMF-d_7. The solution was mixed by using an ultrasound bath. (S)-(-)-1-phenylethylamine (8.77 µL, 0.068 mmol, 1.0 equiv) and DIC (10.65 µL, 0.068 mmol, 1.0 equiv) were added to the stock solution. (S)-(-)-1-phenylethylamine addition was carried out prior to addition of DIC. 170 µL (25% v/v of the solution i.e. ~0.017 mmol based on Fmoc-Gly-OH) of this stock solution was taken out and 0, 5, 10 equiv of DMTS were added to the 170 µL solution. The latter was transferred into a 3 mm NMR tube and transferred to the spectrometer for monitoring at 20°C. 1D ^{1}H NMR acquisition was done after 1 h, 5 h, 10 h and 16 h.

The method used for the determination of HCN concentration is described in section 8.3 of this ESI.

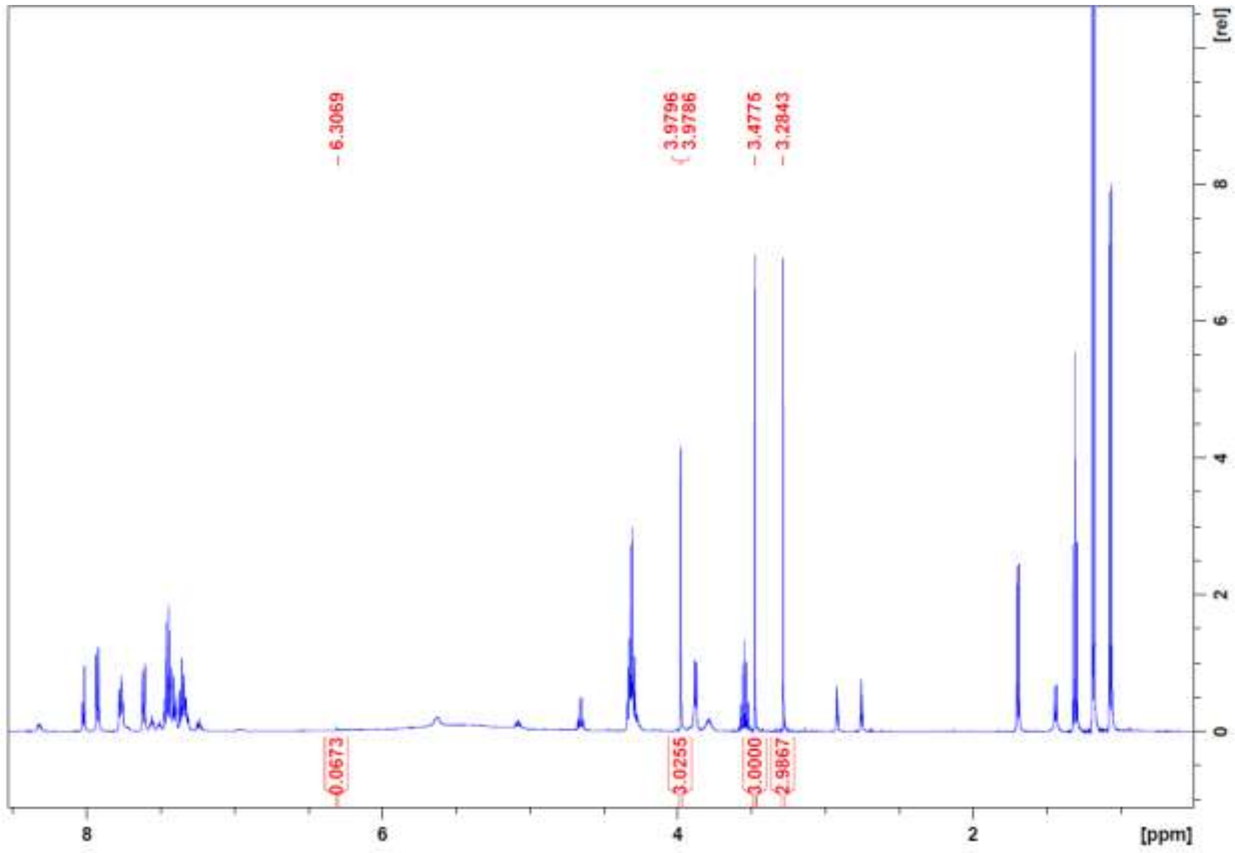

Figure S145. 1D ^{1}H NMR spectrum of Fmoc-Gly-OH/DIC/Oxyma/(S)-(-)-1-phenylethylamine (1:1:1:1) reaction at 0.1M after 1 h in DMF-d_7 (full spectrum).

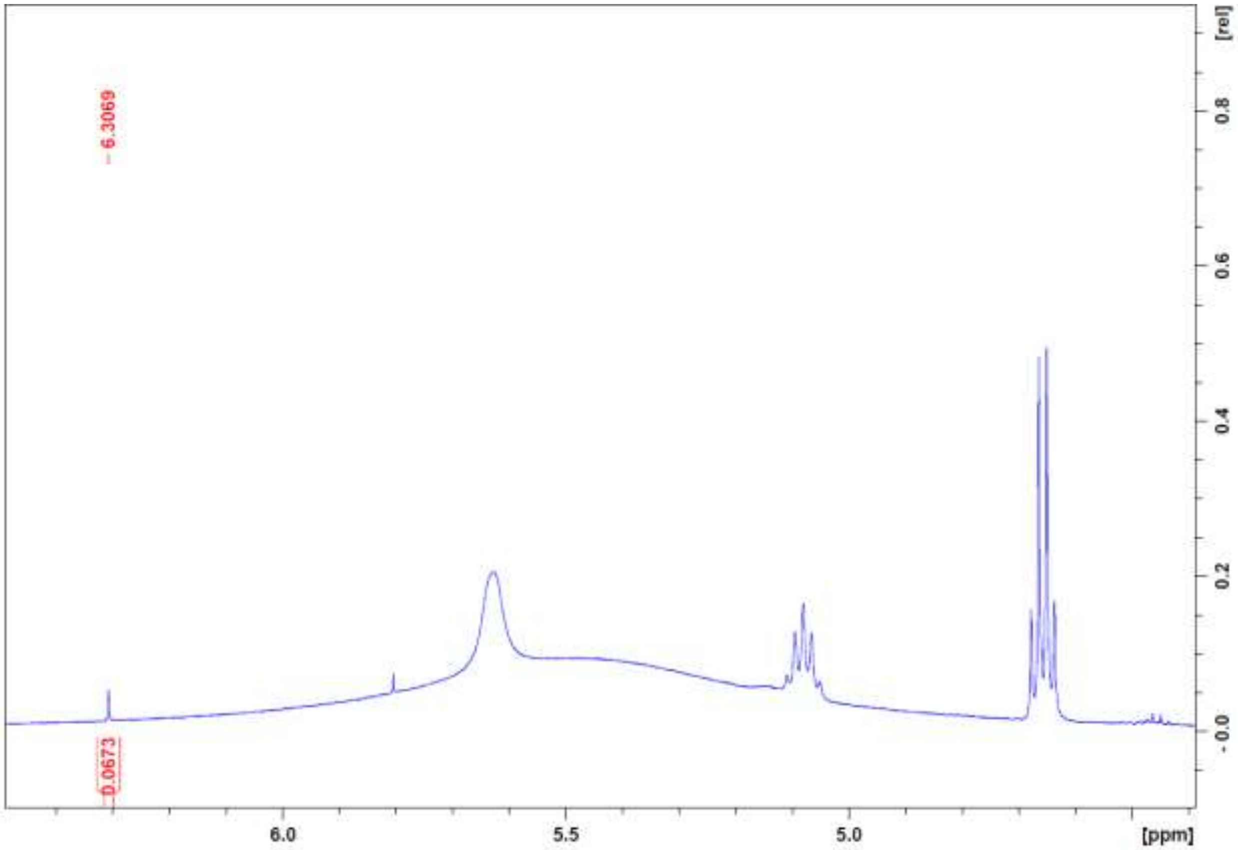

Figure S146. 1D ^{1}H NMR spectrum of Fmoc-Gly-OH/DIC/Oxyma/(S)-(-)-1-phenylethylamine (1:1:1:1) reaction at 0.1M after 1 h in DMF-d_7 (zoom-in).

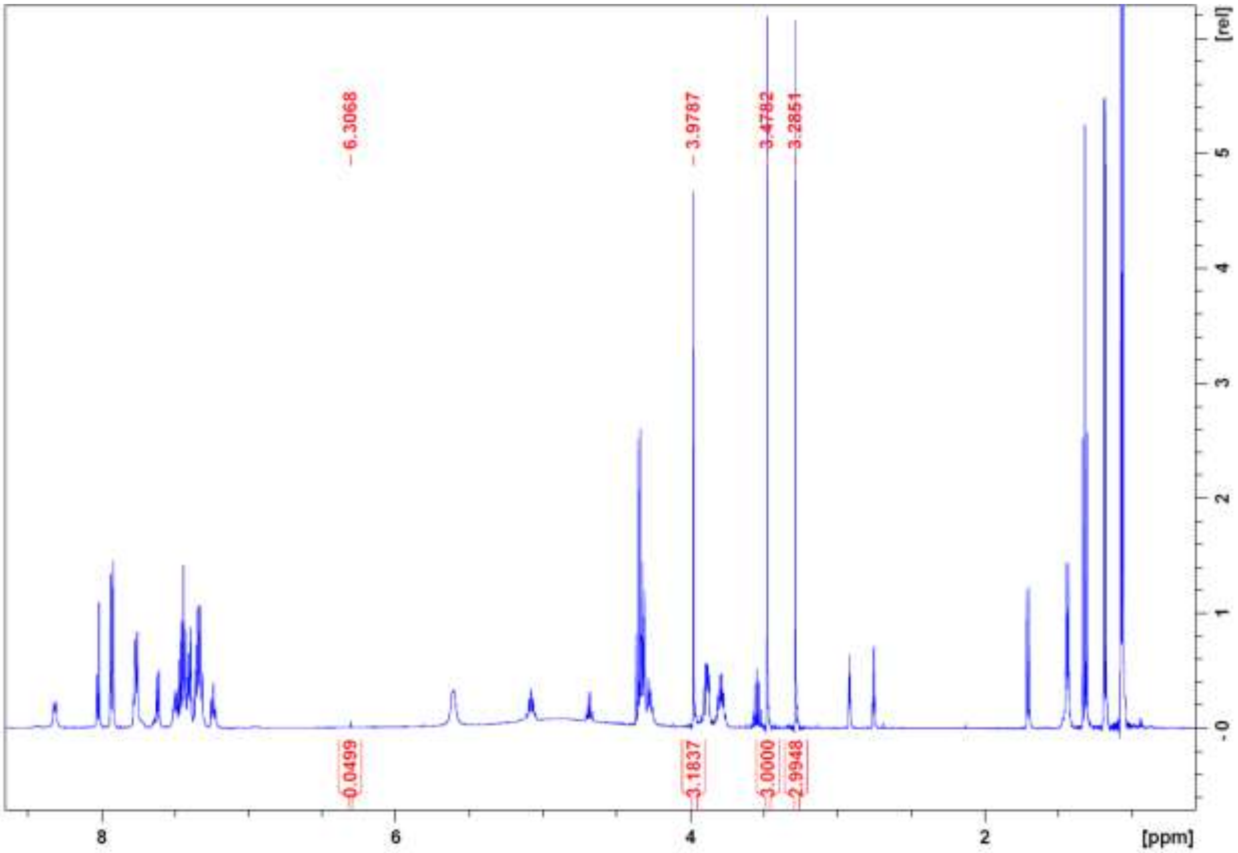

Figure S147. 1D ^{1}H NMR spectrum of Fmoc-Gly-OH/DIC/Oxyma/(S)-(-)-1-phenylethylamine (1:1:1:1) reaction at 0.1M after 5 h in DMF-d_7 (full spectrum).

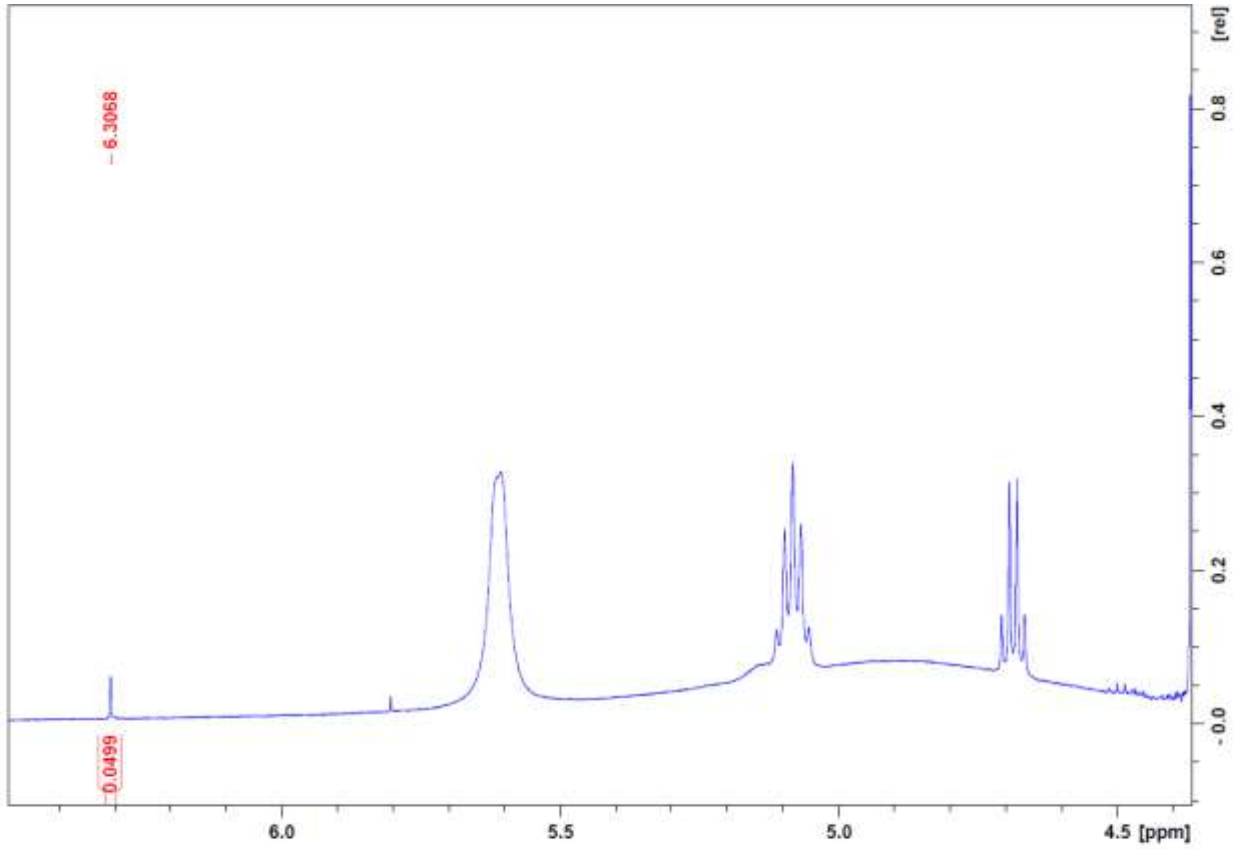

Figure S148. 1D ^{1}H NMR spectrum of Fmoc-Gly-OH/DIC/Oxyma/(S)-(-)-1-phenylethylamine (1:1:1:1) reaction at 0.1M after 5 h in DMF-d_7 (zoom-in).

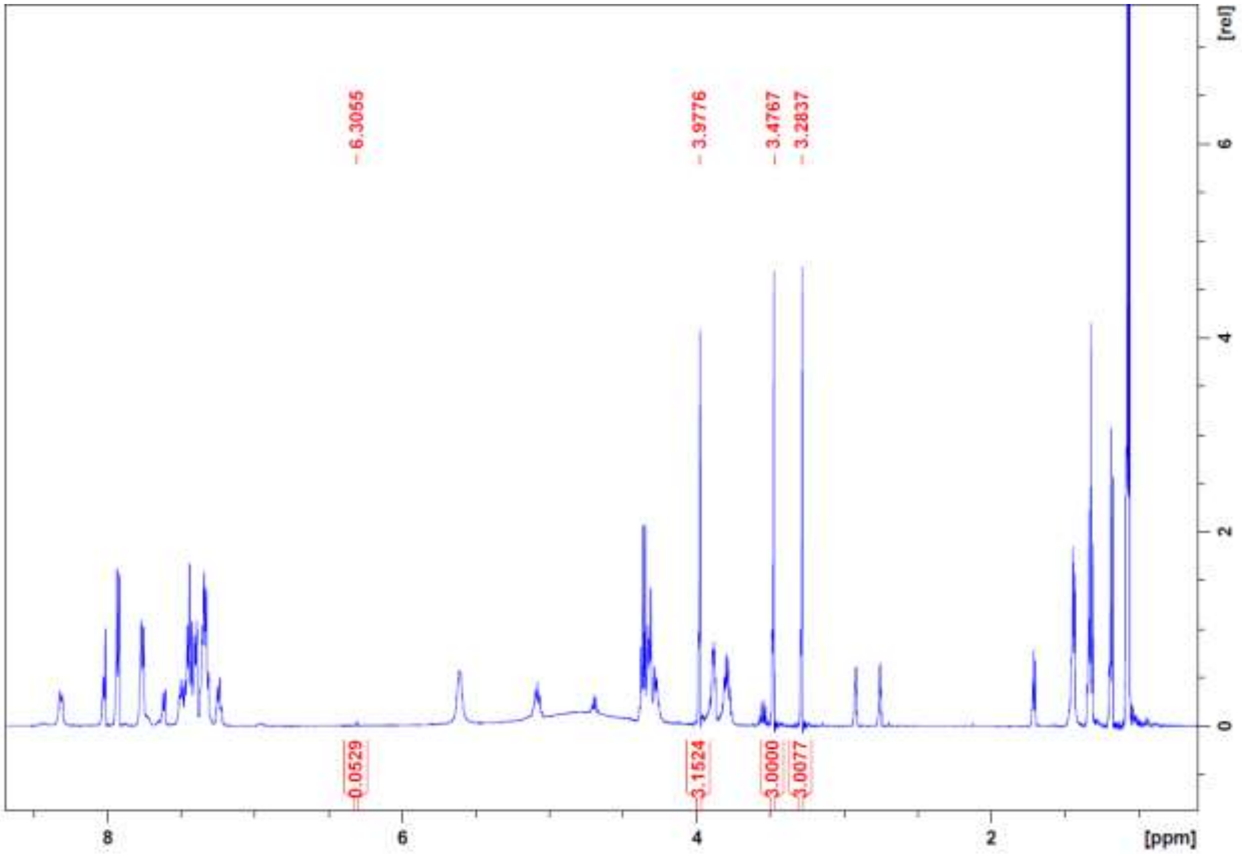

Figure S149. 1D ^{1}H NMR spectrum of Fmoc-Gly-OH/DIC/Oxyma/(S)-(-)-1-phenylethylamine (1:1:1:1) reaction at 0.1M after 10 h in DMF-d_7 (full spectrum).

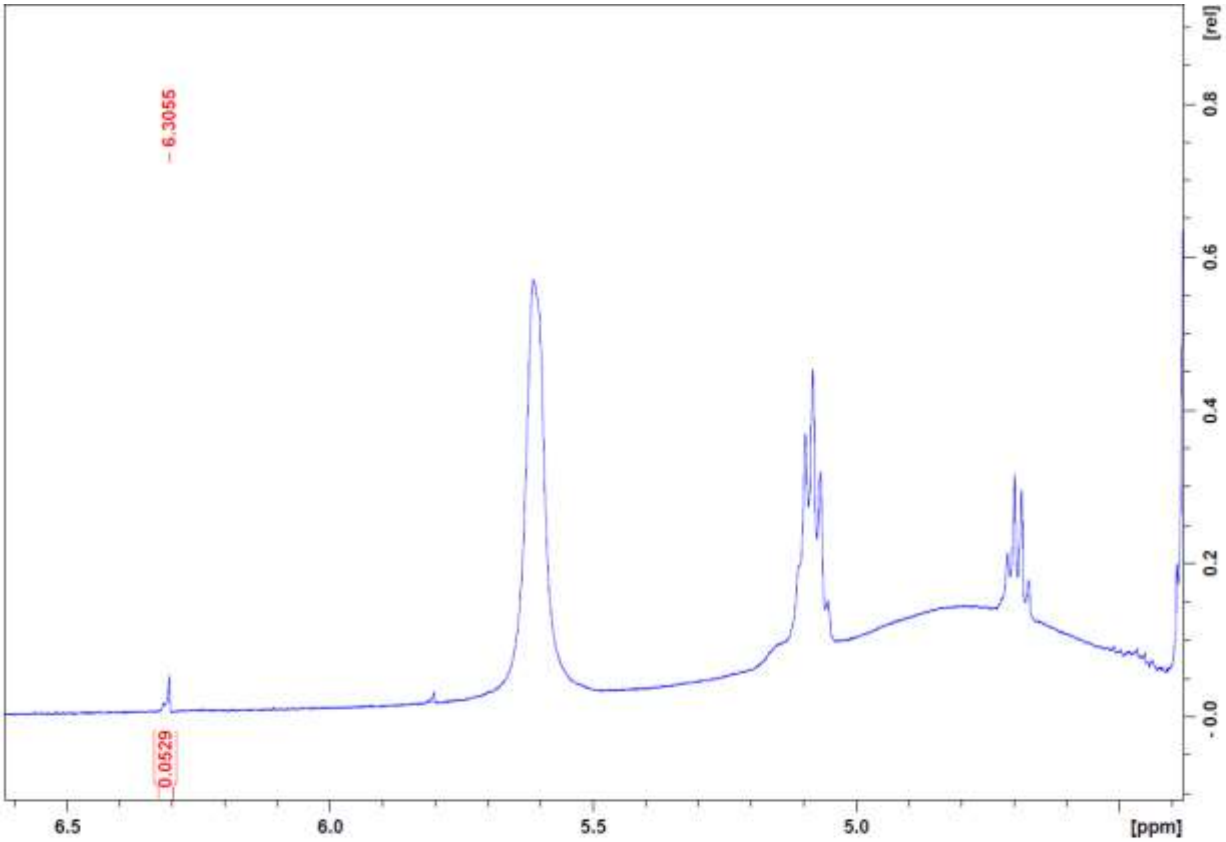

Figure S150. 1D ^{1}H NMR spectrum of Fmoc-Gly-OH/DIC/Oxyma/(S)-(-)-1-phenylethylamine (1:1:1:1) reaction at 0.1M after 10 h in DMF-d$_7$ (zoom-in).

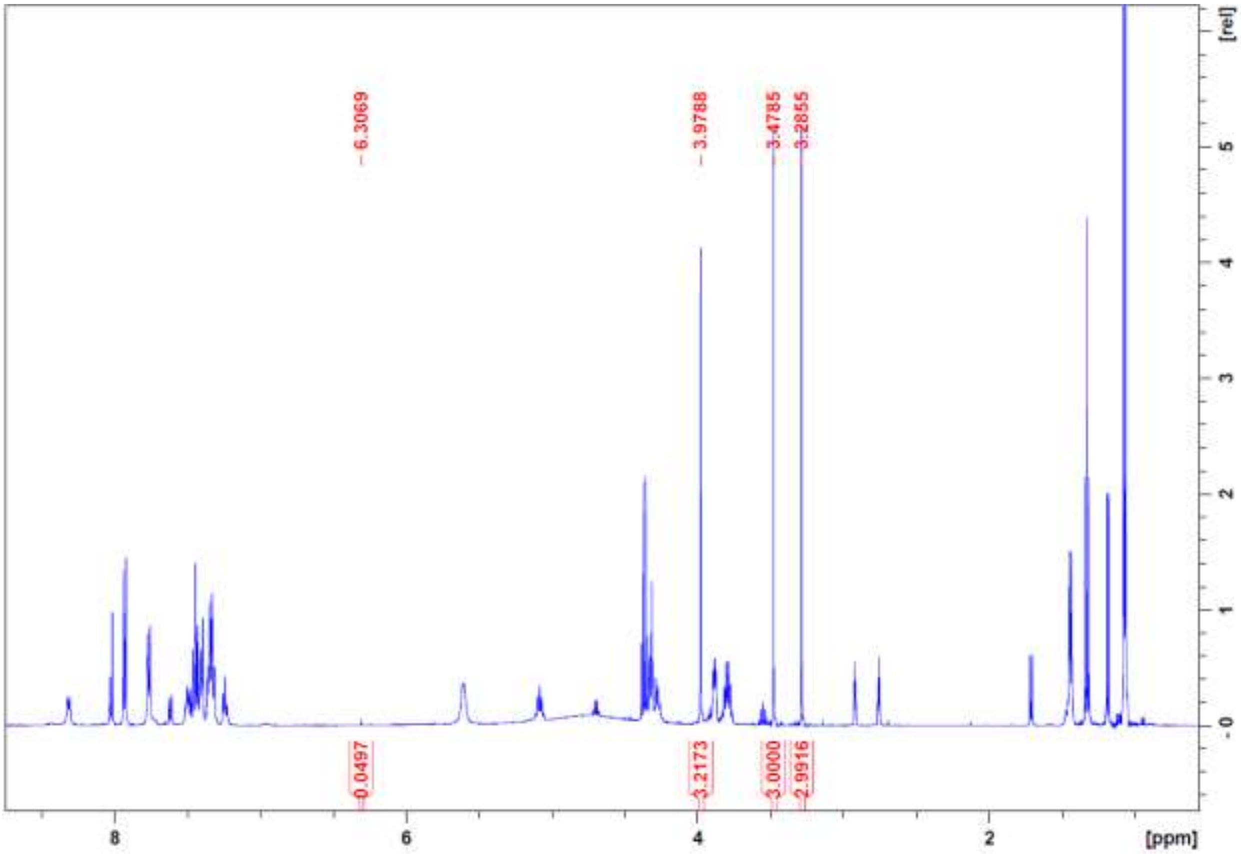

Figure S151. 1D ^{1}H NMR spectrum of Fmoc-Gly-OH/DIC/Oxyma/(S)-(-)-1-phenylethylamine (1:1:1:1) reaction at 0.1M after 16 h in DMF-d_7 (full spectrum).

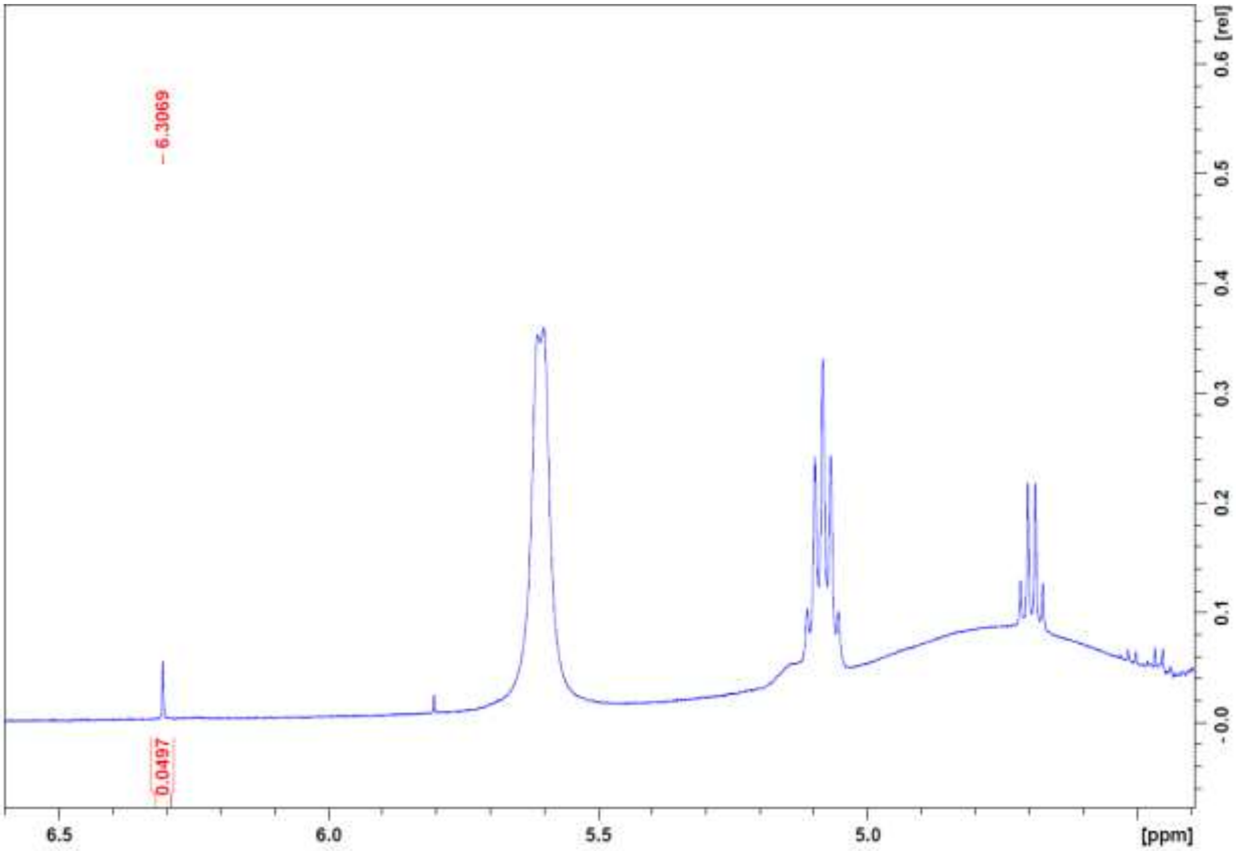

Figure S152. 1D ^{1}H NMR spectrum of Fmoc-Gly-OH/DIC/Oxyma/(S)-(-)-1-phenylethylamine (1:1:1:1) reaction at 0.1M after 16 h in DMF-d_7 (zoom-in).

9.2 Assessment of HCN formation during amide bond formation with 5 equiv DMTS in 0.1 M DMF-d_7

The general procedure for the amide bond formation in DMF-d_7 as described in the section 9.1 of this ESI was followed. The following amount of DMTS was used: (8.96 µL, 0.085 mmol, 5 equiv).

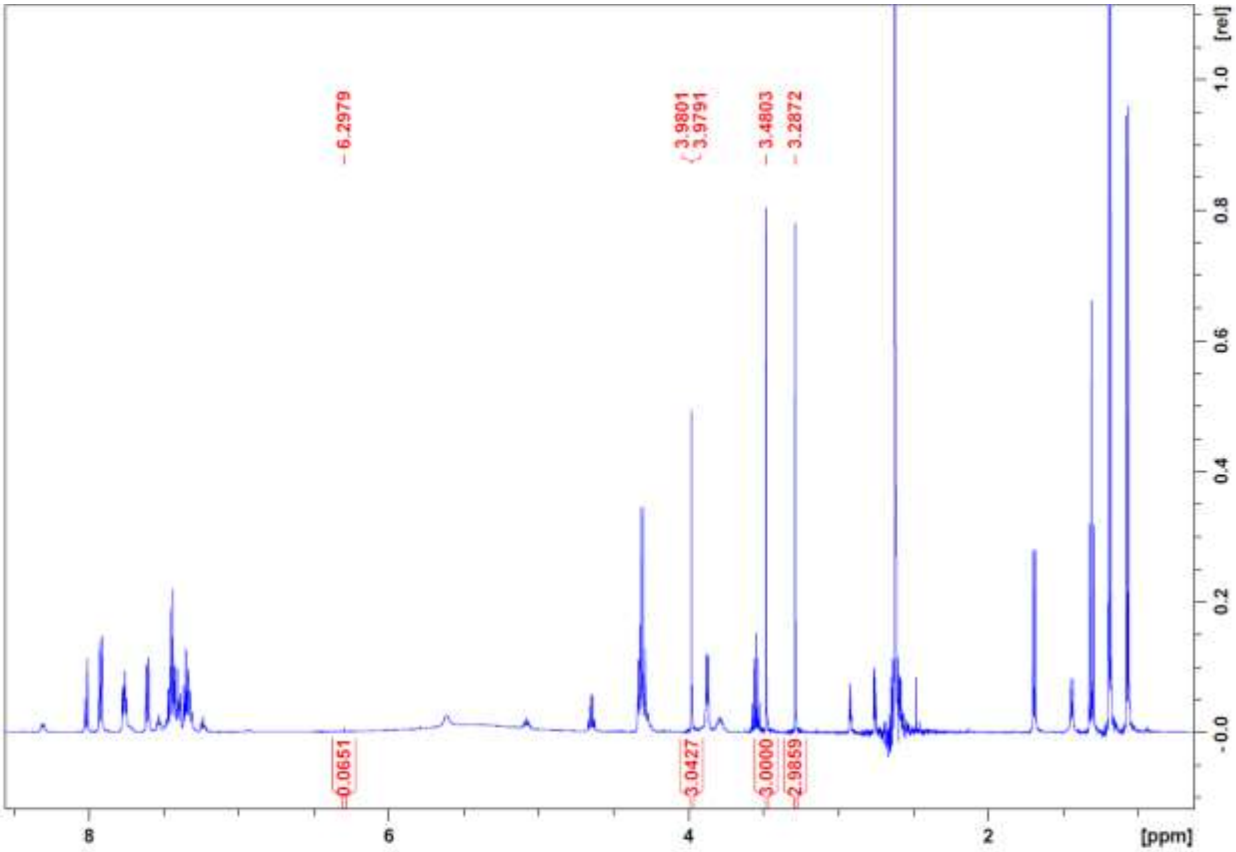

Figure S153. 1D ^{1}H NMR spectrum of Fmoc-Gly-OH/DIC/Oxyma/(S)-(-)-1-phenylethylamine (1:1:1:1) reaction with 5 equiv DMTS at 0.1M after 1 h in DMF-d_7 (full spectrum).

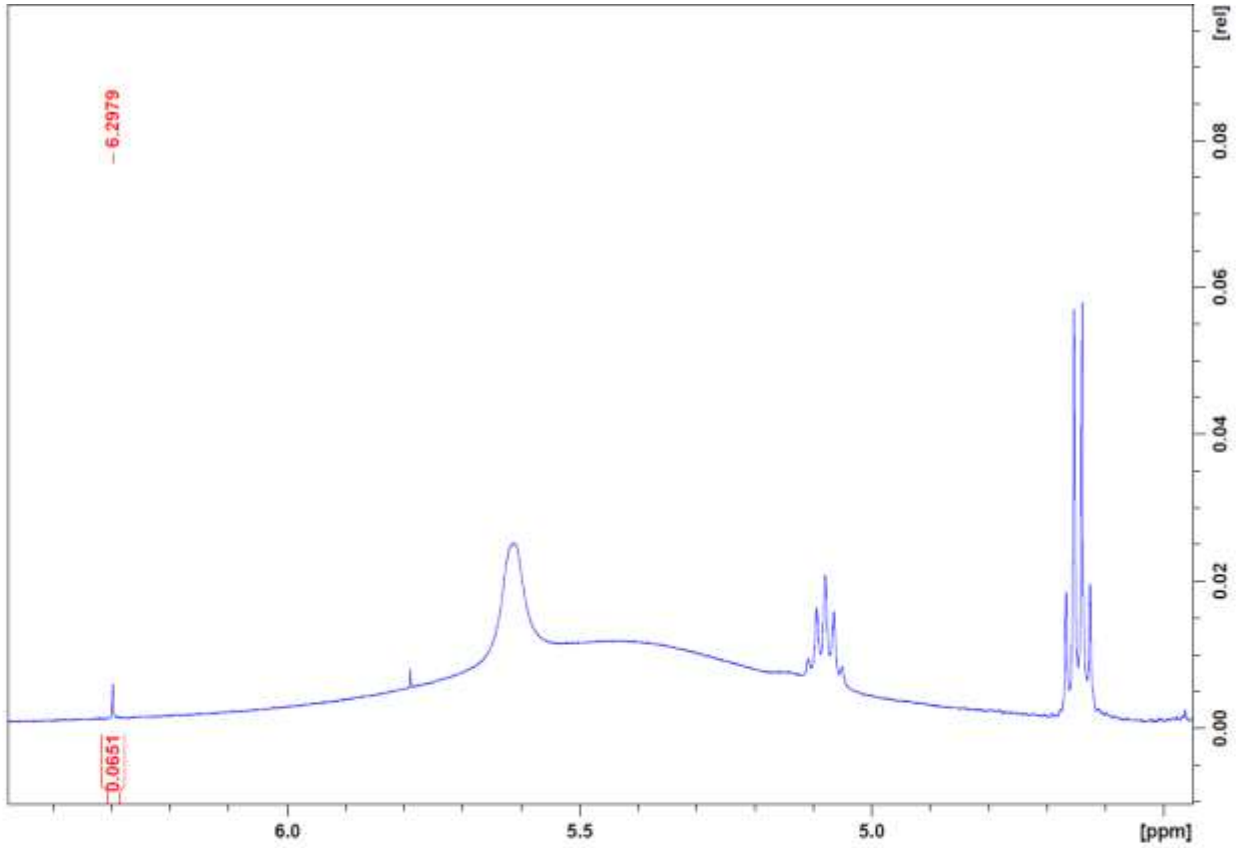

Figure S154. 1D ^{1}H NMR spectrum of Fmoc-Gly-OH/DIC/Oxyma/(S)-(-)-1-phenylethylamine (1:1:1:1) reaction with 5 equiv DMTS at 0.1M after 1 h in DMF-d_7 (zoom-in).

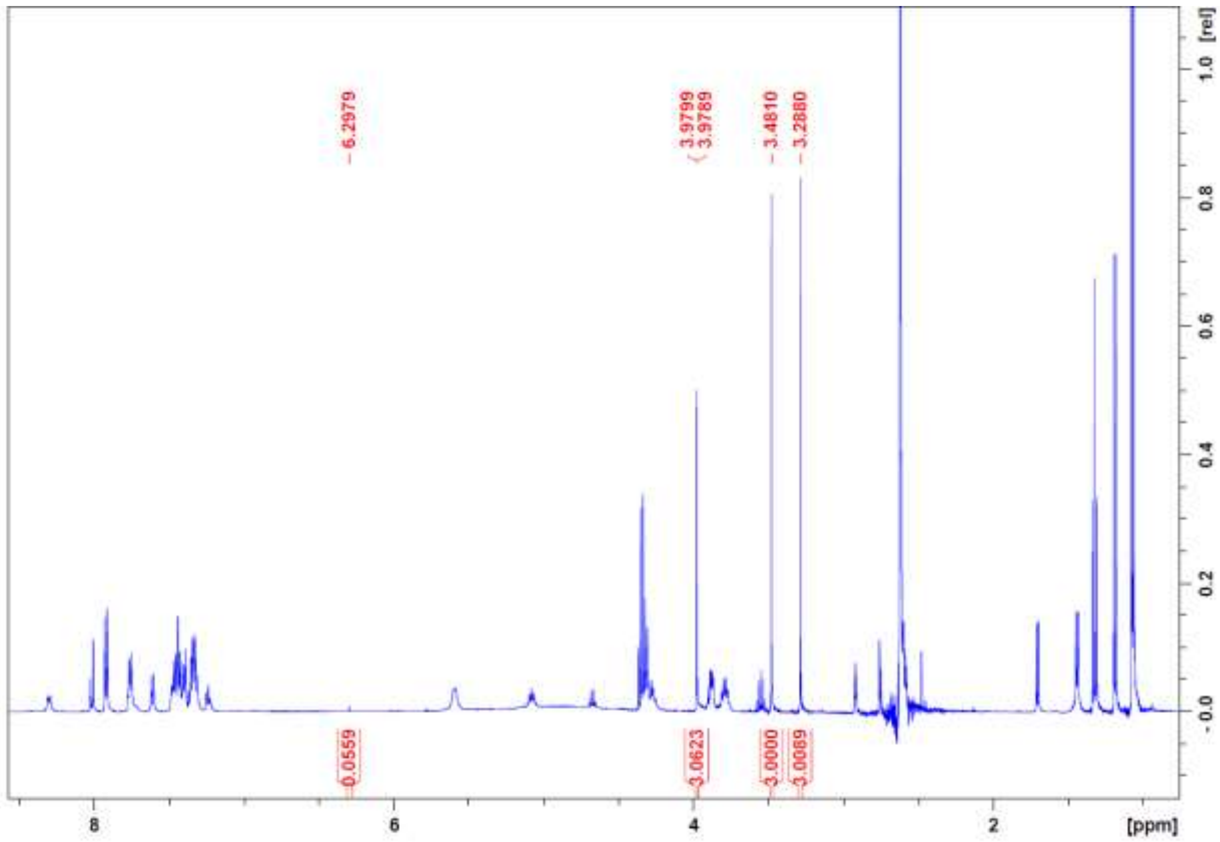

Figure S155. 1D ^{1}H NMR spectrum of Fmoc-Gly-OH/DIC/Oxyma/(S)-(-)-1-phenylethylamine (1:1:1:1) reaction with 5 equiv DMTS at 0.1M after 5 h in DMF-d_7 (full spectrum).

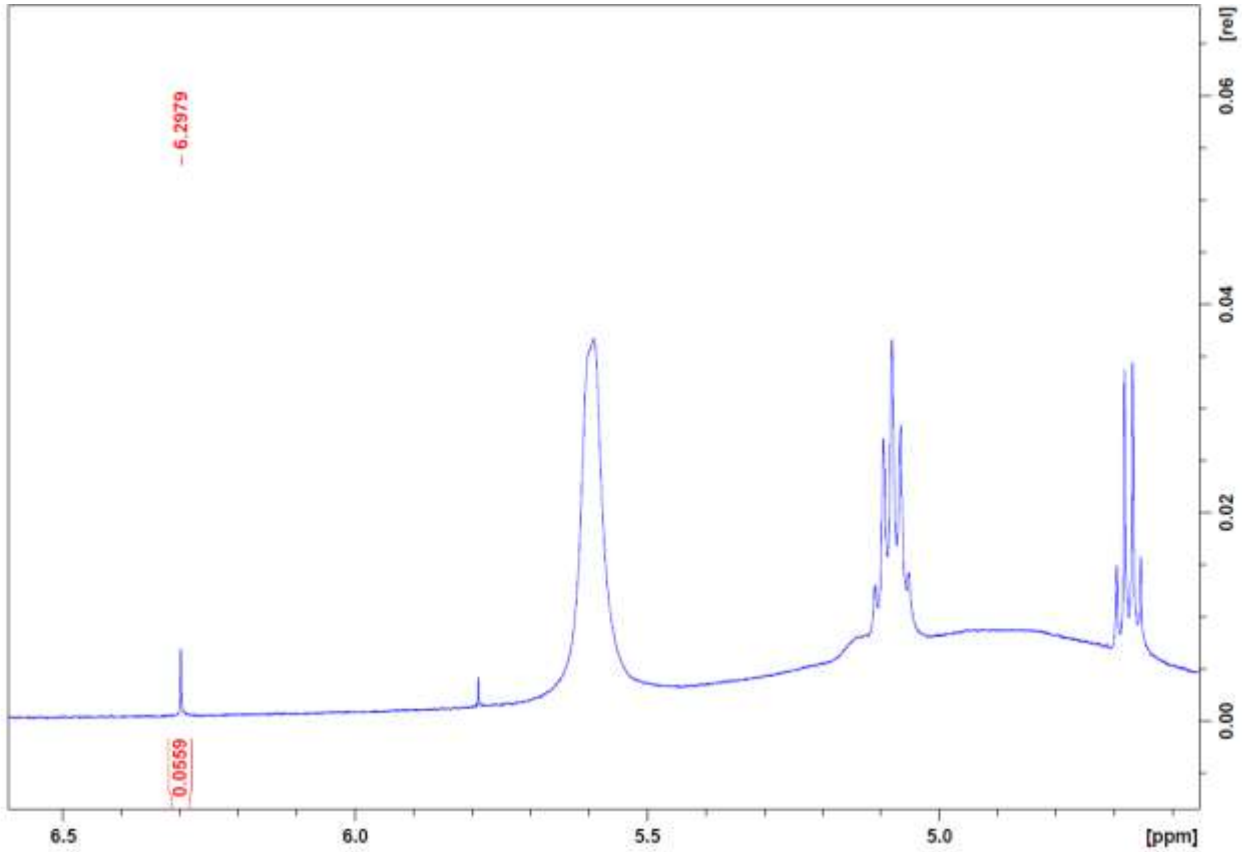

Figure S156. 1D ^{1}H NMR spectrum of Fmoc-Gly-OH/DIC/Oxyma/(S)-(-)-1-phenylethylamine (1:1:1:1) reaction with 5 equiv DMTS at 0.1M after 5 h in DMF-d_7 (zoom-in).

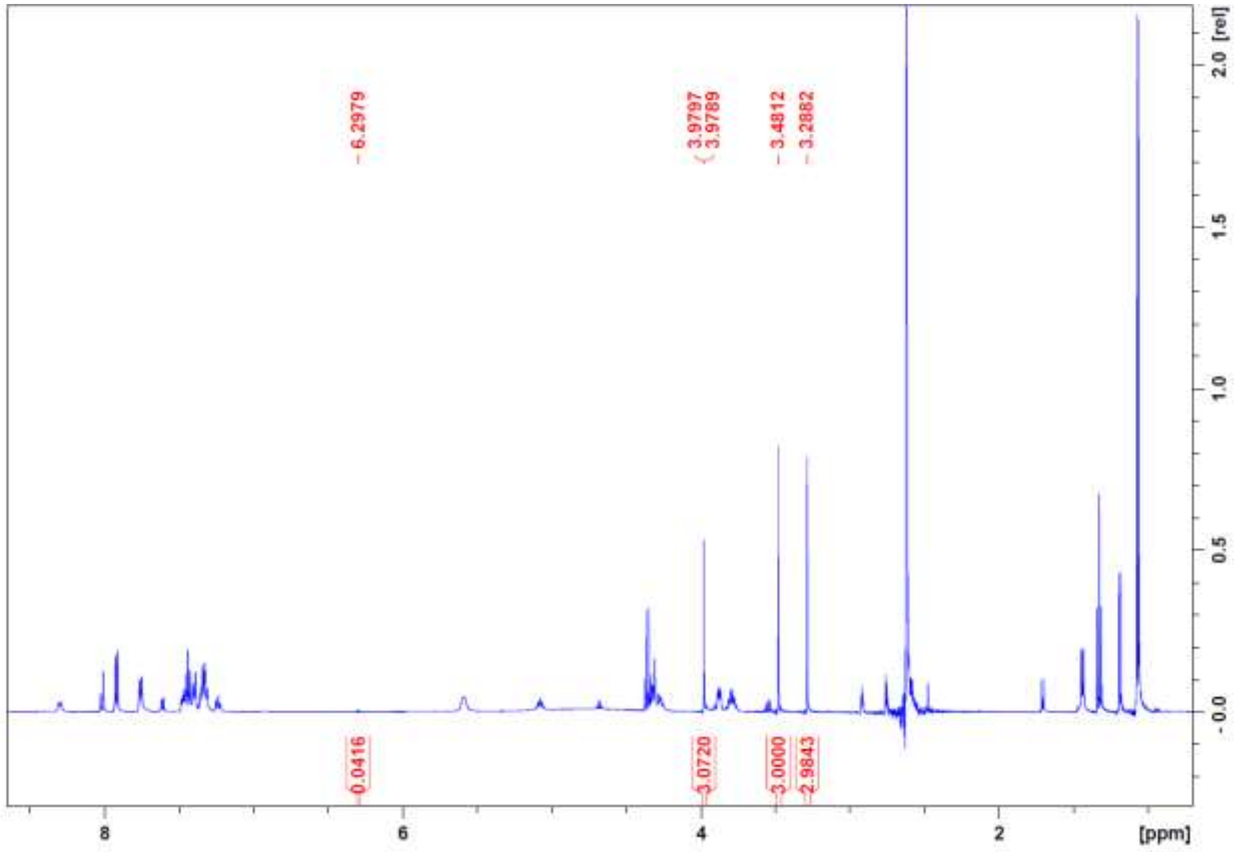

Figure S157. 1D ^{1}H NMR spectrum of Fmoc-Gly-OH/DIC/Oxyma/(S)-(-)-1-phenylethylamine (1:1:1:1) reaction with 5 equiv DMTS at 0.1M after 10 h in DMF-d_7 (full spectrum).

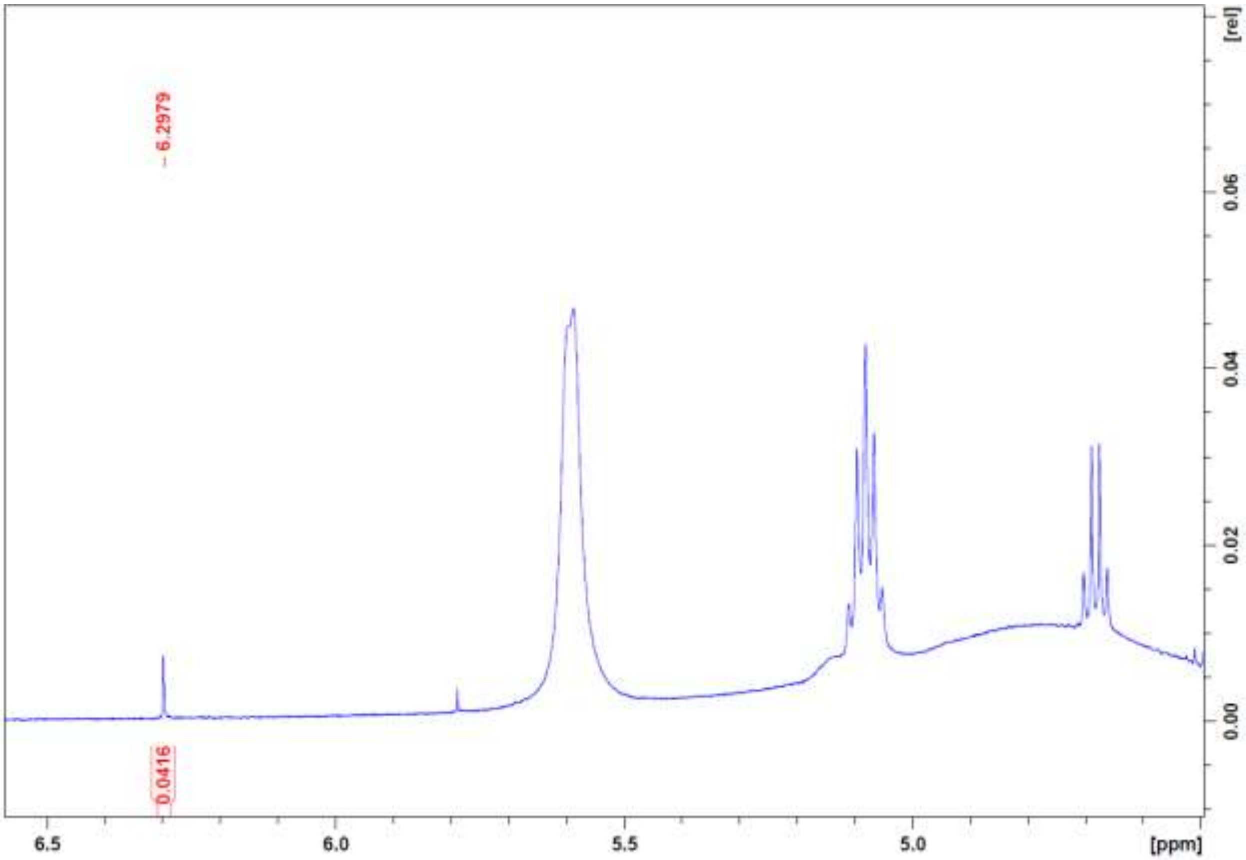

Figure S158. 1D ^{1}H NMR spectrum of Fmoc-Gly-OH/DIC/Oxyma/(S)-(-)-1-phenylethylamine (1:1:1:1) reaction with 5 equiv DMTS at 0.1M after 10 h in DMF-d_7 (zoom-in).

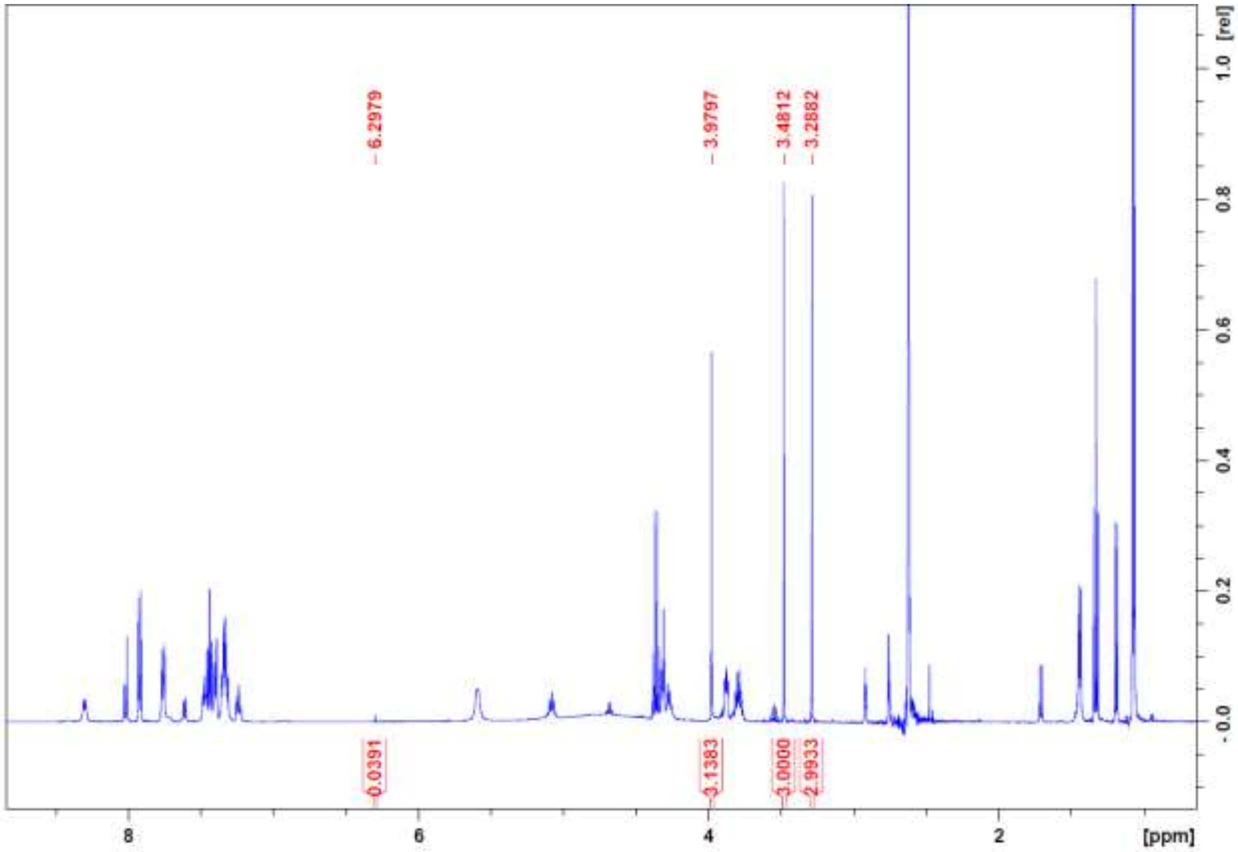

Figure S159. 1D ^{1}H NMR spectrum of Fmoc-Gly-OH/DIC/Oxyma/(S)-(-)-1-phenylethylamine (1:1:1:1) reaction with 5 equiv DMTS at 0.1M after 16 h in DMF-d_7 (full spectrum).

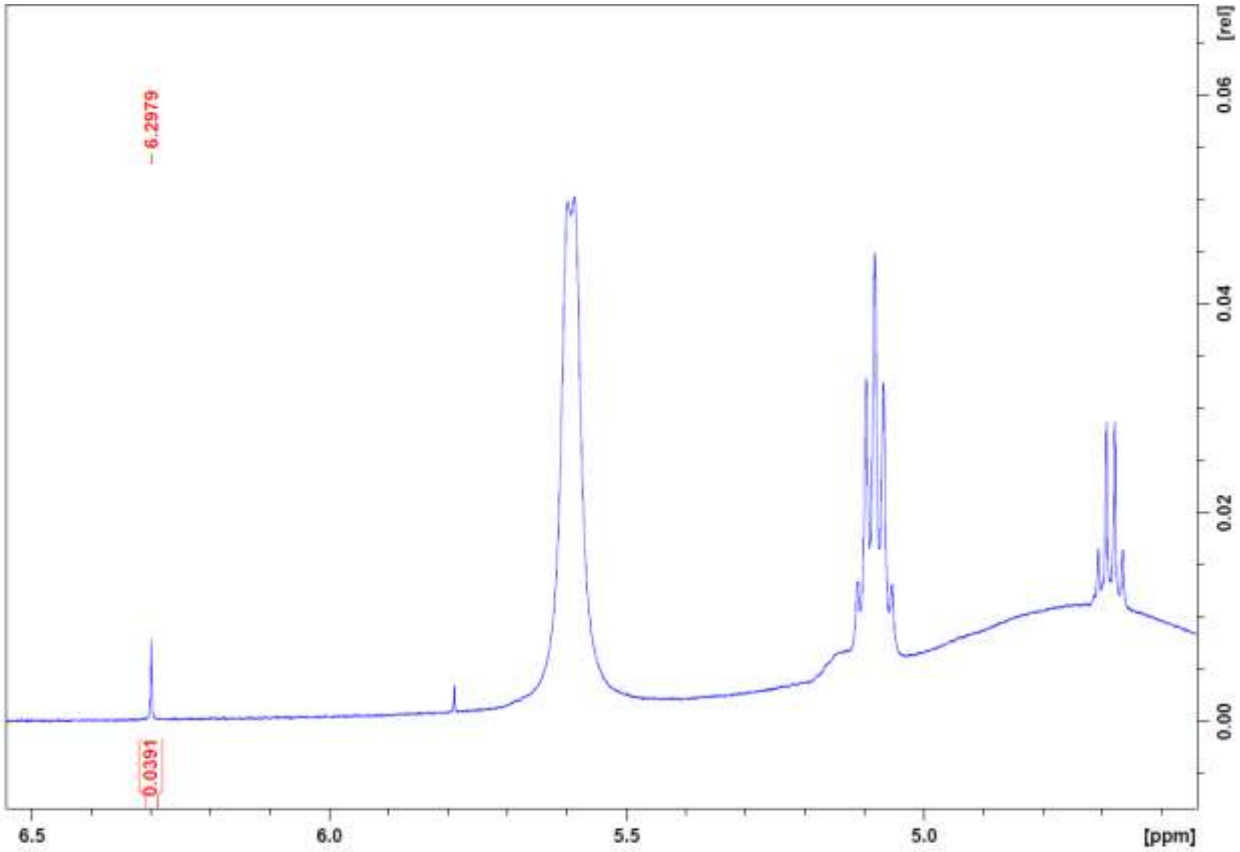

Figure S160. 1D ^{1}H NMR spectrum of Fmoc-Gly-OH/DIC/Oxyma/(S)-(-)-1-phenylethylamine (1:1:1:1) reaction with 5 equiv DMTS at 0.1M after 16 h in DMF-d$_7$ (zoom-in).

9.3 Assessment of HCN formation during amide bond formation with 10 equiv DMTS in 0.1 M DMF-d_7

The general procedure for the amide bond formation in DMF-d7 as described in the section 9.1 of this ESI was followed. The following amount of DMTS was used: (17.92 µL, 0.17 mmol, 10 equiv).

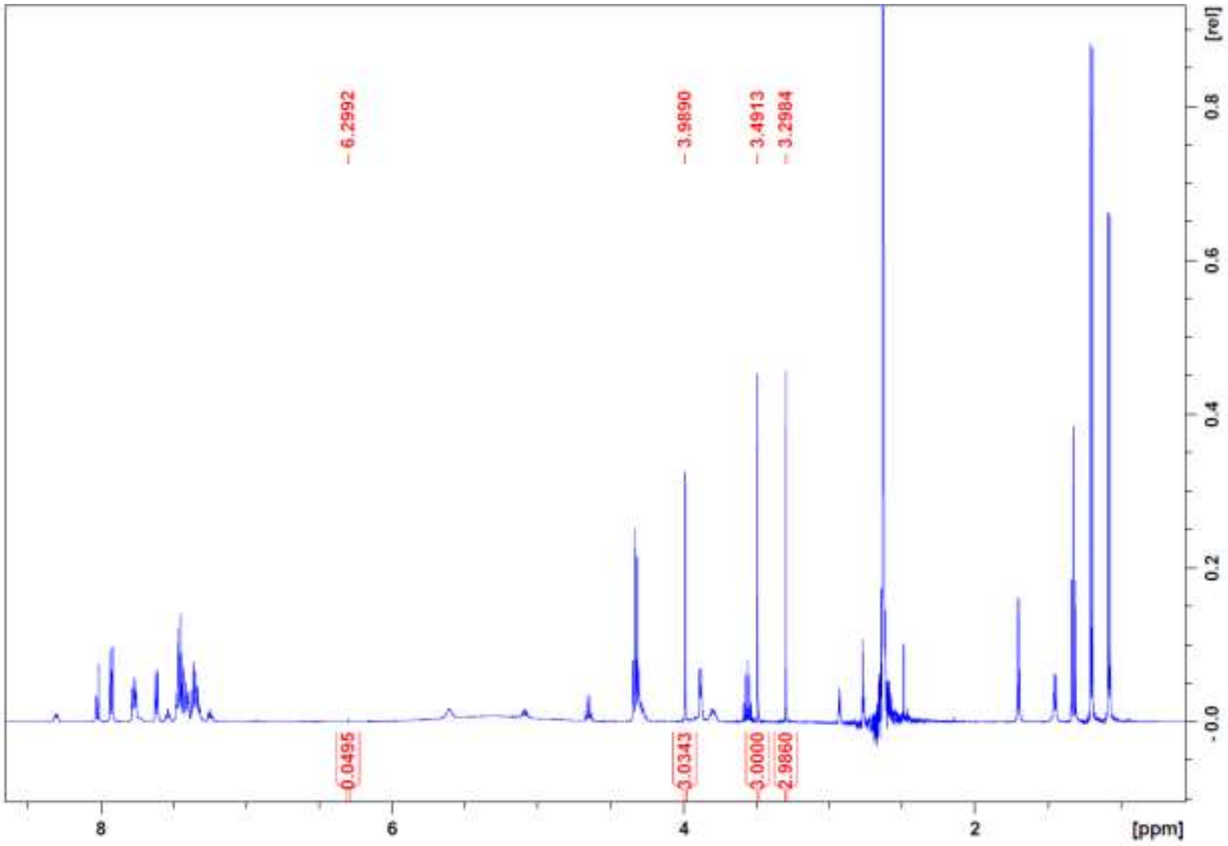

Figure S161. 1D ^{1}H NMR spectrum of Fmoc-Gly-OH/DIC/Oxyma/(S)-(-)-1-phenylethylamine (1:1:1:1) reaction with 10 equiv DMTS at 0.1M after 1 h in DMF-d_7 (full spectrum).

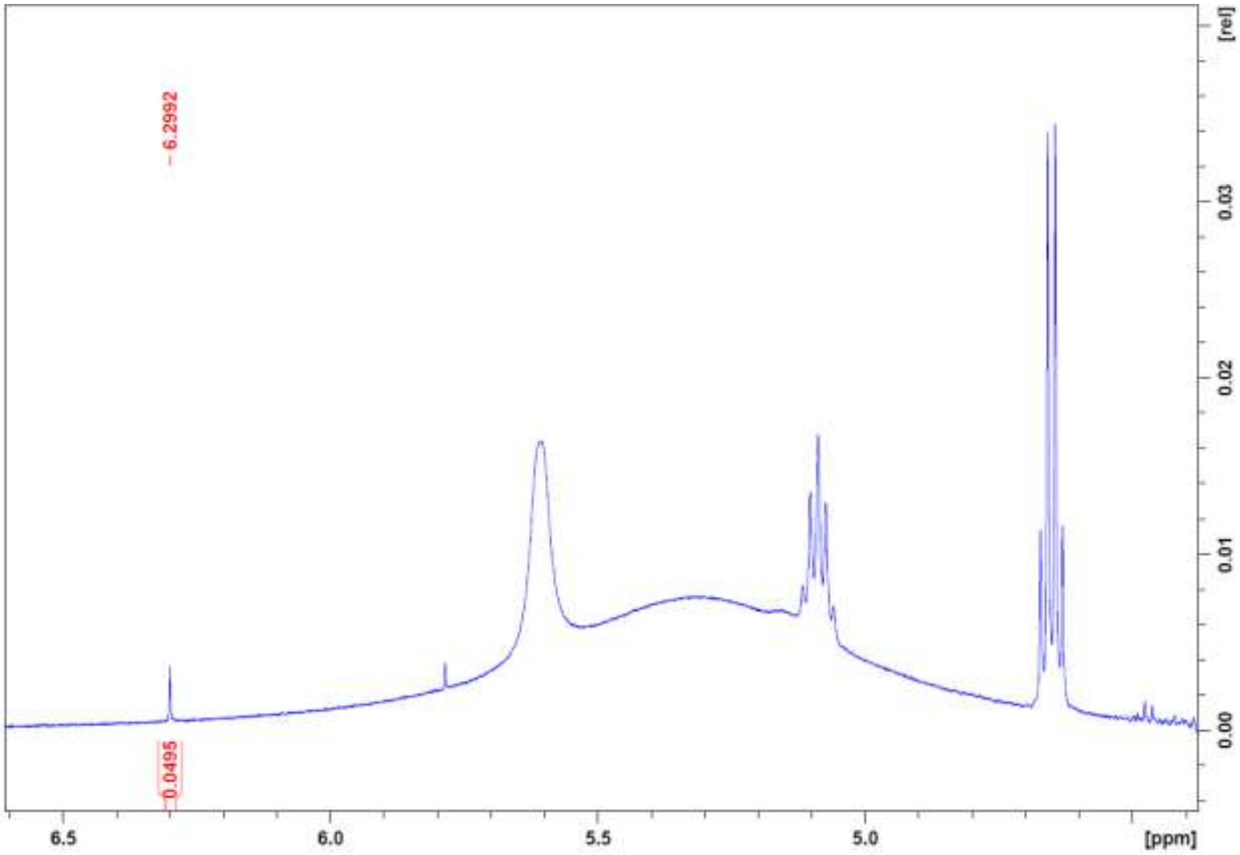

Figure S162. 1D ^{1}H NMR spectrum of Fmoc-Gly-OH/DIC/Oxyma/(S)-(-)-1-phenylethylamine (1:1:1:1) reaction with 10 equiv DMTS at 0.1M after 1 h in DMF-d_7 (zoom-in).

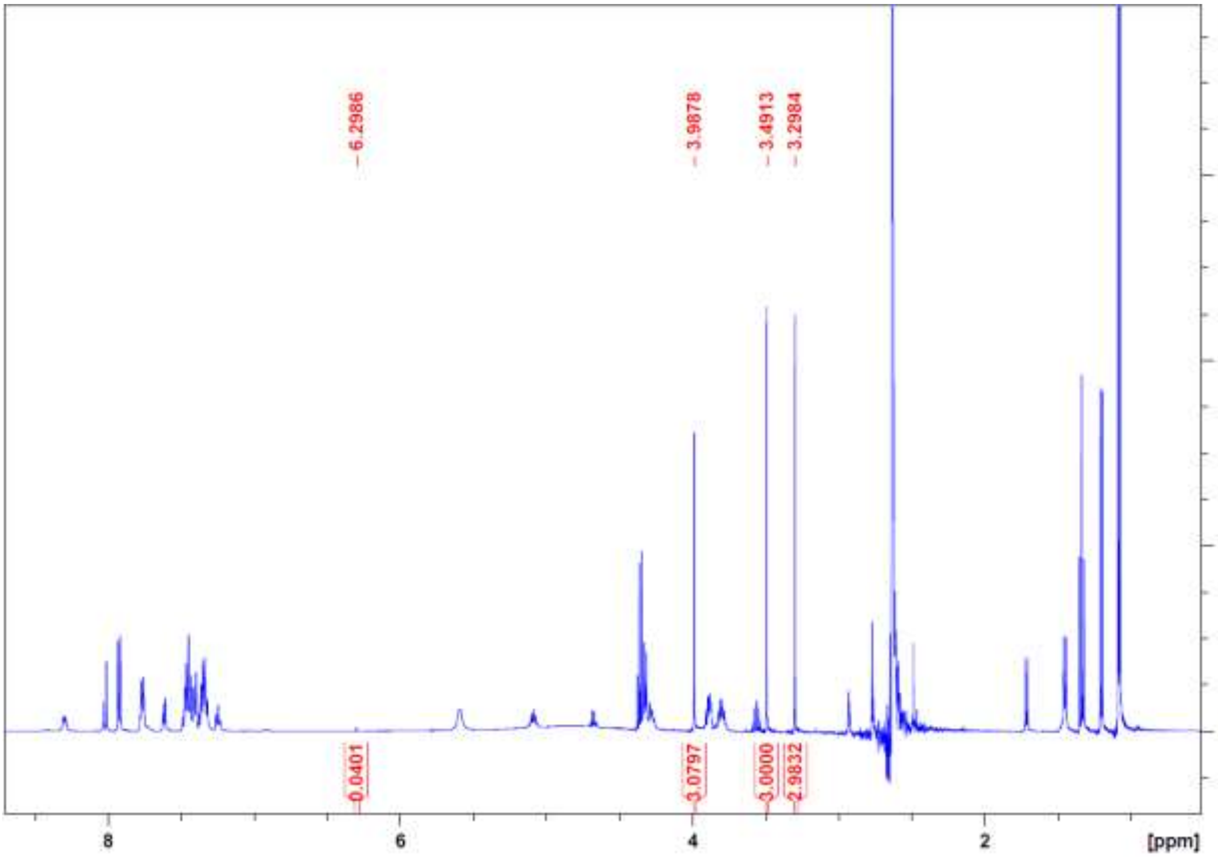

Figure S163. 1D ^{1}H NMR spectrum of Fmoc-Gly-OH/DIC/Oxyma/(S)-(-)-1-phenylethylamine (1:1:1:1) reaction with 10 equiv DMTS at 0.1M after 5 h in DMF-d_7 (full spectrum).

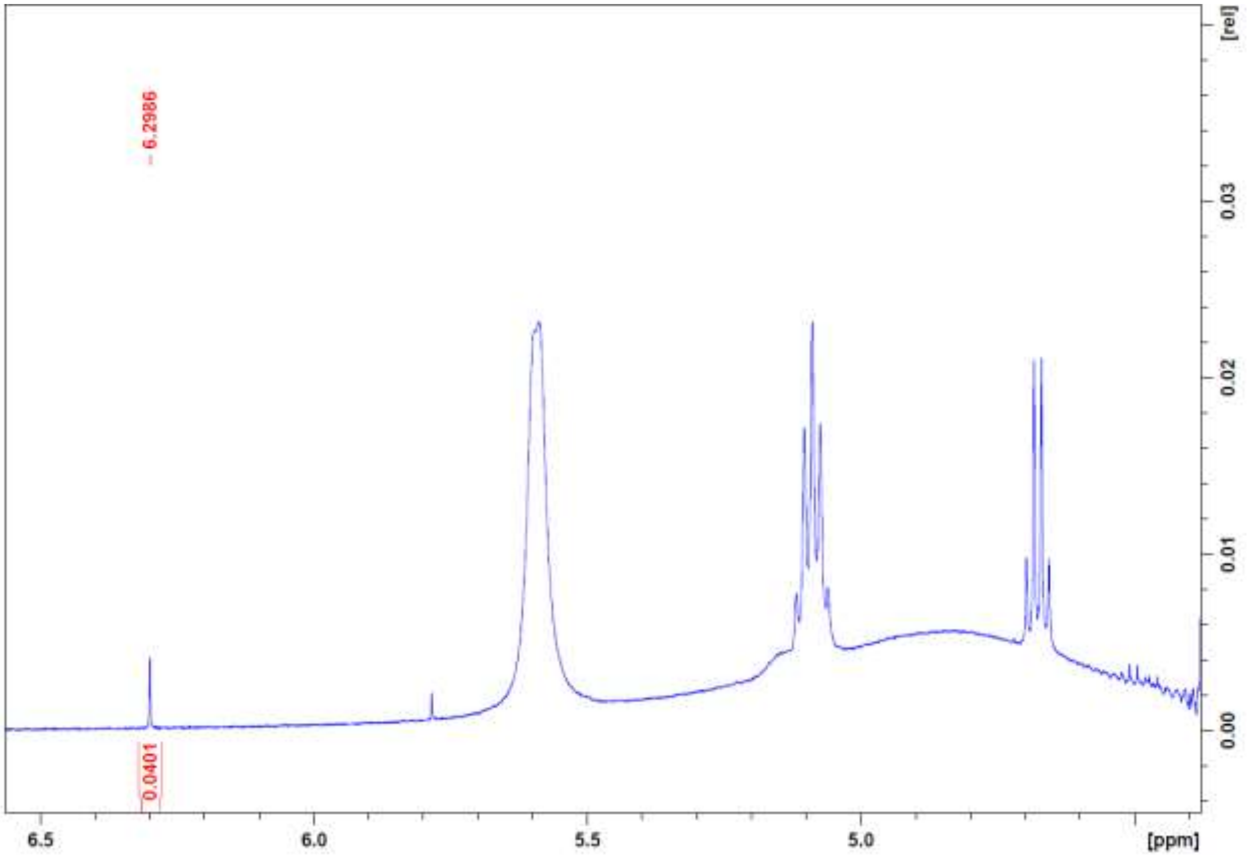

Figure S164. 1D ^{1}H NMR spectrum of Fmoc-Gly-OH/DIC/Oxyma/(S)-(-)-1-phenylethylamine (1:1:1:1) reaction with 10 equiv DMTS at 0.1M after 5 h in DMF-d_7 (zoom-in).

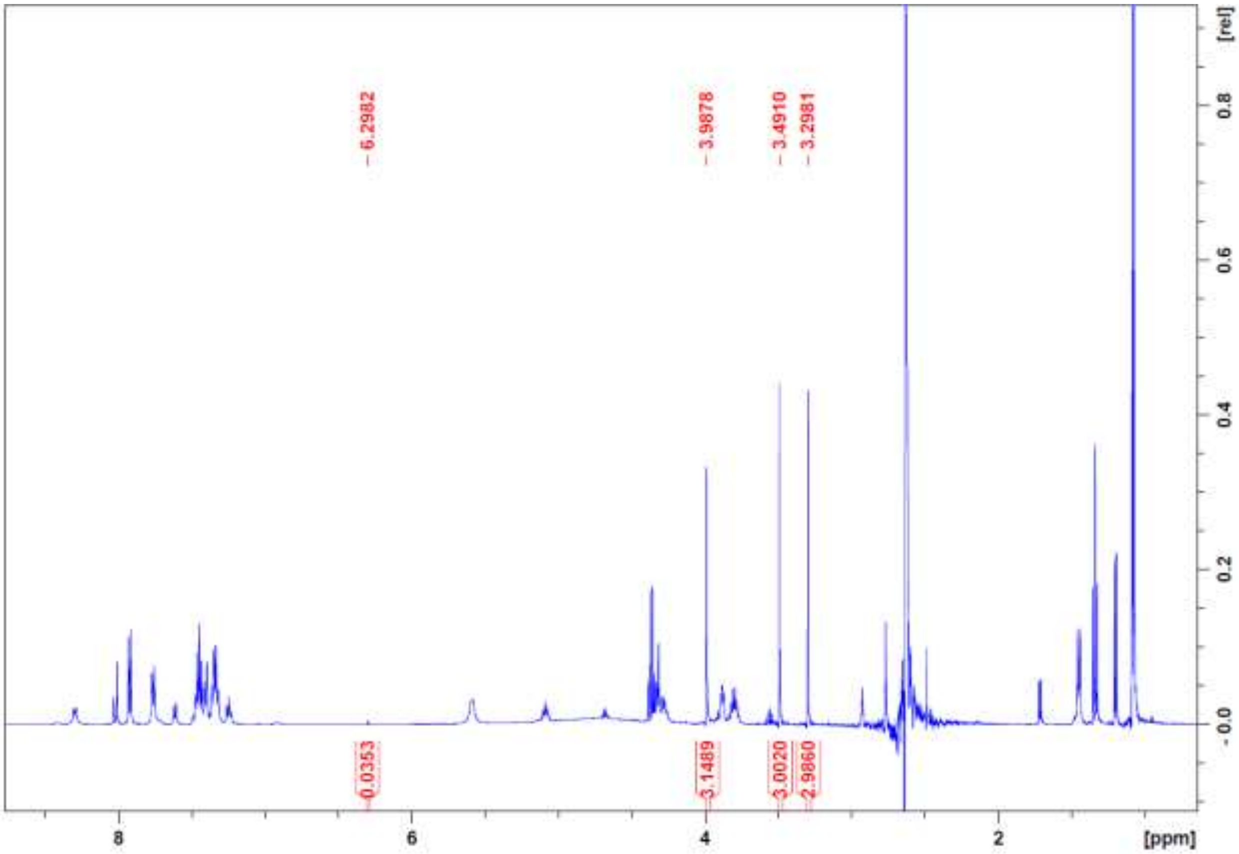

Figure S165. 1D ^{1}H NMR spectrum of Fmoc-Gly-OH/DIC/Oxyma/(S)-(-)-1-phenylethylamine (1:1:1:1) reaction with 10 equiv DMTS at 0.1M after 10 h in DMF-d_7 (full spectrum).

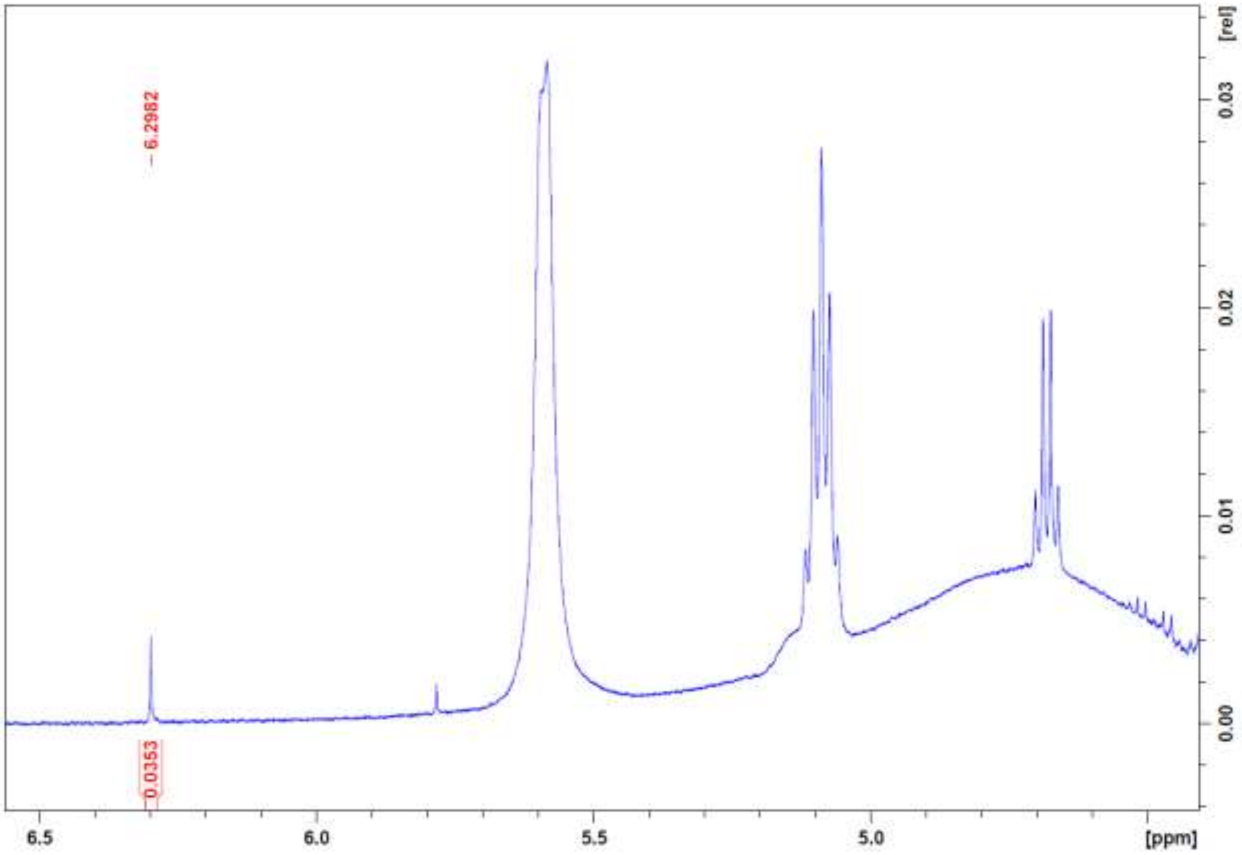

Figure S166. 1D ^{1}H NMR spectrum of Fmoc-Gly-OH/DIC/Oxyma/(S)-(-)-1-phenylethylamine (1:1:1:1) reaction with 10 equiv DMTS at 0.1M after 10 h in DMF-d_7 (zoom-in).

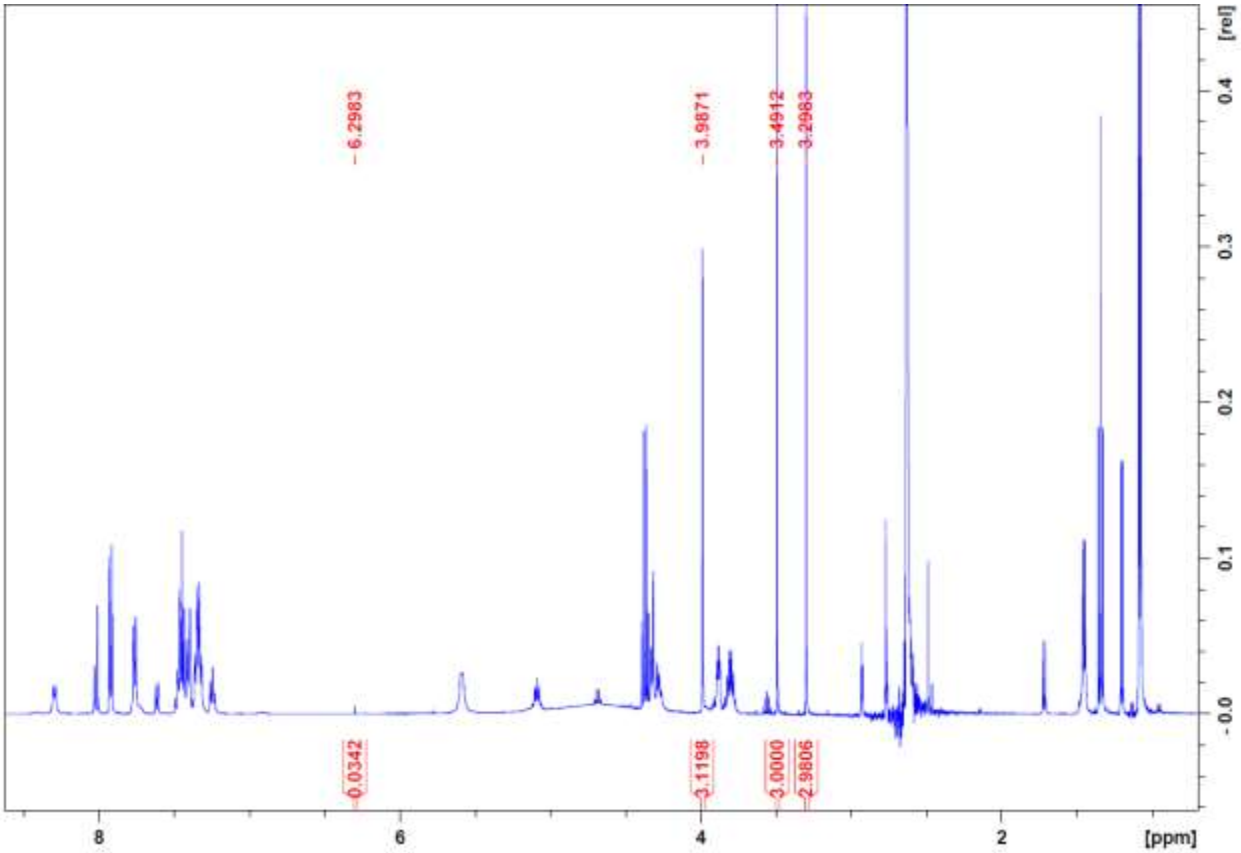

Figure S167. 1D ^{1}H NMR spectrum of Fmoc-Gly-OH/DIC/Oxyma/(S)-(-)-1-phenylethylamine (1:1:1:1) reaction with 10 equiv DMTS at 0.1M after 16 h in DMF-d_7 (full spectrum).

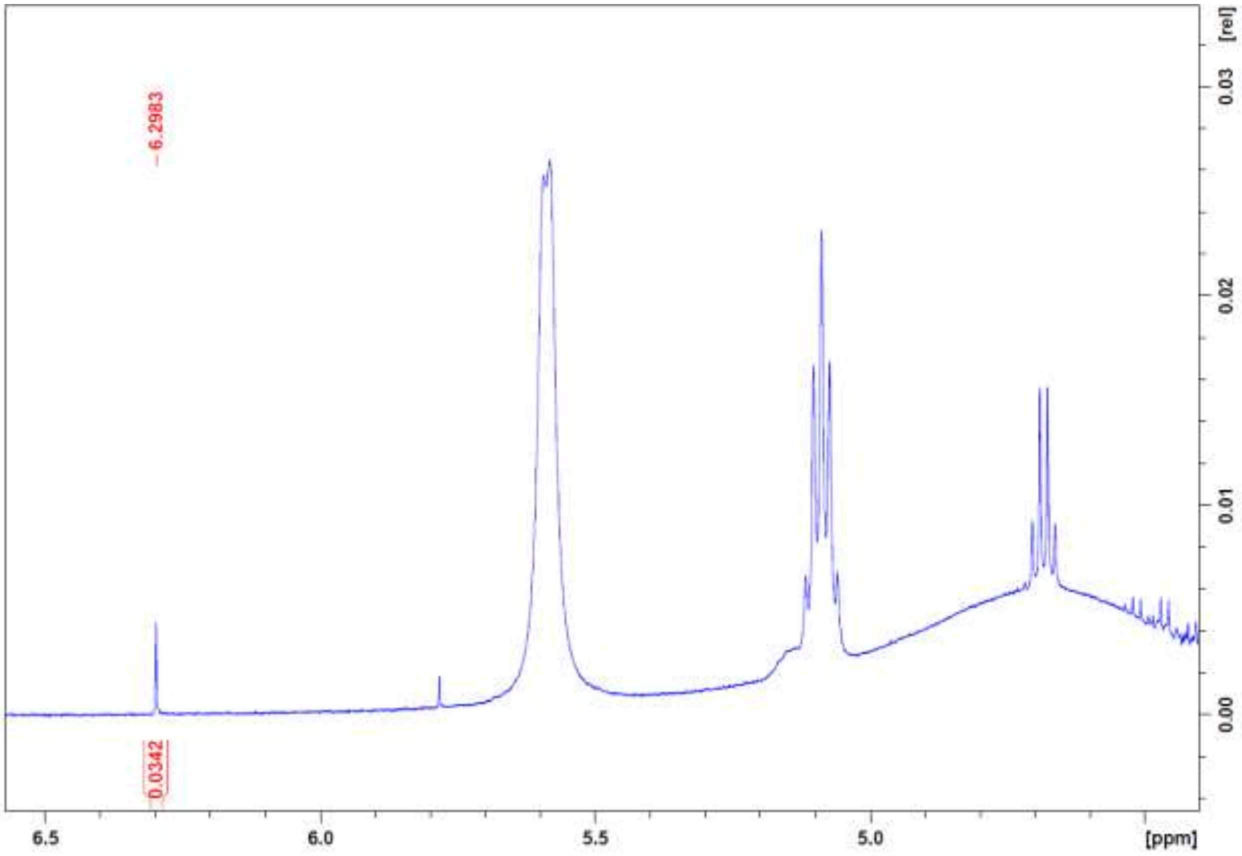

Figure S168. 1D ^{1}H NMR spectrum of Fmoc-Gly-OH/DIC/Oxyma/(S)-(-)-1-phenylethylamine (1:1:1:1) reaction with 10 equiv DMTS at 0.1M after 16 h in DMF-d_7 (zoom-in).

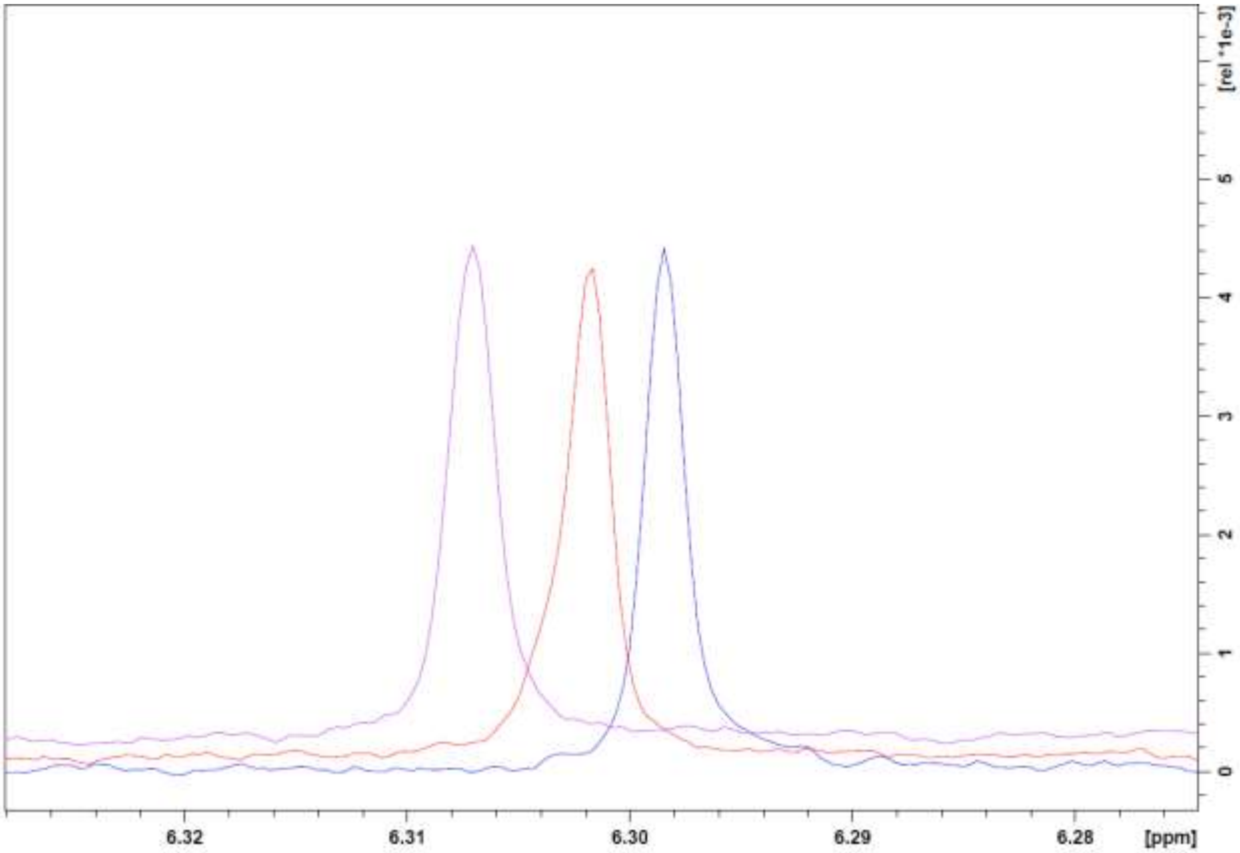

Figure S169. Overlap of ^{1}H NMR spectra of amide bond formation at 0.1M (in purple), with 5 equiv DMTS (in red) and with 10 equiv DMTS (in blue) after 16 h in DMF-d_7 (zoom-in).

9.4 Determination of amidation conversion based on ^{1}H NMR spectra of Fmoc-Gly-OH/DIC/Oxyma/(S)-(-)-1-phenylethylamine (1:1:1:1) reaction mixtures with and without DMTS containing caffeine as internal standard

General method to calculate the amidation conversion.

1) One well defined (without any overlap) signal of a starting material had to be chosen to follow the amount of this starting material over time. The well defined septuplet at 3.55 ppm corresponding to DIC was deemed as a signal suitable for use in amide bond formation conversion calculations (Figure S170).

2) The amount of DIC was calculated using the internal standard (caffeine) which does not react with the constituent of the amide bond forming reaction and has three well defined singlets at 3.28, 3.48 and 3.98 ppm respectively corresponding to its three methyl groups.

3) The calibration was done on the septuplet at 3.55 ppm corresponding to DIC, which corresponds to two protons. We considered that 1 equiv of DIC was in the solution at this time point.

4) Once the calibration was completed, we carried out the integration for the caffeine at 3.28, 3.48 and 3.98 ppm, corresponding to three protons. Comparing the integrated peak ares for 3) and 4) respectively allowed us to determine the area of the DIC peak at the outset of the amide bond forming reaction.

5) The conversion throughout all amide bond forming reactions studied was calculated integrating the peak of the DIC vs the peak of the caffeine reference at a given timepoint.

This method was used to calculate the conversion of the amide bond forming reactions shown in Fig. 5.

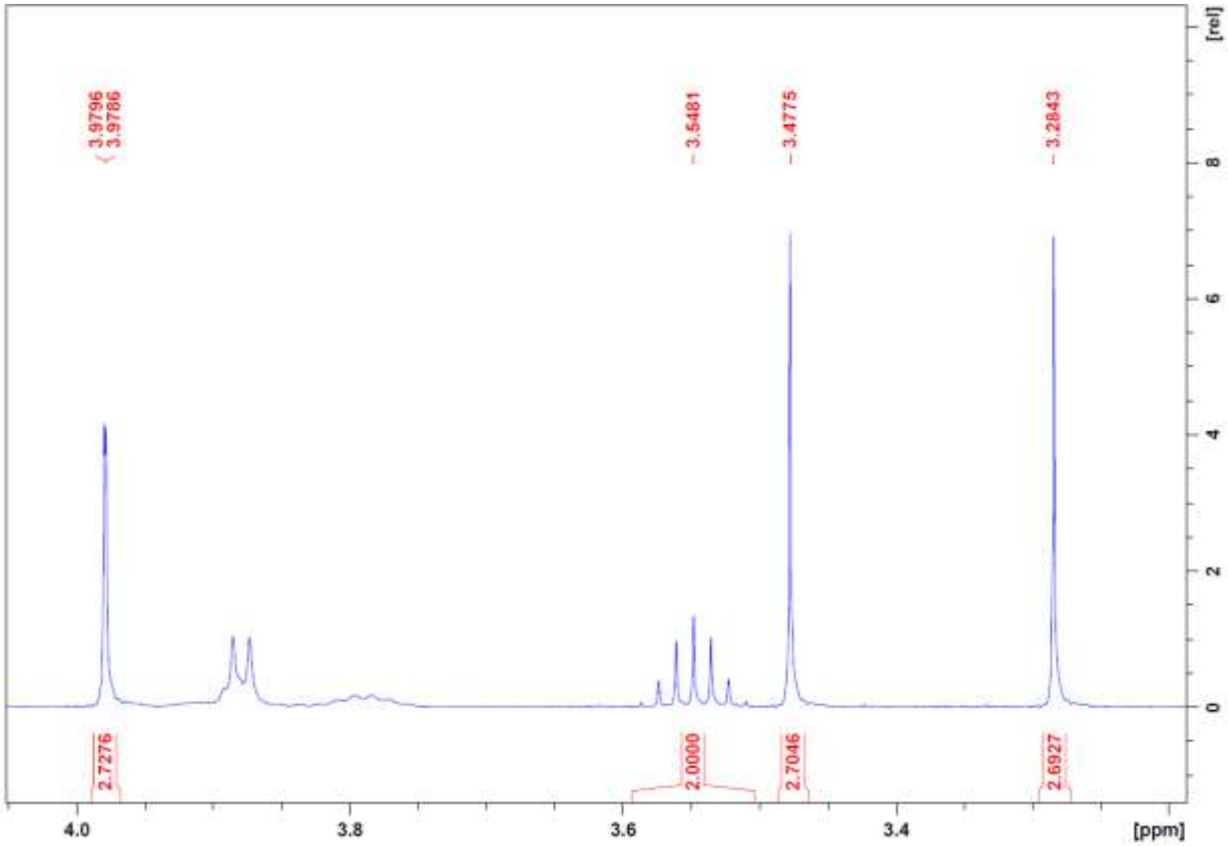

Figure S170. 1D ^{1}H NMR spectrum of Fmoc-Gly-OH/DIC/Oxyma/(S)-(-)-1-phenylethylamine (1:1:1:1) reaction at 0.1M after 1 h in DMF-d_7 (zoom-in).

The results of this section are summarized in Fig. 5.

Specifically, DMTS exhibited good properties in terms of minimizing HCN concentration, both with 5 equiv as well as 10 equiv. The lowering of HCN concentration proceeded faster and more efficiently by using 10 equiv of DMTS. No significant additional peaks were observed by using DMTS, i.e the HCN scavenger does not seem to interfere with the amide bond forming reaction by means of side product formation.

10. Assessment of amide bond formation kinetics during DIC/Oxyma mediated coupling of 1.0 equiv Fmoc-Ser(*t*-Bu)-OH with (S)-(-)-1-phenylethylamine with and without 10 equiv DMTS in DMF and NBP/EtOAc (1:4)

The aim of this section of the ESI was to show that DMTS does not interfere with the amidation using different solvents, for which DMF and NBP/EtOAc (1:4) were evaluated.

The general procedure for the assessment of the kinetics of amide bond formation during DIC/Oxyma mediated couplings of Fmoc-Ser(t-Bu)-OH with (S)-(-)-1-phenylethylamine in DMF and NBP/EtOAc (1:4) as described in the section 6 of this ESI was followed. In this section, the impact of using 10 equiv DMTS on the kinetics of the amide bond formation is described. Specifically, in section 10.2 an experiment carried out in DMF in the presence of 10 equiv DMTS is described and in section 10.4, an experiment carried out in NBP/EtOAc (1:4) in the presence of 10 equiv DMTS is described. In both cases, DMTS addition was carried out prior to addition of DIC. For all four experiments 10 µL of aliquots of reaction mixtures were taken out and quenched with 0.5 % TFA/MeCN (1.0 mL) at 0, 10, 30, 60, 120 and 960 min. The conversions of the amidation reactions were then determined by HPLC using the following analytical system: column: Waters XBridge C18 100Å 3.5 µm 4.6x50mm; column temperature: 25°C; injection volume: 12 µL; sampler temperature: 4°C; detection wavelength: 273 nm, flow: 1.0 ml/min; mobile phase A: 0.1 % TFA in water, mobile phase B: 0.1 % TFA in MeCN. Gradient (Time(min), %B): 0, 10; 15, 100; 20, 10; 25,10. Following peaks were integrated: i) Fmoc-Ser(*t*-Bu)-OH (starting material), rt 11.8 min; ii) Fmoc-Ser(*t*-Bu)- (S)-(-)-1-phenylethylamide (product of amidation reaction), rt 13.7 min.

10.1 Fmoc-Ser(*t*-Bu)-OH/Oxyma/DIC/(S)-(-)-1-phenylethylamine amidation reaction in DMF

Following amounts of starting materials were used: Fmoc-Ser(*t*-Bu)-OH (95.6 mg, 0.25 mmol, 1.0 equiv), Oxyma (35.4 mg, 0.25 mmol, 1.0 equiv), (S)-(-)-1-phenylethylamine (32.2 µL, 0.25 mmol, 1.0 equiv), DIC (39.1 µL, 0.25 mmol, 1.0 equiv) in 5 mL DMF.

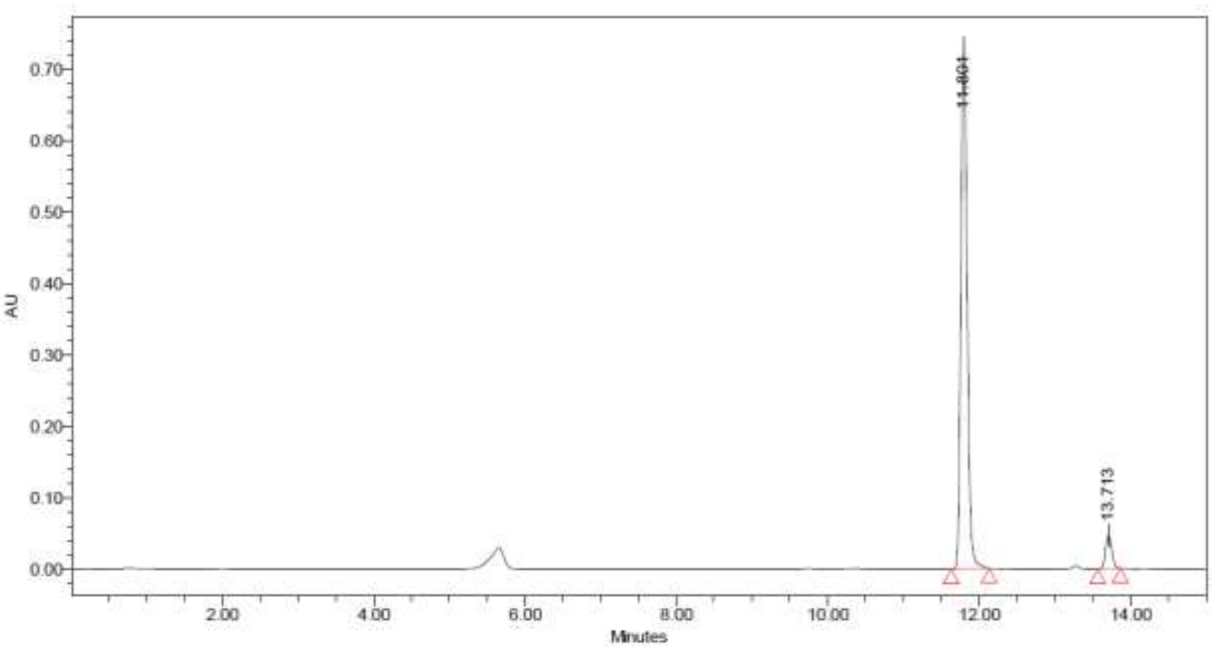

Figure S171. HPLC chromatogram of the Fmoc-Ser(*t*-Bu)-OH/Oxyma/DIC/(S)-(-)-1-phenylethylamine amidation reaction in DMF at t=10 min.

Table S48. Area% for integrated peaks.

	RT	Height	Area	% Area
1	11.801	730370	4178091	93.93
2	13.713	46942	269876	6.07
Sum			4447967.0	

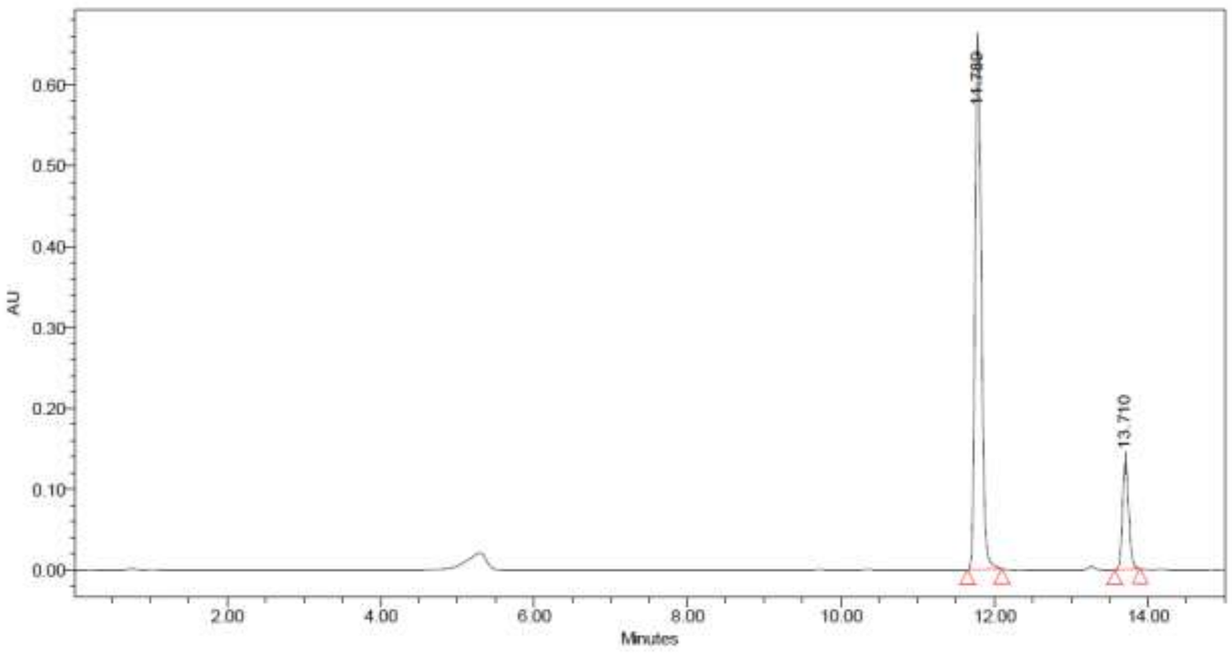

Figure S172. HPLC chromatogram of the Fmoc-Ser(*t*-Bu)-OH/Oxyma/DIC/(S)-(-)-1-phenylethylamine amidation reaction in DMF at t=30 min.

Table S49. Area% for integrated peaks.

	RT	Height	Area	% Area
1	11.789	658758	3751181	83.13
2	13.710	132088	761246	16.87
Sum			4512427.1	

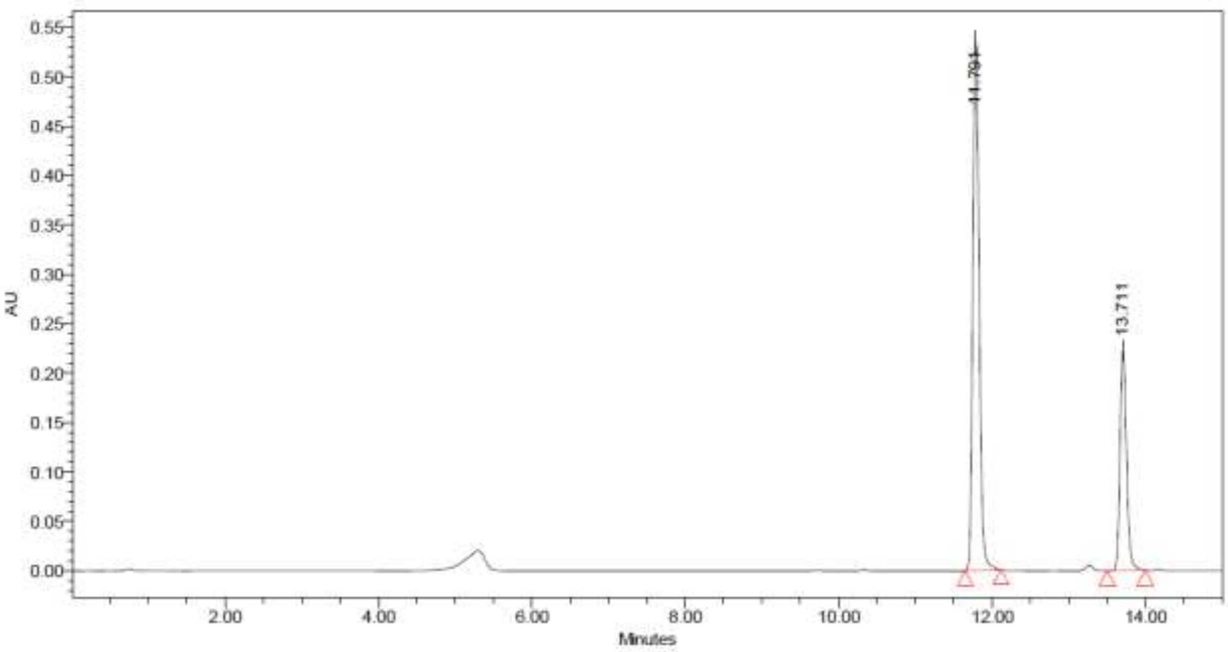

Figure S173. HPLC chromatogram of the Fmoc-Ser(*t*-Bu)-OH/Oxyma/DIC/(S)-(-)-1-phenylethylamine amidation reaction in DMF at t=60 min.

Table S50. Area% for integrated peaks.

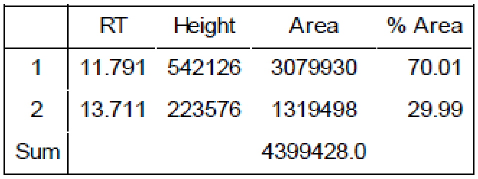

	RT	Height	Area	% Area
1	11.791	542126	3079930	70.01
2	13.711	223576	1319498	29.99
Sum			4399428.0	

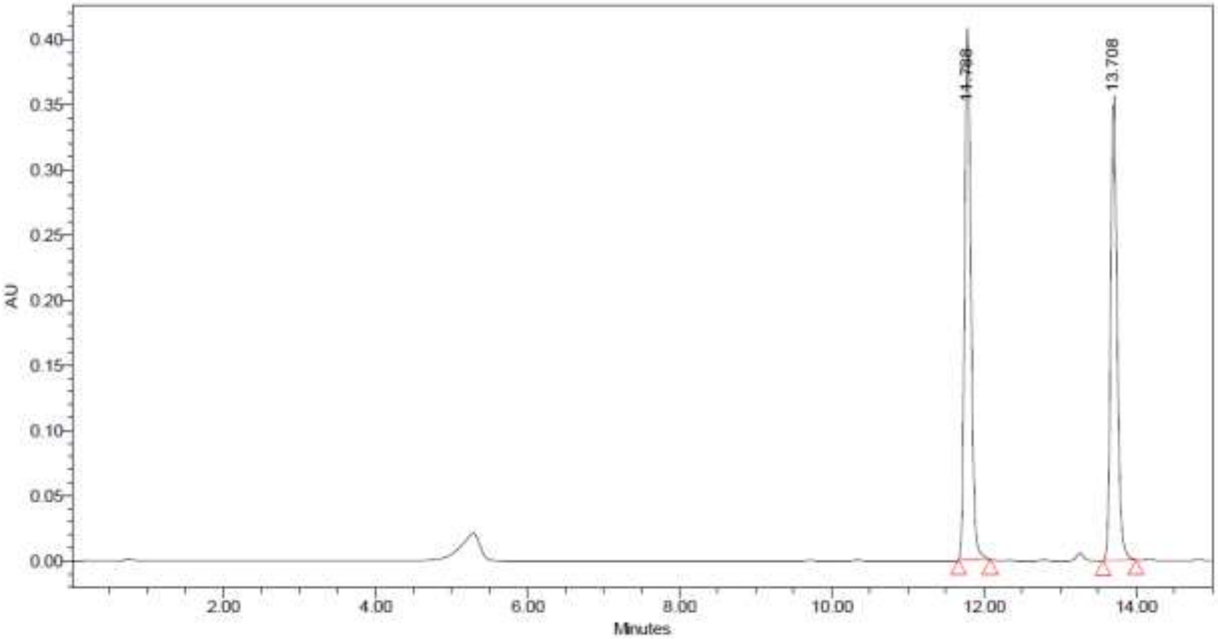

Figure S174. HPLC chromatogram of the Fmoc-Ser(*t*-Bu)-OH/Oxyma/DIC/(S)-(-)-1-phenylethylamine amidation reaction in DMF at t=120 min.

Table S51. Area% for integrated peaks.

	RT	Height	Area	% Area
1	11.788	403677	2325455	52.54
2	13.708	351999	2100488	47.46
Sum			4425942.6	

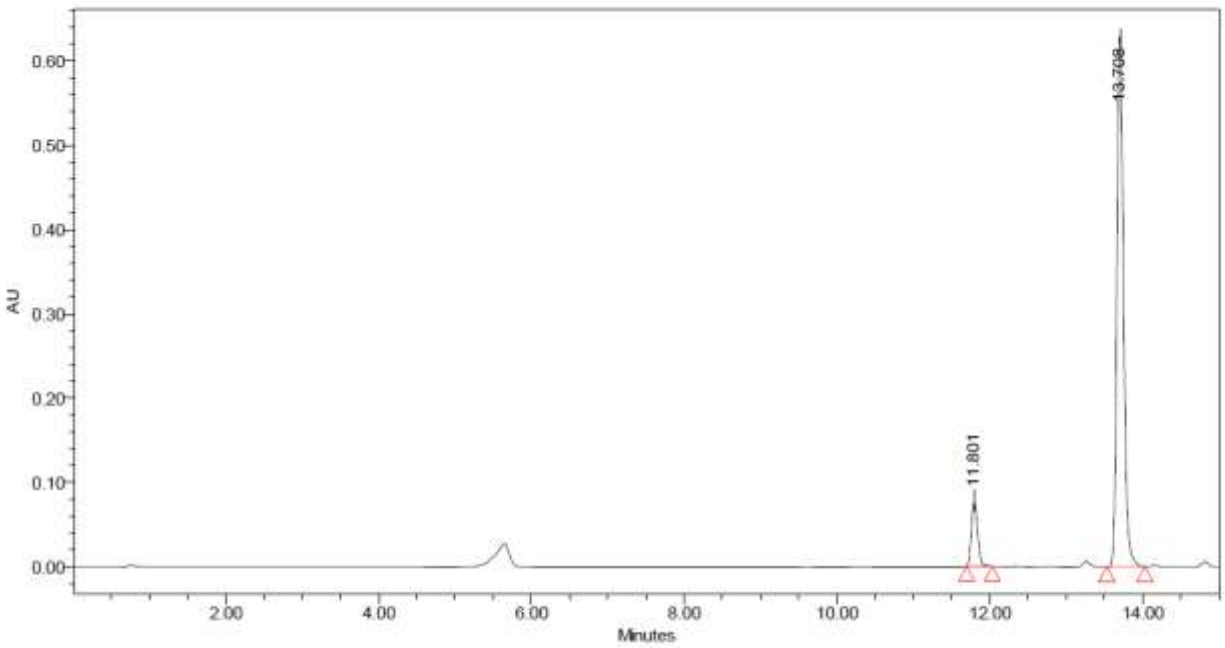

Figure S175. HPLC chromatogram of the Fmoc-Ser(*t*-Bu)-OH/Oxyma/DIC/(S)-(-)-1-phenylethylamine amidation reaction in DMF at t=960 min.

Table S52. Area% for integrated peaks.

	RT	Height	Area	% Area
1	11.801	76905	431896	10.27
2	13.708	633240	3775326	89.73
Sum			4207222.0	

10.2 Fmoc-Ser(*t*-Bu)-OH/Oxyma/DIC/(S)-(-)-1-phenylethylamine amidation reaction with 10 equiv DMTS in DMF

The following amounts of starting materials were used: Fmoc-Ser(*t*-Bu)-OH (95.5 mg, 0.25 mmol, 1.0 equiv), Oxyma (35.4 mg, 0.25 mmol, 1.0 equiv), (S)-(-)-1-phenylethylamine (32.2 µL, 0.25 mmol, 1.0 equiv), DMTS (263.5 µL, 2.5 mmol, 10 equiv), DIC (39.1 µL, 0.25 mmol, 1.0 equiv) in 5 mL DMF.

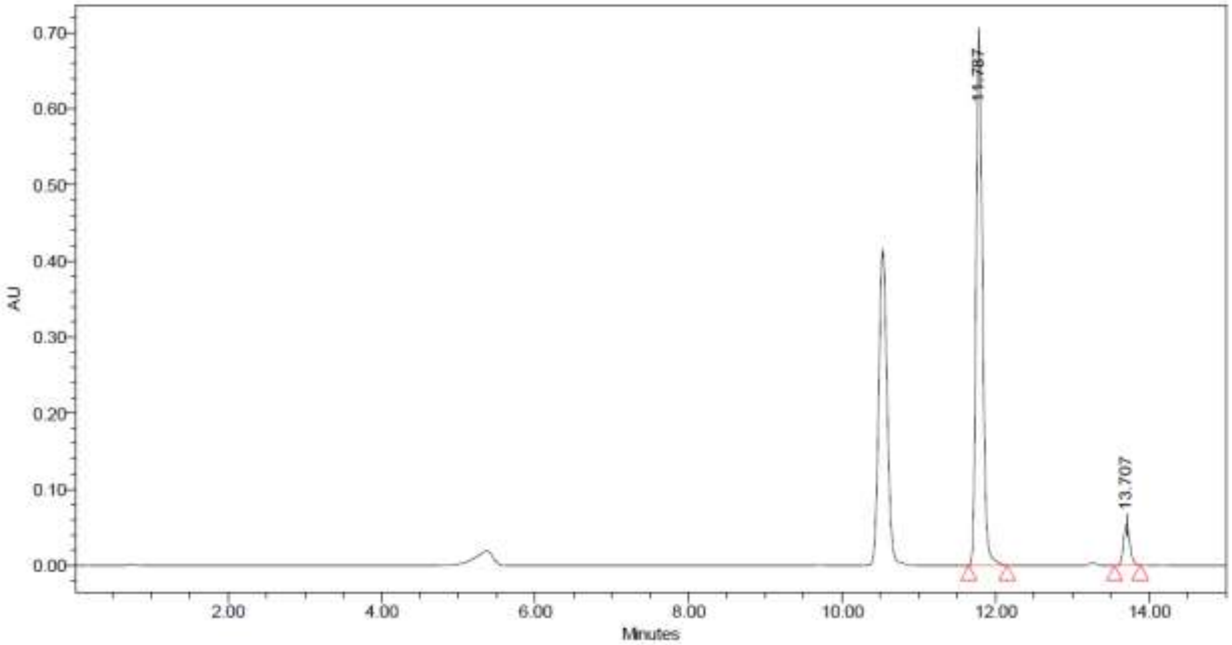

Figure S176. HPLC chromatogram of the Fmoc-Ser(*t*-Bu)-OH/Oxyma/DIC/(S)-(-)-1-phenylethylamine amidation reaction with 10 equiv DMTS in DMF at t=10 min.

Table S53. Area% for integrated peaks.

	RT	Height	Area	% Area
1	11.787	696418	4036771	92.92
2	13.707	53079	307573	7.08
Sum			4344343.4	

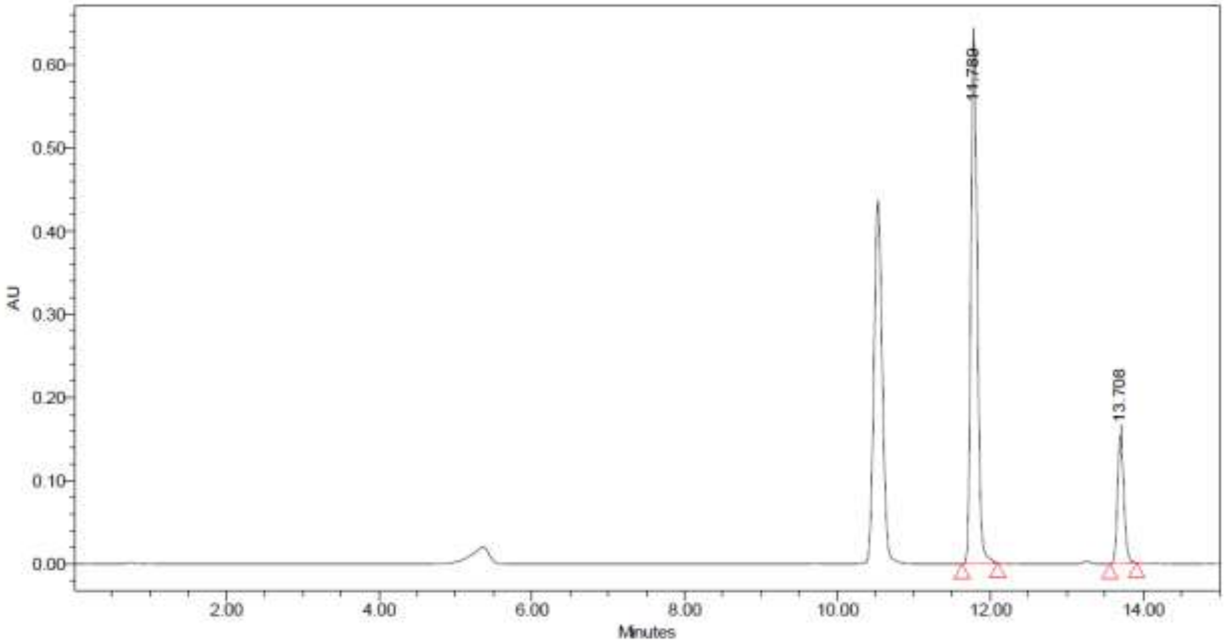

Figure S177. HPLC chromatogram of the Fmoc-Ser(*t*-Bu)-OH/Oxyma/DIC/(S)-(-)-1-phenylethylamine amidation reaction with 10 equiv DMTS in DMF at t=30 min.

Table S54. Area% for integrated peaks.

	RT	Height	Area	% Area
1	11.789	637978	3683668	80.44
2	13.708	154044	895850	19.56
Sum			4579518.0	

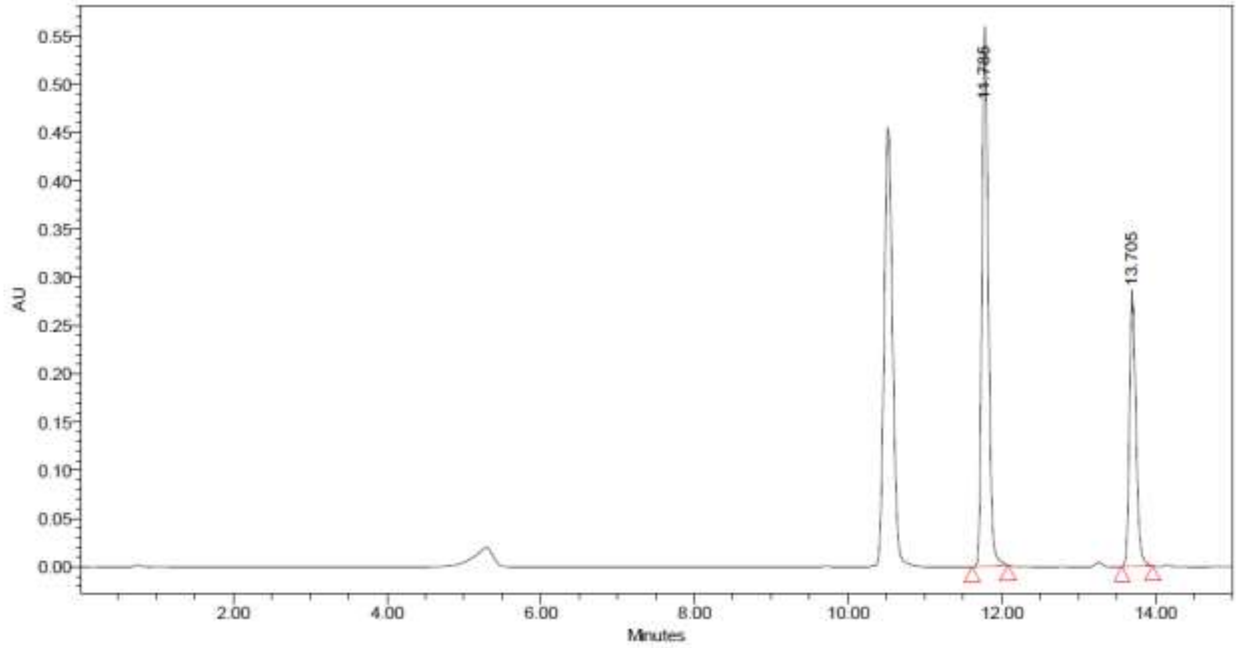

Figure S178. HPLC chromatogram of the Fmoc-Ser(*t*-Bu)-OH/Oxyma/DIC/(S)-(-)-1-phenylethylamine amidation reaction with 10 equiv DMTS in DMF at t=60 min.

Table S55. Area% for integrated peaks.

	RT	Height	Area	% Area
1	11.785	547927	3168506	65.65
2	13.705	278064	1657638	34.35
Sum			4826144.3	

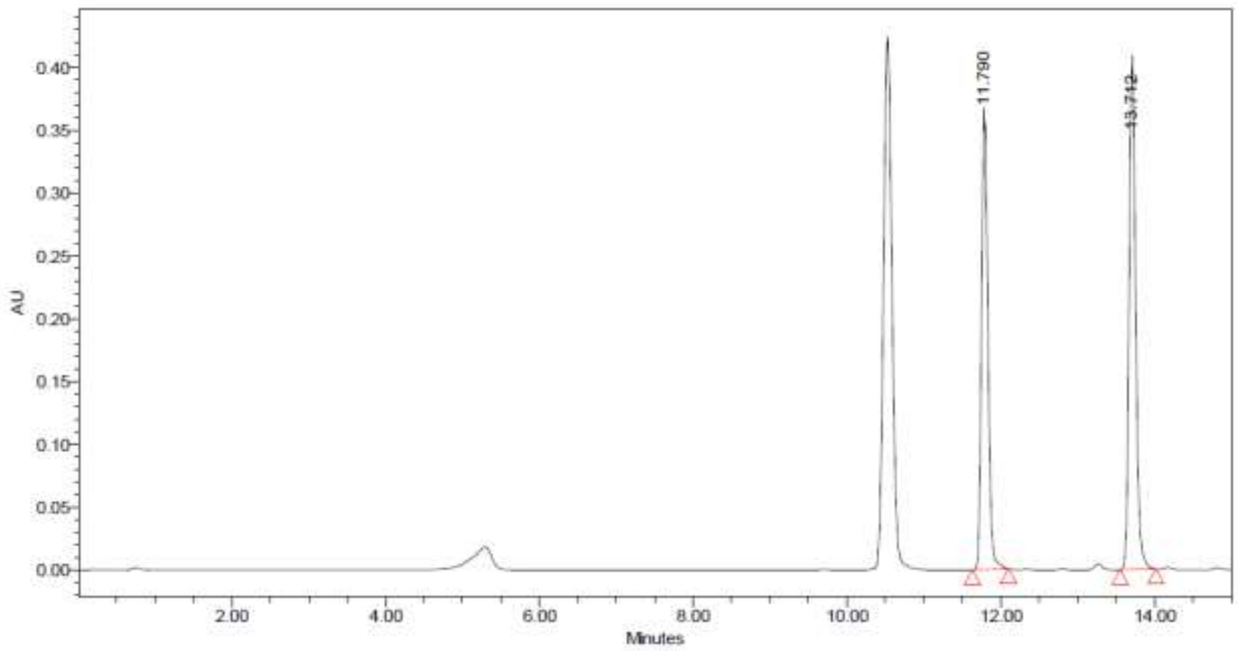

Figure S179. HPLC chromatogram of the Fmoc-Ser(*t*-Bu)-OH/Oxyma/DIC/(S)-(-)-1-phenylethylamine amidation reaction with 10 equiv DMTS in DMF at t=120 min.

Table S56. Area% for integrated peaks.

	RT	Height	Area	% Area
1	11.790	362895	2096326	46.56
2	13.712	402521	2405872	53.44
Sum			4502197.7	

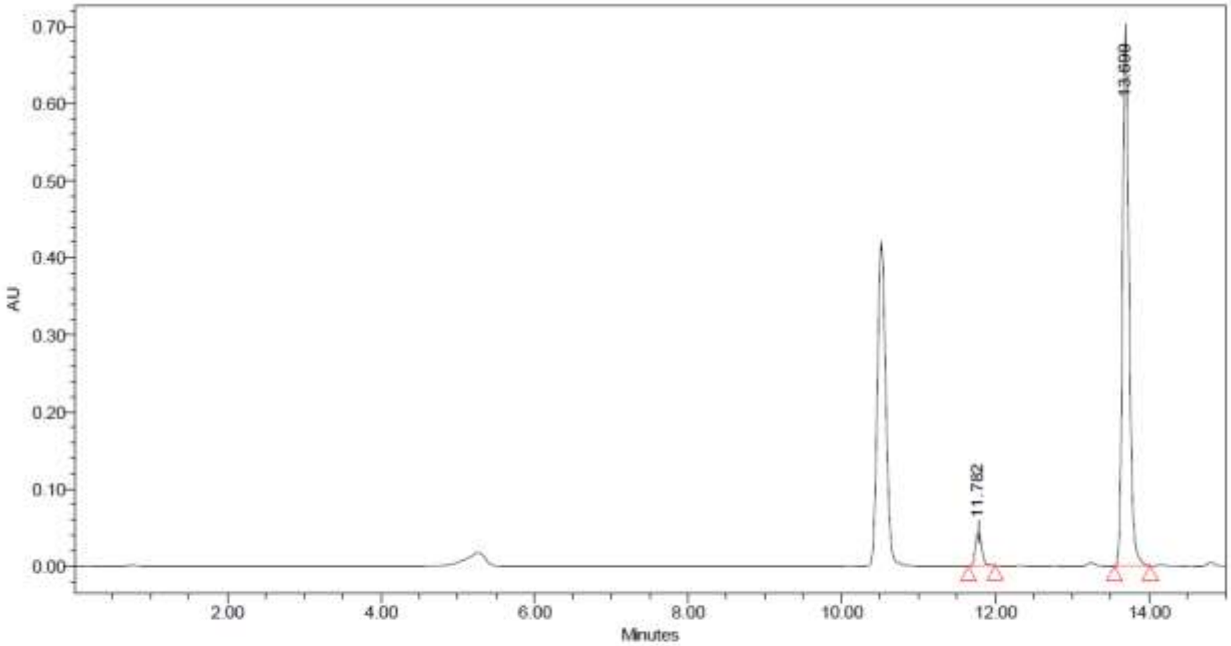

Figure S180. HPLC chromatogram of the Fmoc-Ser(*t*-Bu)-OH/Oxyma/DIC/(S)-(-)-1-phenylethylamine amidation reaction with 10 equiv DMTS in DMF at t=960 min.

Table S57. Area% for integrated peaks.

	RT	Height	Area	% Area
1	11.782	43785	252376	5.75
2	13.699	686673	4135052	94.25
Sum			4387428.4	

10.3 Fmoc-Ser(*t*-Bu)-OH/Oxyma/DIC/(S)-(-)-1-phenylethylamine amidation reaction in NBP/EtOAc (1:4)

The following amounts of starting materials were used: Fmoc-Ser(*t*-Bu)-OH (95.5 mg, 0.25 mmol, 1.0 equiv), Oxyma (35.1 mg, 0.25 mmol, 1.0 equiv), (S)-(-)-1-phenylethylamine (32.2 µL, 0.25 mmol, 1.0 equiv), DIC (39.1 µL, 0.25 mmol, 1.0 equiv) in 5 mL NBP/EtOAc (1:4).

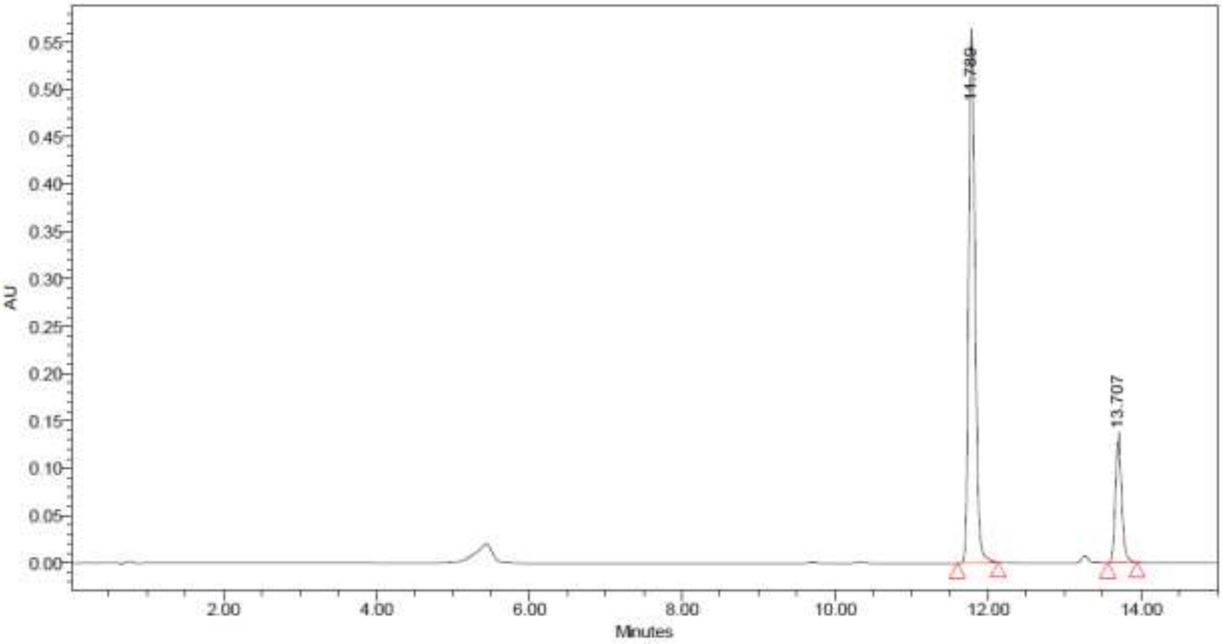

Figure S181. HPLC chromatogram of the Fmoc-Ser(*t*-Bu)-OH/Oxyma/DIC/(S)-(-)-1-phenylethylamine amidation reaction in NBP/EtOAc (1:4) at t=10 min.

Table S58. Area% for integrated peaks.

	RT	Height	Area	% Area
1	11.789	560175	3234886	81.14
2	13.707	127593	751970	18.86
Sum			3986855.9	

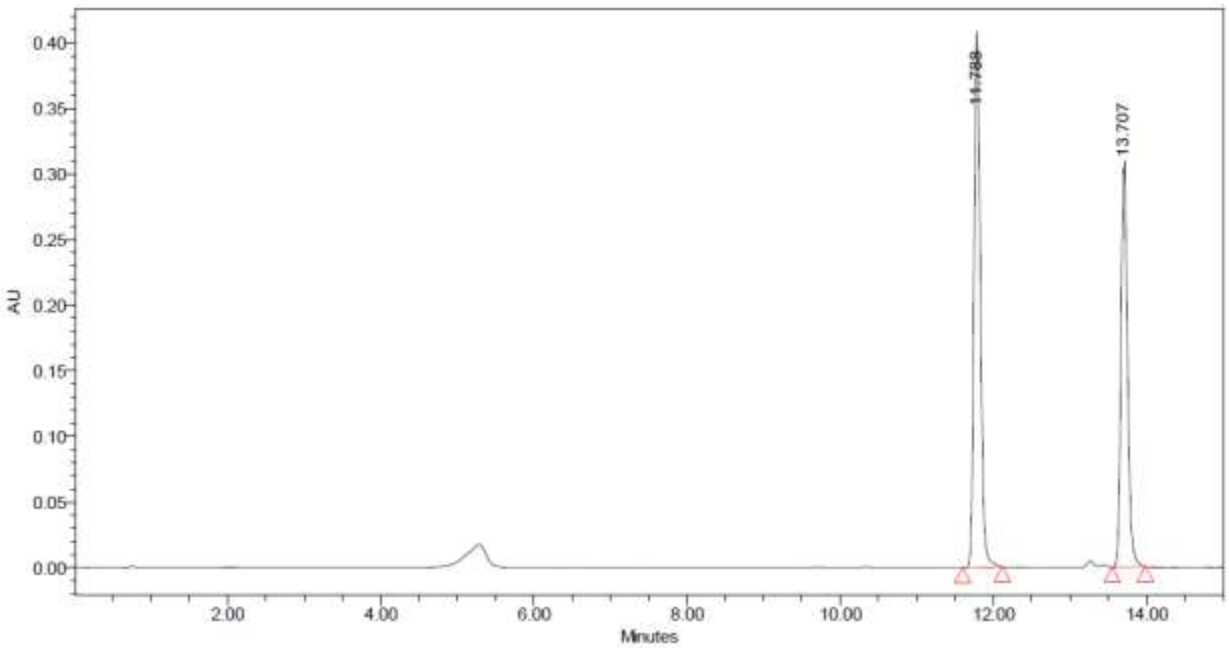

Figure S182. HPLC chromatogram of the Fmoc-Ser(*t*-Bu)-OH/Oxyma/DIC/(S)-(-)-1-phenylethylamine amidation reaction in NBP/EtOAc (1:4) at t=30 min.

Table S59. Area% for integrated peaks.

	RT	Height	Area	% Area
1	11.788	404595	2327562	56.02
2	13.707	305532	1827204	43.98
Sum			4154765.8	

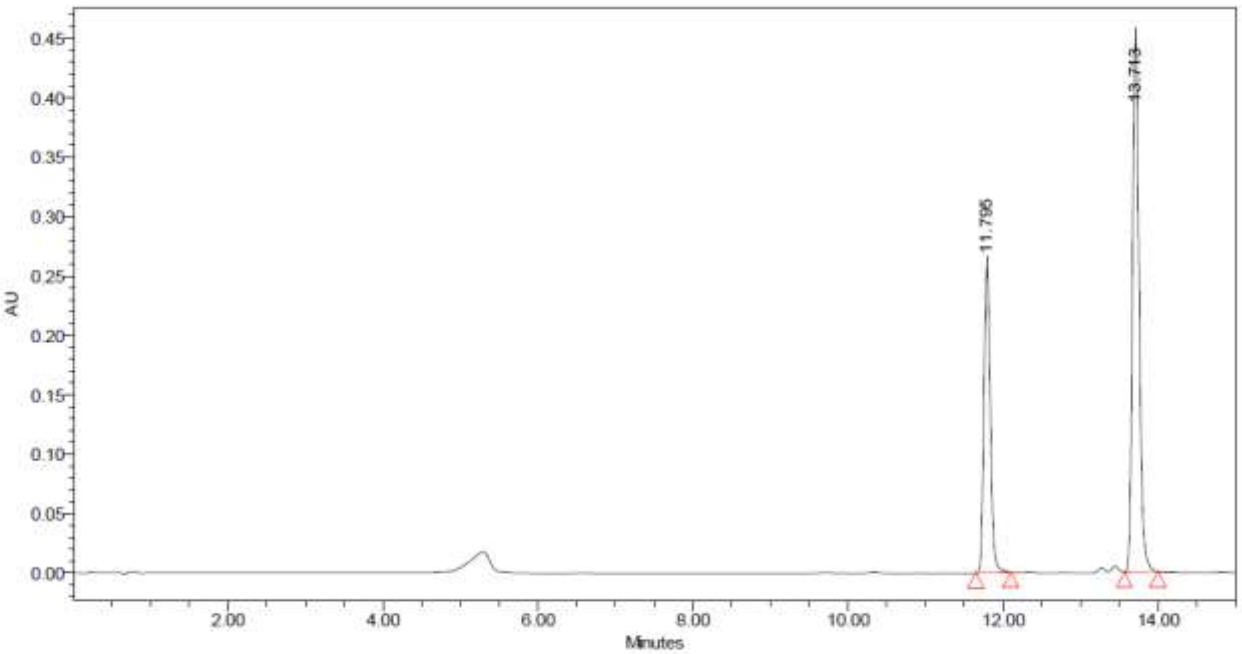

Figure S183. HPLC chromatogram of the Fmoc-Ser(*t*-Bu)-OH/Oxyma/DIC/(S)-(-)-1-phenylethylamine amidation reaction in NBP/EtOAc (1:4) at t=60 min.

Table S60. Area% for integrated peaks.

	RT	Height	Area	% Area
1	11.795	258492	1484410	35.58
2	13.713	450966	2687963	64.42
Sum			4172373.5	

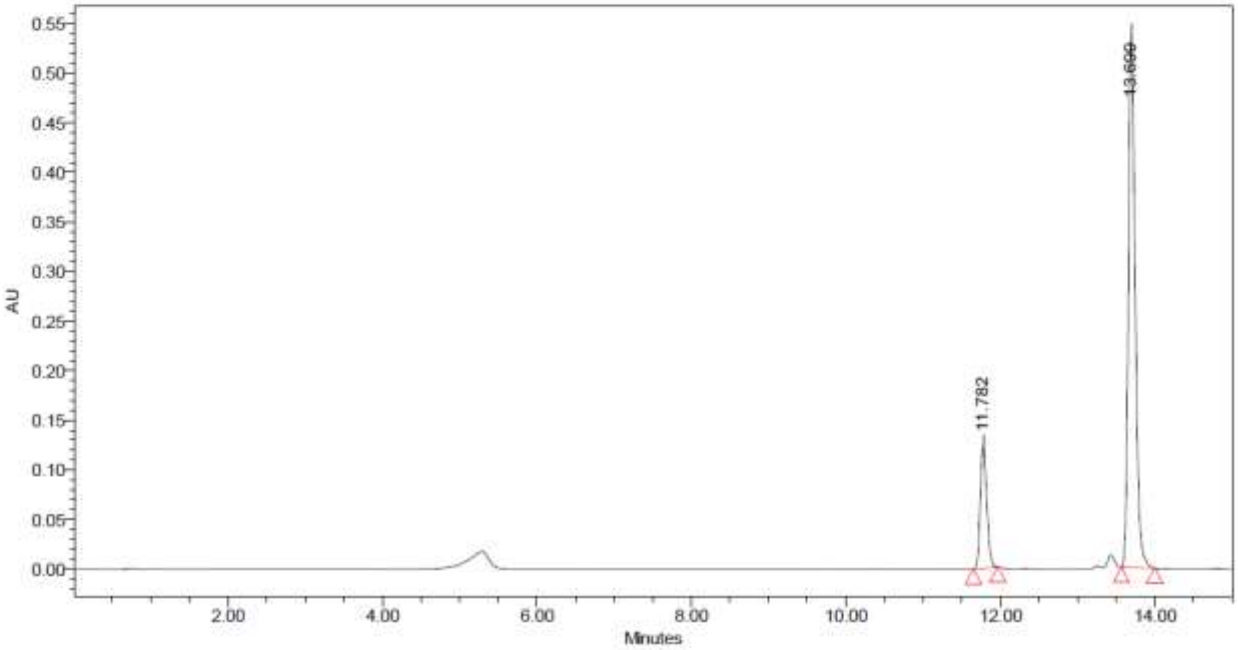

Figure S184. HPLC chromatogram of the Fmoc-Ser(*t*-Bu)-OH/Oxyma/DIC/(S)-(-)-1-phenylethylamine amidation reaction in NBP/EtOAc (1:4) at t=120 min.

Table S61. Area% for integrated peaks.

	RT	Height	Area	% Area
1	11.782	122951	722478	17.86
2	13.699	535258	3322753	82.14
Sum			4045231.1	

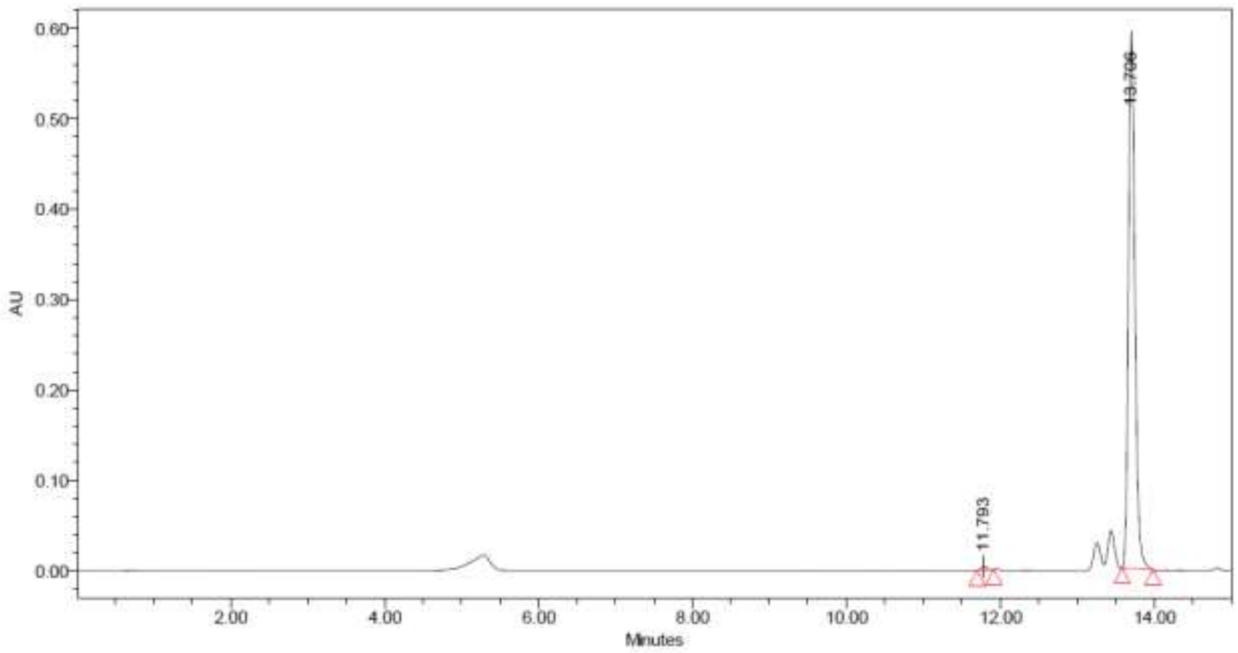

Figure S185. HPLC chromatogram of the Fmoc-Ser(*t*-Bu)-OH/Oxyma/DIC/(S)-(-)-1-phenylethylamine amidation reaction in NBP/EtOAc (1:4) at t=960 min.

Table S62. Area% for integrated peaks.

	RT	Height	Area	% Area
1	11.793	4304	22750	0.65
2	13.706	588928	3457374	99.35
Sum			3480124.5	

10.4 Fmoc-Ser(*t*-Bu)-OH/Oxyma/DIC/(S)-(-)-1-phenylethylamine amidation reaction with 10 equiv DMTS in NBP/EtOAc (1:4)

The following amounts of starting materials were used: Fmoc-Ser(*t*-Bu)-OH (95.8 mg, 0.25 mmol, 1.0 equiv), Oxyma (35.2 mg, 0.25 mmol, 1.0 equiv), (S)-(-)-1-phenylethylamine (32.2 μL, 0.25 mmol, 1.0 equiv), DMTS (263.5 μL, 2.5 mmol, 10 equiv), DIC (39.1 μL, 0.25 mmol, 1.0 equiv) in 5 mL NBP/EtOAc (1:4).

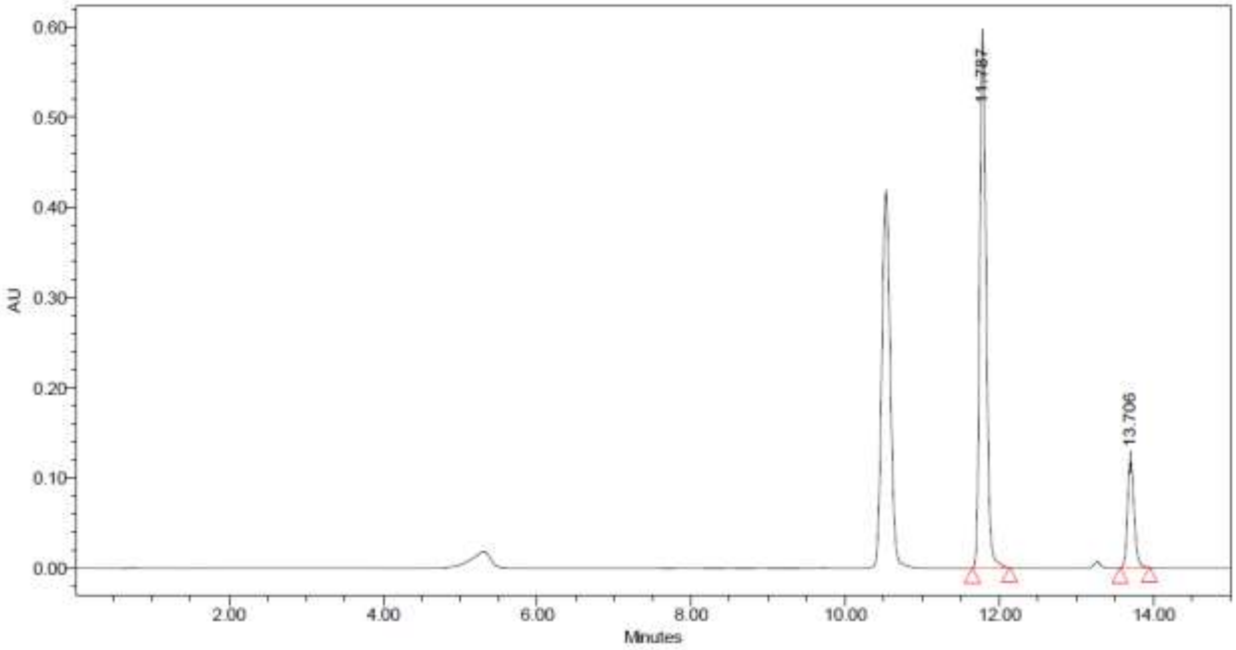

Figure S186. HPLC chromatogram of the Fmoc-Ser(*t*-Bu)-OH/Oxyma/DIC/(S)-(-)-1-phenylethylamine amidation reaction with 10 equiv DMTS in NBP/EtOAc (1:4) at t=10 min.

Table S63. Area% for integrated peaks.

	RT	Height	Area	% Area
1	11.787	590375	3436636	82.96
2	13.706	119033	705902	17.04
Sum			4142538.1	

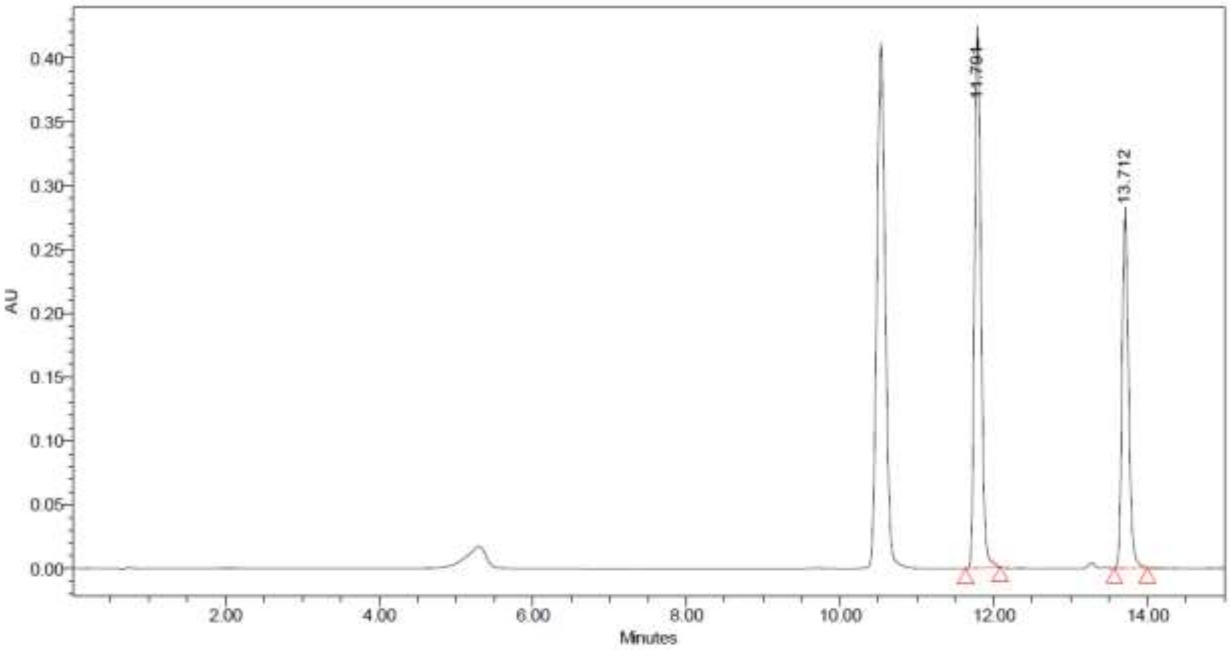

Figure S187. HPLC chromatogram of the Fmoc-Ser(*t*-Bu)-OH/Oxyma/DIC/(S)-(-)-1-phenylethylamine amidation reaction with 10 equiv DMTS in NBP/EtOAc (1:4) at t=30 min.

Table S64. Area% for integrated peaks.

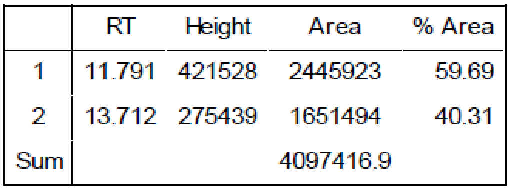

	RT	Height	Area	% Area
1	11.791	421528	2445923	59.69
2	13.712	275439	1651494	40.31
Sum			4097416.9	

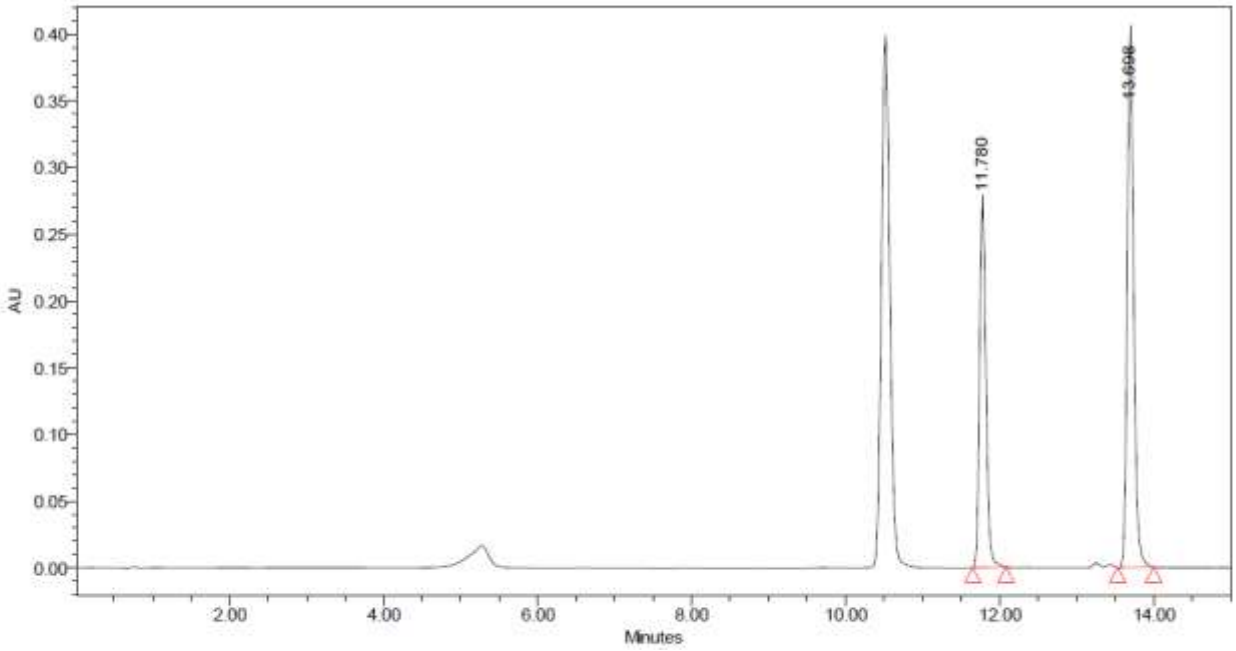

Figure S188. HPLC chromatogram of the Fmoc-Ser(*t*-Bu)-OH/Oxyma/DIC/(S)-(-)-1-phenylethylamine amidation reaction with 10 equiv DMTS in NBP/EtOAc (1:4) at t=60 min.

Table S65. Area% for integrated peaks.

	RT	Height	Area	% Area
1	11.780	271592	1578353	40.07
2	13.698	397067	2360712	59.93
Sum			3939064.6	

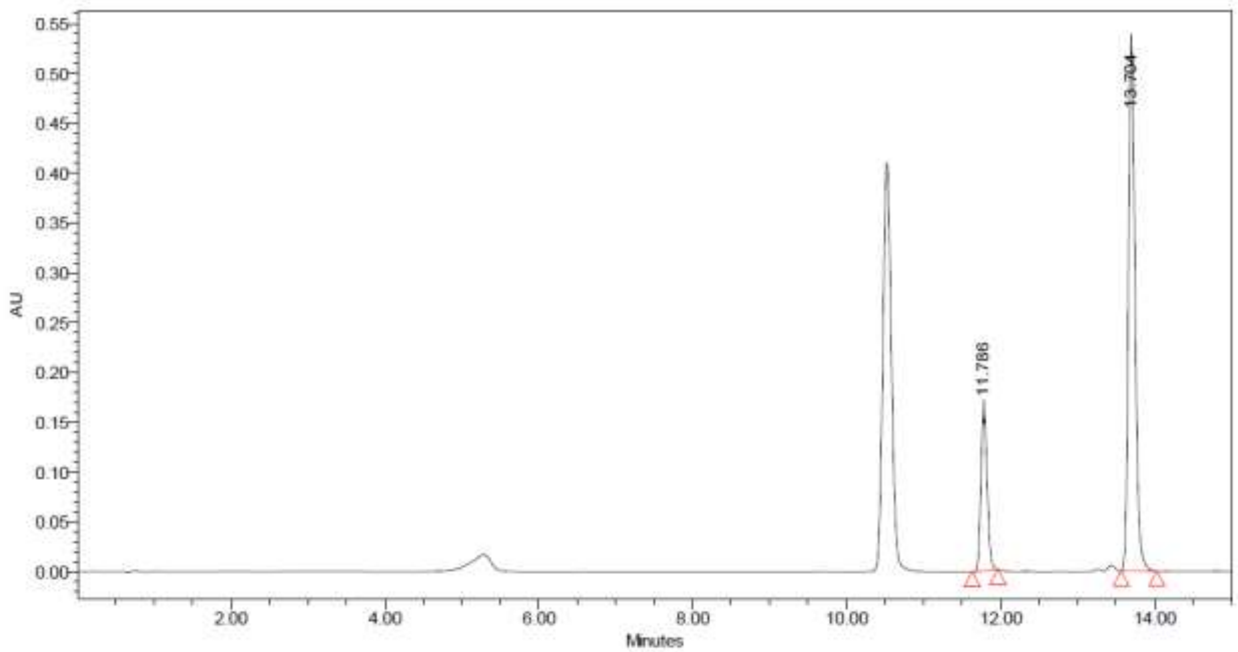

Figure S189. HPLC chromatogram of the Fmoc-Ser(*t*-Bu)-OH/Oxyma/DIC/(S)-(-)-1-phenylethylamine amidation reaction with 10 equiv DMTS in NBP/EtOAc (1:4) at t=120 min.

Table S66. Area% for integrated peaks.

	RT	Height	Area	% Area
1	11.786	160973	905647	22.09
2	13.704	532832	3194348	77.91
Sum			4099995.5	

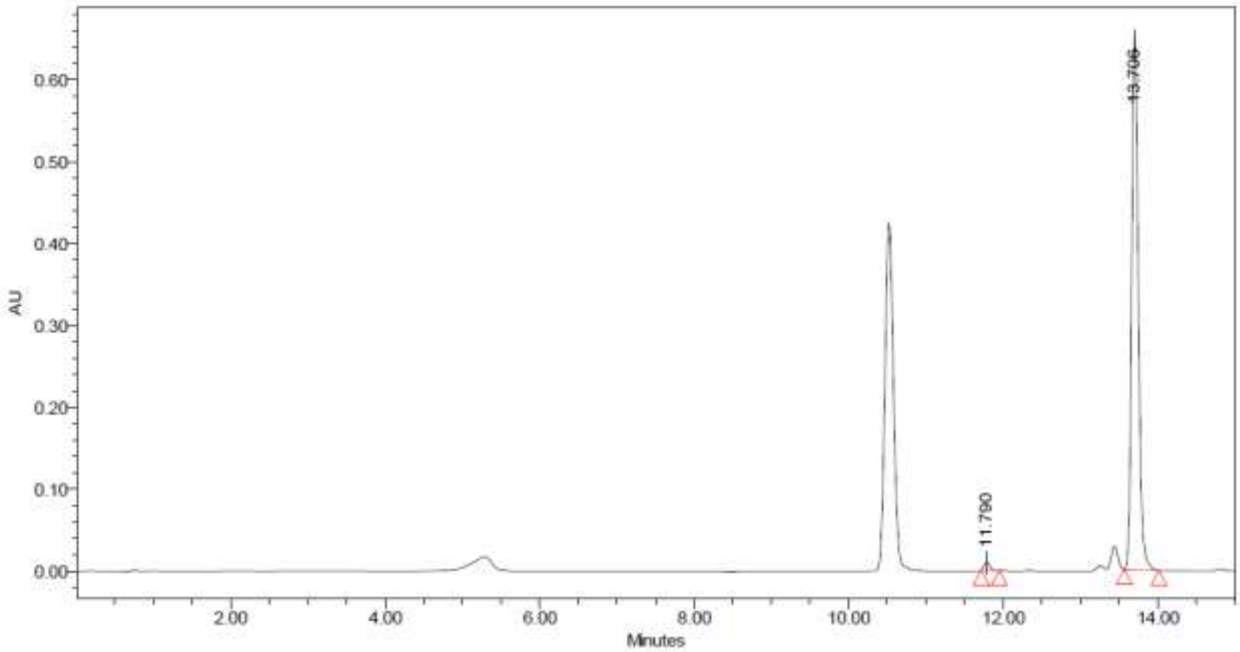

Figure S190. HPLC chromatogram of the Fmoc-Ser(*t*-Bu)-OH/Oxyma/DIC/(S)-(-)-1-phenylethylamine amidation reaction with 10 equiv DMTS in NBP/EtOAc (1:4) at t=960 min.

Table S67. Area% for integrated peaks.

	RT	Height	Area	% Area
1	11.790	9682	50440	1.28
2	13.706	654833	3900331	98.72
Sum			3950770.8	

10.5 Summary of HPLC conversions for amide bond formation kinetics during DIC/Oxyma mediated coupling of Fmoc-Ser(*t*-Bu)-OH with (S)-(-)-1-phenylethylamine with and without 10 equiv DMTS in DMF and NBP/EtOAc (1:4)

Table S68. A summary of conversions during Fmoc-Ser(*t*-Bu)-OH/Oxyma/DIC/(S)-(-)-1-phenylethylamine amidation reactions with and without 10 equiv DMTS in DMF and NBP/EtOAc (1:4).

Solvent	**DMTS**	**Time (min)** 0	 10	 30	 60	 120	 960
		HPLC % conversion					
DMF	**No**	0.0	6.1	16.9	30.0	47.5	89.7
DMF	**Yes**	0.0	7.1	19.6	34.4	53.4	94.3
NBP/EtOAc (1:4)	**No**	0.0	18.9	44.0	64.4	82.1	99.3
NBP/EtOAc (1:4)	**Yes**	0.0	17.0	40.3	59.9	77.9	98.7

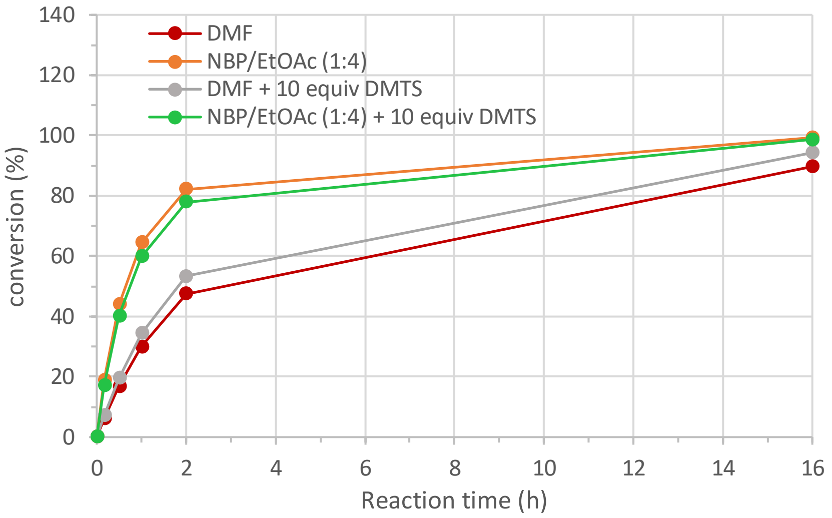

Figure S191. A schematic representation of conversions during Fmoc-Ser(*t*-Bu)-OH/Oxyma/DIC/(S)-(-)-1-phenylethylamine amidation reactions with and without 10 equiv DMTS in DMF and in NBP/EtOAc (1:4).

Conclusions of the experiments summarized in Fig. S191: The presence of DMTS did not have an appreciable impact on the conversion of amide bond forming reaction in neither of the two solvents. Irrespective of whether DMF or NBP/EtOAc (1:4) was used as a solvent no appreciable side reactions were observed as a consequence of addition of DMTS to the DIC/Oxyma mediated amide bond forming reactions.

---

[1] Pawlas, J.; Antonic, B.; Lundqvist, M.; Svensson, T.; Finnman, J.; Rasmussen, J. H., 2D green SPPS: green solvents for on-resin removal of acid sensitive protecting groups and lactamization. *Green Chem*. **2019**, *21*, 2594.

[2] Kaiser, E.; Colescott, R. L.; Bossinger, C. D.; Cook, P. I., Color test for detection of free terminal amino groups in the solid-phase synthesis of peptides. *Anal. Biochem*. **1970**, *34*, 595.

[3] McFarland, A. D.; Buser, J. Y.; Embry, M. C.; Held, C. B.; Kolis, S. P., Generation of Hydrogen Cyanide from the Reaction of Oxyma (Ethyl cyano(hydroxyimino) acetate) and DIC (Diisopropylcarbodiimide). *Org. Process Res. Dev*. **2019**, *23*, 2099.

[4] Pawlas, J.; Svensson, T.; Rasmussen, J. H., 1,4-Benzenedimethanethiol (1,4-BDMT) as a scavenger for greener peptide resin cleavages. *RSC Adv*. **2019**, *9*, 38928.

[5] Gude, M.; Ryf, J.; White, P. D., An accurate method for the quantitation of Fmoc-derivatized solid phase supports. *Lett. Pep. Sci*. **2003**, *9*, 203.